Elevating phosphorus accumulation in waste stabilisation pond algae

A thesis presented in partial fulfilment of the requirements for the degree of

Doctor of Philosophy

in

Environmental Engineering

at Massey University, Palmerston North,

New Zealand.

Matthew Sells

2019

MASSEY
UNIVERSITY

Abstract

Facultative waste stabilisation ponds (WSP) are used globally for wastewater treatment due to their low cost and simple operation. While WSPs can be effective at removing organic pollutants and pathogens, phosphorus removal is typically poor. Algae that are common in WSPs are known to accumulate phosphorus and increase their phosphorus content in the biomass from 1% up to 3.8% (gP/gSS), which is believed to be from the production of intracellular polyphosphate granules. This phenomenon, known as luxury uptake, may be possible to manipulate to improve phosphorus removal in WSPs; however, its occurrence is sporadic and poorly understood. This PhD thesis was undertaken to investigate the conditions that influence phosphorus accumulation in WSP algae. Phosphorus accumulation was quantified using two methods: (1) the traditional phosphorus content in the biomass (gP/gSS), and (2) a new image analysis method developed in this thesis that quantifies stained polyphosphate granules within individual algal cells (μm^2 granule/μm^2 cell).

Following a literature review and screening experiments that sought to identify variables that could affect the phosphorus content in the biomass (gP/gSS), six variables: temperature, phosphorus concentration, light intensity, mixing intensity, organic load, and pH were comprehensively examined using 40 batch factorial experiments (2^{6-1}) and a mixed genus culture from a full-scale WSP. Nine variables and interactions had a significant effect on the phosphorus content in the biomass and were incorporated into a regression equation. This 'mixed genus' regression equation was tested against literature data, where seven out of the eight batch experiments from the literature were successfully predicted.

In order to identify if the batch findings could be applied to a continuous process, which is more typical of full-scale WSPs, a bench-scale novel 'luxury uptake' process was designed, built, and operated under five different scenarios. The regression equation successfully predicted the experimental results for three of the five conditions examined. It was theorised that differences in behaviour at the genus level might explain why all five conditions were not successfully predicted.

In an attempt to improve the prediction capability, the 'black-box' of mixed genus analysis was 'opened' to allow the effects of variables on phosphorus accumulation at the genus level to be directly examined. To achieve this, a new image analysis method was developed that quantified stained polyphosphate granules in individual algal cells. To ensure the granules

being measured were indeed polyphosphate, algal cells were analysed using transmission electron microscopy coupled with energy dispersive X-ray spectroscopy, which confirmed the granules contained higher levels of phosphorus compared to the remaining cell. The image analysis method was then used to quantify stained polyphosphate granules in individual cells from the 40 batch factorial experiments mentioned previously.

The results using the image analysis method showed that, for the five most abundant algal genera, *Micractinium/Microcystis* had the highest average accumulation of polyphosphate granules (17% μm^2 granule/μm^2 cell), followed by *Scenedesmus* (12%), *Pediastrum* (11%), *Monoraphidium* (8%), and *Actinastrum* (4%). Although none of the genera studied had the same combination of significant variables, all five genera preferred a high phosphorus concentration to elevate polyphosphate granule accumulation. Furthermore, a high light intensity, high organic load, or high temperature was preferred by the algae if the variable was significant for that genus.

The culture used in the bench-scale continuous flow 'luxury uptake' process originated from a mixed genus WSP culture; however, it had become dominated by the *Scenedesmus* genus. Therefore, the regression equation was refined to use the batch data for this genus alone. This new *Scenedesmus* regression equation was compared against the experimental data from the 'luxury uptake' process previously mentioned. Polyphosphate granule accumulation was now successfully predicted in all five experimental conditions at the 95% confidence level. This improved prediction capability indicates that an understanding of the algal genus present in a WSP system is required for accurate predictions of the phosphorus accumulation to be obtained, and the batch data can indeed be applied to a continuous process.

An unexpected result of the research was that, contrary to what was believed in the literature, an increase in the phosphorus content in the biomass did not necessarily increase the polyphosphate granule accumulation. Further examination identified that individual cells from the same algal species had varying polyphosphate granule contents from 0% to over 20% (μm^2 granule/μm^2 cell) when exposed to the same conditions. This variation was hypothesised to be from cellular functions influencing the granules differently depending on the individual alga's cell cycle. In addition, when the phosphorus content in the biomass was increased above 2.1% (gP/gSS), no significant effect on the average quantity of polyphosphate granules was observed. This finding indicates that other forms of phosphorus storage must be responsible for attaining a highly elevated phosphorus content in the biomass.

The findings in this thesis have demonstrated that manipulation of phosphorus accumulation in WSP algae is possible, and predictable, albeit at a genus level. These findings pave the way forward for the development of a new algal-based biotechnology capable of harvesting phosphorus from wastewater.

Acknowledgements

Firstly, I would like to thank my supervisors Prof. Andrew Shilton and Dr. Nicola Brown. Their support and guidance throughout my PhD motivated me to produce the highest level of work I possibly could. Their feedback on the many drafts of the research papers was invaluable and greatly appreciated.

Thank you to the Manawatu District Council, Horowhenua District Council, Tararua District Council, and the Palmerston North City Council for their assistance and access to the WSPs that allowed me to undergo my research.

Many thanks to all the staff from the School of Engineering and Advanced Technology at Massey University Palmerston North for their assistance during my PhD. In particular, I would like to thank Ann-Marie Jackson, John Sykes, and John Edwards for their assistance in the laboratory, and Glenda Rosoman and Michele Wagner for their assistance with the administrative aspects of this PhD. Thank you to the team at the Manawatu Microscopy and Imaging Centre, Dr Matthew Savoian, Ms Jordan Taylor, and Mrs Niki Minards, for the training and assistance with the many hours of microscopy work undertaken. I would also like to thank Nihal Jayamaha for his valuable guidance on the statistical analysis conducted in this PhD.

Thanks to all my postgraduate colleagues, Aidan Crimp, Ramsay Huang, Roland Schaap, and Zane Norvill, for their assistance and encouragement during my PhD. In particular, I would like to thank Maxence Plouviez for his assistance with the *Chlamydomonas reinhardtii* culture, and Paul Chambonniere for access to the pilot scale Palmerston North WSP that he used for his research.

I would also like to thank the Royal Society of New Zealand for financially supporting this research through the Marsden Fund (MAU1103). Thank you also to the Massey University scholarship office for their financial support through the Doctoral Scholarship.

Finally, thank you to all my friends and family for their support and encouragement throughout the PhD journey.

Table of Contents

Table of Figures

Table of Tables

Table of Equations

Structure of the thesis

The chapters in this thesis are adapted from a series of scientific papers that have been published or are ready for submission to international peer-reviewed journals. While the presented content of the chapters is the same as the papers they are based on, the following changes have been made to improve the clarity of the thesis:

- Formatting changes have been conducted to ensure a consistent style throughout the thesis,
- The introductions of each chapter have been shortened to reduce repetition,
- If a method is repeated in later chapters, a reference back to the first mention of the method has been used, and
- Changing the references of papers produced in this PhD to their corresponding chapter number (i.e. a reference to the paper Sells *et al.* (2018) has been changed to Chapter 2).

A preface has been included at the beginning of each chapter to help link the individual chapters together and illustrate their contribution towards the research objectives of this thesis. The content presented in Chapters 1 through 5 has been used to produce the thesis conclusions that are discussed after Chapter 5.

The structure of this thesis complies with the Massey University "Guidelines for Doctoral Thesis by Publications", 2015 issued by the graduate research school (GRS).

List of papers and contribution

A list of the chapters and relevant publications are given below. Along with these publications, an overview of the initial findings of this thesis was presented at the "11th IWA Specialist Group Conference on Wastewater Pond Technologies, 2016" in Leeds, UK.

Chapter 2

Sells, M. D., Brown, N., & Shilton, A. N. (2018). Determining variables that influence the phosphorus content of waste stabilization pond algae. *Water Research, 132*, 301-308. doi:10.1016/j.watres.2018.01.013

Chapter 3

Sells, M.D., Brown, N. and Shilton, A.N. Interactions between environmental and process variables influence phosphorus accumulation in waste stabilisation pond algae. *In preparation for submission to Water Research.*

Chapter 4

Sells, M.D., Brown, N. and Shilton, A.N. The conditions for phosphorus accumulation in algae are genus dependent. *In preparation for submission to Ecological Engineering.*

Chapter 5

Sells, M.D., Brown, N. and Shilton, A.N. Relating polyphosphate granule accumulation to the algal phosphorus content. *In preparation for submission to Environmental Science and Technology.*

Matthew Sells was the main contributor and lead author on all the papers mentioned above, with advice and editing assistance being obtained from his supervisors Prof. Andrew Shilton and Dr. Nicola Brown. Matthew Sells designed, conducted, and analysed the experimental work. The "statement of contribution to doctoral thesis containing publications" for the published paper can be found at the end of the appendices.

Introduction

Thousands of small communities around the world rely on facultative waste stabilisation ponds (WSP) for their wastewater treatment due to their relatively low cost and simple operation. Although WSPs can be effective at removing organic pollutants and pathogens, phosphorus removal is typically low with removal rates of 15 to 50% (Garcia *et al.* 2000; Ghazy *et al.* 2008; Mburu *et al.* 2013). With regulators becoming stricter on phosphorus discharge, WSP operators globally are being faced with costly upgrades to improve phosphorus removal.

Currently, two main options are available to improve phosphorus removal in WSPs: addition of chemical dosing, or a shift to the activated sludge based enhanced biological phosphorus removal (EBPR) process. Chemical dosing with coagulants such as aluminium sulphate (alum) or ferric salts is the most common upgrade option for WSPs due to the consistently high phosphorus removal possible. However, the increased operating costs associated with the coagulants and, in particular, the disposal of the resulting chemical sludge is a drawback for smaller communities. Instead of using chemicals for phosphorus removal, it is possible to utilise microorganisms. EBPR uses microorganisms to accumulate phosphorus as polyphosphate and thereby reduce the phosphorus concentration in the effluent. However, EBPR is a complex system that requires careful control to achieve phosphorus removal. When we reflect on why small communities selected WSPs to start with (i.e. low operating costs and simple operation), the combined operating and capital costs of an EBPR system makes this option often seen as an inappropriate replacement for WSPs. This leaves a problem for these smaller communities relying on WSP systems. Instead of focusing on these less suitable phosphorus removal options for WSPs, consideration should be given to improving WSP design to optimise the processes that are already naturally occurring.

An important process already occurring in WSPs is the algal assimilation of phosphorus. For normal cellular growth, algae typically have a phosphorus content of about 1% (gP/gSS) (Azad & Borchardt 1970; Goldman 1980; Kaplan *et al.* 1986). However, algae in WSPs have shown the ability to accumulate phosphorus far in excess of that needed for cellular growth, where the algae are believed to store this extra phosphorus intracellularly as polyphosphate granules (Harold 1966; Elgavish *et al.* 1980; Bolier *et al.* 1992; Siderius *et al.* 1996; Eixler *et al.* 2006). This phenomenon, known as luxury uptake, has been shown to increase the phosphorus content of the algal biomass from 1% up to 3.8% (gP/gSS) (Powell *et al.* 2011a; Crimp *et al.* 2018). If this higher phosphorus content of the algal biomass could be consistently achieved, and these algae harvested, phosphorus removal could be drastically improved in WSP systems.

For example, as shown in Figure 0.1, at an average WSP biomass concentration of 100 mgSS/L (Crimp *et al.* 2018), increasing the phosphorus content of the biomass from 1% up to 3.8% (gP/gSS) represents an increased phosphorus removal by the algae of nearly 3 mgP/L.

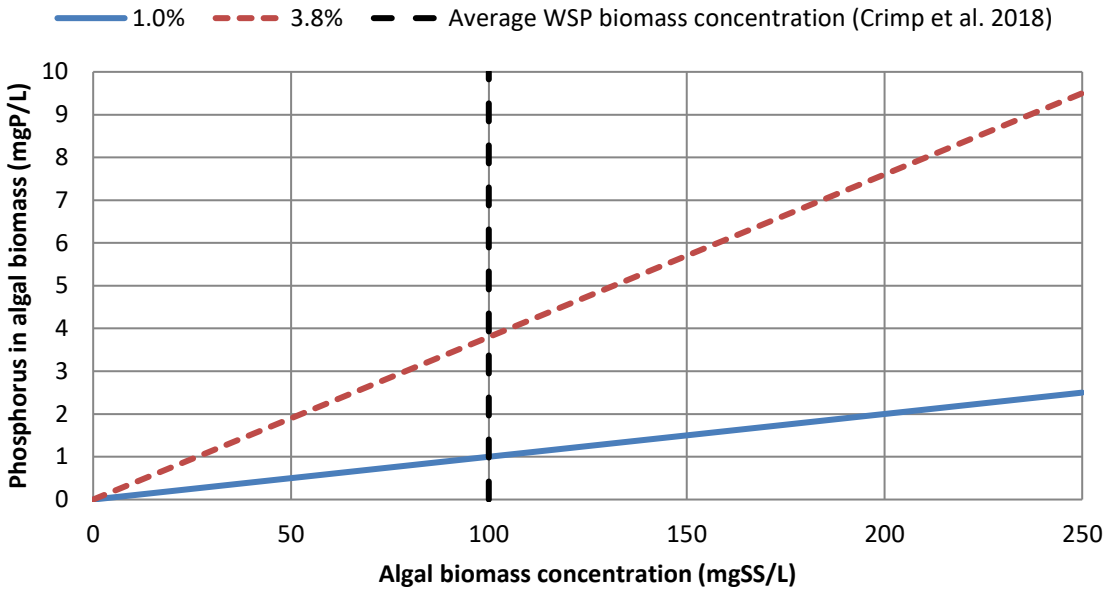

Figure 0.1: Phosphorus concentration in the biomass at luxury uptake levels of 1.0% or 3.8% (gP/gSS). Adapted from Powell *et al.* (2008).

Unfortunately, while algal luxury uptake has been observed, its occurrence is sporadic, and the conditions that influence this phenomenon are not fully understood. This results in a knowledge gap that is preventing the transition of algal luxury uptake from an interesting observation to a new engineered biotechnology. For progression towards an engineered 'luxury uptake' process to occur, the conditions that reliably increase phosphorus accumulation in WSP algae need to be understood. In particular, we need to know:

1. What variables influence phosphorus accumulation under WSP conditions?
2. What effect do these variables have on phosphorus accumulation in WSP biomass?
3. What influence does the algal genus have on polyphosphate granule accumulation?

In order to answer these questions, this thesis aims to address the following objectives:

1. Screen for environmental and process variables that influence the phosphorus content of WSP biomass,
2. Investigate the conditions that influence phosphorus accumulation in a mixed genus WSP biomass, and

3. Examine how the algal genus influences the conditions for polyphosphate granule accumulation.

Furthermore, while the literature indicates polyphosphate granules are produced during phosphorus accumulation; unexpected findings in Chapter 4 of this thesis suggest that this accepted understanding may be incorrect. As a result, an additional fourth objective was added:

4. Examine the relationship between polyphosphate granules in single algal cells and the phosphorus content of the biomass.

Chapter 1

Literature Review

1.1 Waste stabilisation pond (WSP) overview

WSPs are used for wastewater treatment by thousands of small communities around the world due to their relatively low cost, simple design, and straightforward operation. When appropriately designed, WSPs can achieve high organic and pathogen removal, however, these systems are often plagued by poor nutrient removal with phosphorus removal efficiencies ranging from 15 to 50% (Garcia *et al.* 2000; Ghazy *et al.* 2008; Mburu *et al.* 2013).

WSPs can be grouped into four general pond systems: anaerobic, facultative, maturation, and high-rate algal (HRAP). These pond types are described briefly below.

Anaerobic ponds are designed for high organic removal and are usually the first pond in a WSP series if they are present. The pond is typically 2 to 5 meters deep to reduce oxygen diffusion and maintain anaerobic conditions (Kayombo *et al.* 2004; Shilton & Walmsley 2005). These anaerobic conditions mean there is low phosphorus assimilation by the bacteria (Oliveira & Von Sperling 2008), resulting in the main phosphorus removal pathway being the sedimentation of solids containing phosphorus. This pond type is not discussed further due to the limited algal abundance in anaerobic ponds.

Facultative ponds have both aerobic and anaerobic sections that can support algae, aerobic bacteria, and anaerobic bacteria. The pond is typically 1.5m deep. The aerobic bacteria and algae dominate the upper layer, but as the depth of the pond increases the environment becomes increasingly anaerobic, with the sludge layer being entirely anaerobic (Shilton & Walmsley 2005). Retention times of these ponds are commonly weeks long (Kayombo *et al.* 2004; Shilton & Walmsley 2005). Facultative ponds can be designed to include a fermentation pit. This fermentation pit receives the raw influent and acts like a small anaerobic pond within the facultative pond to improve organics removal (Shilton & Walmsley 2005).

Maturation ponds are ordinarily last in the series of ponds and are used for pathogen removal (Mara & Pearson 1998). Maturation ponds are generally shallower than facultative ponds at about 1m depth to optimise aerobic conditions and light penetration (Menya *et al.* 2013).

HRAPs are typically constructed in a raceway or single loop configuration. The HRAP depth can vary between 0.2 to 1.0m deep, however for standard wastewater treatment the depth is typically 0.3 to 0.5m (Craggs 2005). A paddle wheel is used to create circulation around the pond. These pond systems can include CO_2 addition to improve algal productivity (Craggs *et al.* 2015). While settling of traditional facultative pond algae can be difficult, algal settling ponds

following HRAPs have been used to successfully harvest the algae (García *et al.* 2000; Park *et al.* 2011b; Craggs *et al.* 2015). Algal settleability may potentially be improved in HRAP systems by recycling part of the harvested biomass back into the HRAP (Park *et al.* 2011b).

Anaerobic, facultative, maturation and HRAP ponds are often combined in a WSP system to achieve the required level of treatment. An example of a traditional WSP system would be an anaerobic pond followed by a secondary facultative pond, and final maturation ponds (Shilton & Walmsley 2005). The anaerobic pond can be substituted by a primary facultative pond; however, this considerably increases the overall size of the pond system. New combinations of pond systems, referred to as "advanced integrated wastewater ponds", are becoming increasingly popular in an attempt to improve the performance of traditional WSP systems. Some examples of these advanced integrated wastewater ponds are:

1. An advanced facultative pond with a fermentation pit, followed by a HRAP, algal settling ponds, and final maturation ponds (Craggs 2005),
2. A covered anaerobic pond, followed by a HRAP, algal settling ponds, and final maturation ponds (Craggs *et al.* 2015), or
3. Biological trickling filter, followed by a HRAP, algal settling ponds, and wetlands with a denitrification filter (Park *et al.* 2018)

While these advanced integrated wastewater ponds can improve solids and nutrient removal compared to traditional WSP systems, phosphorus removal still remains an issue with an average removal of about 65% in the HRAP (Park *et al.* 2018).

The differences in the WSP designs mentioned often result in the algal genera varying between the pond types. The typical algal genera found in these systems have been summarised in Table 1.1.

Table 1.1: Key algal genera present in facultative ponds (7 studies), maturation ponds (5 studies), and HRAPs (7 studies) (Shelef 1982; Banat *et al.* 1990; Cromar *et al.* 1996; Pearson 2005; Godos *et al.* 2009; Shanthala *et al.* 2009; Park & Craggs 2010; Pham *et al.* 2014; Ariesyady *et al.* 2016; Mehrabadi *et al.* 2016; Crimp *et al.* 2018). Classification of class and order is based on Guiry and Guiry (2017). ✓ = present, × = no mention of presence, F-WSP = facultative WSP, and M-WSP = Maturation WSP.

Class	Order	Genus	F-WSP	M-WSP	HRAP
Chlorophyceae	Chaetophorales	*Protoderma*	×	×	✓
		Stigeoclonium	✓	×	×
	Chlamydomonadales	*Carteria*	✓	✓	×
		Chlamydomonas	✓	✓	✓
		Chlorogonium	✓	✓	×
		Eudorina	✓	✓	×
		Pandorina	✓	✓	×
		Pyrobotrys	✓	✓	×
		Tetraspora	✓	✓	×
		Volvox	✓	×	×
	Sphaeropleales	*Ankistrodesmus*	✓	✓	✓
		Coelastrum	✓	✓	✓
		Desmodesmus	✓	✓	✓
		Kirchneriella	✓	×	×
		Korshikoviella	✓	✓	×
		Monoraphidium	✓	✓	✓
		Pediastrum	✓	×	✓
		Planktosphaeria	✓	✓	×
		Scenedesmus	✓	✓	✓
		Schroederia	✓	✓	×
		Selenastrum	✓	✓	×
		Tetraedron	✓	×	×
Chrysophyceae	Chromulinales	*Chromulina*	✓	×	×
	Pyrenomonadales	*Chroomonas*	✓	✓	×
Conjugatophyceae	Desmidiales	*Closterium*	✓	×	×
		Cosmarium	✓	×	×
		Euastrum	✓	×	×
Cryptophyceae	Cryptomonadales	*Cryptomonas*	✓	✓	×
	Pyrenomonadales	*Rhodomonas*	×	✓	×
Euglenophyceae	Euglenales	*Euglena*	✓	✓	✓
		Phacus	✓	✓	×
		Trachelomonas	✓	✓	×
Trebouxiophyceae	Chlorellales	*Actinastrum*	✓	✓	✓
		Chlorella	✓	✓	✓
		Closteriopsis	×	✓	×
		Crucigeniella	✓	×	×
		Dictyosphaerium	✓	✓	×
		Micractinium	✓	✓	✓
		Oocystis	✓	✓	✓

1.2 Phosphorus removal pathways in WSPs

Phosphorus removal in WSP systems is achieved through the following pathways: biological assimilation, adsorption, precipitation, and sedimentation.

Bacteria and algae contribute towards the biological assimilation of phosphorus in WSPs. The relationship between bacteria and algae in WSPs is complex. Heterotrophic bacteria undergo respiration that consumes oxygen and produces carbon dioxide (CO_2). Autotrophic algae and cyanobacteria can undergo photosynthesis that consumes CO_2 and produces oxygen. CO_2 consumption increases the pH in the pond, which can affect phosphorus adsorption and precipitation.

Adsorption occurs when phosphorus chemically or physically binds to the surface of a solid material, whereas precipitation occurs when phosphorus reacts with dissolved cations (such as calcium or magnesium) in the wastewater to form a solid precipitate. Both adsorption and precipitation are influenced by the pH, redox potential, and the concentration of the binding material (Nurdogan & Oswald 1995; Maurer *et al.* 1999; Peng *et al.* 2007).

Biological assimilation, adsorption, and precipitation take the dissolved phosphorus and turn it into a solid form. To then achieve phosphorus removal from the wastewater, the solid phosphorus forms need to be harvested and removed from the wastewater. Most WSPs do not have dedicated harvesting systems and instead rely on sedimentation within the ponds to remove the phosphorus solids. This results in the build-up of phosphorus compounds in the anaerobic sludge layer at the bottom of the ponds. This sludge layer is rarely removed, about every ten years (Walmsley & Shilton 2005), meaning that interactions between the sludge at the bottom of the pond and the liquid above it impact the overall phosphorus removal in the WSP. Phosphorus release has been observed in the sludge layer of full-scale WSP systems to range from 4.3 to 12.4 μgP/(gTSS.d) (Powell *et al.* 2011b).

The combination of these previously discussed pathways results in the overall phosphorus removal in WSPs. However, the phosphorus removal in WSP systems is typically low and variable with removal efficiencies of 15 to 50%. While the exact cause of this has not been identified in the literature, algal phosphorus uptake has been proposed as the dominant phosphorus removal pathway in WSPs (Larsdotter *et al.* 2007; Powell *et al.* 2011b). The following section considers algal phosphorus uptake in more detail.

1.3 Algal phosphorus uptake dynamics

Phosphorus is a critical nutrient that fulfils a range of cellular functions from cell structure, to cellular energy, to genetic information storage and transfer (Blank 2012). This wide range of functions requires a variety of different phosphorus compounds, such as adenosine triphosphate (ATP), nucleotides, RNA, DNA, phosphoproteins, phosphorylated carbohydrates, phospholipids, and polyphosphates (Kuhl 1977).

Algae normally uptake phosphorus as inorganic phosphate (typically $H_2PO_4^-$ or HPO_4^{2-}), but organic phosphorus can also be used after hydrolysing the substrate with extracellular or cell wall bound phosphatase enzymes (Kuhl 1977; Cembella *et al.* 1982; Kaplan *et al.* 1986). Phosphorus uptake is an active process controlled by a carrier enzyme in the cell membrane that transports phosphorus into the cell against the electrochemical gradient (Kuhl 1977; Cembella *et al.* 1982). This active uptake process follows four main stages as shown in Figure 1.1. The first stage is diffusion of the phosphate next to the membrane, followed by adsorption onto the carrier enzyme, passage through the membrane, and release from the carrier enzyme within the cell (Cembella *et al.* 1982).

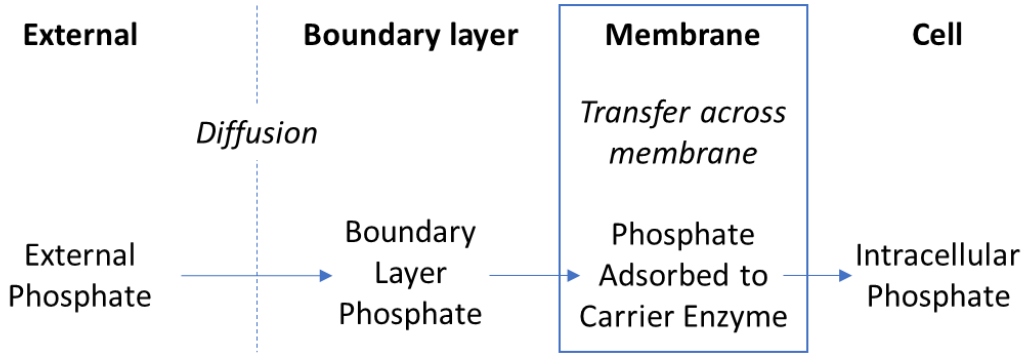

Figure 1.1: Phosphate transfer into an algal cell according to Cembella *et al.* (1982).

Although phosphorus is involved in multiple cellular processes, the actual phosphorus content of the algal biomass is typically only 1% (gP/gSS) (Azad & Borchardt 1970; Goldman 1980; Kaplan *et al.* 1986). This phosphorus content can decrease below 1% (gP/gSS); however, this generally has an adverse effect on the growth rate (Azad & Borchardt 1970). More intriguing is the ability of the algae to increase their phosphorus content above 1% (gP/gSS), with values of 4% (gP/gSS) (Krauss 1976; Kaplan *et al.* 1986) and in one study up to 6.5% (gP/gSS) (Azad & Borchardt 1970) being observed. This increase in phosphorus content is believed to be from the algae storing phosphorus intracellularly as polyphosphate granules (Harold 1966; Elgavish

et al. 1980; Bolier *et al.* 1992; Siderius *et al.* 1996; Eixler *et al.* 2006). This storage process is suggested to be an evolutionary response to the varying phosphorus conditions found naturally in lakes. Algae are suggested to store phosphorus during times of high phosphorus flux as a competitive response to allow continued growth during the more typical low phosphorus concentration periods (Azad & Borchardt 1970; Portielje & Lijklema 1994; Carey *et al.* 2012; Yue *et al.* 2013). The next section will look at polyphosphate in more detail.

1.4 The role of polyphosphate in the algal cell

Polyphosphates are linear polymers made up of multiple phosphate residues that are linked by ATP like energy-rich phosphoanhydride bonds (Kornberg *et al.* 1999; Kulaev *et al.* 2004; Achbergerová & Nahálka 2011). The formation of polyphosphate is an energy demanding process (Smith 1966; Aitchison & Butt 1973), which results in the algal cell having an energy compromise between growth and production of polyphosphate.

Polyphosphate can be classified as either acid soluble (ASP) or acid-insoluble (AISP) polyphosphate. While this classification is based on extraction techniques rather than biological function, these different forms of polyphosphate are involved in distinctly different biological processes. ASP are shorter chain polyphosphates involved in metabolism, synthesis of cellular components (Kuhl 1962), and short-term phosphorus storage (Powell *et al.* 2009), whereas AISP are longer chain polyphosphates used in the storage of phosphorus (Miyachi *et al.* 1964). These polyphosphate forms were defined further into four fractions by Miyachi and colleagues (Miyachi & Miyachi 1961; Miyachi & Tamiya 1961a, b; Miyachi *et al.* 1964). These forms were referred to as polyphosphate “A”, “B”, “C”, and “D” and had distinct functions in the alga *Chlorella*. Polyphosphate “A” and “C” are intermediates between cellular orthophosphate and synthesis of DNA and phosphoproteins, while “B” and “D” are considered phosphorus reserves for use in the absence of external phosphorus (Miyachi *et al.* 1964). These different polyphosphate fractions were also found in different parts of the cell. Polyphosphate “A” is a component of polyphosphate granules, “C” is located next to the chloroplasts, and fractions “B” and “D” are found in multiple cellular structures (Kulaev *et al.* 2004). The relationships between the polyphosphate groups and other cellular phosphorus fractions have been summarised in Figure 1.2.

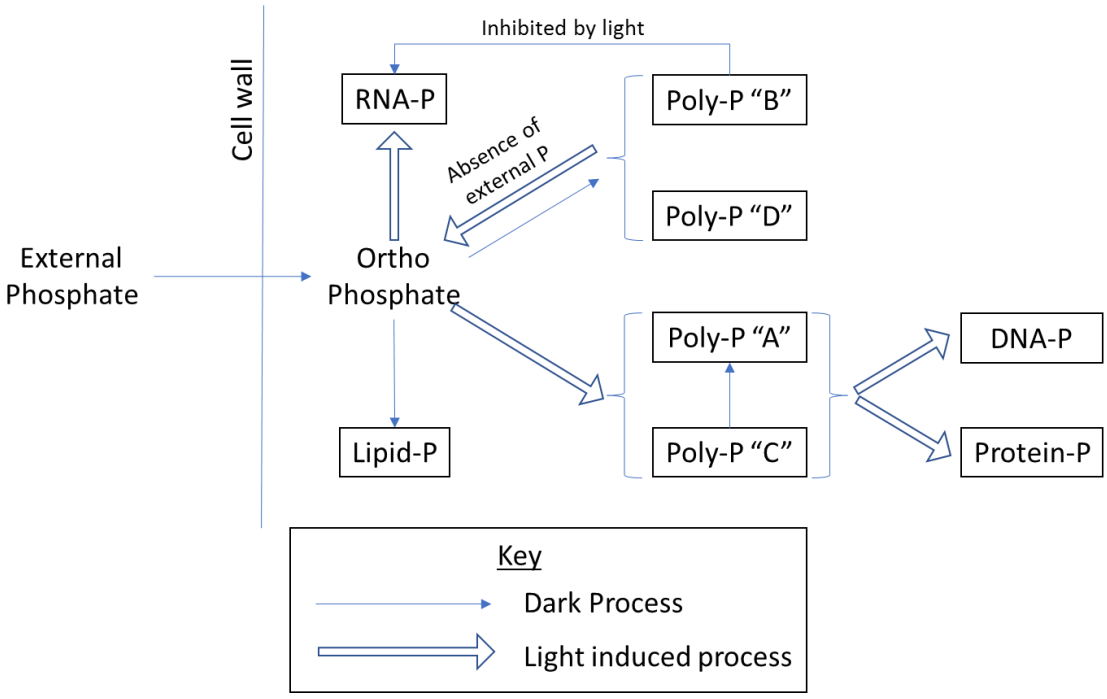

Figure 1.2: Relationships between the polyphosphate groups and other cellular phosphorus fractions. RNA-P, DNA-P, Lipid-P, and Protein-P refer to the phosphorus associated with the respective compounds. Poly-P refers to polyphosphate with A, B, C, and D referring to the different fractions. Adapted from Miyachi *et al.* (1964).

Polyphosphate can also fulfil biological functions other than just a phosphorus reservoir. Polyphosphate has been found in the nucleus, mitochondria, cytoplasm, endoplasmic reticulum, vacuoles (Kulaev *et al.* 2004), and the cell wall (Werner *et al.* 2007). The function of the polyphosphate may depend on its location within the cell. For example, Werner *et al.* (2007) found polyphosphate would accumulate in the cell wall of *Chlamydomonas reinhardtii*, which they hypothesised was a defence mechanism against toxins or pathogens.

Changes in the polyphosphate concentration have been linked to cell division (Miyachi & Miyachi 1961; Baker & Schmidt 1964; Herrmann & Schmidt 1965; Werner *et al.* 2007). Miyachi and Miyachi (1961) identified that the polyphosphate fraction defined by Miyachi as "A" increased in concentration until cell division occurred, after which the concentration was drastically reduced. Similar findings were also observed by Baker and Schmidt (1963) for AISP concentrations in *Chlorella*. This relationship of polyphosphate being linked to the cell cycle has also been observed in bacterial cells (Henry & Crosson 2013; Racki *et al.* 2017).

The main accumulation of polyphosphate in algal cells is believed to be as polyphosphate granules (Harold 1966; Elgavish *et al.* 1980; Bolier *et al.* 1992; Siderius *et al.* 1996; Eixler *et al.* 2006; Markou *et al.* 2014). These polyphosphate granules vary in size from 0.3 to 2 micron

(Bolier *et al.* 1992; Diaz *et al.* 2009). Diaz *et al.* (2009) further examined the phosphorus content of polyphosphate granules in the *Chlamydomonas* and *Chlorella* algal species. They found the average phosphorus content of polyphosphate granules for both species was 7±2 (µgP/cm^2 of granule) which was twice the phosphorus content of the remaining cell (3±1 µgP/cm^2 of cell) (Diaz *et al.* 2009). Granular polyphosphates are typically found in the vacuoles of the cells (Smith 1966; Solovchenko *et al.* 2016). These are sometimes referred to as acidocalcisomes due to their high calcium concentrations (Ruiz *et al.* 2001; Kulaev *et al.* 2004), with molar ratios of P:Ca of around 8±2 (Diaz *et al.* 2009). While this calcium may only be included to counteract osmotic disturbances (Harold 1966; Bental *et al.* 1990; Leitao *et al.* 1995), it is also possible that the incorporation of calcium is used to regulate the calcium concentration and control signalling processes (Siderius *et al.* 1996). The polyphosphate granules can also contain cations other than calcium, such as potassium, magnesium, iron, zinc, manganese, and titanium (Lins & Farina 1999; Schonborn *et al.* 2001; Hupfer *et al.* 2008; Diaz *et al.* 2009).

The next step to enhance our understanding of this phosphorus accumulation phenomenon is to examine the effect of environmental and process variables on phosphorus accumulation in algae. To achieve this, section 1.5 will first analyse methods to quantify phosphorus accumulation in algae, before leading into section 1.6 that examines the current understanding of variables that influence phosphorus accumulation in algae.

1.5 Methods to quantify phosphorus accumulation in algae

A method to reliably detect phosphorus accumulation in algae is required before the conditions that affect this phenomenon can be identified. The traditional method found in the literature for achieving this is to measure the phosphorus content of the biomass (%P, gP/gSS), as shown in Equation 1.1 (Krauss 1976; Kaplan *et al.* 1986; Eixler *et al.* 2006; Powell *et al.* 2008; Schmidt *et al.* 2016; Crimp *et al.* 2018):

$$\%P = \frac{(TP - DP)}{SS} \times 100$$

Equation 1.1: Calculating the phosphorus content of the biomass, %P (gP/gSS), multiplied by 100 to change into a percentage. Where: TP = total phosphorus concentration (gP/L), DP = dissolved phosphorus concentration (gP/L), and SS = biomass suspended solids concentration (gSS/L).

The methods to calculate the values of total phosphorus, dissolved phosphorus, and suspended solids have been well researched and can be found in the Standard Methods for the Examination of Water and Wastewater (Rice *et al.* 2017).

This method is suitable for understanding the overall effect of variables on an entire algal culture. However, this method cannot be used to understand the influence of individual algal genera from a mixed WSP culture. The effect of the individual algal genera is important to understand as the conditions required to improve phosphorus accumulation may change depending on the algae present in the WSP. In order to identify this potential effect, a method is required that can quantify phosphorus accumulation in single algal cells from a mixed genus culture. The following techniques have been identified to allow phosphorus accumulation to be quantified in single algal cells:

- Raman microscopy,
- Electron microscopy coupled with energy dispersive X-Ray spectroscopy (EM-EDS), and
- Polyphosphate granule staining coupled with image analysis.

These methods are discussed in the following sections.

1.5.1 Raman microscopy

Raman microscopy is an analytical method that can be used to image and determine the chemical composition of microorganisms (Majed *et al.* 2009; Parab & Tomar 2012). This method is based on inelastic light scattering between a photon and the molecule. In brief, when the photon interacts with the molecule it enters a virtual energy state (Parab & Tomar 2012) or an excited vibrational state (Colthup *et al.* 1990). The return of the photon from the virtual energy state to the ground state results in inelastic scattering. The wavelength and amount of scattered photons will determine the position and intensity of the peaks on the Raman spectrum (Parab & Tomar 2012). The position of the peaks refers to different compounds that can be identified through characteristic peaks. Raman microscopy has benefits for analysing biological systems, such as the easy to identify and relatively weak signal intensity of water which allows for 'wet' samples to be analysed, the non-destructive analysis of the sample, and the relatively low sample preparation (Schuster *et al.* 2000; Majed *et al.* 2012; Parab & Tomar 2012). The preparation required for analysis can be as simple as placing a sample onto a microscope slide and sealing closed to reduce water evaporation during the

analysis (Dementjev & Kostkeviciene 2013), or centrifuging and washing of the biomass followed by fixing to the slide through drying (Schuster *et al.* 2000).

Raman microscopy has been used on bacterial cells to identify and quantify phosphorus molecules including polyphosphate (Majed *et al.* 2009; Majed *et al.* 2012; Parab & Tomar 2012). Majed *et al.* (2009) used Raman microscopy to identify polyphosphate-accumulating organisms from the enhanced biological phosphorus removal (EBPR) process and quantify the intracellular polyphosphate content of the polyphosphate-accumulating organisms. In a Raman spectrum, polyphosphate inclusions appear as peaks at 700 and 1175 cm^{-1} (Majed *et al.* 2009). The peak at 700 cm^{-1} is due to P-O-P bonds, while the peak at 1175 cm^{-1} is due to PO_2^- bonds which are both associated with polyphosphate (Majed & Gu 2010). The intensity of these peaks can be used as a direct measure of the quantity of the compound of interest (Majed *et al.* 2009).

Raman microscopy has been successfully used to quantify compounds in algae, such as carotene, carotenoids, and chlorophyll (Brahma *et al.* 1983; Wood *et al.* 2005; Heraud *et al.* 2006; Parab & Tomar 2012; Dementjev & Kostkeviciene 2013; Wei *et al.* 2014). Polyphosphate has also been quantified in algal cells using Raman microscopy (Moudříková *et al.* 2017). However, when this was attempted within the research group at Massey University, issues with the fluorescence of the algae prevented the detection of polyphosphate (Brown unpublished). Due to this fluorescence issue, Raman microscopy was not used in this thesis for quantifying polyphosphate.

1.5.2 Electron microscopy coupled with energy dispersive X-ray spectroscopy (EM-EDS)

Electron microscopy (EM) can be used to locate and visualise polyphosphate in cells (Majed *et al.* 2012), with polyphosphate granules appearing as electron dense areas (Hupfer *et al.* 2008). In order to quantify the phosphorus concentration in the polyphosphate granules, the electron microscopy needs to be coupled with energy dispersive X-ray spectroscopy (EDS) (Majed *et al.* 2012). X-ray spectroscopy can be used at a single location within the cell or in a mapping mode over a larger area (Hupfer *et al.* 2008). The benefit of this technique is that a large amount of information can be obtained on the abundance of specific elements within the algal cell.

The sample preparation required depends on the desired level of information. To obtain quantifiable EDS outputs, the surface of the analysed sample needs to be flat to prevent

unwanted deflection of the EDS laser. This is achieved by washing the sample, followed by dehydrating, and finally embedding the sample in a resin (Bode *et al.* 1993; Hupfer *et al.* 2008). This resin can then be cut using an ultramicrotome into thin flat sections for analysis (Bode *et al.* 1993; Goldberg *et al.* 2001; Hupfer *et al.* 2008). This cutting of the sample can make it difficult to identify the algae when using a mixed genus culture typical of WSP systems. Detection of polyphosphate in algal cells can be made without the need for the slicing preparation; however, the resulting EDS outputs cannot be used to quantify the amount of phosphorus due to possible deflections of the EDS laser.

Transmission electron microscopy (TEM) coupled with EDS has been used to identify polyphosphate within individual bacterial (Hupfer *et al.* 2008; Majed *et al.* 2012) and algal cells (Diaz *et al.* 2009). The polyphosphate was observed as granules that also contained calcium, potassium, magnesium, iron, zinc, and manganese concentrations (Diaz *et al.* 2009).

As shown by Diaz *et al.* (2009), this method can be used to quantify polyphosphate granules in single algal cells successfully. However, the disadvantages of this method are the increased sample preparation time, and for mixed culture WSP samples, the resulting difficulties in identification of the algae after the sample preparation. Although these disadvantages do not rule out TEM-EDS as a potential analysis tool, its applicability to a mixed genus culture such as those found in WSPs is reduced.

1.5.3 Polyphosphate granule staining coupled with image analysis

Polyphosphate staining has frequently been used in the literature to identify polyphosphate granules in single algal cells. A common stain used for identifying polyphosphate granules in algal cells is the modified Ebel's cytochemical stain (Ebel *et al.* 1958; Bolier *et al.* 1992; Powell *et al.* 2006a; Crimp *et al.* 2018). This stain is applied in two stages. The first stage relies on the substitution of counter-ions located within the granules, such as calcium and potassium, with lead ions. This is then followed by the second stage where the lead ions react with sulphide to form black lead sulphide granules that can be visualised under a light microscope (Bolier *et al.* 1992). A key benefit of this method is that the algal cells maintain their morphology after the staining protocol, allowing for identification of the algae during the microscopy. Furthermore, the staining and microscopy process is relatively fast compared to the other methods discussed, allowing for a larger number of cells to be analysed in the same period.

Once the staining and microscopy have occurred, quantification of the polyphosphate granule content needs to be conducted. This can be achieved through a simple manual ranking of the polyphosphate granules in individual cells, as used by Crimp (2015); however, this approach is subjective and does not give a quantifiable result. Instead, image analysis of the stained algal cells should be used. Image analysis can give a quantitative output for individual algal cells of both the area of the polyphosphate granules and the area of the cell. This image analysis method would need to be specifically developed, however, as the software is currently unavailable for this purpose.

1.5.4 Summary of the methods to quantify phosphorus accumulation in algae

Three methods were compared to identify potential techniques to analyse phosphorus accumulation in single algal cells.

Raman microscopy has been used to quantify polyphosphate in algal cells (Moudříková *et al.* 2017). However, when attempted at Massey University, the fluorescence of the algae prevented detection of polyphosphate (Brown unpublished), and therefore Raman microscopy was not used in this thesis for quantifying polyphosphate.

EM-EDS can be used on WSP algae for polyphosphate quantification. The benefit of this technique is the large amount of information obtained on the abundance of specific elements through the EDS analysis. However, the disadvantages of this method are the increased sample preparation time, and, for mixed genus WSP samples, the resulting difficulties in identifying the algae after the sample preparation. As mentioned, this sample preparation can be reduced if quantification using EDS is not required; however, polyphosphate staining and light microscopy would then give a similar result in a shorter period.

Polyphosphate staining can be coupled with image analysis to allow identification and quantification of polyphosphate granules in individual cells. The benefits of this method are the speed of analysis and the ability to identify the algal genera after sample preparation has occurred. The latter point is of particular importance when analysing a mixed genus culture such as those found in WSPs. The disadvantage of this method is the requirement for image analysis software that would need to be developed for this purpose.

These findings suggest that EM-EDS or polyphosphate staining with image analysis can be used to quantify polyphosphate granules in algal cells. The use of either of these methods would depend on the requirement of the research being undertaken.

1.6 Phosphorus accumulation mechanisms

Phosphorus accumulation in algae is classified by two different mechanisms depending on the phosphorus condition of the algae. The first mechanism occurs when algae accumulate phosphorus after an initial phosphorus starvation period. This phosphorus accumulation is classified as over-compensation (Aitchison & Butt 1973; Stevenson & Stoermer 1982; Chopin *et al.* 1997), overshoot (Cembella *et al.* 1984), or over-plus (Voelz *et al.* 1966; Bolier *et al.* 1992). Over-compensation is unlikely to occur in WSPs due to their typically nutrient-rich conditions (Garcia *et al.* 2000; Ghazy *et al.* 2008; Mburu *et al.* 2013) which would prevent a starvation period from occurring. The second mechanism, however, occurs when algae accumulate phosphorus without any prior starvation period. This phosphorus accumulation is referred to as luxury uptake, and, due to the starvation period not being required, luxury uptake can occur in WSP systems.

This section will review both over-compensation and luxury uptake in algae. While over-compensation is unlikely to occur in WSPs, it is useful to review as some of the effects may be transferable to the luxury uptake mechanism.

1.6.1 Variables influencing over-compensation

Over-compensation occurs when the algae accumulate phosphorus after an initial phosphorus starvation period (Aitchison & Butt 1973; Stevenson & Stoermer 1982; Chopin *et al.* 1997). Phosphorus starvation refers to reducing not only the external phosphorus concentration but also the internal phosphorus content of the algae (Ren *et al.* 2009). This starvation period can have a substantial effect on the amount of phosphorus accumulation possible. For example, algae exposed to a phosphorus pulse after a starvation period had over double the phosphorus accumulation compared to algae exposed to the same phosphorus pulse without a starvation period (Azad & Borchardt 1970; Aitchison & Butt 1973). However, if the starvation period is too long, cellular damage can occur, resulting in reduced phosphorus accumulation (Azad & Borchardt 1970). The length of the starvation period required is dependent on the algal species and environmental factors (Azad & Borchardt 1970).

The algae need to be exposed to a phosphorus pulse after the starvation period for over-compensation to occur. This pulse needs to have a phosphorus concentration above a minimum level. While this minimum level is likely to vary with the algal species studied, the minimum phosphorus concentration for over-compensation to occur in *Chlorella vulgaris* was 1 mgP/L (Aitchison & Butt 1973). The amount of over-compensation increased with a higher

phosphorus concentration in the pulse (Aitchison & Butt 1973; Stevenson & Stoermer 1982; Chopin *et al.* 1997).

Over-compensation can result in an initial growth lag occurring while the phosphorus is being accumulated within the algae (Azad & Borchardt 1970; Nyholm 1978). This lag is proposed to be caused by metabolic shifts from the starved phase into a new exponential growth phase (Healey 1979). The lag phase is species dependent and can vary from less than one day for *Scenedesmus quadricauda* (Healey 1979) and *Chlorella pyrenoidosa* (Nyholm 1978), to four days for *Staurastrum chaetoceras* and *Cosmarium abbreviatum* (Spijkerman & Coesel 1998).

After this initial growth lag has occurred, the amount of phosphorus accumulation is then influenced by the growth rate of the algae. As depicted in Figure 1.2 (cellular use of polyphosphate fractions), a rapid growth rate will use the stored polyphosphate as a phosphorus reservoir to synthesise cellular components such as DNA and phosphoproteins (Aitchison & Butt 1973; Nyholm 1978; Stevenson & Stoermer 1982; Yue *et al.* 2013). Aitchison and Butt (1973) noted that if the growth rate can be limited by a factor other than the phosphorus concentration, storage of polyphosphate can be increased.

The amount of over-compensation possible is closely related to the algal species (Rosemarin 1982; Stevenson & Stoermer 1982; Whitton *et al.* 1991). Smaller algal species with large surface to volume ratios were found to uptake more phosphorus under low phosphorus conditions (Laws 1975; Smith & Kalff 1982; Kooijman *et al.* 1991). However, when a high phosphorus pulse occurred, larger cells could accumulate more phosphorus (Turpin & Harrison 1979; Lean 1984; Suttle *et al.* 1987). Using this relationship to cell size, Suttle *et al.* (1987) found that the average size of the algal cells increased when the concentration of the phosphorus pulse increased.

1.6.2 Variables influencing luxury uptake of phosphorus

Luxury uptake is the accumulation of phosphorus without a prior starvation period. Since a starvation period is not required, luxury uptake is possible in WSPs that are typically nutrient-rich. This phenomenon has indeed been observed in full-scale WSPs where algae have increased their phosphorus content in the biomass from the standard 1% (gP/gSS) up to 3.85% (gP/gSS) (Powell *et al.* 2011a; Crimp *et al.* 2018).

This section will review the current knowledge on variables that influence luxury uptake of phosphorus with an emphasis on WSPs. The leading studies on luxury uptake in WSP

conditions are from Powell and colleagues (Powell *et al.* 2006b; Powell *et al.* 2008; Powell *et al.* 2009; Powell *et al.* 2011a), Schmidt *et al.* (2016) and Crimp *et al.* (2018). As these studies are discussed in detail in the following sections, a summary of the different experimental methods used for each of these studies is given in Table 1.2. It should be noted that the work by Crimp *et al.* (2018) was part of the same Marsden funded project as this PhD.

Table 1.2: Experimental methods used in the key literature on luxury uptake under WSP conditions

Study	Culture	Variables examined	Experimental setup
Powell *et al.* (2006b)	WSP inoculum dominated by the *Scenedesmus* genus	• Phosphorus concentration • Temperature • Light intensity • Diurnal light cycle • Nitrogen concentration	• Laboratory scale batch • Factorial (2^5) experiment looking at 2-way interactions • Analysed phosphorus removal and biomass produced
Powell *et al.* (2008)	WSP inoculum dominated by the *Scenedesmus* genus	• Phosphorus concentration • Temperature • Light intensity	• Laboratory scale continuous • Factorial (2^3) experiment looking at 2-way interactions • Analysed luxury uptake
Powell *et al.* (2009)	WSP inoculum dominated by the *Scenedesmus* genus	• Phosphorus concentration • Temperature • Light intensity	• Laboratory scale batch • Main effects of the variables • Analysed luxury uptake
Powell *et al.* (2011a)	Algae from four different full-scale WSPs	• N/A (Observations of luxury uptake)	• Grab samples from four full-scale WSPs in New Zealand over a year • Variable levels uncontrolled due to the field-based nature of the work • Analysed luxury uptake
Schmidt *et al.* (2016)	*Chlorella vulgaris* and *Chlamydomonas reinhardtii*	• Phosphorus concentration • Temperature • Light intensity	• Laboratory scale batch • Factorial (2^3) experiment looking at 2-way interactions • Analysed luxury uptake
Crimp *et al.* (2018)	Algae from 15 different full-scale WSPs	• Phosphorus concentration • Temperature • Light intensity • pH • Dissolved oxygen (DO) • Biomass concentration • Rainfall • Algal genus	• Grab samples from 15 full-scale WSPs across New Zealand over a year • Variable levels uncontrolled due to the field-based nature of the work • Analysed luxury uptake and polyphosphate granules

1.6.2.1 Phosphorus concentration

The phosphorus concentration has been found to influence luxury uptake in full-scale WSPs (Crimp *et al.* 2018), lakes (Selig *et al.* 2006), and saline algae (Sforza *et al.* 2018), where the minimum phosphorus concentration to trigger luxury uptake was dependent on the algal species present (Selig *et al.* 2006). Further work on the effect of changing the phosphorus concentration on luxury uptake under WSP conditions has been summarised in Table 1.3.

Table 1.3: The effect of increasing the phosphorus concentration on luxury uptake in WSP algae. "N/A" refers to unavailable data, and "not significant" is the result of a p-value greater than 0.1 suggesting less than 90% confidence.

Phosphorus concentration	Acid soluble polyphosphate (ASP)	Acid-insoluble polyphosphate (AISP)	Luxury uptake (gP/gSS)	Source
5 to 15 mg P/L	Not significant	Not significant	Not significant	(Powell *et al.* 2008)
5 to 30 mg P/L	Positive	Positive	Positive	(Powell *et al.* 2009)
7.5 to 15 mg P/L	N/A	N/A	Positive (95% confidence)	(Schmidt *et al.* 2016)
Variable WSP concentrations	N/A	N/A	Positive (95% confidence)	(Crimp *et al.* 2018)

As shown in Table 1.3, Powell *et al.* (2009), Schmidt *et al.* (2016), and Crimp *et al.* (2018) all found increasing the phosphorus concentration increased luxury uptake, with Powell *et al.* (2009) finding both ASP and AISP concentrations increased. While Powell *et al.* (2008) found the phosphorus concentration had no main effect on luxury uptake, they did find interactions of phosphorus concentration with both light intensity and temperature to be significant. The fact that these interactions observed by Powell *et al.* (2008) were significant indicates that the phosphorus concentration is still an important variable to consider, which agrees with the other studies shown in Table 1.3. The effects of these interactions on luxury uptake in WSPs are shown in Table 1.4.

Table 1.4: Effect on luxury uptake of interactions involving the phosphorus concentration

Interactions involving the phosphorus concentration	Powell *et al.* (2008)	Schmidt *et al.* (2016)
Temperature	Negative (90% confidence)	Negative (90% confidence)
Light intensity	Positive (95% confidence)	Not significant

As shown in Table 1.4, both Powell *et al.* (2008) and Schmidt *et al.* (2016) found a negative interaction effect between the phosphorus concentration and the temperature. This suggests

that, if the phosphorus concentration is high ('high' depends on the values tested in these studies), increasing the temperature would have a negative effect on luxury uptake. Schmidt *et al.* (2016) propose this is due to an increased growth rate at higher temperatures.

Interestingly, only Powell *et al.* (2008) found the interaction between phosphorus concentration and light intensity to be significant. The fact that Schmidt *et al.* (2016) did not identify an interaction between the phosphorus concentration and light intensity may be due to the range of light intensities examined. Powell *et al.* (2008) studied light intensities over a range of 90 $\mu E/m^2.s$ (60 to 150 $\mu E/m^2.s$), whereas Schmidt *et al.* (2016) only covered a range of 50 $\mu E/m^2.s$ (100 to 150 $\mu E/m^2.s$).

These interactions agree with previous findings based on natural systems that suggest that the phosphorus concentration alone does not trigger luxury uptake, but instead, it is influenced by a combination of variables such as phosphorus concentration, temperature, and light (Selig *et al.* 2006).

1.6.2.2 Nitrogen concentration

The effect of the nitrogen concentration on phosphorus uptake has been studied in both eutrophic lakes (Jones 1990) and WSP systems (Powell *et al.* 2006b). Initial work by Jones (1990) using a eutrophic lake found increasing the nitrogen concentration by 200 mgN/L did not affect algal phosphorus uptake, suggesting the nitrogen concentration was not limiting at the lowest levels tested. Further studies by Powell *et al.* (2006b) under typical WSP nitrogen concentrations (35 to 70 mgN/L) also found no effect on phosphorus removal or algal biomass production. This finding suggests that the nitrogen concentration at typical WSP levels does not affect algal luxury uptake.

1.6.2.3 Organic load

The organic load varies within a WSP series, with primary WSPs having higher organic loading than secondary WSPs. Although the algal genera vary between WSP systems, common algal genera present in WSPs have been identified as mixotrophic (Pollingher & Berman 1975; Bouarab *et al.* 2004; Perez-Garcia *et al.* 2011; Zhao *et al.* 2013), suggesting the algae will undergo respiration and utilise the organic carbon for energy. This energy is known to increase algal growth, which in turn can improve the phosphorus removal (Perez-Garcia *et al.* 2011; Zhao *et al.* 2013); however, the effect on luxury uptake was not examined in these studies.

The effect of organic load on luxury uptake under conditions for biofuel production was studied by Qu *et al.* (2008). They observed that the introduction of glucose to a *Chlorella* culture had a negative effect on luxury uptake. Although this effect has not yet been studied under WSP conditions, the findings by Qu *et al.* (2008) suggest that the organic load should be considered as a potential variable for influencing luxury uptake under WSP conditions.

1.6.2.4 Cation concentration

Cations such as calcium, magnesium, potassium, iron, zinc, and manganese have been consistently identified in polyphosphate granules that occur during luxury uptake in algae (Diaz *et al.* 2009) and bacteria (Lins & Farina 1999; Schonborn *et al.* 2001; Hupfer *et al.* 2008). These cations are suggested to be included to counteract osmotic disturbances of the polyphosphate (Harold 1966; Bental *et al.* 1990; Leitao *et al.* 1995); however, other reasons are possible as discussed in section 1.4. If these cations are included in polyphosphate granules to counteract the osmotic disturbance, it is then also possible that if these cations are limiting in the wastewater, luxury uptake could be reduced.

The influence of the cation concentration on luxury uptake has been studied in algae from the eutrophic Lake Michigan. Schelske and Sickogoad (1990) found that at a phosphorus concentration of 8 µgP/L, increasing the concentration of the cations: cobalt (1 to 10µg/L), manganese (1 to 10µg/L), zinc (5 to 50µg/L), and iron (10 to 100µg/L), increased luxury uptake in algae. No effect of cation addition was observed when the phosphorus concentration was reduced to 2 µgP/L (Schelske & Sickogoad 1990). This suggests a possible positive interaction between the phosphorus concentration and the cation concentration. Since this work is currently limited to one study on a eutrophic lake, further research is required to identify if an effect of cation concentration on luxury uptake under WSP conditions is also observed.

1.6.2.5 Temperature

Temperature can influence both growth and biological phosphorus removal in algal systems (Powell *et al.* 2006b; Wu *et al.* 2013). The effect of the temperature on luxury uptake under WSP conditions has been summarised in Table 1.5.

Table 1.5: The effect of increasing the temperature on luxury uptake in WSP algae. "N/A" refers to unavailable data, "not significant" is the result of a p-value greater than 0.1 suggesting less than 90% confidence, [a] inferred from effects on both ASP and AISP

Temperature	Acid soluble polyphosphate (ASP)	Acid-insoluble polyphosphate (AISP)	Luxury uptake (gP/gSS)	Source
15 to 25°C	Not significant	Positive (95% confidence)	Positive (95% confidence)	(Powell *et al.* 2008)
15 to 25°C	Not significant	Positive (90% confidence)	Positive [a]	(Powell *et al.* 2009)
10 to 15°C	N/A	N/A	Not significant	(Schmidt *et al.* 2016)
4 to 28°C	N/A	N/A	Not significant (No correlation)	(Crimp *et al.* 2018)

As shown in Table 1.5, increasing the temperature was observed to have a positive effect (Powell *et al.* 2008; Powell *et al.* 2009), and no significant effect (Schmidt *et al.* 2016; Crimp *et al.* 2018) on the luxury uptake. The positive effect on luxury uptake in both Powell papers was due to an increase in AISP concentration, as indicated in Table 1.5, with Powell *et al.* (2009) showing the positive effect was due to a peak in AISP concentration at 25°C that was not present at 15°C. This would explain why no significant effect on luxury uptake was observed by Schmidt *et al.* (2016) who only studied temperatures up to 15°C and would, therefore, have not observed an increase in AISP concentration. The fact that Crimp *et al.* (2018) found temperature did not correlate with luxury uptake in full-scale WSP systems is likely due to the low temporal resolution of their data. In full-scale WSP systems, there is substantial variation in temperature throughout a day/night cycle as well as across different days. Therefore, a grab sample of a single point in time may not represent the actual condition in the pond.

Further research by Powell *et al.* (2008) and Schmidt *et al.* (2016) identified that the effect of temperature is more complex due to interactions with the phosphorus concentration (as previously discussed in section 1.6.2.1) and the light intensity as shown in Table 1.6.

Table 1.6: Effect of interactions of temperature with other variables for luxury uptake of phosphorus

Interactions involving the temperature	Powell *et al.* (2008)	Schmidt *et al.* (2016)
Phosphorus concentration	Negative (90% confidence)	Negative (90% confidence)
Light intensity	Negative (95% confidence)	Not significant

The negative effect of the interaction between temperature and phosphorus concentration (Powell *et al.* 2008; Schmidt *et al.* 2016) suggests that, if the phosphorus concentration is high, increasing the temperature will have a negative effect on luxury uptake, which is opposite to the main effect observed in Table 1.5. Schmidt *et al.* (2016) suggested this is due to increased growth rates at higher temperatures. A similar effect is also observed by Powell *et al.* (2008) for the light intensity and temperature interaction which could be explained by the same reasoning.

1.6.2.6 Light conditions

Algae are photosynthetic organisms; therefore, light can have a significant impact on cellular energy. This can affect growth and phosphorus uptake processes within the cell. Two variables are considered for light conditions: the diurnal light cycle and the light intensity.

The diurnal light cycle refers to the daylight hours available and is dependent on both the geographical location and the season. To understand the effect of the diurnal light cycle on the luxury uptake in WSP conditions, Powell *et al.* (2006b) studied algal growth and algal phosphorus removal under two different diurnal light cycles: New Zealand summer of 15 hours light, 9 hours dark; and New Zealand winter of 9 hours light, 15 hours dark. Powell *et al.* (2006b) found the diurnal light cycle had no main effect on phosphorus removal but had a significant (95% confidence) effect on the biomass concentration due to growth. Effects of light conditions influencing luxury uptake have also been proposed by Selig *et al.* (2006) for algae in eutrophic lakes, although a connection to diurnal light cycle or light intensity specifically was not established.

The light intensity experienced by individual algae within a WSP is dependent on the intensity of the incidence light, the position of the algae within the WSP, and the degree of vertical mixing. This effect is typically represented by Beer's law that describes the exponential decrease of light intensity with depth (Torzillo *et al.* 2003; Zhang *et al.* 2008). The effect of the light intensity on luxury uptake under WSP conditions has been summarised in Table 1.7.

Table 1.7: The effect of increasing the light intensity on luxury uptake in WSP algae. "N/A" refers to unavailable data, "not significant" is the result of a p-value greater than 0.1 suggesting less than 90% confidence, *Effect is only initially positive, [a] inferred from effects on both ASP and AISP, [b] measured above the water surface

Light intensity	Acid soluble polyphosphate (ASP)	Acid-insoluble polyphosphate (AISP)	Luxury uptake (gP/gSS)	Source
60 to 150 $\mu E/m^2.s$	Negative (95% confidence)	Not significant	Negative (95% confidence)	(Powell *et al.* 2008)
60 to 150 $\mu E/m^2.s$	Positive* (90% confidence)	Not significant	Positive [a]	(Powell *et al.* 2009)
100 to 150 $\mu E/m^2.s$	N/A	N/A	Positive (95% confidence)	(Schmidt *et al.* 2016)
51 to 299[b] W/m^2	N/A	N/A	Not significant (No correlation)	(Crimp *et al.* 2018)

As shown in Table 1.7, the effect of light intensity varies widely throughout the literature, with negative (Powell *et al.* 2008), positive (Powell *et al.* 2009; Schmidt *et al.* 2016), and no significant (Crimp *et al.* 2018) effects being observed. Part of this discrepancy between studies observed in Table 1.7 could be accounted for by the negative interaction between temperature and light intensity observed by Powell *et al.* (2008). This negative interaction suggests that, at low temperatures, increasing the light intensity would have a positive effect on luxury uptake. This interaction agrees with the findings of Schmidt *et al.* (2016), shown in Table 1.7, who found that under cold climate conditions, increasing the light intensity did indeed have a positive effect on luxury uptake. The finding of Crimp *et al.* (2018) that light intensity had no significant effect on luxury uptake in full-scale WSP systems may be due to the low temporal resolution of their data combined with the natural variation in the WSPs, as explained previously for the effect of temperature in section 1.6.2.5.

Interestingly, the AISP concentration was not influenced by the light intensity (Powell *et al.* 2008; Powell *et al.* 2009) suggesting long-term phosphorus storage in algae is not influenced by the light intensity.

1.6.2.7 pH

The pH in WSPs changes with heterotrophic and autotrophic growth, and can be modified with carbon dioxide (CO_2) addition (Park & Craggs 2010). These factors cause the pH in WSPs to vary from below 7 to above 11 (Curtis *et al.* 1992; Mayo & Noike 1996; Davies-Colley *et al.* 1999; Crimp *et al.* 2018). This pH variation can affect the biological and physiochemical processes

occurring in WSP systems, such as the permeability of the membrane and the ionic form of the phosphate (Kuhl 1962).

The concentration of CO_2 in WSPs is often the limiting factor for algal growth (Martinez *et al.* 2000). This limitation can be overcome by artificial addition of CO_2, which has been shown to increase the biomass yield in WSP systems by up to 30% (Park & Craggs 2010; Zhou *et al.* 2012). CO_2 addition can also increase the phosphorus removal in the WSP (Park & Craggs 2010; Zhou *et al.* 2012); however, this is likely a result of the increased growth . The effect on luxury uptake was not identified.

To date, only Crimp *et al.* (2018) has attempted to correlate the effect of pH in full-scale WSPs to luxury uptake. Crimp *et al.* (2018) found that while the pH in full-scale WSPs varied from 6.6 up to 9.8, no correlation to the observed level of luxury uptake could be made. More research is required on the effect of pH under controlled conditions before the pH can be omitted as an influential variable for algal luxury uptake.

1.6.2.8 Dissolved oxygen concentration

The dissolved oxygen concentration in WSPs is related to both heterotrophic and autotrophic growth, with heterotrophs reducing dissolved oxygen through respiration and autotrophs producing dissolved oxygen through photosynthesis. The dissolved oxygen at the surface of facultative WSPs can vary from as low as 0.2 to over 20 mg/L (Crimp *et al.* 2018) or in excess of 200% saturation (Molina *et al.* 2001; Park & Craggs 2010). Dissolved oxygen levels above saturation have been found to reduce algal productivity, with a 25% reduction observed when the dissolved oxygen levels were at 300% saturation (Molina *et al.* 2001).

Crimp *et al.* (2018) attempted to correlate the dissolved oxygen levels in full-scale WSPs to the observed luxury uptake. They found that while the dissolved oxygen levels varied from 0.2 to 20 mg/L, no significant correlation to the luxury uptake could be made.

1.6.2.9 Rainfall

An interesting observation in studies of full-scale WSPs by Crimp *et al.* (2018) was the negative effect on luxury uptake of increased monthly rainfall. Two potential mechanisms for this effect were hypothesised by Crimp *et al.* (2018) to explain this observation. The first mechanism was a dilution of the phosphorus concentration by the increased rainfall, which, as shown in section 1.6.2.1, would likely cause a negative effect on luxury uptake. The second mechanism was a reduction in hydraulic retention time due to the increased flow rate from infiltration.

This reduced hydraulic retention time would increase the washout of biomass, which could trigger the algae to transition towards growth to replace the lost biomass over luxury uptake.

1.6.2.10 Mixing

Mixing is a relatively easy to manipulate process variable in wastewater systems. The amount of mixing in a WSP is influenced by the presence of mechanical aerators, influent momentum, and wind shear. The presence of mixing has been observed to increase algal productivity in both *Scenedesmus obliquus* (Martinez *et al.* 2000) and *Chlorella* (Silva-Benavides & Torzillo 2012), with Weissman *et al.* (1988) observing that once mixing was occurring, variations to the mixing intensity did not affect algal productivity. Phosphorus removal by *Scenedesmus obliquus* was not affected by the presence of mixing; however, the time to achieve phosphorus removal was reduced with mixing (Martinez *et al.* 2000).

There is currently no literature available on the effect of mixing on luxury uptake in WSPs. The closest link was from Crimp *et al.* (2018) who studied the effect of different types of WSP systems. In their work, typical facultative WSPs were compared to HRAPs. The HRAPs studied had a paddlewheel mixer to provide consistent mixing and create a circulating flow pattern. Through this comparison, Crimp *et al.* (2018) identified that HRAPs had significantly lower levels of luxury uptake compared to facultative WSPs. While not stated by Crimp *et al.* (2018), as shown in Table 1.1, the algal genera often differ between HRAP and facultative WSPs. The potentially different algal genera along with the many other differences between HRAPs and facultative WSPs (i.e. depth, influent conditions, and light experienced by the algae), may explain the differences in HRAPs and WSPs observed by Crimp *et al.* (2018). More research on the effect of mixing on luxury uptake is required to confirm this observation.

1.6.2.11 The prior phosphorus content of the biomass

It is known that phosphorus starvation followed by sudden exposure to phosphorus increases the phosphorus uptake (over-compensation) by algae in natural systems such as lakes (Eixler *et al.* 2006). While algae are unlikely to undergo phosphorus starvation in WSPs due to their typically nutrient-rich conditions, the phosphorus content of the biomass does vary from less than 1% up to 3.8% (gP/gSS) (Powell *et al.* 2011a; Crimp *et al.* 2018). While not currently known, it is possible that the prior phosphorus content of the biomass could affect the future luxury uptake possible, similar to how a starvation period influences over-compensation.

1.6.2.12 Biomass concentration

The algal biomass concentration in a pond is dependent on a multitude of factors, including environmental variables such as light intensity and pH, or process variables such as WSP depth and biomass recycling. A preliminary study by Crimp *et al.* (2018) attempted to correlate the luxury uptake observed in full-scale WSPs to the biomass concentration. Although the biomass concentration varied from 28 to 687 mgVSS/L (average of 114 mgVSS/L), no correlation to the level of luxury uptake was observed (Crimp *et al.* 2018). This is different to Powell *et al.* (2011a) who observed, through simple observations of full-scale WSPs, that high biomass concentrations typically resulted in low levels of luxury uptake.

1.6.2.13 Algal genus

The algal genus is known to affect phosphorus removal and growth rates of algae (Ruiz-Marin *et al.* 2010; Su *et al.* 2012). In order to identify if the occurrence of luxury uptake in WSPs also differs between algal genera, the frequency of polyphosphate granule accumulation was studied by Crimp *et al.* (2018) for 17 algal genera in full-scale WSP systems. Through their work, it was identified that all 17 algal genera (shown in Table 1.8) could accumulate polyphosphate granules under typical WSP conditions. Table 1.8 shows that polyphosphate granule accumulation is widespread among all WSP algae. Furthermore, the frequency of observed polyphosphate granules differed between the algal genera, indicating the conditions that cause this phenomenon may vary between algal genera. Unfortunately, this work by Crimp *et al.* (2018) was unable to identify the variables responsible for polyphosphate granule accumulation in the specific algal genera. Further work should, therefore, be conducted to identify the variables that influence this phenomenon in specific algal genera.

Table 1.8: The ability of algal genera typically found in New Zealand WSPs to accumulate polyphosphate granules. *Microcystis is a cyanobacterium. *Chlamydomonas/Cryptomonas* and *Micractinium/Microcystis could not be differentiated and were therefore grouped. Adapted from Crimp *et al.* (2018).**

Algal genera	The frequency of observed polyphosphate granules
Actinastrum	46%
Chlamydomonas/Cryptomonas	68%
Closterium	65%
Crucigeniella	65%
Cyclotella	17%
Elakatothrix	50%
Euglena	73%
Kirchneriella	14%
*Micractinium/Microcystis**	50%
Monoraphidium	37%
Oocystis	41%
Pandorina	50%
Pediastrum	82%
Phacus	53%
Scenedesmus	73%
Schroederia	79%
Tetraedron	30%

1.7 Summary

Algal phosphorus removal and growth in WSPs has been frequently studied in the literature; however, few researchers have examined the conditions that influence phosphorus accumulation in WSP algae. The current understanding of phosphorus accumulation in WSP algae has been summarised in Table 1.9, which shows only a few variables are known to have a significant effect. Furthermore, while it was recently shown that most algal genera in WSPs can accumulate polyphosphate granules, the conditions that influence this accumulation for individual algal genera are still unknown. In order to move this phosphorus accumulation phenomenon from an interesting observation towards a new algal-based phosphorus removal process, an improved understanding of the variables responsible for phosphorus accumulation and the effect of individual algal genera within the WSP is required.

Table 1.9: The effect of key variables on luxury uptake in algae. [1] Effect is putative as it has not been studied under WSP conditions, [2] Effect on luxury uptake was estimated based on growth and phosphorus removal data

Variable	Effect on growth	Effect on biological phosphorus removal	Effect on luxury uptake (gP/gSS)
Phosphorus concentration	Not significant (Powell *et al.* 2006b)	Positive (Powell *et al.* 2006b)	Positive @ 5 to 30 mgP/L (Powell *et al.* 2009; Schmidt *et al.* 2016; Crimp *et al.* 2018)
Nitrogen concentration	Not significant (Powell *et al.* 2006b)	Not significant (Powell *et al.* 2006b)	Not significant @ 35 to 70 mgN/L (Jones 1990; Powell *et al.* 2006b)
Organic load	Positive (Perez-Garcia *et al.* 2011; Zhao *et al.* 2013)	Positive (Perez-Garcia *et al.* 2011; Zhao *et al.* 2013)	Negative for biofuel[1] @ 5 to 43 gCOD/L (Qu *et al.* 2008)
Cation concentration	Unknown	Unknown	Positive for lakes[1] @ variable levels (Schelske & Sickogoad 1990)
Temperature	Significant (Powell *et al.* 2006b; Wu *et al.* 2013)	Significant (Powell *et al.* 2006b; Wu *et al.* 2013)	Positive @ 15 to 25°C (Powell *et al.* 2008; Powell *et al.* 2009) Not significant @ 10 to 15°C (Schmidt *et al.* 2016) No correlation @ 4 to 28°C (Crimp *et al.* 2018)
Diurnal light cycle	Significant (Powell *et al.* 2006b)	Not significant (Powell *et al.* 2006b)	Significant [2] @ variable levels (Powell *et al.* 2006b)
Light intensity	Significant (Powell *et al.* 2006b)	Significant (Powell *et al.* 2006b)	Positive @ 60 to 150 µE/m^2.s (Powell *et al.* 2009; Schmidt *et al.* 2016) Negative @ 60 to 150 µE/m^2.s (Powell *et al.* 2008) No correlation @ 51 to 299 W/m^2 (Crimp *et al.* 2018)
pH	Negative (Park & Craggs 2010; Zhou *et al.* 2012)	Unknown	No correlation @ pH of 6.6 to 9.8 (Crimp *et al.* 2018)
Dissolved oxygen	Negative [1] (Molina *et al.* 2001)	Unknown	No correlation @ 0.2 to 20 mgDO/L (Crimp *et al.* 2018)
Rainfall	Unknown	Unknown	Negative @10 to 328 mm rainfall (Crimp *et al.* 2018)
Mixing	Positive (Martinez *et al.* 2000)	Positive (Martinez *et al.* 2000)	Unknown
The prior phosphorus content of the biomass	Unknown	Unknown	Unknown for luxury uptake Positive for over-compensation[1] (Azad & Borchardt 1970; Aitchison & Butt 1973)
Biomass concentration	Unknown	Positive (Lau *et al.* 1995)	No correlation @ 28 to 687 mgVSS/L (Crimp *et al.* 2018)
Algal genus	Significant (Ruiz-Marin *et al.* 2010; Su *et al.* 2012)	Significant (Ruiz-Marin *et al.* 2010; Su *et al.* 2012)	Significant (Crimp *et al.* 2018)

Chapter 2
Screening of variables

Preface

The first objective of this thesis was to "screen for environmental and process variables that influence the phosphorus content of WSP biomass". Through the literature review in Chapter 1, variables with a potential to have an effect on phosphorus accumulation under WSP conditions were identified as the organic load, cation concentration, pH, mixing, prior phosphorus content of the biomass, and the biomass concentration. The purpose of this chapter is to screen these potential variables to determine which ones influence the phosphorus content of the WSP biomass and require further investigation in later chapters of this thesis.

This chapter is based on the following publication that has resulted from this PhD research:

Sells, M. D., Brown, N., & Shilton, A. N. (2018). Determining variables that influence the phosphorus content of waste stabilization pond algae. *Water Research, 132*, 301-308. doi:10.1016/j.watres.2018.01.013

Abstract

It is known that WSP algae can accumulate phosphorus within their cells in excess of that needed for cellular function. If phosphorus accumulation could be triggered at the higher range of WSP cell concentrations, phosphorus removal from domestic wastewater could be significantly improved. However, this phenomenon is sporadic and still not fully understood. This chapter examines eight previously untested variables that may influence the phosphorus content of WSP biomass. Although calcium, magnesium, and potassium are key constituents of polyphosphate granules, the concentrations tested were not limiting to phosphorus accumulation. While literature also pointed to the biomass concentration and prior phosphorus accumulation as potentially having an impact, no significance was found in this research. Conversely, three important new variables where identified that significantly (90% confidence) affected the phosphorus content of WSP biomass. An increase in the phosphorus content of the biomass was observed by decreasing the organic load or allowing the pH to increase as compared to pH control. By contrast, the presence of mixing decreased the phosphorus content of the WSP biomass.

2.1 Introduction

Phosphorus accumulation in WSP algae is sporadic, and the conditions that influence the phenomenon are not fully understood. The literature has given some insights into the significant variables for algal phosphorus accumulation in a WSP environment. As previously summarised in Table 1.9 of the literature review, the current knowledge on phosphorus accumulation in WSP algae is limited to only a few variables. While these variables give vital information towards understanding this phenomenon, a multitude of variables remain that have not been considered. To provide a more comprehensive understanding, the effect on phosphorus accumulation of the environmental and process variables: mixing intensity; biomass concentration; organic load; pH; prior phosphorus content of the biomass; and concentration of calcium, magnesium, and potassium cations needs to be examined.

The research in this chapter aims to improve our understanding of phosphorus accumulation in WSP algae by identifying, for the first time, the effect of these new variables on the phosphorus content of the biomass under WSP conditions. While some effects of these variables on algal growth and phosphorus removal have previously been identified (Table 2.1), their link to the phosphorus content of the WSP biomass remains unknown.

Table 2.1: Identification of variables that could potentially influence the phosphorus content of the biomass

Variable	Identification of variables that could potentially influence the phosphorus content of the WSP biomass
Mixing intensity	Mixing is a relatively easy to manipulate process variable that is influenced by the presence of mechanical aerators, influent momentum, and wind shear. Although the mixing intensity is known to affect algal growth and phosphorus removal in WSPs (Martinez *et al.* 2000), its effect on the phosphorus content of WSP biomass is unknown.
Biomass concentration	The biomass concentration is an important variable in WSPs as it can be influenced by environmental variables such as light intensity and pH, or controlled by process variables such as WSP depth and biomass recycling. A preliminary study by Crimp *et al.* (2018) attempted to correlate the biomass concentration to the phosphorus content of the biomass observed in full-scale WSPs; however, no correlation could be made. Further research under controlled laboratory conditions is required to confirm this observation.
Organic load	The organic load varies within a WSP series, with primary WSPs having higher organic loading than secondary WSPs. The organic load is known to affect heterotrophic growth and consequently phosphorus removal (Perez-Garcia et al. 2011; Zhao et al. 2013). While not observed under WSP conditions, the addition of glucose to a *Chlorella* culture had a negative effect on the phosphorus content of the biomass (Qu *et al.* 2008), indicating the organic load should be considered as a potential variable for phosphorus accumulation under WSP conditions.
pH	The pH in WSPs varies with heterotrophic and autotrophic growth, and can be modified with carbon dioxide (CO_2) addition (Park & Craggs 2010). Crimp *et al.* (2018) attempted to link the pH to the phosphorus content of the biomass observed in full-scale WSPs; however, no correlation could be determined. Since pH is known to affect algal growth (Park & Craggs 2010) and phosphorus removal (Cembella et al. 1982), further research is required before pH can be eliminated as a significant variable.
The prior phosphorus content of the biomass	It is known that phosphorus starvation followed by sudden exposure to phosphorus increases the phosphorus uptake (over-compensation) by algae in natural systems such as lakes (Eixler et al. 2006). While algae are unlikely to undergo phosphorus starvation in WSPs due to their typically nutrient-rich conditions, the phosphorus content of the biomass does vary from less than 1% up to 3.8% (gP/gSS) (Powell *et al.* 2011a; Crimp *et al.* 2018). While not currently known, it is possible that the prior phosphorus content of the biomass could affect the future phosphorus accumulation, similar to how a starvation period influences over-compensation.
The concentration of calcium, magnesium, and potassium cations	Cations such as calcium, magnesium, and potassium have been identified in polyphosphate granules that occur during phosphorus accumulation in algae (Diaz et al. 2009). Furthermore, the addition of cations to lakes was previously observed to improve phosphorus accumulation in algae (Schelske & Sickogoad 1990). Before cations can be confirmed as a significant variable for phosphorus accumulation in WSPs, research is required to confirm this observation occurs under WSP conditions that are largely different to lakes.

2.2 Methodology

A two-litre inoculum reactor was started from a facultative WSP at Ashhurst, New Zealand. Collection of the sample was within the algal band (below the surface but no more than 30 cm deep) near the outlet of the secondary pond at Ashhurst. The reactor was mixed using a magnetic stirrer in a constant temperature room at 25 °C. The light source consisted of two fluorescent lights (Philips daylight bulbs 36 W) producing a light intensity of 100 µE/m^2.s (Irradiance sensor: Biospherical Instruments QSL-2101) at the surface of the reactor. 100 µE/m^2.s represents a light intensity on a sunny day below the surface of a full-scale WSP but within the algal band as measured by (Powell *et al.* 2006b) and confirmed in this thesis at Rongotea WSP. Every seven days one litre of culture was removed and replaced with one litre of fresh synthetic wastewater (Davis & Wilcomb 1967), with the composition of the wastewater shown in Appendix 8.2.1. This synthetic wastewater was used as it represents a typical secondary wastewater with chelating chemicals to prevent phosphorus precipitation (Davis & Wilcomb 1967). Apart from sodium citrate that was required as a chelating chemical, no organic carbon was added in order to limit heterotrophic bacterial growth. In order to obtain a consistent inoculum culture for the experimental reactors, the inoculum was maintained in the laboratory under the constant environmental conditions mentioned previously. The consistency of the inoculum culture was checked by microscopic observation at the start and end of the experimental period. Although the inoculum culture originated from a mixed genus WSP culture, it had become dominated by the *Scenedesmus* genus, which remained dominant throughout the experimental period.

The experimental reactors used to test the variables were one litre in volume conical flasks as shown in Figure 2.1. These reactors were given the same conditions as the inoculum reactor described above, and started with 10% inoculum, with the remaining 90% volume comprised of synthetic wastewater (composition is shown in Appendix 8.2.1) unless otherwise stated.

Figure 2.1: Example of the experimental reactors used during the screening experiments.

Eight variables were tested in duplicate at three levels resulting in 48 individual reactors. Each of the 48 reactors was run for seven days and analysed daily for suspended solids using a 0.45μm membrane filter (Lee & Shen 2007) and phosphate concentration using ion chromatography (Dionex ICS-2000) (Powell *et al.* 2008). The seven day experimental time was used as previous work by Powell *et al.* (2009) showed that, for batch cultures, the effect of changing variable levels on the phosphorus content of the biomass would be observed within seven days.

The variable levels can be seen in Table 2.2, with further explanation given in section 2.2.1.

Table 2.2: Variable levels examined

Variable	Units	Low	Medium	High
Organic load	(mgCOD/L)	105	1175	2245
Calcium concentration	(mgCa/L)	15	20	30
Magnesium concentration	(mgMg/L)	4	6	8
Potassium concentration	(mgK/L)	33	49	66
Prior phosphorus content of the biomass	(gP/gSS)	0.2%	1.9%	2.6%
Biomass concentration	(mgSS/L)	22	33	73
pH control	(pH range)	Uncontrolled	8-9	7-8
Mixing intensity	(RPM)	0	100	500

2.2.1 Variable selection

Organic loading

The organic load was manipulated by adding COD in the form of glucose to the reactors to achieve concentrations of 105, 1175, and 2245 mgCOD/L. Glucose was used as the COD source to allow for rapid heterotrophic growth during the batch experiments. An organic load of 105 mgCOD/L was used to limit bacterial heterotrophic growth and represents the wastewater at the end of a WSP series in a tertiary maturation pond; 1175 mgCOD/L is at the high range for standard domestic wastewater (Rani & Dahiya 2008); and 2245 mgCOD/L represents a domestic wastewater with industrial inputs (Carrera *et al.* 2004). In retrospect, the high levels of organic load selected in this work are rather too high as they more representative of the influent concentrations as opposed to within the WSP system.

Concentration of calcium, magnesium and potassium

The concentrations of calcium, magnesium, and potassium cations used in these experiments were based on secondary wastewater characteristics from Davis and Wilcomb (1967). The cation concentrations were modified using calcium hydroxide, magnesium sulphate, or potassium sulphate.

Prior phosphorus content of the biomass

The prior phosphorus content of the biomass was manipulated by changing the wastewater phosphorus concentration of the inoculum. As indicated by the literature (Powell *et al.* 2009; Schmidt *et al.* 2016; Crimp *et al.* 2018), this is expected to give a range of phosphorus contents in the biomass. To manipulate the phosphorus content of the biomass, three separate portions of the original inoculum reactor were fed with the following phosphorus concentrations: 0 mgP/L, 5 mgP/L, and 15 mgP/L. These cultures were maintained for one week before being used as the inoculum for these experiments.

Equation 2.1 was used to determine the phosphorus content of the inoculum reactors:

Equation 2.1: Calculating the phosphorus content of the inoculum reactors

$$\%P\left(\frac{gP}{gSS}\right) = \frac{TP(gP/L) - DP(gP/L)}{SS\ (gSS/L)} \times 100$$

Where: %P is the phosphorus content in the biomass (gP/gSS) multiplied by 100 to change into a percentage, TP is the total phosphorus concentration (gP/L), DP is the dissolved phosphate concentration in the solution (gP/L), and SS is the biomass suspended solids concentration (gSS/L). TP was determined using sulphuric acid-nitric acid digestion with ascorbic acid colourimetry (Rice *et al.* 2017).

Biomass concentration

The biomass concentration in WSPs is dependent on a multitude of factors such as light intensity, pH and biomass recycle. At local WSPs in Rongotea and Halcombe, New Zealand, the biomass concentration was found to vary from 25 to 250 mgSS/L, with an average of 100 mgSS/L. These values are similar to observations found in the literature (Arauzo *et al.* 2000; Furtado *et al.* 2009). Due to these experiments being batch operated, biomass concentrations in the low to average range were used to allow growth to occur in the reactors. In retrospect, higher biomass concentrations could have been used to allow the wider range of levels observed in WSP systems to be studied.

The biomass concentrations used in these experiments were controlled by varying the inoculum biomass concentration. The inoculum biomass concentrations used in the reactors were, on average, 22, 33, and 73 mgSS/L. This was achieved by varying the amount of inoculum culture added. To ensure the same concentration of wastewater components for all reactors, the inoculum was centrifuged (3000 RCF for 5 minutes) and part of the filtrate

removed to produce an inoculum volume of 100 mL (10% reactor volume) for all inoculum biomass concentrations.

Wastewater pH

pH control was achieved using the addition of 5% CO_2 in air with a Thermo Scientific Alpha 190 series pH controller. 5% CO_2 in air represents the typical CO_2 concentrations in combustion flue gas (Arbib *et al.* 2013), which has previously been used in algal-based wastewater treatment (Zhou *et al.* 2012). Due to the direct effect of CO_2 on photosynthesis, a separate experiment with the controlled addition of 10% hydrochloric acid (HCl) was used as an alternative pH control method. Although the volume of HCl used was less than 5% of the reactor volume, corrections to the measurements were applied to account for dilution.

Mixing intensity

The mixing intensity in a WSP is difficult to measure and represent at the laboratory scale, therefore estimates based on the typical flow patterns were used. Circulating flow just suspends the algae in the wastewater, where surface aerators supply rapid localised mixing. At laboratory scale using a 1L conical flask with a magnetic stir bar (length 38.1mm, diameter 9.5 mm), 0 RPM resulted in 'unmixed', 100 RPM 'just suspended' the biomass, and 500 RPM resulted in 'rapid' mixing. The unmixed reactor was briefly stirred immediately prior to taking a sample to ensure it was representative of the entire reactor contents.

2.2.2 Data analysis

Equation 2.2 was used to identify the effect of variables on the phosphorus content of the biomass:

Equation 2.2: Calculating the phosphorus content of the biomass (gP/gSS)

$$Phosphorus\ content of\ the\ biomass\left(\frac{gP}{gSS}\right) = \frac{DP_{(t=0)} - DP_{(t)}}{SS_{(t)} - SS_{(t=0)}} \times 100$$

Where: Phosphorus content of the biomass is the amount of phosphorus removed per amount of biomass produced (gP/gSS) multiplied by 100 to change into a percentage, DP is the dissolved phosphate concentration in the solution (mgP/L), SS is the biomass suspended solids concentration (mgSS/L), and t is the time (days).

An average phosphorus content of the biomass from day 1 to day 7 inclusive was used as the output from the experiments. This will allow for variables with significant effects to be

identified, irrespective of the time the effect occurs. Although it should be noted that the exact effect of the variable cannot be determined using this method. Day 0 was not included as this represents the inoculum conditions rather than the experimental conditions.

A control reactor was used to estimate the experimental error in the phosphorus content of the biomass. The control reactor was 1L in volume, given the same conditions as the inoculum reactor, and started with 10% inoculum, with the remaining 90% volume synthetic wastewater according to Davis and Wilcomb (1967). A new control reactor was operated for each variable examined, resulting in nine replications (one for each of the eight variables examined, with one extra for the two pH control methods). The average phosphorus content of the biomass for these reactors from day 1 to day 7 was compared and found to have a difference of ± 0.21% at 90% confidence. 90% confidence was used at this stage of experimentation to ensure that any potential variable with a significant effect was not removed during these initial screening experiments conducted in this chapter. This is common practice for screening experiments, as stated by Cohen (1992, pg. 156) "*α represents a policy: the maximum risk attending such a rejection… α = 0.01, 0.05, and 0.10, the last for circumstances in which a less rigorous standard for rejection is desired, as, for example, in exploratory studies*". This 90% confidence level is shown on all phosphorus content of the biomass figures (Figure 2.2 to Figure 2.7) as the error bars. A variable is considered significant at 90% confidence if the error bars of the different levels do not overlap.

2.3 Results and discussion

The effects on the phosphorus content of the biomass of the eight variables studied in this research are summarised in Table 2.3 and discussed in more detail in the following sections. The growth and phosphorus removal data used to produce the phosphorus content graphs have been summarised in Table 2.3 and discussed in more detail in Appendix 8.2.2.

Table 2.3: Effect of increasing the studied variable level on the phosphorus content of the biomass, growth, and phosphorus removal. Effects (negative or positive) are significant at 90% confidence. N/A is no significant effect at 90% confidence.

Variable	Figure	Phosphorus content of the biomass	Growth	Phosphorus removal	Appendix
Organic loading	Figure 2.2	Negative	Positive	N/A	8.2.2.1
Calcium concentration	Figure 2.3A	N/A	N/A	N/A	8.2.2.2
Magnesium concentration	Figure 2.3B	N/A	N/A	N/A	8.2.2.2
Potassium concentration	Figure 2.3C	N/A	N/A	N/A	8.2.2.2
Prior phosphorus content of the biomass	Figure 2.4	N/A	N/A	N/A	8.2.2.3
Biomass concentration	Figure 2.5	N/A	Positive	Positive	8.2.2.4
Wastewater pH	Figure 2.6	Positive	Negative	N/A	8.2.2.5
Mixing intensity	Figure 2.7	Negative	Positive	Positive	8.2.2.6

2.3.1 Organic loading

The dominant algal genus in this study was *Scenedesmus*, which is known to be mixotrophic (Pollingher & Berman 1975) allowing utilisation of the organic load for energy. While this energy can be used for many cellular processes, it was hypothesised that increasing the organic loading would cause a reduction in the phosphorus content of the biomass due to increased heterotrophic growth. As shown in Figure 2.2, this hypothesis was confirmed (90% confidence) and increasing the organic loading resulted in about 200 mgSS/L of extra growth, but because the phosphorus content of the biomass also lowered, there was no significant (90% confidence) effect on the phosphorus removal (Appendix 8.2.2.1). This finding agrees

with the literature, where the addition of glucose had a negative effect on the phosphorus content of the biomass in *Chlorella* grown for biofuel production (Qu *et al.* 2008).

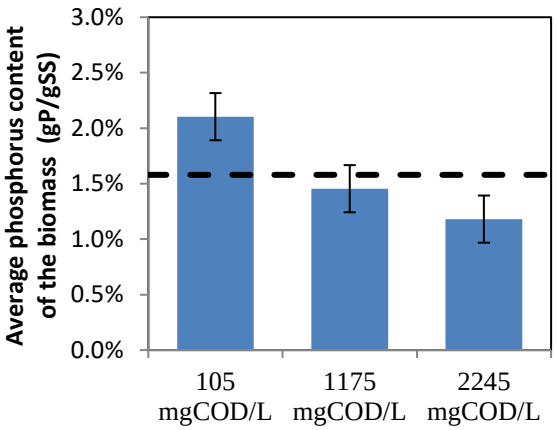

Figure 2.2: Effect of organic load on the average phosphorus content of the biomass. Error bars are 90% confidence intervals. The black dashed horizontal line represents the average of the three levels.

A secondary effect may also be due to changes in the light intensity. Although the light intensity at the surface of the reactor was kept constant, the light attenuation in the reactors would change due to the relationship between light attenuation and biomass concentration (Cornet *et al.* 1994; Cornet *et al.* 1995; Pottier *et al.* 2005; Pruvost *et al.* 2009). Increasing the organic load was observed to increase the biomass concentration by 200 mgSS/L. This would consequently reduce the light received by individual cells, which was previously linked in the literature to a reduction in the phosphorus content of the biomass (Powell *et al.* 2009; Schmidt *et al.* 2016).

It is also possible that the addition of organic load caused bacterial growth to occur. Bacteria typically have a phosphorus content in the biomass of 2% (gP/gSS) (Fagerbakke *et al.* 1996) which is double the typical value of 1% (gP/gSS) for algae (Goldman 1980; Kaplan *et al.* 1986). This suggests the presence of bacteria would shift the phosphorus content of the biomass towards 2% (gP/gSS). However, as seen in Figure 2.2, when the organic load is increased, a reduction in the phosphorus content of the biomass is instead observed.

2.3.2 Concentration of calcium, magnesium and potassium cations

Figure 2.3 shows that changing the concentration of calcium, magnesium, or potassium, within the typical WSP levels tested, had no statistically significant effect on the phosphorus content of the biomass (90% confidence).

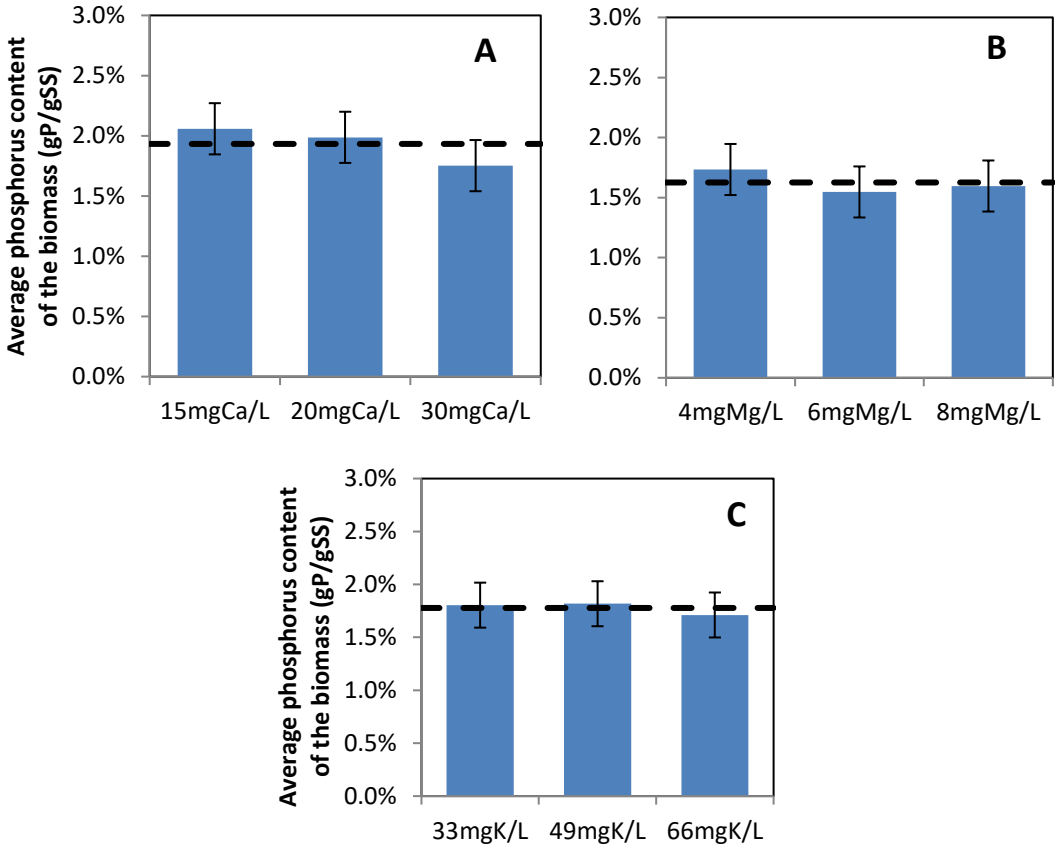

Figure 2.3: Effect of cations calcium (A), magnesium (B), and potassium (C) on the average phosphorus content of the biomass. Error bars are 90% confidence intervals. The black dashed horizontal lines represent the average of the three levels.

This result of no significant effect was unexpected as these cations are key components of polyphosphate granules formed during luxury uptake (Schonborn *et al.* 2001; Diaz *et al.* 2009). For example, under freshwater conditions for both *Chlamydomonas* sp. and *Chlorella* sp., calcium was present within polyphosphate granules at a P:Ca molar ratio of 8±2 (90% confidence) (Diaz *et al.* 2009).

The fact that there was no effect indicates that the concentration of the cations used in these experiments was above the limiting concentration required for polyphosphate granule formation. Analysing calcium, in particular, the P:Ca molar ratios used in this experiment were based on typical secondary wastewater characteristics (Davis & Wilcomb 1967), resulting in P:Ca molar ratios of 0.15 to 0.30 in the wastewater. While this is not the P:Ca ratio in the polyphosphate granules, based on the results from this experiment the typical calcium concentrations in wastewater should not limit polyphosphate granule formation.

Since the concentrations of magnesium and potassium also had no significant effect, it is likely that the typical WSP concentrations of the cations tested are sufficient for polyphosphate granule formation.

2.3.3 Prior phosphorus content of the biomass

The prior phosphorus content of the biomass is an important variable to understand if considering recycling of algal biomass. If the phosphorus content of the biomass has a significant effect, preconditioning of the algae before recycling may be required. However, as shown in Figure 2.4, the prior phosphorus content of the biomass was found to have no significant effect (90% confidence) on the future phosphorus content of the biomass.

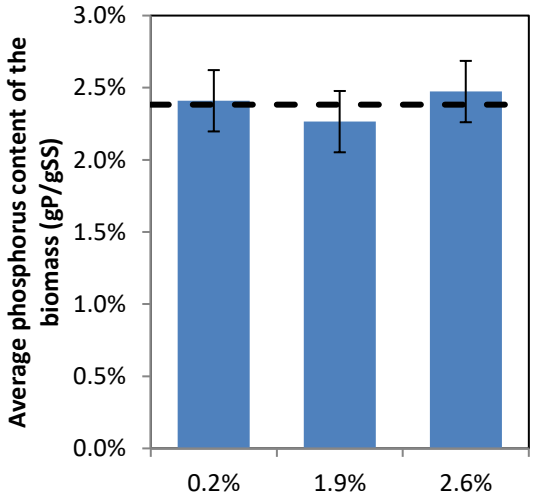

Figure 2.4: Effect of the prior phosphorus content of the biomass (i.e. different levels in the inoculum) on the average phosphorus content of the biomass. Error bars are 90% confidence intervals. The black dashed horizontal line represents the average of the three levels.

This finding agrees with the literature on natural water systems, where it was observed that *Chlorella* exposed to a phosphorus spike without a starvation period, showed either no significant increase (Aitchison & Butt 1973) or a significantly reduced increase in phosphorus accumulation (Eixler *et al.* 2006) compared to phosphorus-starved cells. While the lowest level examined in this experiment of 0.2% suggests phosphorus starvation may have occurred (Goldman 1980; Kaplan *et al.* 1986), the duration of this starvation period may have been insufficient to cause a significant effect on the phosphorus accumulation. Aitchison and Butt (1973) observed that longer starvation periods in *Chlorella* allow for an increased phosphorus content in the biomass after a phosphorus spike. Phosphorus starvation in WSPs is unlikely to occur due to their typically nutrient-rich conditions (Garcia *et al.* 2000; Ghazy *et al.* 2008;

Mburu *et al.* 2013) meaning there is always a reasonable phosphorus concentration available. Therefore, irrespective of any phosphorus starvation effect, the results from this research suggest that the prior phosphorus content of the biomass will not significantly (90% confidence) influence the future phosphorus content in WSP algae.

2.3.4 Biomass concentration

Similar to the prior phosphorus content of the biomass, the biomass concentration is an important variable to understand if considering recycling of algal biomass. It was hypothesised that increasing the biomass concentration would increase cellular competition for phosphorus, resulting in less phosphorus available for individual cells, and a reduction in the phosphorus content of the biomass. However, as shown in Figure 2.5, varying the biomass concentration in the inoculum had no statistical effect on the phosphorus content of the biomass (90% confidence).

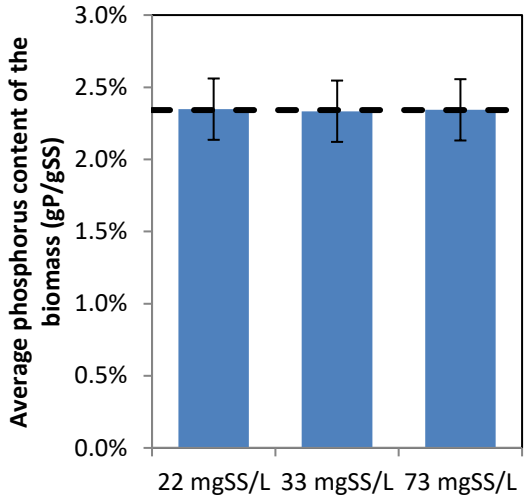

Figure 2.5: Effect of the inoculum biomass concentration on the average phosphorus content of the biomass. Error bars are 90% confidence intervals. The black dashed horizontal line represents the average of the three levels.

This result was unexpected, especially when considering the final biomass concentration in the 73 mgSS/L reactor reached 340 mgSS/L, which is in the high range of suspended solids for WSPs (Arauzo *et al.* 2000; Furtado *et al.* 2009; Crimp *et al.* 2018). This suggests that typical WSP biomass concentrations, as tested in this chapter, will have no effect (90% confidence) on the phosphorus content of the biomass. This is in agreement with the findings of Crimp *et al.* (2018) who found the biomass concentration had no correlation to the phosphorus content of the biomass in full-scale WSP systems.

2.3.5 Wastewater pH

The results from Figure 2.6 show that reducing the pH has a negative effect on the phosphorus content of the WSP biomass. For CO_2 addition (Figure 2.6A) the effect was significant between the uncontrolled and controlled (pH 7-8 and pH 8-9) conditions, whereas for HCl addition (Figure 2.6B) the effect was only significant between the uncontrolled and pH 7-8 controlled conditions (90% confidence).

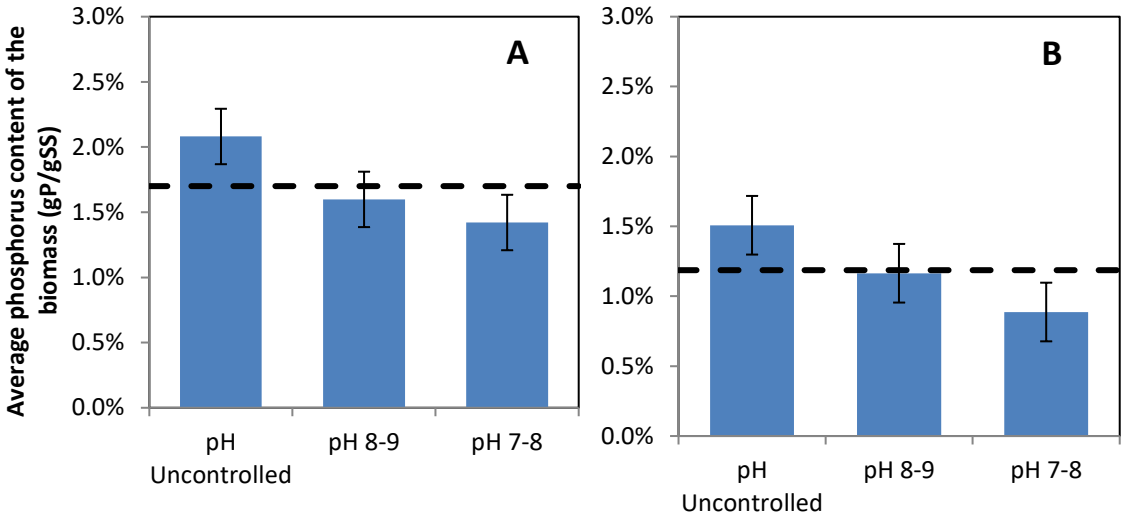

Figure 2.6: Effect of using CO_2 (A) or HCl (B) pH control on the average phosphorus content of the biomass. Error bars are 90% confidence intervals. The black dashed horizontal lines represent the average of the three levels.

This negative effect is likely due to an increased biomass yield when controlling the pH (Appendix 8.2.2.5). Algal photosynthesis consumes aqueous CO_2 from the wastewater. If the wastewater is CO_2 limited, the carbonate equilibrium shifts to replace CO_2 through consumption of carbonate and H^+ ions, causing an increase in pH. This was observed in these experiments with the pH increasing to above 10 in the uncontrolled reactors suggesting CO_2 limitation was occurring.

Using pH control reduced the CO_2 limitation in these experiments either directly through CO_2 dissolution or indirectly through interactions between HCl and the carbonate equilibrium. This allowed for an increased biomass yield of 38% for CO_2 addition and 22% for HCl addition. Similar increases in biomass yields of around 30% have previously been reported for wastewater algae when the pH was controlled to between 7 and 8 with CO_2 addition (Park & Craggs 2010; Zhou *et al.* 2012).

Changes in pH can also influence phosphorus uptake kinetics through changes in membrane permeability and ionic form of phosphate (Cembella *et al.* 1982); however, no effect on

phosphorus removal from the wastewater was observed at the levels tested in this experiment.

2.3.6 Mixing intensity

As seen in Figure 2.7, introducing mixing had a significant negative effect on the phosphorus content of the biomass; however further increasing the mixing beyond a just suspended state had no statistical effect (90% confidence).

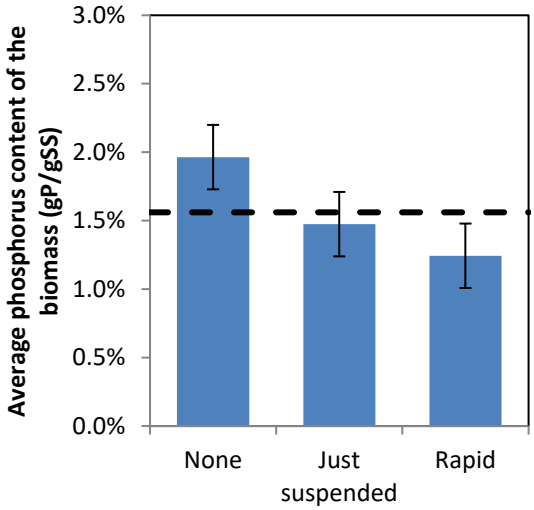

Figure 2.7: Effect of mixing intensity on the average phosphorus content of the biomass. Error bars are 90% confidence intervals. The black dashed horizontal line represents the average of the three levels.

As summarised in Table 2.3 (data shown in Appendix 8.2.2.6), while the biomass concentration and phosphorus removal were increased with mixing, the negative effect on the phosphorus content of the biomass suggests the biomass growth was greater than the increased phosphorus removal. This effect of mixing increasing the biomass concentration has previously been observed in literature (Kim *et al.* 2014; Sutherland *et al.* 2014) and is suggested to be due to improved distribution, and therefore more efficient utilisation, of the light across the cells in the culture (Hadiyanto *et al.* 2013; Sutherland *et al.* 2014). Mixing can also improve phosphorus uptake kinetics through reductions in nutrient gradients and boundary layers (Hadiyanto *et al.* 2013; Sutherland *et al.* 2014). Improved phosphorus removal has previously been observed for *Scenedesmus obliquus* (Martinez *et al.* 2000), *Chlorella vulgaris* (Kim *et al.* 2014) and mixed high rate algal pond cultures (Sutherland *et al.* 2014).

This result shows introducing mixing reduces the phosphorus content in WSP biomass.

2.4 Conclusions

The research presented in this chapter provides an advance in our understanding of phosphorus accumulation in WSP algae by identifying key variables for increasing the phosphorus content of the biomass. Of the eight potentially influential variables studied, only three variables were found to significantly (90% confidence) affect the phosphorus accumulation. The results from this chapter show, for the first time, the phosphorus content in WSP biomass is increased by a reduced organic loading, reduced mixing intensity, or increased pH (90% confidence). These variables should be considered in future work on phosphorus accumulation in WSP algae.

Chapter 3
Variables affecting phosphorus accumulation in a mixed genus WSP biomass

---

Preface

Through the literature review in Chapter 1 and the screening experiments in Chapter 2, six environmental and process variables have been identified that influence the phosphorus content of the biomass under WSP conditions. This chapter now takes these six influential variables and analyses them in batch factorial experiments to identify their effect on phosphorus accumulation in a mixed genus WSP biomass, as well as any interactions between the variables. These variables and interactions are incorporated into a regression equation to predict the conditions required to increase phosphorus accumulation in a mixed genus WSP biomass. This regression equation is then examined using a bench-scale 'luxury uptake' process to identify if the batch findings could be applied to a continuous process, which is more typical of full-scale WSPs. The findings from this chapter will address the second objective of this thesis, which was to "Investigate the conditions that influence phosphorus accumulation in a mixed genus WSP biomass".

This chapter is based on a draft paper that is in preparation for submission to Water Research:

Sells, M.D., Brown, N. and Shilton, A.N. Interactions between environmental and process variables influence phosphorus accumulation in waste stabilisation pond algae. In preparation for *submission to Water Research.*

Abstract

The phosphorus content of WSP algae is known to be influenced by the six variables temperature, phosphorus concentration, light intensity, mixing intensity, organic load, and pH. Furthermore, a few 2-way interactions between some of these variables have previously been identified. The fact that interaction effects have been identified for a limited number of these variables indicates that, in order to move towards the design of a 'luxury uptake' process that increases the phosphorus content of WSP algae, the effects and interactions of all six influential variables needs to be identified. To achieve this understanding, this chapter comprehensively examined the six variables in 40 batch factorial experiments (2^{6-1}) using a mixed genus culture from a full-scale WSP system. Nine variables and interactions had a significant effect on the phosphorus content in the biomass and were incorporated into a regression equation. This regression equation was tested against literature data, where seven out of the eight batch experiments from the literature were successfully predicted.

In order to identify if the batch findings could be applied to a continuous process, which is more typical of full-scale WSPs, a bench-scale novel 'luxury uptake' process was designed, built, and operated under five different scenarios. The regression equation successfully predicted the experimental results for three of the five conditions examined within the 95% confidence bounds (±0.25%). It was theorised that differences in behaviour at the genus level might explain why all five conditions were not successfully predicted.

3.1 Introduction

In order to work towards the development of a new algal-based phosphorus removal process, the conditions to increase phosphorus accumulation in WSP algae needs to be understood. The first step towards this understanding was conducted in Chapter 1 and Chapter 2 by identifying the variables that influence phosphorus accumulation in WSP biomass. Through the literature review in Chapter 1, the variables phosphorus concentration (Powell *et al.* 2009; Schmidt *et al.* 2016; Crimp *et al.* 2018), temperature (Powell *et al.* 2008; Powell *et al.* 2009), and light intensity (Powell *et al.* 2009; Schmidt *et al.* 2016) were identified as influential for phosphorus accumulation in WSP algae. The number of influential variables was then expanded in Chapter 2 with the addition of organic loading, mixing intensity, and pH. These findings gave a good understanding of how the six influential variables behave independently from each other; however, interactions between these variables can also be significant (Powell *et al.* 2008; Schmidt *et al.* 2016), and as a result, need to be considered.

This chapter examines the effects and interactions of these six previously identified variables in a batch factorial experimental design. This will allow a regression equation to be produced to predict the combination of conditions to increase phosphorus accumulation in WSP biomass. These conditions will then be used to design and operate a bench-scale semi-continuous flow 'luxury uptake' process to identify if the batch findings from the factorial experiment could be applied to a continuous process, which is more typical of full-scale WSPs.

3.2 Methodology

The aim of this thesis was to "Elevate phosphorus accumulation in WSP algae". This chapter identifies the conditions to do this in a mixed genus culture, which are then used to inform the design and operation of a 'luxury uptake' process to increase phosphorus accumulation in the biomass. To achieve this, two separate stages of experimentation were used. The first stage is the batch factorial experiments that were conducted to identify the significant variables and interactions that increase the phosphorus content of the biomass. The second stage is the bench-scale semi-continuous flow 'luxury uptake' process that was designed based on stage one findings and used to identify if the regression equation produced from the factorial experiments in stage one could be applied to a continuous process that is more typical of full-scale WSPs

3.2.1 Batch factorial experiment

The following sections describe the methods related to:

1. The inoculum culture used in the reactors,
2. The setup and conditions of the experimental reactors,
3. The analytical methods used to obtain the input numbers required to calculate the phosphorus content of the culture, and
4. The statistical analysis conducted to identify the effects and interactions of the variables.

3.2.1.1 Inoculum

The seed culture was obtained from two field ponds during the experimental period. For the first 20 experiments, the seed culture was obtained from the secondary WSP at Rongotea, New Zealand. This pond has a typical WSP arrangement of a primary facultative pond followed by a secondary facultative pond. After using the Rongotea WSP for the first 20 reactors, unforeseen desludging at the WSP resulted in the removal of the algal biomass. This

desludging made the pond unfeasible for further use, and consequently, a new seed culture was required. Extensive analysis of nine local WSP systems (shown in Appendix 8.3.1) identified the Palmerston North pilot scale WSP, which was originally seeded from Rongotea WSP, as having similar algal genera and phosphorus accumulation response compared to Rongotea WSP. This pilot scale WSP was set up as an HRAP with an oval raceway shape and paddlewheel for mixing and circulation. The Palmerston North WSP was used as the seed culture for the remaining 20 experiments. Statistical analysis of the different seed culture sources showed no significant difference (95% confidence) when comparing the phosphorus content of the biomass (shown in Appendix 8.3.2).

At the start of each experiment, a seed culture was obtained from the field WSPs mentioned previously. The collection was from the middle of the WSP length within the algal band (below the surface but no more than 30 cm deep). The seed culture was centrifuged at 3000 RCF (Pembrey *et al.* 1999) for 15 minutes (microscope observation conducted identified this formed a pallet with live cells and no visual lysis), and then re-suspended in reverse osmosis water to a concentration of 1 gSS/L to produce the inoculum culture. The experimental reactors shown in Table 3.2 were started with 10% inoculum culture, with the remaining 90% volume synthetic wastewater according to Davis and Wilcomb (1967) (recipe shown in Appendix 8.2.1) unless otherwise stated. The most abundant algal genera in the inoculum culture over the entire factorial experiment were: *Scenedesmus* (35%)*, Micractinium/Microcystis* (14%)*, Pediastrum* (8%)*, Monoraphidium* (8%)*, Actinastrum* (6%)*,* and other genera that individually had less than 6% occurrence (30%). The percentage occurrence was determined by manual counting of individual algae (a colony of multiple cells was counted as 1 algae) observed in the inoculum culture at the start of each factorial experiment using a light microscope.

3.2.1.2 Experimental setup

From the literature and Chapter 2, the phosphorus concentration (Powell *et al.* 2009; Schmidt *et al.* 2016; Crimp *et al.* 2018), temperature, light intensity (Powell *et al.* 2009; Schmidt *et al.* 2016), mixing intensity, organic load, and pH (Chapter 2) were identified as influencing the phosphorus content of the biomass. The influence of each of these variables on the phosphorus content of the biomass and any interactions between these variables were analysed in 40 experimental reactors in a 2^{6-1} fractional factorial experiment with eight centre point runs. A summary of the variable levels examined is given in Table 3.1. The full matrix is

shown later in Table 3.2 (page 79) alongside the experimental results to allow easy reference between the results and experimental conditions. Some of these variable levels are slightly different to what was previously used in Chapter 2. In retrospect, the organic load used in Chapter 2 was high compared to a typical WSP system, and therefore was reduced in this chapter to be more reasonable. The "no mixing" level considered in Chapter 2 was removed in this chapter as this is not feasible to achieve in a full-scale WSP.

Table 3.1: Summary of the variable levels examined. The full matrix of experiments is shown in Table 3.2.

Variable	Units	Low level	Centre point	High level
Temperature	(°C)	10	17.5	25
Phosphorus concentration	(mgP/L)	4	9.5	15
Light intensity	($\mu E/m^2.s$)	60	105	150
Mixing intensity	(RPM)	100	300	500
Organic load	(mgCOD/L)	105	455	805
pH	(pH)	7	9	11 (uncontrolled)

The centre point runs were conducted for two reasons. The first reason is they allow identification of any non-linear response occurring between the levels of the variables tested; however, this does not allow the variable responsible for this non-linear response to be identified. The second reason is they allow the reproducibility of the phosphorus content of the biomass to be estimated for all 40 experimental reactors. This is based on the assumption that the difference in phosphorus content of the biomass of the eight centre point reactors would be the same if any other condition was replicated. This use of centre points to estimate the error is common practice in factorial experiments (Bisgaard 1997). The estimation of the error is further quantified in Minitab using observations that are not required in the factorial analysis. Unrequired observations occur when non-significant factors are removed from the regression analysis which can result in replicated non-centre point experimental runs. From all eight centre point reactors, the average phosphorus content of the biomass was 1.17%±0.07% (gP/gSS), showing a low error, and therefore suggesting that the results are reproducible. The error was calculated as a 95% confidence interval using the average phosphorus content of the biomass of the eight centre point reactors. Further details of this analysis are given in Appendix 8.3.2.

The experiments were conducted in batch two-litre Erlenmeyer flasks for seven days inclusive. The reactors were mixed using magnetic stirrers (50 mm stir bars) in a constant temperature

room. The light setup and pH control with CO_2 addition have been described previously in section 2.2. The experimental reactors shown in Table 3.2 were fed with synthetic wastewater according to Davis and Wilcomb (1967) (wastewater recipe is shown in Appendix 8.2.1), with modifications of phosphorus concentration using KH_2PO_4 and organic load using glucose according to the concentrations required by Table 3.2. The synthetic wastewater contained chelating chemicals to prevent phosphorus precipitation at high pH and ensure phosphorus removal was due to biological uptake. Glucose was used as the carbon source as it is readily available to the microorganisms for heterotrophic growth. The reactors were weighed daily and adjusted for evaporation by addition of reverse osmosis water.

3.2.1.3 Analytical methods

Samples of the reactors were taken daily for seven days and analysed for suspended solids using a 0.45µm filter paper (Lee & Shen 2007), total dissolved phosphorus using the filtrate from a 0.45µm filter paper, pH, dissolved oxygen and temperature. Total phosphorus samples were taken on day 0 and day 7 from each reactor. Total phosphorus and total dissolved phosphorus samples were analysed using sulfuric/nitric acid digestion and ascorbic acid colourimetric analysis according to Standard Methods (Rice *et al.* 2017).

Equation 3.1 was used to calculate the phosphorus content of the biomass (%P):

Equation 3.1: Phosphorus content of the biomass (%P) using total dissolved phosphorus

$$\%P\left(\frac{gP}{gSS}\right) = \frac{TP\left(\frac{gP}{L}\right) - TDP\left(\frac{gP}{L}\right)}{SS\left(\frac{gSS}{L}\right)} \times 100$$

Where: %P (gP/gSS) is the phosphorus content of the biomass multiplied by 100 to change into a percentage; TP (gP/L) is the total phosphorus concentration in the reactor sample (includes liquid and solid phosphorus), TDP (gP/L) is the total dissolved phosphorus concentration in the filtrate of the reactor sample; and SS (gSS/L) is the biomass suspended solids concentration.

3.2.1.4 Statistical analysis

Minitab® Statistical Software (Minitab 2010) was used to analyse the significance of the variables and interactions. Depending on the P-value, a variable is considered significant either at the 95% confidence level when the P-value is less than 0.05, or significant at the 90% confidence level when the P-value is between 0.1 and 0.05. Due to potential confounding when using the 2^{6-1} experimental design, only up to two-way interactions were considered in this analysis. Further explanation of this confounding is given in Appendix 8.3.3. The effect of

multicollinearity was assessed using the variance inflation factor (VIF) calculated by Minitab. The VIF for all significant variables and interactions was 1 suggesting no multicollinearity.

Only one value for each of the 40 experiments can be used as the input into the Minitab analysis. As the aim of this thesis is to "Elevate phosphorus accumulation in WSP algae", the maximum phosphorus content of the biomass that was measured from day two to seven was used as the input into the Minitab analysis for each of the 40 reactors. Day zero and one were ignored as they were considered an adjustment period between the field conditions and the experimental conditions.

3.2.2 Semi-continuous flow 'luxury uptake' process

This section describes the semi-continuous flow 'luxury uptake' process that was designed based on the findings of the experiments described above. It should be noted that as this is the first step towards a process to increase the phosphorus content of the biomass, the growth and therefore phosphorus removal have not been optimised in this work. The conditions in the growth stage are instead set by the wastewater concentrations and environmental variables of the luxury uptake stage.

A diagram of the bench-scale 'luxury uptake' process is shown in Figure 3.1 and Figure 3.2, with further description of the process given in Appendix 8.3.4. The luxury uptake stage and the growth stage were each split into three reactors that were connected in series with subsurface pipes to avoid hydraulic short-circuiting. Essentially this was designed to represent a single pond with two internal baffles. Note that in Figure 3.2, two setups of the process are shown. This was done to allow different wastewater concentrations to be tested at the same time.

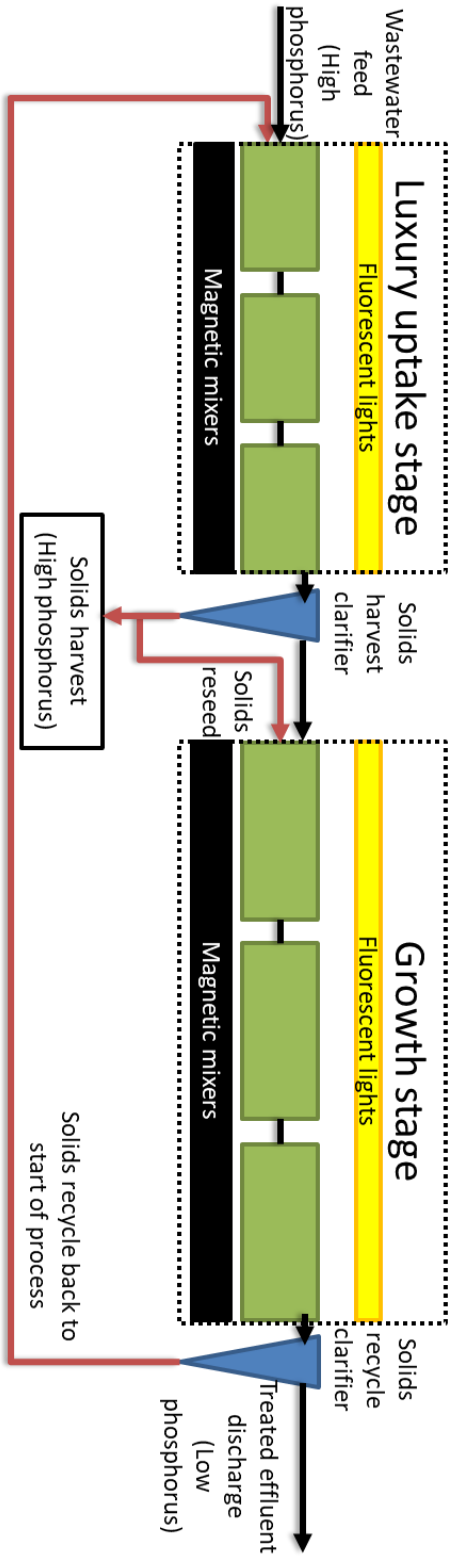

Figure 3.1: Schematic of the bench-scale 'luxury uptake' process design. Black lines represent the flow of the 'liquid' wastewater, and red lines represent the flow of 'solids'. Green rectangles represent reactors. The first three reactors are the luxury uptake stage, and the final three reactors are the growth stage. Solids harvesting occurs in the blue central clarifier. Solids recycle occurs in the final blue clarifier before the treated wastewater is discharged.

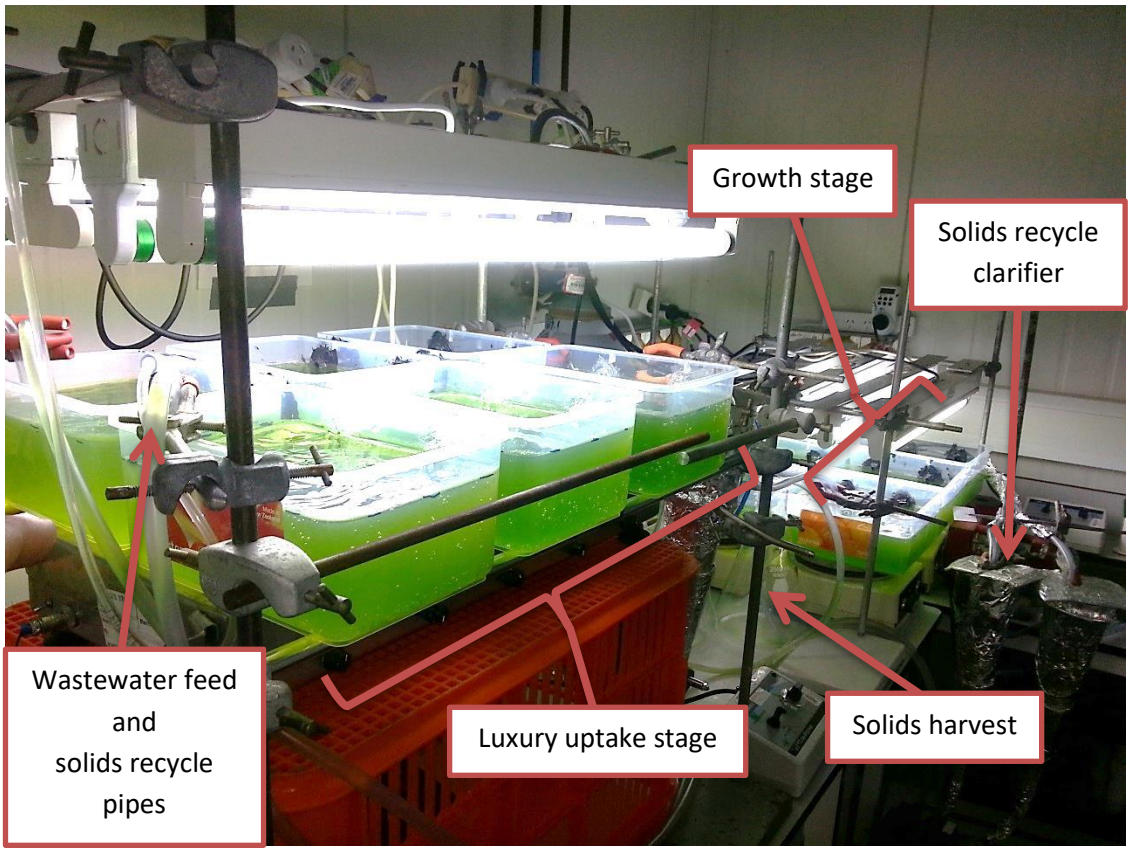

Figure 3.2: The bench-scale 'luxury uptake' process used in experimentation. Two separate experiments are shown, with one set of conditions tested in the front setup, and the second set of conditions tested in the back setup.

The luxury uptake stage reactors were 225 mm (length) by 170 mm (width) by 60 mm (depth) each giving a volume of 2.3L per reactor and a total volume of 7L for the luxury uptake stage. The hydraulic retention time (HRT) in the luxury uptake stage was 3 days. This was based on the time to reach the peak phosphorus content in the biomass from the batch reactors shown in Appendix 8.3.5. The growth stage reactors were 265 mm (length) by 235 mm (width) by 62 mm (depth) giving a volume of 3.9L per reactor and a total volume of 11.7L for the growth stage. The HRT of the growth stage was based on the range of HRT's observed in HRAPs of between 2 to 9 days (Young *et al.* 2017). A midpoint of 5 days was used as the HRT for the growth stage, giving the entire 'luxury uptake' process a total HRT of 8 days.

The HRT of the luxury uptake stage was increased to 5 days for only the third run of the 'luxury uptake' process (Experiment #3 in Table 3.5 shown later in the discussion). This was done to coincide with the peak polyphosphate granule content for the operating conditions, which are identified in Chapter 4 later in this thesis. This resulted in the HRT of the growth stage being increased to 8.4 days as a consequence of the lower feed flowrate.

The sides and bottom of the reactor walls were scraped every 2 to 3 days to re-suspend any attached solids. The inoculum culture used for the 'luxury uptake' process is described in section 2.2. This inoculum culture originated from a mixed genus WSP culture; however, it had become dominated by the *Scenedesmus* genus with no other genera being observed under light microscopy during any of the visual analysis. This *Scenedesmus* dominance was confirmed throughout the experimental period (start and each sampling time) for each of the five 'luxury uptake' process conditions examined. The mixing setup, lighting setup, and synthetic wastewater used in the 'luxury uptake' process have been described previously in section 3.2.1.2. Although water evaporation was not directly accounted for, the relative humidity of the constant temperature room was set to 90% to reduce any potential effects from evaporation.

The 'luxury uptake' process reactors were analysed once a quasi-steady state was reached, which was typically after two months of operation. Quasi-steady state was determined when the phosphorus and biomass concentrations of the luxury uptake stage reactors for two consecutive sampling periods were within 10%. Once quasi-steady state had been reached, the reactors were analysed for pH, dissolved oxygen, temperature, suspended solids, phosphate concentration, total dissolved phosphorus, and total phosphorus as described in section 3.2.1.3. The phosphorus content of the biomass was calculated according to Equation 3.1 also in section 3.2.1.3. The samples were obtained between 2 pm and 6 pm and taken at the midpoint (± 15 minutes) of the semi continuous feed time. A period of at least five days took place before another sampling period occurred.

Table 3.2: The randomised fractional factorial matrix of experiments. Blocking was conducted on the temperature due to only one temperature control room being available at any one time. 'c' in the run order denotes a centre point control experiment.

Run order (#)	Temperature (°C)	Phosphorus concentration (mg P-PO_4/L)	Light intensity (µE/m^2s)	Mixing intensity (RPM)	Organic load (mg COD/L)	CO_2 concentration (pH)
1	10	15	60	100	105	11
2	10	4	60	100	105	7
3	10	4	150	500	805	11
4	10	15	150	100	105	7
5c	17.5	9.5	105	300	455	9
6	25	15	150	100	105	11
7	25	15	60	500	805	7
8	25	4	150	100	105	7
9	25	15	60	100	805	11
10c	17.5	9.5	105	300	455	9
11	10	15	150	100	805	11
12	10	4	150	500	105	7
13	10	4	60	500	105	11
14	10	15	60	100	805	7
15c	17.5	9.5	105	300	455	9
16	10	4	150	100	105	11
17	10	15	150	500	105	11
18	10	4	60	500	805	7
19	10	15	60	500	105	7
20c	17.5	9.5	105	300	455	9
21	25	15	150	500	105	7
22	25	4	150	100	805	11
23	25	4	60	500	805	11
24	25	15	150	100	805	7
25c	17.5	9.5	105	300	455	9
26	10	4	60	100	805	11
27	10	15	60	500	805	11
28	10	15	150	500	805	7
29	10	4	150	100	805	7
30c	17.5	9.5	105	300	455	9
31	25	15	60	100	105	7
32	25	15	150	500	805	11
33	25	4	60	100	105	11
34	25	4	60	100	805	7
35c	17.5	9.5	105	300	455	9
36	25	4	60	500	105	7
37	25	4	150	500	105	11
38	25	15	60	500	105	11
39	25	4	150	500	805	7
40c	17.5	9.5	105	300	455	9

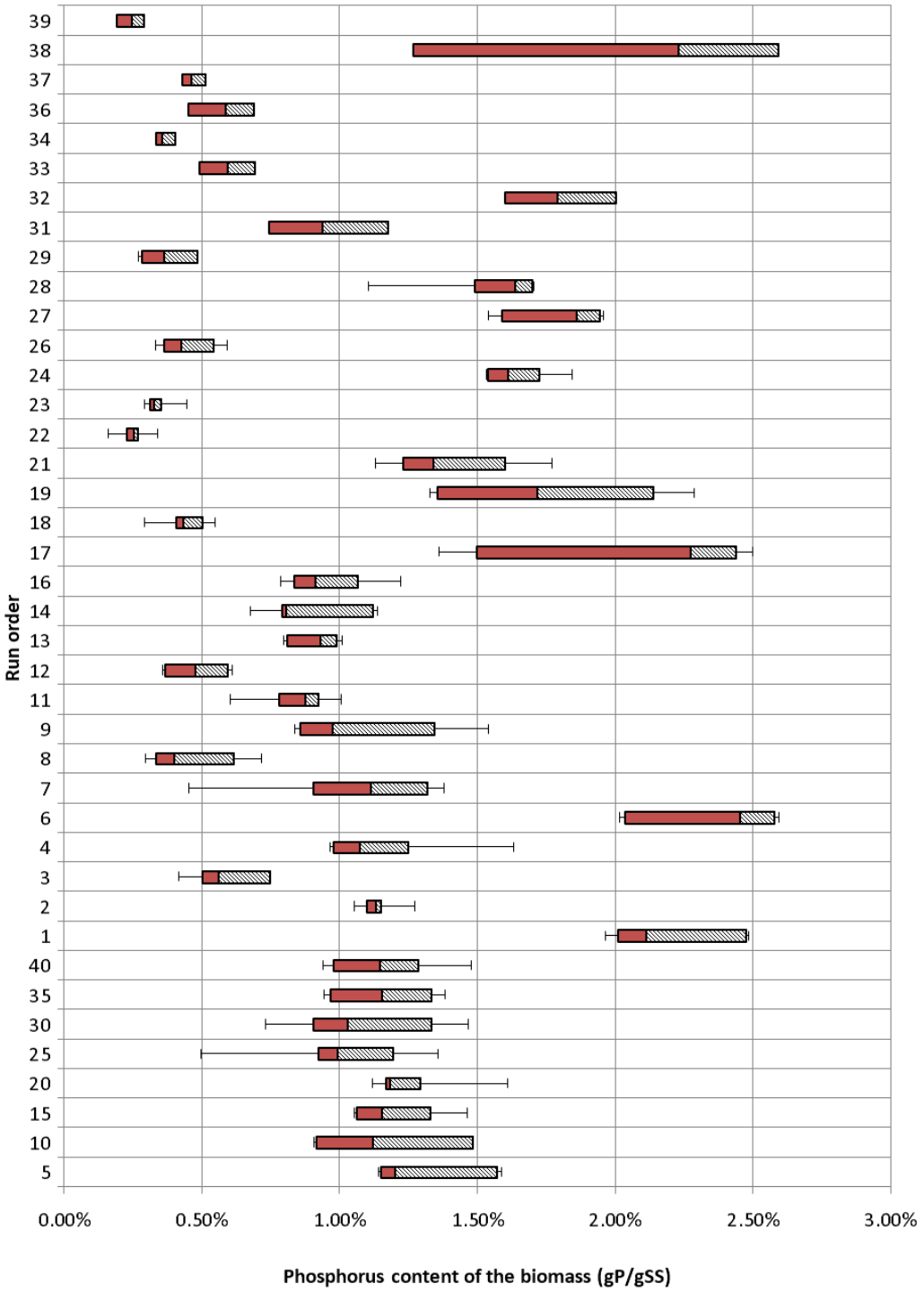

Figure 3.3: Range of phosphorus contents of the biomass achieved in the 40 factorial experiments from day 2 to 7 inclusive. Run order refers to the reactors and conditions described in Table 3.2. The eight centre point reactors have been grouped at the bottom of the figure. The error bar on the right represents the maximum value, the right of the diagonal line box represents the 3rd quartile, the line between the diagonal line box and red box is the median, the left of the solid red box represents the 2nd quartile, and the error bar on the left represents the minimum value.

3.3 Results and discussion

This section first discusses the results of the factorial experiment conducted to identify the combination of conditions to increase the phosphorus content of the WSP biomass (3.3.1). These conditions were used to propose implications for WSP system design and operation (3.3.2), which were then used to design and operate a bench-scale semi-continuous flow 'luxury uptake' process to examine the prediction capability of the batch findings (3.3.3).

3.3.1 Identification of significant variables and interactions

The range of phosphorus contents in the biomass from day 2 to 7 are shown in Figure 3.3 for all 40 experimental reactors. As can be seen in Figure 3.3, the phosphorus contents of the biomass varied from a minimum of 0.2% (gP/gSS) to a maximum of 2.7% (gP/gSS) with an average across all 40 reactors of 1.1% (gP/gSS). In order to identify the conditions that increase the phosphorus content of the WSP biomass, the effects and interactions of the six variables need first to be understood. This was investigated by analysing the phosphorus content of the biomass from all 40 batch factorial experiments, with the significant effects and interactions of the variables summarised in Table 3.3. Coded effects are shown in Table 3.3 to allow a direct comparison between the effects of the variables and interactions. Coded effects refer to +1 being used for the variables high level, and -1 being used for the variables low level. For example, the phosphorus concentration levels would change from 15 mgP/L to +1, and 4 mgP/L to -1. This coding of the variable levels is automatically done when designing a factorial experiment in the statistical software Minitab.

Of the 21 variables and interactions studied, Table 3.3 summarises the nine that had a significant (≥90% confidence) effect on the phosphorus content of the biomass at the levels tested. While no significant main effect of mixing intensity (p-value of 0.198) and light intensity (p-value of 0.451) were observed, the significant interactions involving these variables indicate that they still influence the phosphorus content of the biomass. The coded effects in Table 3.3 show that, at the range of levels tested, the phosphorus concentration of the wastewater had the largest effect on the phosphorus content of the biomass, with an effect of +1.21% (gP/gSS). This is followed next by the organic load with an effect of -0.42% (gP/gSS). The remaining significant variables shown in Table 3.3 have effects between ±0.25% (gP/gSS).

Table 3.3: Coded effects of the significant variables and interactions on the maximum phosphorus content of the biomass observed over days 2 to 7. * Denotes an interaction between variables, and N/A is not applicable as the variable is not significant.

	Variable	Standardised effect	P-value	Significance
Main effects	**Phosphorus concentration**	1.21%	0.000	95%
	Organic load	-0.42%	0.000	95%
	Mixing intensity	N/A	0.198	N/A
	pH	0.24%	0.011	95%
	Temperature	-0.15%	0.088	90%
	Light intensity	N/A	0.451	N/A
2 way interactions	**Phosphorus Concentration * Mixing Intensity**	0.20%	0.028	95%
	Phosphorus Concentration * pH	0.20%	0.031	95%
	Phosphorus Concentration * Temperature	0.17%	0.066	90%
	Organic Load * pH	-0.20%	0.028	95%
	Temperature * Light Intensity	0.15%	0.097	90%

A regression equation was produced to incorporate the effects of the variables and interactions from Table 3.3. This regression equation (Equation 3.2) can be used to identify the combination of variable levels that increase the phosphorus content in the biomass. This regression equation uses the 'uncoded' or 'true' values of the variables. For example, using the phosphorus concentration variable, the true value of 15 mgP/L, 4 mgP/L or any other actual phosphorus concentration should be used as the input into Equation 3.2.

Equation 3.2: Regression equation produced to predict the maximum phosphorus content in the biomass over days 2 to 7, %P (gP/gSS), as a percentage. T = temperature (°C), P = phosphorus concentration (mgP/L), L = light intensity (µE/m².s), M = mixing intensity (RPM), C = organic load (mgCOD/L), and pH = pH. '×' refers to an interaction effect between the variables. Note: the input value of the variables should be their initial value from day 0.

$$Phosphorus\ content\ of\ the\ biomass = \%P\left(\frac{gP}{gSS}\right)$$
$$= 1.405 - 0.0341(P) - 0.0006(M) + 0.0248(pH) + 0.0007(C)$$
$$- 0.0527(T) - 0.0046(L) + 0.0001(P \times M) + 0.0090(P \times pH)$$
$$+ 0.0020(P \times T) - 0.0001(pH \times C) + 0.0002(T \times L)$$

The adjusted R^2 and prediction R^2 of Equation 3.2 were calculated in Minitab to be 86% and 76% respectively, suggesting the linear regression is a good fit to the data. The prediction R^2 is

calculated in Minitab by removing one of the 40 experimental observations, calculating a new regression equation, then determining how well the new regression equation predicts the removed experimental observation. A high prediction R^2, such as the one observed here, suggests Equation 3.2 should have a reasonable prediction capability for new observations outside of the 40 experimental reactors. Analysis of the residuals in appendix 8.3.6 suggests the assumption of normal distribution of the residuals is correct. It should be noted; however, that curvature in Equation 3.2 was significant at the 90% confidence level. This suggests that one or more of the variables has a non-linear relationship with the phosphorus content of the biomass when changing the value of the variable, and caution should be used if applying this regression equation with values outside of the range tested.

To provide independent validation of the prediction capability of Equation 3.2, experimental data was obtained from Schmidt *et al.* (2016) (Nova Scotia, Canada) and used to compare to the predicted values obtained using Equation 3.2. Their work was used for comparison as it was also conducted on luxury uptake in WSPs under batch conditions. The comparison is shown in Figure 3.4.

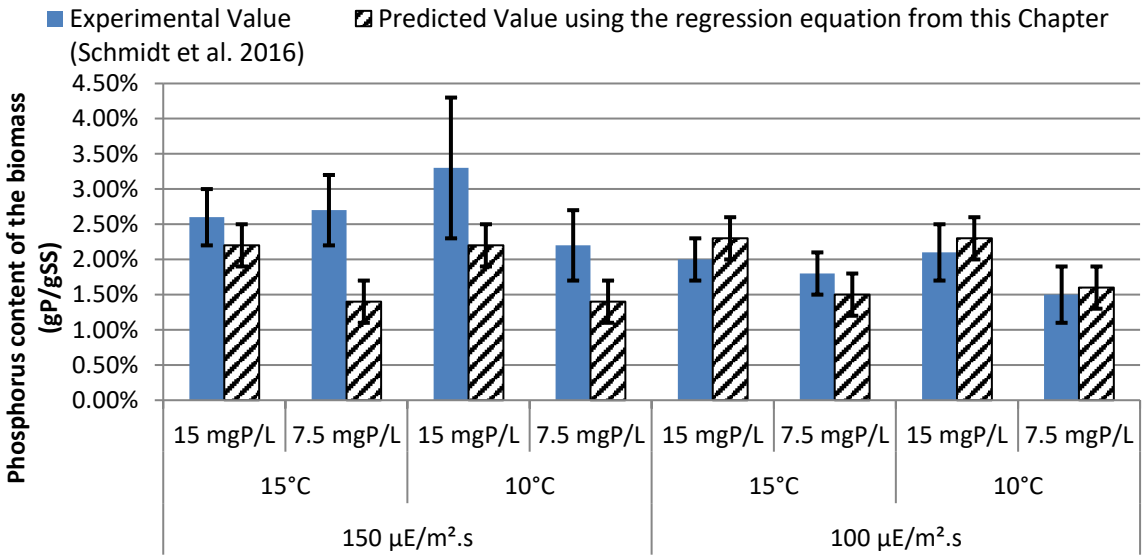

Figure 3.4: Comparison between the phosphorus content of the biomass observed by Schmidt *et al.* (2016) and that predicted by Equation 3.2. Error bars are 95% confidence intervals.

Figure 3.4 shows that Equation 3.2 successfully predicted the phosphorus content of the biomass in seven out of the eight conditions studied by Schmidt *et al.* (2016). Only one set of conditions (150 µE/m^2.s, 15°C, and 7.5 mgP/L) was not successfully predicted, which may be due to the non-linearity in Equation 3.2 as previously mentioned. Equation 3.2 appears to slightly under predict for high light intensity and over predict for low light intensity when

compared to Schmidt *et al.* (2016) work. While the predictions are within the error bounds, the non-linearity combined with the significant temperature and light intensity interaction shown in Table 3.3 may explain this slight variation in predication. Overall, this high prediction capability gives confidence in using Equation 3.2 for further predictions.

Before Equation 3.2 can be used to predict the conditions to increase the phosphorus content of the biomass, the practical limitations should be discussed. These practical limitations are associated with the environmental variables of temperature and light intensity, which are difficult to control in full-scale WSPs. Although a degree of control over these environmental variables can be achieved through dynamic control of the WSP depth (Bechet *et al.* 2016), their levels are typically based on the climatic conditions. Therefore, in a practical sense, these variables are linked together, as the temperature typically increases at the same time as light intensity. With these practical limitations in mind, Equation 3.2 was used to predict the conditions to increase the phosphorus content of the biomass. The best set of conditions was found to be a 'winter' condition (low light intensity and low temperature); however, a 'summer' condition (high light intensity and high temperature) was also included to account for the practical limitations associated with temperature and light intensity. These conditions are shown in Table 3.4.

Table 3.4: The combination of variable levels proposed in this study to increase the phosphorus content of WSP biomass. Error in the predicted value is a 95% confidence interval produced in Minitab from analysis of the factorial experiment.

	Phosphorus Concentration (mgP/L)	Mixing Intensity (RPM)	pH	Organic load (mgCOD/L)	Temperature (°C)	Light Intensity (µE/m².s)	Predicted phosphorus content of the biomass (gP/gSS)
Winter	15	500	No control	105	10	60	2.7%±0.3%
Summer	15	500	No control	105	25	150	2.6%±0.3%

In Table 3.4, it can be seen that there is no significant difference between the predicted phosphorus content of the biomass for the winter and summer sets of conditions. Both combinations of conditions suggest the phosphorus content of the biomass will be increased

with a high phosphorus concentration, high mixing intensity, and high pH, while having a low organic load. These conditions are discussed further below.

A high phosphorus concentration is proposed in Table 3.4 to increase the phosphorus content of the biomass. This effect was expected based on the phosphorus uptake mechanism for algal cells (Cembella *et al.* 1982) and is in agreement with the literature for algae in both temperate (Powell *et al.* 2009; Crimp *et al.* 2018) and cold climate (Schmidt *et al.* 2016) WSP systems.

As shown in Table 3.4, the mixing intensity should be high in order to increase the phosphorus content of the biomass. This result initially opposes the finding in Chapter 2, where increasing the mixing intensity was found to have a negative effect. The difference between these findings can be explained by the significant interaction between the mixing intensity and phosphorus concentration shown in Table 3.3. This interaction indicates that increasing the mixing intensity under low phosphorus conditions will have a negative effect on the phosphorus content of the biomass, while under high phosphorus conditions a positive effect would be observed. The phosphorus concentration used in Chapter 2 was 4.6 mgP/L, which is near the low level of 4 mgP/L examined in this chapter. Therefore, increasing the mixing intensity at this low phosphorus concentration would be expected, and was observed in Chapter 2, to have a negative effect on the phosphorus content of the biomass. This highlights the importance of understanding not only the main effects of variables but also how interactions between the variables influence the phosphorus content of the biomass.

A high pH is proposed in Table 3.4 to increase the phosphorus content of the biomass. A high pH was achieved by reducing the pH control mechanism of CO_2 addition. This finding is in agreement with Chapter 2 and is likely due to the effect of pH on biomass growth. Since algae are photosynthetic, reducing CO_2 addition was expected (Park & Craggs 2010; Zhou *et al.* 2012) and consequently observed (Appendix 8.3.7 and Chapter 2) to have a negative effect on the biomass growth.

The dominant algae in this study were mixotrophic (Pollingher & Berman 1975; Bouarab *et al.* 2004; Zhao *et al.* 2013), allowing the algae to undergo respiration and utilise the organic carbon for energy. While this energy can be used for a range of cellular processes involved in growth and phosphorus uptake, the results in this chapter show that a high organic load decreases the phosphorus content of the biomass. This negative effect on the phosphorus content of the biomass agrees with the findings from Chapter 2.

3.3.2 Implications on WSP system design and operation

This section will first discuss the implications on WSP system design and operation based on the findings from the factorial experiments shown in Table 3.4. These implications will then be used to design and operate a bench- scale 'luxury uptake' process in section 3.3.3.

To achieve a high phosphorus concentration, a small size 'luxury uptake pond' could be used at the start of the WSP system to reduce dispersion and dilution of influent phosphorus into the larger main WSP. The inclusion of baffles in this pond can also be used to increase the phosphorus gradient by making the pond more plug flow and reducing short-circuiting. However, as shown in Table 3.4, a low organic load is also required, which is typically present at the end of the WSP system. To meet both requirements, an anaerobic pond at the start of the WSP system could be used prior to the 'luxury uptake pond'. Anaerobic ponds typically have good removal of organics while having low phosphorus removal, allowing for both the low organic load and high phosphorus concentration requirements to be met.

A high mixing intensity is difficult to achieve in WSPs without large mechanical mixers. However, it is possible to increase the mixing intensity through changes to the inlet manifold and placement of baffles (Shilton & Sweeney 2005).

The pH in WSPs changes with heterotrophic and autotrophic growth and can be modified with carbon dioxide (CO_2) addition (Park & Craggs 2010) as was done in the batch experiments. Although pH control through CO_2 addition is not typically used in traditional WSP systems, pilot-scale high rate algal ponds are known to use pH control to increase biomass concentrations (Park & Craggs 2010; Zhou *et al.* 2012). While pH control could be used in the traditional main pond, it should be avoided in the 'luxury uptake pond' to achieve a higher pH.

The temperature and light intensity are difficult to control in full-scale WSPs. A level of control over these environmental variables can be possible through dynamic control of the pond depth (Bechet *et al.* 2016). By including an outlet that can be raised and lowered in the 'luxury uptake pond' would allow this dynamic control to be achieved. However, the conditions indicated in Table 3.4 represent typical winter and summer conditions, and therefore, control over the temperature and light intensity may not be required.

The findings in Chapter 2 showed that the biomass concentration had no effect on the phosphorus content of the biomass. This indicates that increasing the biomass concentration in the 'luxury uptake pond' should increase the phosphorus removed in the system. For

example, assuming that the phosphorus content of the biomass in the 'luxury uptake pond' is at 2% (gP/gSS), and, based on Chapter 2 findings, this does not change with an increased biomass concentration. If the biomass concentration (gSS/L) in the 'luxury uptake pond' was then doubled, the phosphorus associated with the biomass (gP/L) must also double to ensure the 2% (gP/gSS) phosphorus content of the biomass is maintained. A high biomass concentration in the 'luxury uptake pond' could be achieved through recycling of algal biomass from a 'growth pond' that is placed after the 'luxury uptake pond'. This 'growth pond' could be an advanced pond system such as a HRAP, or a traditional facultative pond that has been similarly modified to improve algal productivity and settleability. Final harvesting of the high phosphorus content algal biomass should be conducted immediately following the 'luxury uptake pond' to remove the phosphorus from the WSP system.

Incorporating these proposed implications into a final design to increase the phosphorus content of the biomass would result in a WSP system similar to that shown in Figure 3.5.

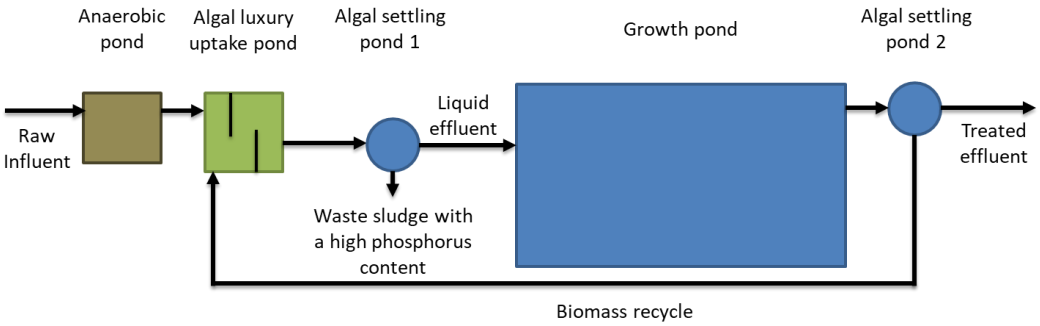

Figure 3.5: Diagram of potential 'luxury uptake' process using the information obtained from this chapter. The pond sizes are not to scale. Arrows show the direction of flow.

This proposed 'luxury uptake' process in Figure 3.5 has similarities to the bacterial based enhanced biological phosphorus removal (EBPR) process. The process therefore also incurs similar downsides that are preventing the uptake of EBPR in small communities currently using WSP systems – high operating and capital costs. However, the major differences between EBPR and this new proposed 'luxury uptake' system are:

1. Does not require large aeration capacity which is typically the main operating cost to a wastewater treatment plant,
2. It is possible to redesign existing WSP systems, into which millions of dollars have already been invested, which would reduce the capital costs required, and

3. The accumulated phosphorus is more stable in algal biomass (days) compared to bacterial biomass (hours), potentially allowing for easier processing of the harvested algal biomass into a slow-release fertiliser or feedstock (Shilton *et al.* 2012).

3.3.3 Operation of a laboratory scale 'luxury uptake' process

The 'luxury uptake' process proposed in section 3.3.2 was used as the basis for a bench-scale semi-continuous process. The only change to the system proposed in Figure 3.5 was the removal of the anaerobic pond, as the organic load could instead be simply controlled through the preparation of the synthetic wastewater feed solution. The 'luxury uptake' process was operated under the conditions identified in Table 3.4 that were proposed to increase the phosphorus content of the biomass (experiment #1 and #2 in Table 3.5). Additional conditions were also tested to analyse the prediction capability of Equation 3.2 (experiment #3, #4, and #5 in Table 3.5). These additional conditions were chosen to give a range of phosphorus contents of the biomass. The experimental conditions are shown in Table 3.5, with the corresponding predicted and experimental phosphorus contents of the biomass after operating the 'luxury uptake' process shown in Figure 3.6. In order to ensure the 'luxury uptake' process was at steady state, each set of conditions shown in Table 3.5 were operated for at least 2 months before the experimental phosphorus content of the biomass could be obtained. Additional operational data including pH, dissolved oxygen, solids concentration and phosphorus concentration is shown in Appendix 8.3.8. A mass balance was considered for studying the overall system operation, however since the growth stage has not been optimised, a mass balance at this stage would not likely add any important information as the biomass concentration needs to also be increased for overall phosphorus removal to be targeted.

Table 3.5: Experimental conditions used to operate the 'luxury uptake' process. Winter and summer refer to the conditions in Table 3.4.

	Phosphorus Concentration (mgP/L)	Mixing Intensity (RPM)	pH	Organic load (mgCOD/L)	Temperature (°C)	Light Intensity (μE/m^2.s)
#1 Winter	15	500	No control	105	10	60
#2 Summer	15	500		105	25	150
#3	15	500		805	25	150
#4	5	100		105	25	150
#5	5	100		105	10	60

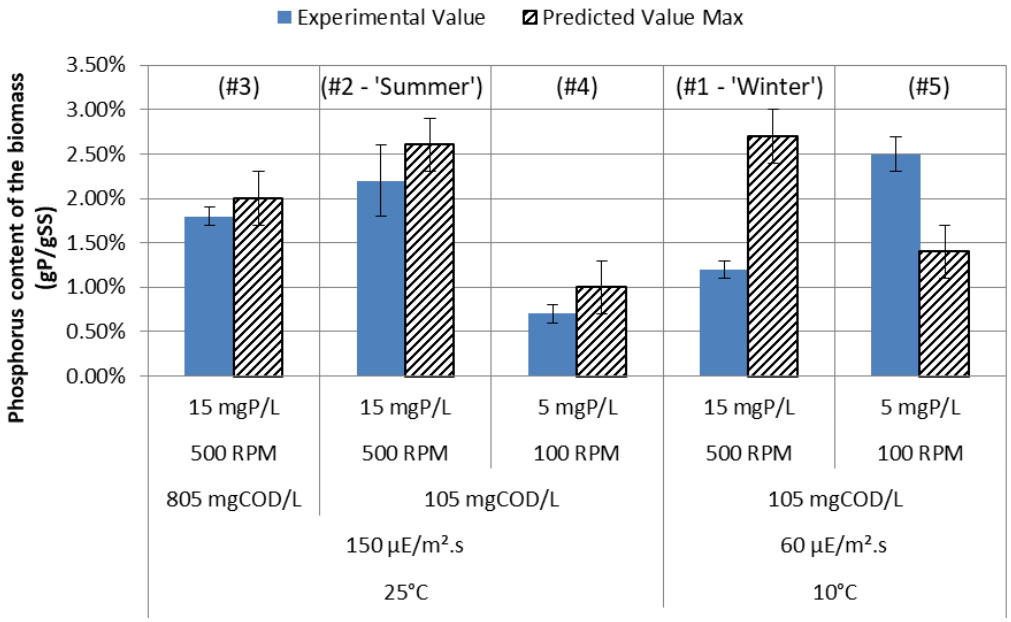

Figure 3.6: Experimental and predicted phosphorus contents of the biomass when operating the 'luxury uptake' process. Calculation of the predicted values is based on Equation 3.2. Predicted error bars are a 95% confidence interval calculated from Minitab analysis of the factorial experiment. Experimental error bars are 95% confidence intervals from repeated sampling (n = 2 to 6). The numbers in the brackets refer to the experiment number in Table 3.5.

Experiment #1 (winter) and #2 (summer) shown in Figure 3.6 were proposed from the batch factorial experiments to achieve the highest phosphorus content of the biomass. While both the winter and summer conditions achieved a phosphorus content in the biomass above 1% (gP/gSS), indicating luxury uptake was occurring (Goldman 1980; Kaplan *et al.* 1986), only the summer condition obtained a phosphorus content in the biomass similar to that predicted by Equation 3.2. When comparing the entire data set, three of the five conditions tested were successfully predicted using Equation 3.2.

Three reasons have been examined to explain these differences between the predicted and experimental values.

1. Changing from batch-based predicted values to semi-continuous based experimental values,
2. The hydraulic retention time (HRT) required for an increase in the phosphorus content of the biomass may be different depending on the experimental conditions, and
3. The algal culture changed from a mixed genus WSP inoculum in the batch experiments to a *Scenedesmus* genus dominated inoculum in the semi-continuous experiments.

The difference between the predicted and experimental values may be due to changing from batch experiments to semi-continuous experiments. Although the predictions using Equation 3.2 were based on the best available information, this information is centred on small-scale batch laboratory experiments. Differences in the phosphorus content of the biomass between batch and continuous experiments have previously been observed in the literature. For example, it was observed that light intensity had a positive effect on the phosphorus content of the biomass in batch studies by Powell *et al.* (2009) and Schmidt *et al.* (2016), whereas, light intensity was observed to have a negative effect in continuous studies by Powell *et al.* (2008).

It is also possible that the HRT required to achieve the predicted phosphorus content of the biomass would change depending on the experimental conditions. This relationship between HRT and environmental conditions has been observed in HRAPs, where it was shown that the HRT could be increased in winter months to achieve the same removal performance as observed in the summer months (García *et al.* 2000). This relationship between HRT and environmental conditions is possible in the 'luxury uptake' process, as both the incorrectly predicted experiments (#1 and #5) were exposed to the same environmental conditions of low light intensity and low temperature. However, this would not explain why experiment #1 was overpredicted, and experiment #5 was underpredicted. Furthermore, in the batch experiments under the low light and low temperature environmental conditions (Run 1 in Table 3.2), the phosphorus content of the biomass was observed to peak on day three at 2.5% (gP/gSS) and then decrease to 2.0% (gP/gSS) by day seven. This indicates that increasing the HRT would instead have a negative effect on the phosphorus content of the biomass, and is therefore unlikely the reason for the differences between the predicted and experimental values observed in Figure 3.6.

The final potential reason for these differences is that the algal culture changed from a mixed genus WSP inoculum in the batch experiments used to produce Equation 3.2, to a *Scenedesmus* dominated inoculum in the semi-continuous experiments. Although the effect of different algal genera on the conditions for phosphorus accumulation are unknown, algal genera in full-scale WSPs have been observed to accumulate polyphosphate granules at different times (Crimp *et al.* 2018). This suggests that the conditions for phosphorus accumulation may differ between the algal genera, which could explain the difference observed in Figure 3.6. Further research is required to confirm this hypothesis.

3.4 Conclusions

The phosphorus content of the biomass in the batch experiments varied from 0.2% to 2.7% (gP/gSS). All six variables studied were involved in nine significant main effects and interactions (≥90% confidence), with the phosphorus concentration and organic load having the largest effects on the phosphorus content of the biomass. These significant effects and interactions were incorporated into a regression equation that successfully predicted seven out of the eight batch experiments from the literature. The combination of conditions to increase the phosphorus content of the biomass (gP/gSS) was predicted using the regression equation as:

- High phosphorus concentration (15 mgP/L), high mixing intensity (500 RPM), and high pH (11), while having a low organic load (105 mgCOD/L), and
- Temperature and light intensity need to be either both low (winter: 10°C and 60 $\mu E/m^2.s$) or both high (summer: 25°C and 150 $\mu E/m^2.s$).

A bench-scale 'luxury uptake' process, designed based on these conditions, was used to assess the prediction capability of the regression equation in a continuous flow system, in which three of the five conditions examined were successfully predicted. Of the two conditions predicted to increase the phosphorus content of the biomass, the summer condition successfully achieved a high phosphorus content in the biomass of 2.2%±0.4% (gP/gSS), which was within the 95% confidence bounds of the predicted value of 2.6%±0.3% (gP/gSS).

Chapter 4
The effect of individual algal genera on phosphorus accumulation

Preface

The findings in this thesis up to now have been based on the 'black box' approach of analysing the phosphorus content of a mixed genus WSP biomass (gP/gSS). While this has advanced our understanding of phosphorus accumulation in a mixed genus culture, this approach ignores any potential effects of individual algal genera. Furthermore, it was indicated at the end of Chapter 3 that the conditions to increase phosphorus accumulation might indeed be different for individual algal genera. In order to understand this potential effect and identify the conditions that influence phosphorus accumulation in individual algal genera, this chapter reanalyses the factorial experiments from Chapter 3 using a new image analysis method to quantify polyphosphate granule accumulation in individual cells. These new findings in this chapter will then be examined using the bench-scale 'luxury uptake' process previously proposed in Chapter 3 to identify if the prediction capability can be improved.

The findings from this chapter will address the third objective of this thesis that was to "Examine how the algal genus influences the conditions for polyphosphate granule accumulation".

This chapter is based on a draft paper that is in preparation for submission to Ecological Engineering:

Sells, M.D., Brown, N. and Shilton, A.N. The conditions for phosphorus accumulation in algae are genus dependent. In preparation for *submission to Ecological Engineering.*

Abstract

The current knowledge on phosphorus accumulation in WSPs is limited to a mixed algal population, meaning we do not know what algal genera are being affected nor to what extent. This chapter examines the environmental, biological, and process conditions that influence polyphosphate granule accumulation by 'drilling down', for the first time, to study algal responses at the individual cell level. To achieve this, a new image analysis method was developed that quantified stained polyphosphate granules in individual algal cells. To ensure the granules being measured were indeed polyphosphate, algal cells were analysed using transmission electron microscopy coupled with energy dispersive X-ray spectroscopy, which confirmed the granules contained higher levels of phosphorus compared to the remaining cell. The image analysis method was then used to quantify stained polyphosphate granules in individual cells from forty batch factorial experiments (2^{6-1}) using a mixed genus WSP inoculum. All twelve algal genera that were identified in the inoculum could accumulate polyphosphate granules. Of the five most abundant genera, *Micractinium/Microcystis* had the highest average accumulation of polyphosphate granules (17% μm^2 granule/μm^2 cell), followed by *Scenedesmus* (12%), *Pediastrum* (11%), *Monoraphidium* (8%) and *Actinastrum* (4%). Although none of the genera studied had the same combination of significant variables, all five genera preferred a high phosphorus concentration to elevate polyphosphate granule accumulation. Furthermore, a high light intensity, high organic load, or high temperature was preferred by the algae if the variable was significant for that genus. The conditions that influence polyphosphate granule accumulation in *Scenedesmus* were incorporated into a regression equation. The bench-scale 'luxury uptake' process previously operated in Chapter 3 with a prediction capability of three out of five was reanalysed using this new *Scenedesmus* regression equation. The prediction capability was improved with all five conditions being successfully predicted within the 95% confidence bounds. This improved prediction capability indicates that an understanding of the algal genus present in a WSP system is required for accurate predictions of the phosphorus accumulation to be obtained.

4.1 Introduction

The current understanding of phosphorus accumulation in WSP algae is based on a mixed culture analysis of the WSP biomass. This has identified the variables temperature (Powell *et al.* 2008; Powell *et al.* 2009; Chapter 3), phosphorus concentration (Powell *et al.* 2009; Schmidt *et al.* 2016; Crimp *et al.* 2017; Chapter 3), light intensity (Powell *et al.* 2008; Powell *et al.* 2009; Schmidt *et al.* 2016; Chapter 3), mixing intensity, organic load, and pH (Chapter 2; Chapter 3)

as impacting phosphorus accumulation. While that work gave vital information on phosphorus accumulation in WSP systems, it was limited to a mixed algal culture 'black box' approach that ignores any effect of individual algal genera in the mixed culture (i.e. we do not know what algae are being affected nor to what extent).

Preliminary research into the algae responsible for phosphorus accumulation in WSPs has been conducted by Crimp *et al.* (2018). This work was part of the same Marsden funded project as this PhD. Crimp *et al.* (2018) identified through field-based observations that the algal genera accumulated polyphosphate granules at different times. However, as a consequence of variation in field conditions and limited temporal data, they were unable to identify the variables responsible for this observation.

The crucial next step to take this luxury uptake phenomenon from an interesting occurrence to the basis of a new environmental biotechnology is to open this 'black box' and determine:

1. Are there WSP algal genera capable of accumulating larger quantities of polyphosphate granules compared to other WSP genera?
2. What is the effect of key process and environmental variables on polyphosphate granule accumulation in individual WSP algal genera?

The work presented in this chapter aims to address these questions by 'drilling down' to study polyphosphate granule accumulation at the individual cell level. In order to achieve this, a new method is required to quantify phosphorus accumulation in individual algal genera from a mixed algal WSP culture. This new method will be used to reveal the algal genera capable of accumulating large quantities of polyphosphate granules and identify the combination of conditions required to increase polyphosphate granule accumulation in the five most abundant algal genera. These conditions will then be examined using the bench-scale 'luxury uptake' process previously proposed in Chapter 3 to identify if the prediction capability can be improved by understanding the influence of the algal genus.

4.2 Methodology

This methodology section is separated into two main parts. The first being the development of a method that can quantify the polyphosphate granule content of individual algal cells (4.2.1), with the second being the procedure for identifying variables that influence polyphosphate granule accumulation in individual algal genera (4.2.2). Using the traditional phosphorus content of the biomass method with single algal genera was considered for this work; however, since full-scale WSPs are mixed genus cultures, studying the effect on phosphorus

accumulation of single algal genera within a mixed genus culture was preferable to keep the experiments as relatable as possible to full-scale.

4.2.1 Developing the polyphosphate granule quantification method

The typical method for identifying phosphorus accumulation in algae is to quantify the phosphorus content as a percentage by weight of the biomass (gP/gSS) (Powell *et al.* 2009; Schmidt *et al.* 2016; Crimp *et al.* 2018). While effective at quantifying the phosphorus content of an entire algal culture, this method is unable to be used on individual algal cells. Other methods are available to quantify the phosphorus content in individual cells, such as electron microscopy (EM) coupled with energy dispersive X-ray spectroscopy (EDS) (Hupfer *et al.* 2008; Majed *et al.* 2012). EM-EDS can provide a large amount of information about the abundance of elements within the algal cell. However, sample preparation for EM-EDS is time intensive, as the sample is required to be washed, embedded in a resin, and then thinly sliced before it can be accurately analysed (Bode *et al.* 1993; Hupfer *et al.* 2008). Not only is this procedure timely, but the slicing of the sample causes difficulties when identifying the algal genera from a mixed genus culture, such as the ones found in WSPs. To provide a way forward, an image analysis method was developed that allows polyphosphate granules to be quantified in individual algal cells.

4.2.1.1 Experimental procedures used during the development of the polyphosphate granule quantification method

This section describes the algal culture and the three analytical methods used during the method development: scanning transmission electron microscopy (STEM) coupled with energy dispersive X-ray spectroscopy (EDS), scanning electron microscopy (SEM) coupled with EDS, and polyphosphate staining and light microscope visualisation.

Electron Microscopy Culture

A two-litre culture, referred to from here as the 'EM culture', was inoculated using a sample isolated from Ashhurst WSP, New Zealand. Although the EM culture originated from a mixed genus WSP sample, it had become dominated by the algal genus *Scenedesmus*. The culture was located in a constant temperature room at 25°C and mixed using a 50 mm magnetic stirrer bar to suspend the algae. The light source consisted of two fluorescent lights (Philips daylight bulbs 36 W) resulting in a light intensity of 100 $\mu E/m^2.s$ measured at the surface of the reactor using an irradiance sensor (Biospherical Instruments QSL-2101). Every seven days one litre of culture was removed and replaced with one litre of fresh synthetic wastewater according to

Davis and Wilcomb (1967) (standard composition shown in Appendix 8.2.1) with a reduced phosphorus concentration of 1 mg $P\text{-}PO_4$/L. The synthetic wastewater contained chelating chemicals to prevent phosphorus precipitation at high pH.

The EM culture was spiked to a concentration of 15 mg $P\text{-}PO_4$/L three days before any electron microscopy was conducted (referred to from here as the 'high phosphorus EM culture'). Based on the work in Chapter 3, after three days the *Scenedesmus* exposed to the phosphorus spike are expected to have undergone luxury uptake and contain polyphosphate granules.

STEM-EDS

A 60 mL algal sample from the high phosphorus EM culture was centrifuged at 4000 RPM for 5 minutes with the supernatant liquid being removed. The sample was washed twice with distilled water and centrifuged again to remove the remaining medium. The final centrifuged pallet was embedded into a resin and cut into 100nm thick sections using an ultramicrotome. Analysis of the slices was conducted using an FEI Company Tecnai™ G2 F20 TWIN transmission electron microscope coupled with an EDAX Phoenix energy dispersive x-ray spectroscopy detector.

SEM-EDS

A 0.5 mL algal sample from the high phosphorus EM culture was fixed on a microscope slide by drying in a 105°C oven for 20 minutes. The slide was carbon coated and analysed using an FEI Quanta 200 Environmental Scanning Electron Microscope with EDAX module.

This sample preparation allows for identification of elements within the sample and an estimation of their elemental abundance. To obtain an accurate measure of the abundance of the specific elements would require a sample preparation similar to that outlined for the STEM-EDS above.

Polyphosphate staining and light microscope visualisation

A 0.5 mL algal sample from the high phosphorus EM culture was fixed to a microscope slide by drying in a 105°C oven for 20 minutes. The slide was stained using a modified Ebel's cytochemical stain according to Bolier *et al.* (1992). The stain consists of two stages: 2.5g $Pb(NO_3)_2$ in 100 mL of 5% HNO_3 (stain A) was applied to the slide for 5 minutes. The slide was rinsed with reverse osmosis water before 18% NH_4S (stain B) was applied for 15 seconds. After rinsing and drying, the slide was examined using a Zeiss Axiophot light microscope with 100

times oil immersion lens and colour CCD camera. Polyphosphate granules appear as black granules (lead sulphide) within the algal cell (Bolier *et al.* 1992).

4.2.1.2 Development of the polyphosphate granule quantification method

The stain used to identify polyphosphate granules in this study does not directly react with polyphosphate. Instead, the cytochemical stain interacts with the counter-ions, such as calcium or potassium (Lins & Farina 1999; Diaz *et al.* 2009), which are found within the granules (Bolier *et al.* 1992). This stain produces black lead sulphide granules within the algal cell as shown in Figure 4.1.

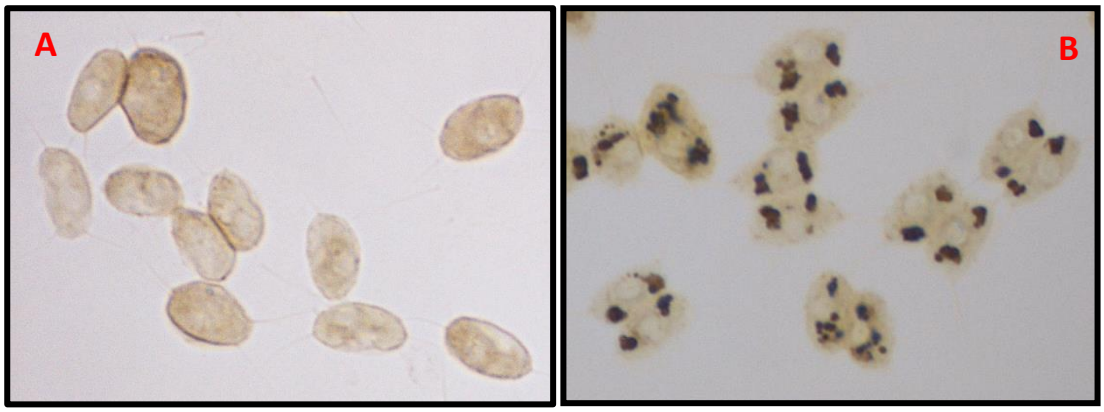

Figure 4.1: Example of *Scenedesmus* cells that have been stained using Ebel's cytochemical stain. A: Low phosphorus culture without polyphosphate granules. B: High phosphorus culture with polyphosphate granules shown as black areas within the cells.

In order to develop a reliable method to visualise and then quantify polyphosphate granules, the following questions needed to be analysed:

1. Is phosphorus stored as polyphosphate granules within algal cells?
2. Can polyphosphate granules be reliably identified in single algal cells?
3. How can the polyphosphate granules be quantified?

Is phosphorus stored as polyphosphate granules within algal cells?

STEM-EDS was conducted to quantify the abundance of elements within a single algal cell and identify if elevated levels of phosphorus are present in granules. An example of a STEM image of a *Scenedesmus* cell high in phosphorus from this work is shown in Figure 4.2.

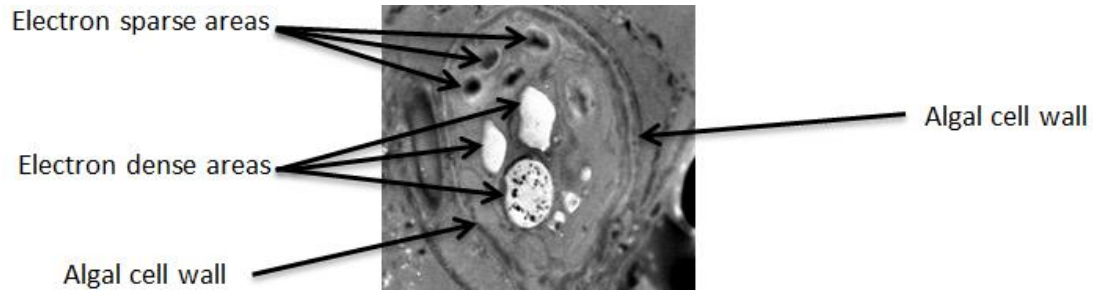

Figure 4.2: STEM image of a *Scenedesmus* cell. Note: STEM images are contrast inverted therefore electron dense areas appear as white.

As shown in Figure 4.2, the *Scenedesmus* cell has large electron-dense areas (shown as white in the STEM image) localised within the cell. Polyphosphate granules are known to be electron dense (Hupfer *et al.* 2008), giving an initial indication of the presence of polyphosphate granules. EDS was conducted on the *Scenedesmus* cell from Figure 4.2 to identify the elemental abundance of specific areas within the algal cell. An example of this EDS analysis can be seen in Figure 4.3.

The electron dense areas of interest in the STEM image from Figure 4.3 have been indicated by the black dashed and solid red circles. These black dashed and solid red circles are also shown on the EDS outputs in Figure 4.3 for phosphorus (P), oxygen (O), carbon (C), and calcium (Ca) to highlight the position of these electron-dense areas on the corresponding elemental abundance outputs. The abundance of the different elements is shown on the y-axis of the EDS outputs in Figure 4.3, with the x-axis showing the position (left to right) along the orange EDS laser line shown in the STEM image. As shown in Figure 4.3, the circled electron dense areas in the STEM image have an increased abundance of phosphorus, oxygen, and calcium, while having a decreased carbon abundance. Accounting for the baseline of oxygen in the remaining cell, the ratio of P:O in the electron-dense granules is approximately 1:3 suggesting a polyphosphate (PO_3) molecular ratio. The fact that these are polyphosphate granules is further justified by the increased calcium abundance (bottom plot in Figure 4.3) which is known to be included in polyphosphate granules (Schonborn *et al.* 2001; Diaz *et al.* 2009). The decreased carbon abundance is a result of the extra volume taken up by the non-carbon based polyphosphate granules. Figure 4.3 also shows that the abundance of phosphorus in other areas of the cell is significantly lower than in the granules. This result shows that phosphorus is stored in granules within the cells with a molecular ratio of PO_3 that is indicative of polyphosphate.

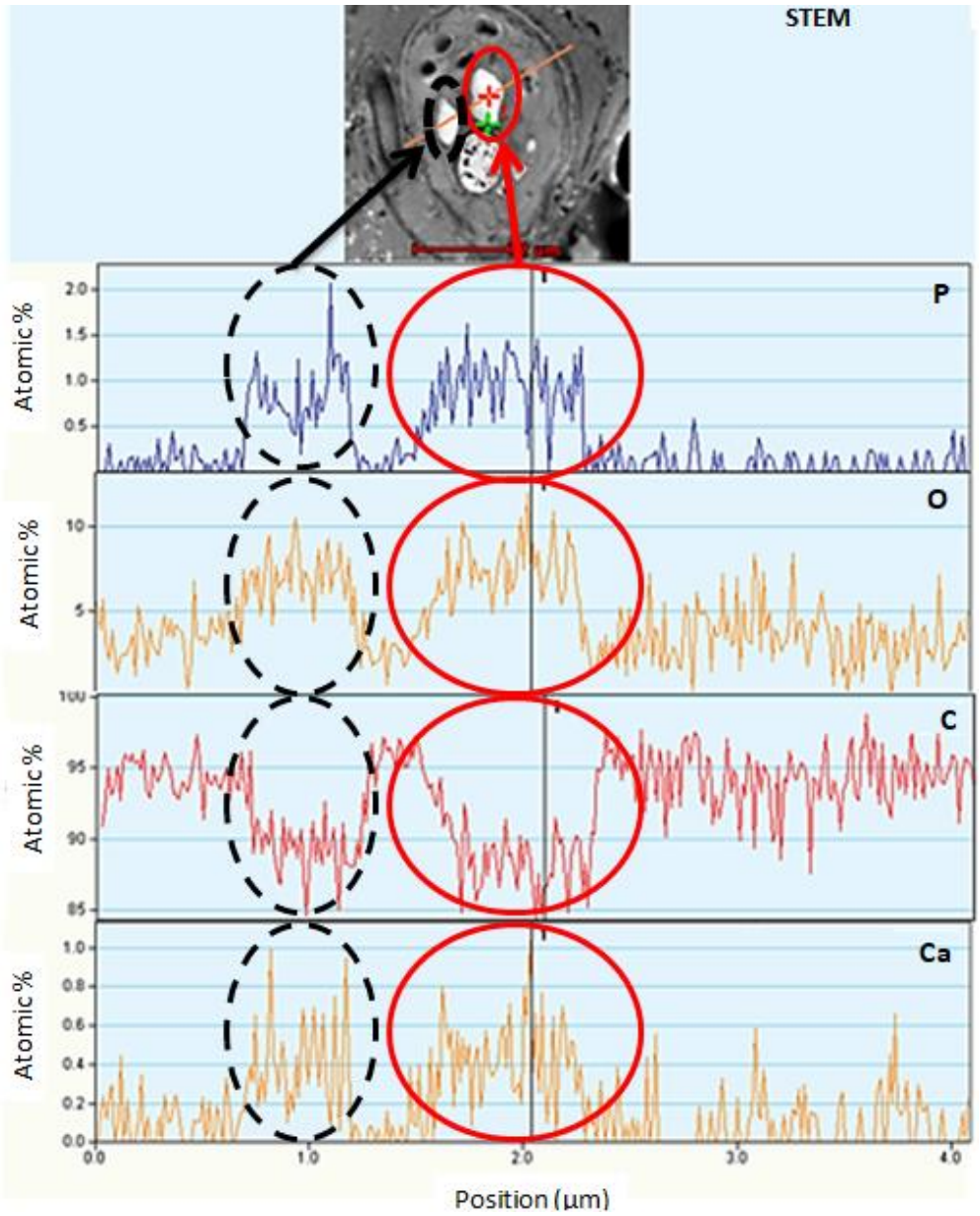

Figure 4.3: Typical STEM-EDS output from a *Scenedesmus* algal cell with polyphosphate granules. Top: STEM image of *Scenedesmus* cell (contrast inverted) showing electron-dense areas as white. Bottom: Phosphorus (P), oxygen (O), carbon (C), and calcium (Ca) spectrometric output as EDS laser goes from left to right along the orange line in the STEM image shown at the top. Black-dashed and solid red circles highlight areas of two separate polyphosphate granules in the STEM image and the corresponding position in the P, O, C, and Ca spectrometric outputs.

Can polyphosphate granules be reliably identified in single algal cells?

It has been shown using STEM-EDS that algae store phosphorus as polyphosphate granules that have an increased phosphorus concentration compared to the remaining cell. However, the STEM-EDS analysis requires a relatively large time for sample preparation, and, for mixed

genus WSP samples, it is difficult to identify the algae after sample preparation has occurred. Therefore, an alternative method to quantify polyphosphate granules was required.

Ebel's cytochemical stain has previously been used in the literature to visualise polyphosphate granules in algae (Bolier *et al.* 1992; Powell *et al.* 2006a; Crimp *et al.* 2018). This stain operates in two parts. The first part of the stain substitutes the counter-ions within the polyphosphate granules (such as calcium and potassium) with lead. The second part involves the reaction of NH_4S with the lead. This produces lead sulphide that appears as black granules under standard light microscopy (Bolier *et al.* 1992).

Previous work has used Ebel's stain to visualise polyphosphate granules, however the specificity of the stain to the polyphosphate granules has not previously been examined. While a direct comparison between the polyphosphate granules observed in a STEM-EDS image and the same algal cell stained using Ebel's stain would be desirable, the sample preparation required for STEM-EDS and the ability to be able to then locate the same algal cell for both sample techniques makes this very difficult, if not impossible, to achieve. Instead, to give confidence that Ebel's cytochemical stain can be used to identify polyphosphate granules within single algal cells, SEM-EDS analysis was conducted on *Scenedesmus* cells stained using Ebel's modified cytochemical stain. If the stain is specific to polyphosphate granules, a peak in both lead and phosphorus should occur when the EDS laser passes through electron dense areas. A SEM-EDS output produced from this work is shown in Figure 4.4. It should be noted that when comparing Figure 4.3 and Figure 4.4, the number and size of the polyphosphate granules in the *Scenedesmus* cells vary considerably. As shown later in this chapter, the amount of polyphosphate granules can vary widely within individual cells from the same algal culture which would explain this observed variation between the two EM-EDS methods.

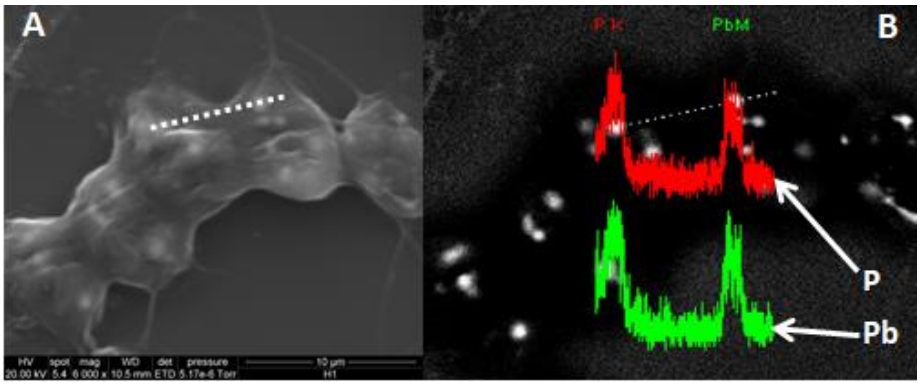

Figure 4.4: (A): Electron microscope image of a *Scenedesmus* alga. (B): SEM backscatter detection image of *Scenedesmus* alga with overlaid phosphorus (P) in red/top and lead (Pb) in green/bottom EDS outputs. The white dotted line in all images shows the EDS laser path.

The SEM image in Figure 4.4A allows the *Scenedesmus* cell to be visualised before further analysis was conducted in Figure 4.4B. This *Scenedesmus* cell remains in the same position for all Figure 4.4 images. Figure 4.4B uses SEM with backscatter detection to show electron-dense granules as white areas. EDS was used along the white dotted line shown in all Figure 4.4 images to estimate the elemental abundance of phosphorus and lead. The peaks in Figure 4.4B indicate an increase in the concentration of phosphorus and lead. These increases occurred simultaneously in the electron dense areas, suggesting that Ebel's cytochemical stain is specific to phosphorus-dense localisations in the cell. This shows that polyphosphate granules can be reliably identified in single algal cells using Ebel's cytochemical stain and light microscopy.

How can the polyphosphate granules be quantified?

Up to this point, it has been shown that polyphosphate is stored as granules within the cell, and Ebel's cytochemical stain is specific to these polyphosphate granules. This allows polyphosphate granules to be visualised using light microscopy; however, in order to quantify these polyphosphate granules, an image analysis method was required.

This image analysis method was developed in the computing software Matlab. In general, this method measures the area of the polyphosphate granules and the area of the algal cell to give a percentage of the cell that is polyphosphate granules. This is achieved in the following steps:

1. Prepare a microscope slide with the algal sample,
2. Stain the sample for polyphosphate granules using the modified Ebel's cytochemical stain as described in section 4.2.1.1,
3. Capture light microscope images of the sample,
4. Quantify the polyphosphate granule content in individual algal cells using the image analysis program developed in Matlab (code given in Appendix 8.4.1).

The robustness of the image analysis program was tested (as shown in Appendix 8.4.2), where the ability of the program to detect stained polyphosphate granules, and the use of a 2-dimensional image to represent a 3-dimensional object are discussed. While these issues may have a minor effect on the quantification of polyphosphate granules in a single cell, the findings suggest that due to the large number of cells analysed, the results obtained using this method should not be affected.

A description of how the image analysis program quantifies the polyphosphate granules is shown below. Effectively the image analysis program works by stepping through the following stages:

1. Isolate the individual cell from the image
2. Remove the background leaving only the algal cell remaining
3. Count the pixels of the cell
4. Count the pixels of the granules
5. Divide the pixels of the granules by the pixels of the cell to obtain a percentage of the cell that is polyphosphate granules (μm^2 granule/ μm^2 cell)

1. Isolate the individual cell from the image

The input into the Matlab program is a light microscope image of a stained algal sample such as that shown in Figure 4.5.

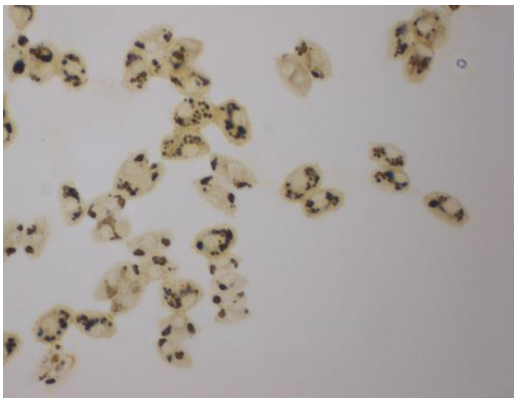

Figure 4.5: Raw image obtained from microscopic observation of stained *Scenedesmus* cells

Using the "Algal selection" program developed in Matlab (code shown in Appendix 8.4.1.1), individual cells are manually isolated from the culture and grouped into their different genera. This produces multiple new images of single algal cells such as that shown in Figure 4.6A. The next steps are conducted using the "Polyphosphate granule quantification" code shown in Appendix 8.4.1.2.

2. Remove the background leaving only the algal cell remaining

The next step is to take the isolated image, as shown in Figure 4.6A, and remove the background to leave only the algal cell, as shown in Figure 4.6D.

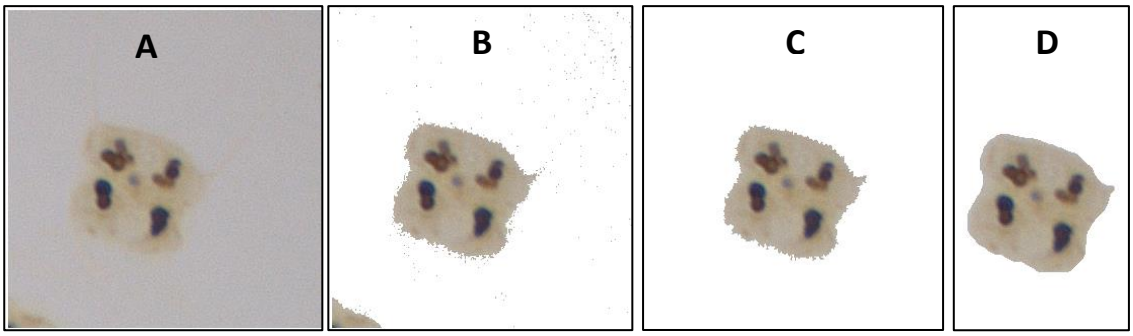

Figure 4.6. A: original image, B: initial background removed, C: small non-cell objects removed, and D: edge corrected

Three background removal stages occur. The initial background removal is shown in Figure 4.6B. This removal is based on a threshold that isolates the cell from the background. This threshold is empirically calculated based on the average background colour of the image. The next step involves the removal of small non-cell objects as shown in Figure 4.6C. This is achieved using a removal technique based on the size of objects in the image, with the assumption that the cell is the largest object. Then finally, edge correction is applied to the algal cell to smooth the pixelated edges that occur in the previous steps (Figure 4.6D). Due to the use of wastewater samples, this background removal stage can encounter situations that prevent successful isolation of the cell. To overcome this issue, a manual check of each cell, and, if necessary, a manual background removal is conducted. Once the background has been successfully removed, the cell is passed onto the granule detection and quantification stage.

3. Count the pixels of the cell

The background-removed cell (Figure 4.6D) is then converted into a black and white image. This is then used as the input for a Matlab function that counts the pixels of the cell.

4. Count the pixels of the granules

Before the pixels of the granules can be counted, a threshold is required to isolate the granules from the remaining cell. A dynamic threshold based on the mean cell colour was used to account for any variations in the cell colour. An empirical relationship was developed based on the manual selection of the threshold for varying cell colours, as shown in Figure 4.7 for *Scenedesmus* cells. A linear trend line was fitted to produce an empirical relationship with an R^2 value of 0.75 suggesting a good fit.

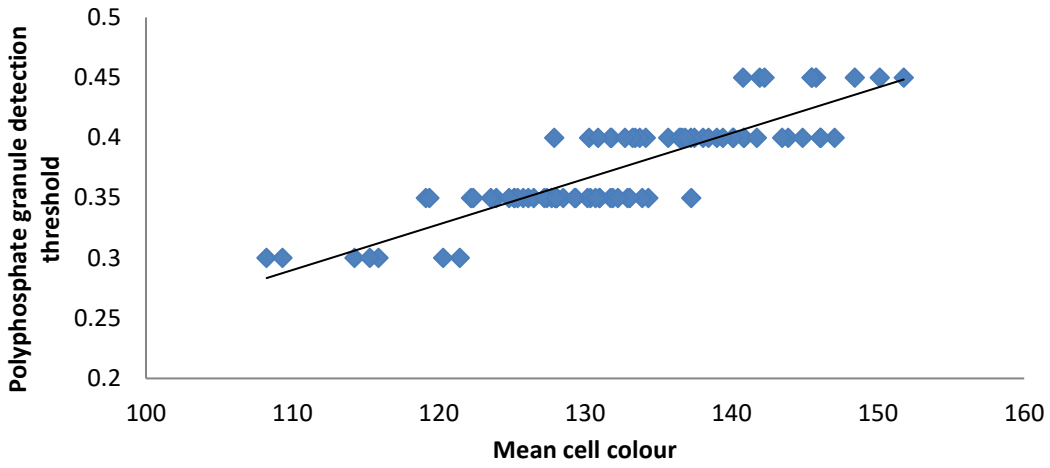

Figure 4.7: Empirical relationship between mean cell colour and polyphosphate granule detection threshold (Note: a higher cell colour results in a lighter cell)

This threshold can then be applied to the background-removed image from Figure 4.6D to isolate the polyphosphate granules from the cell as shown in Figure 4.8.

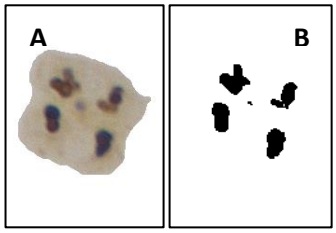

Figure 4.8: Using the threshold to isolate the polyphosphate granules (B) from the algal cell (A)

A Matlab function is then applied that counts the black pixels that now only represent the polyphosphate granules (Figure 4.8B). To ensure that the granules were detected correctly, a slightly higher and lower threshold are also applied and used as a comparison when manually inspecting each alga.

5. Divide the pixels of the granules by the pixels of the cell to obtain a percentage of the cell that is polyphosphate granules (µm² granule/ µm² cell)

The final step is to take the pixels from the granules (step 4) and the pixels from the cell (step 3) and divide the two values to get a percentage as shown in Equation 4.1.

$$Polyphosphate\ granule\ content\ of\ cell\ \left(\frac{\mu m^2\ granule}{\mu m^2\ cell}\right) = \frac{Pixels\ of\ granules}{Pixels\ of\ cell}$$

Equation 4.1: Calculating the polyphosphate granule content (µm² granule/µm² cell) of a single algal cell.

4.2.2 Procedure for identifying variables that influence polyphosphate granule accumulation in individual algal genera

Section 4.2.1 described the development of a new image analysis method to quantify polyphosphate granules in individual algal cells. This section describes the experiments that utilised this new method to identify the effect of variables on polyphosphate granule accumulation in individual algal genera.

4.2.2.1 Batch factorial experimental method

The same factorial experiments that were used in Chapter 3 were analysed again in this chapter using the new image analysis method for quantifying polyphosphate granules in individual cells developed in section 4.2.1. Details of the factorial experiment are given in section 3.2.1.

Minitab® Statistical Software (Minitab 2010) was used to analyse the significance of the variables and interactions. Variables are considered significant at the 95% confidence level when the p-value is less than 0.05, or the 90% confidence level when the p-value is between 0.1 and 0.05. Only one value for each of the 40 factorial experiments can be used as the input into the Minitab analysis. Therefore, to obtain one number from the seven days of analysis, the maximum polyphosphate granule content of the algae for day two to seven was used. Day zero and one were ignored as they were considered an adjustment period between the field conditions and the experimental conditions.

In order to reduce the analysis time, the identification of the peak polyphosphate granule day was conducted by visual observations. Visual observations involved a simple ranking from zero to five of the amount of polyphosphate granules observed in each algal genus, with zero being no granules and five being the most granules. As this manual ranking method is subjective, once the peak polyphosphate granule day was identified, the image analysis method described in section 4.2.1 was used to quantify the polyphosphate granule content of the individual cells. This peak day varied between the algal genera; therefore, this process of identifying the peak day was conducted for each algal genus, resulting in over 30,000 individual cells being visually quantified.

Confirmation of the algal genus identification was conducted at the start of the experiment by Cawthron Institute, an independent organisation from Nelson, New Zealand. This was conducted as quality assurance to ensure identification of algal genera throughout the

experiment was accurate. Twelve genera were identified in the inoculum culture as *Actinastrum, Ankistrodesmus, Closterium, Coelastrum, Crucigeniella, Cyclotella/Cryptomonas, Kirchneriella, Micractinium, Monoraphidium*, *Oocystis, Pediastrum, and Scenedesmus*. The five most abundant genera overall were identified, in order, as *Scenedesmus* (35%)*, Micractinium* (14%)*, Pediastrum* (8%)*, Monoraphidium* (8%), and *Actinastrum* (6%). The percentage occurrence was determined by manual counting of individual algae (a colony of multiple cells was counted as 1 algae) observed in the inoculum culture at the start of each factorial experiment using a light microscope. Due to difficulties in differentiating between small round colonial genera after staining with Ebel's cytochemical stain, there is potential that *Microcystis* are included within the *Micractinium* grouping.

4.2.2.2 'Luxury uptake' process experimental method

The bench-scale semi-continuous flow 'luxury uptake' process is described in section 3.2.2. Polyphosphate granules were quantified according to the image analysis method described in section 4.2.1, and the phosphorus content of the biomass (gP/gSS) was analysed according to section 3.2.1.3.

4.3 Results and discussion

The image analysis method developed in section 4.2.1 was used to identify the conditions responsible for increasing polyphosphate granule accumulation in individual algal genera (section 4.3.1). These findings are then used to predict the polyphosphate granule accumulation in a bench-scale semi-continuous flow 'luxury uptake' process (section 4.3.2).

4.3.1 Variables responsible for polyphosphate granule accumulation in individual WSP algal genera

All 12 algal genera identified in the inoculum culture could accumulate polyphosphate granules; however, the conditions at which this occurred varied between the genera. In order to identify the conditions that influence polyphosphate granule accumulation, a factorial experiment was conducted which analysed the five most abundant algal genera from the inoculum culture (*Scenedesmus, Micractinium/Microcystis, Pediastrum, Monoraphidium,* and *Actinastrum*). This allowed the effects of the variables phosphorus concentration, light intensity, organic load, pH, temperature, and mixing intensity to be identified, and are shown in Table 4.1.

Eixler *et al.* (2006) previously observed that "polyphosphate storage can be strongly influenced by other environmental factors" other than phosphorus concentration; however, these environmental factors were not identified in their work. The work conducted in this chapter and shown in Table 4.1 has now allowed the effect of these environmental factors to be identified. While some variables influence all genera, the combinations of variables that effect polyphosphate granule accumulation differ between the algal genera studied. Along with the main effects of phosphorus concentration, light intensity, pH, and temperature, ten interactions between the variables were also found to be significant (90% confidence).

Table 4.1: Effect of variables and interactions with a significant effect on polyphosphate granule accumulation for the algal genera *Scenedesmus, Micractinium/Microcystis, Pediastrum, Monoraphidium,* and *Actinastrum*. N/A = not applicable as the P-value is greater than 0.10 and no interaction involving the variable is significant, * represents an interaction, '+' is a positive effect, '-' is a negative effect. Significant effects have been highlighted yellow.

	Variable	Effect	*Scenedesmus*	*Micractinium/ Microcystis*	*Pediastrum*	*Monoraphidium*	*Actinastrum*
Main Effects	Phosphorus (P)	+	0.002	0.010	0.222	0.014	0.842
	Light intensity (L)	+	0.087	0.326	0.952	0.121	N/A
	Organic load (O)	N/A	0.554	0.700	0.569	0.344	N/A
	pH	-	N/A	0.062	0.142	0.865	0.139
	Temperature (T)	+	0.051	0.081	0.014	N/A	0.081
	Mixing intensity (M)	N/A	N/A	0.500	N/A	0.641	0.705
2-way interactions	P*L	+	0.001	0.029	0.034	0.033	N/A
	P*O	+	0.046	0.096	0.044	N/A	N/A
	P*pH	-	N/A	0.063	N/A	N/A	0.070
	P*T	+	N/A	N/A	0.039	N/A	N/A
	P*M	-	N/A	N/A	N/A	N/A	0.083
	L*T	+	0.081	0.056	N/A	N/A	N/A
	O*M	-	N/A	0.044	N/A	N/A	N/A
	O*pH	+	N/A	N/A	N/A	0.076	N/A
	pH*T	-	N/A	0.061	0.008	N/A	0.009
	pH*M	+	N/A	N/A	N/A	0.083	N/A

The maximum amount of polyphosphate granules accumulated by each algal genus was also observed to vary. Of the five genera studied, *Micractinium/Microcystis* had the highest average accumulation of polyphosphate granules (17% μm^2 granule/μm^2 cell), followed by *Scenedesmus* (12%), *Pediastrum* (11%), *Monoraphidium* (8%) and *Actinastrum* (4%). This shows that under typical WSP conditions, certain algal genera are 'high performers' and are able to accumulate much larger quantities of polyphosphate granules. Selecting for these 'high performing' genera may provide an improvement to the biological phosphorus removal in WSP systems.

In order to predict the conditions to increase polyphosphate granule accumulation, individual regression equations were produced that incorporate the effects shown in Table 4.1 for each algal genus (regression equations used are shown in Appendix 8.4.3). Using these regression equations, the combinations of variable levels to increase polyphosphate granule accumulation from this study were predicted and shown in Table 4.2.

Table 4.2: Combination of variable levels predicted to increase polyphosphate granule accumulation in the individual algal genera based on the levels tested in this study. N/A is due to no significant effect of the variable on polyphosphate granule accumulation.

Genus	Phosphorus concentration	Light intensity	Organic load	CO_2	Temperature	Mixing intensity
Scenedesmus	High	High	High	N/A	High	N/A
Micractinium/ Microcystis	High	High	High	High	High	Low
Pediastrum	High	High	High	High	High	N/A
Monoraphidium	High	High	High	Low	N/A	High
Actinastrum	High	N/A	N/A	High	High	Low

Table 4.2 shows that all algal genera preferred a high phosphorus concentration to increase polyphosphate granule accumulation. Furthermore, a high light intensity, high organic load, or high temperature was preferred by the algae if the variable was significant for that genus. *Monoraphidium* was the only genera to prefer a low CO_2 addition and high mixing intensity to increase polyphosphate granule accumulation.

The preference for a high phosphorus concentration was expected, as increasing the external phosphorus concentration would allow for increased phosphorus mass transfer into the algal cell. While this effect of phosphorus concentration on polyphosphate granules has not previously been observed in the literature, a positive effect on the total phosphorus content of WSP algae has been observed in Chapter 3 and the literature (Powell *et al.* 2009; Schmidt *et al.* 2016; Crimp *et al.* 2018).

The significance of high light intensity and organic load suggest a link between polyphosphate granules and energy. All algal genera included in this study were mixotrophic (Pollingher & Berman 1975; Bouarab *et al.* 2004; Zhao *et al.* 2013) and could, therefore, utilise an increased light intensity or organic compounds for energy production, assuming no other limiting factors. No significant effect of light intensity or organic load for *Actinastrum* may be due to this genus

having an overall low level of polyphosphate granule accumulation (maximum culture average of 4% μm^2 granule/μm^2 cell). This could result in the effect of light intensity and organic load not being detected for *Actinastrum*.

Monoraphidium was the only genera to prefer low CO_2 conditions, while *Micractinium/Microcystis*, *Pediastrum*, and *Actinastrum* all preferred high CO_2 conditions. As no information on the effect of CO_2 concentrations on polyphosphate granule accumulation in algae was found, literature on the effect of CO_2 tolerance of these different algal genera with respect to growth is instead discussed. While algae need CO_2 for photosynthesis, some algae have been found to have a negative effect when CO_2 addition is introduced. For example, 5% CO_2 addition to a *Monoraphidium* culture was observed to have a negative effect on growth compared to standard air addition (Heo *et al.* 2015). This negative relationship between *Monoraphidium* and CO_2 may explain why this algal genus also prefers low CO_2 addition to increase polyphosphate granule accumulation.

Apart from *Monoraphidium* that was found to have no significant effect of temperature, the remaining algal genera preferred a high temperature to increase polyphosphate granule accumulation. While not specifically for polyphosphate granules, the cellular reaction rates for all algal genera in this study are known to increase when the temperature is elevated to 25°C (Moss 1973; Sánchez *et al.* 2008; Woertz *et al.* 2009; Lurling *et al.* 2013; Sonmez *et al.* 2016). While the increased cellular reaction rates could also increase algal growth, the findings in Table 4.2 suggest the rate of polyphosphate granule accumulation is increased beyond any additional growth.

Micractinium/Microcystis, Actinastrum, and *Monoraphidium* had significant effects due to mixing intensity. *Micractinium/Microcystis* and *Actinastrum* both require a low mixing intensity, while *Monoraphidium* requires a high mixing intensity. The effect of mixing intensity on photosynthetic activity is known to be genus dependent (Leupold *et al.* 2012). For example, Leupold *et al.* (2012) found the mixing intensity in *Chlorella* cultures could be increased four times higher than the mixing intensity for *Chlamydomonas* without a negative effect on the photosynthetic activity being observed. No literature could be found relating an effect of mixing intensity to the algal genera *Micractinium/Microcystis, Monoraphidium,* or *Actinastrum* specifically. However, this species dependent effect of mixing on photosynthetic activity shown by Leupold *et al.* (2012) could be used to explain the different effects of mixing on polyphosphate granule accumulation observed in this chapter for the different algal genera.

4.3.2 Bench-scale semi-continuous flow 'luxury uptake' process

A bench-scale semi-continuous flow 'luxury uptake' process was proposed in Chapter 3 and operated under the conditions shown in Table 4.3. The conditions proposed in Chapter 3 to increase the phosphorus content of a mixed genus biomass (gP/gSS) are shown in Table 4.3 as experiment number 1 (Winter) and 2 (Summer). The culture used in the bench-scale 'luxury uptake' process originated from a mixed genus WSP culture; however, it had become dominated by the *Scenedesmus* genus. Therefore, the conditions to increase polyphosphate granule accumulation were predicted using the *Scenedesmus* regression equation produced in section 4.3.1, and are included in Table 4.3 as experiment number 3 (Granule).

Table 4.3: Experimental conditions used to operate the 'luxury uptake' process. 'Winter' and 'Summer' refer to the conditions proposed in Chapter 3 to increase the phosphorus content of a mixed genus culture. 'Granule' refers to the conditions that are proposed to increase polyphosphate granule accumulation in the *Scenedesmus* genus.

Number	Phosphorus Concentration (mgP/L)	Mixing Intensity (RPM)	pH	Organic load (mgCOD/L)	Temperature (°C)	Light Intensity (µE/m².s)
1 (Winter)	15	500	No control	105	10	60
2 (Summer)	15	500		105	25	150
3 (Granule)	15	500		805	25	150
4	5	100		105	25	150
5	5	100		105	10	60

The 'luxury uptake' process was analysed for polyphosphate granule accumulation in the *Scenedesmus* genus for each of the five experiments shown in Table 4.3. These experimental values were then compared back to the predicted values obtained from the *Scenedesmus* regression equation produced in section 4.3.1 (Regression equation shown in appendix 8.4.3.1). This comparison is shown in Figure 4.9.

As shown in Figure 4.9, the experimental values under all five conditions examined were successfully predicted within the 95% confidence bounds. Furthermore, the conditions proposed in this chapter to increase polyphosphate granule accumulation in *Scenedesmus* did indeed achieve the largest polyphosphate granule content observed in this study of 6.8%±0.6% (μm^2 granule/μm^2 cell), which was within the 95% confidence bounds of the predicted value of 8%±2% (μm^2 granule/μm^2 cell).

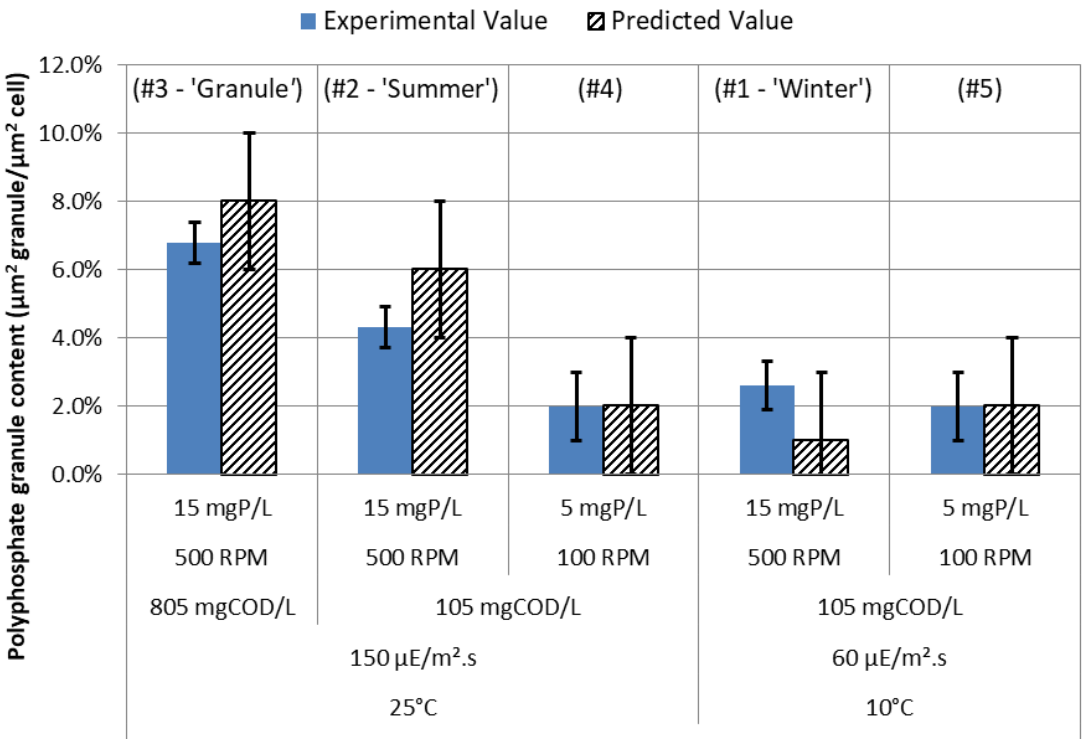

Figure 4.9: Experimental and predicted polyphosphate granule accumulation in *Scenedesmus* cells when operating the 'luxury uptake' process. Calculation of the predicted values is based on the *Scenedesmus* regression equation shown in Appendix 8.4.3. Predicted error bars are a 95% confidence interval calculated from Minitab analysis of the factorial experiment. Experimental error bars are 95% confidence intervals from samples of multiple *Scenedesmus* cells (n>5). The numbers in brackets refer to the experiment number in Table 4.3.

The *Scenedesmus* regression equation produced in this chapter provides an improvement to the previous mixed genus regression equation from Chapter 3. As previously shown in Chapter 3, only three of the five 'luxury uptake' process conditions were successfully predicted when phosphorus accumulation is analysed at the mixed genus level. However, as shown in this chapter, all five conditions can be successfully predicted when studying polyphosphate granule accumulation in individual algal genera. This improved prediction capability suggests that an understanding of the algal genus present in a WSP system is required for accurate predictions of the polyphosphate granule accumulation to be obtained, and the batch data can indeed be applied to a continuous process.

4.3.3 Comparing the polyphosphate granule content to the phosphorus content in the biomass

It is well established in the literature that algae increase their phosphorus content of the biomass by accumulating polyphosphate granules (Harold 1966; Elgavish *et al.* 1980; Bolier *et al.* 1992; Siderius *et al.* 1996; Eixler *et al.* 2006). For example:

1. "Polyphosphate is stored in electron-dense bodies together with calcium." (Siderius, et al., 1996, pg 402)
2. "Microalgae accumulate and store inorganic phosphorus as polyphosphate granules" (Eixler, et al., 2006, pg 53)
3. "In algae, as in many other organisms, phosphorus can be stored in the form of polyphosphate granules" (Bolier, et al. 1992, pg 113)

It is therefore expected to observe a relationship of increasing polyphosphate granule accumulation with increasing phosphorus content in the biomass. To investigate this relationship, a comparison between the polyphosphate granule accumulation (μm^2 granule/μm^2 cell) observed in this chapter, and the phosphorus content in the biomass (gP/gSS) observed in Chapter 3 was conducted on the values obtained from operating the 'luxury uptake' process. This comparison is shown in Figure 4.10.

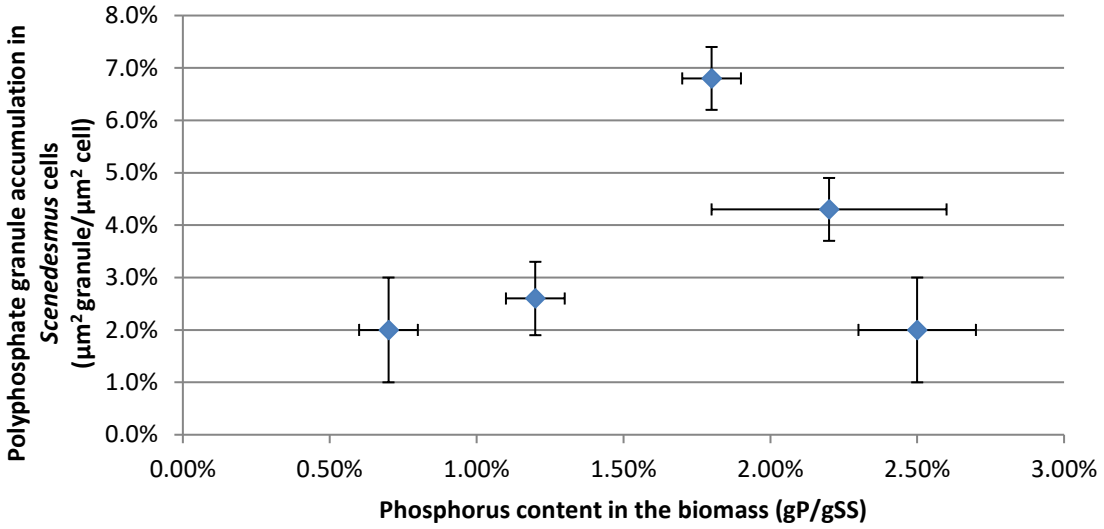

Figure 4.10: Relationship between polyphosphate granule accumulation in *Scenedesmus* cells and the phosphorus content of the culture observed in the bench-scale 'luxury uptake' process. Experimental error bars are 95% confidence intervals from repeated sampling (n ≥ 3 for all error bars except for the phosphorus content of the biomass at 2.5% where n = 2 which corresponds to the standard deviation).

As shown in Figure 4.10, the relationship between the polyphosphate granule content of *Scenedesmus* and the phosphorus content of the biomass appears more complex than previously indicated in the literature. The relationship appears non-linear, with the highest polyphosphate granule accumulation achieved at a phosphorus content in the biomass of 1.8%±0.1% (gP/gSS). From these findings, it appears that increasing the phosphorus content of the biomass does not necessarily increase the polyphosphate granule content. Further research should be conducted to analyse this unexpected relationship between polyphosphate

granule accumulation in individual cells and the phosphorus content of the entire biomass, which is conducted in Chapter 5 of this thesis.

4.4 Conclusions

A new method was developed using image analysis that could quantify stained polyphosphate granules in individual algal cells from a mixed genus WSP culture. All twelve algal genera identified in the WSP could accumulate polyphosphate granules. Of the five most abundant genera, *Micractinium/Microcystis* had the highest average accumulation of polyphosphate granules (17% μm^2 granule/μm^2 cell), followed by *Scenedesmus* (12%), *Pediastrum* (11%), *Monoraphidium* (8%), and *Actinastrum* (4%). Although none of the genera studied had the same combination of significant variables, all five genera preferred a high phosphorus concentration to increase polyphosphate granule accumulation. Furthermore, a high light intensity, high organic load, or high temperature was preferred by the algae if the variable was significant for that genus. The conditions to increase polyphosphate granule accumulation in the *Scenedesmus* genus were identified as high temperature (25°C), high phosphorus concentration (15 mgP/L), high light intensity (150 $\mu E/m^2.s$), and high organic load (700 mgCOD/L). These conditions were used to successfully operate a bench-scale 'luxury uptake' process, resulting in a polyphosphate granule content of 7%±1% (μm^2 granules/μm^2 cell) which was within the 95% confidence bounds of the predicted value of 8%±2%. Furthermore, the results from this work allowed successful prediction of the polyphosphate granule content of *Scenedesmus* cells in all five conditions examined in the 'luxury uptake' process. These findings indicate that an understanding of the algal genus present in a WSP system is required for accurate predictions of the phosphorus accumulation to be obtained, and the batch data can indeed be applied to a continuous process.

Chapter 5

Relating polyphosphate granules in algal cells to the phosphorus content of the biomass

---

Preface

It is well established in the literature that algae increase their phosphorus content of the biomass by accumulating polyphosphate granules (Harold 1966; Elgavish *et al.* 1980; Bolier *et al.* 1992; Siderius *et al.* 1996; Eixler *et al.* 2006). This relationship was briefly examined at the end of Chapter 4, where the polyphosphate granule accumulation (μm^2 granules/μm^2 cell) achieved in the 'luxury uptake' process was correlated against the phosphorus accumulation of the total biomass (gP/gSS). Based on the literature, a relationship of increasing polyphosphate granule accumulation with increasing phosphorus content in the biomass was expected to be observed. However, an unexpected finding revealed that increasing the phosphorus content of the biomass does not necessarily increase the polyphosphate granule content. This finding suggests that the accepted understanding in the literature may be incorrect, and as a result, an additional fourth objective was added to this thesis. This objective was to "Examine the relationship between polyphosphate granules in single algal cells and the phosphorus content of the biomass", which is addressed in this chapter.

This chapter is based on a draft paper that is in preparation for submission to Environmental Science and Technology:

Sells, M.D., Brown, N. and Shilton, A.N. Relating polyphosphate granule accumulation to the algal phosphorus content. In preparation for *submission to Environmental Science and Technology.*

Abstract

Algae are known to accumulate phosphorus as polyphosphate granules that are believed to increase the phosphorus content of the biomass (gP/gSS). While this relationship is widely accepted in the literature, the only link between these metrics is the presence of polyphosphate granules at phosphorus contents in the biomass above 1% (gP/gSS). For the first time in the literature, this chapter investigates this relationship using image analysis to quantify polyphosphate granules in individual algal cells (μm^2 granule/μm^2 cell) over a range of phosphorus contents in the biomass (gP/gSS). Far from having a standard response, this chapter showed that individual cells from the same algal species have varying polyphosphate granule contents from 0% to over 20% (μm^2 granule/μm^2 cell) when exposed to the same conditions. This variation was hypothesised to be from cellular functions influencing the granules differently depending on the individual alga's cell cycle. In addition, when the phosphorus content in the biomass was increased from 2.1% to 3.4% (gP/gSS), no significant effect on the average quantity of polyphosphate granules was observed. This finding indicates that other forms of phosphorus storage must be responsible for attaining a highly elevated phosphorus content in the biomass.

5.1 Introduction

It is widely accepted in the literature that intracellular polyphosphate granules indicate an increase in the phosphorus content of the biomass (Harold 1966; Kuhl 1977; Elgavish *et al.* 1980; Bolier *et al.* 1992; Eixler *et al.* 2006; Markou *et al.* 2014). While these polyphosphate granules are known to contain elevated levels of phosphorus compared to the remainder of the cell (Diaz *et al.* 2009), phosphorus is also contained in a variety of other compounds within the cell, such as ATP, nucleotides, RNA, DNA, and phospholipids to name a few (Kuhl 1977). Furthermore, polyphosphate is not always stored in a granular form. Although not shown in algal cells, Jacobson *et al.* (1982) previously observed that granular polyphosphate isolated from vacuoles of yeast only accounted for 14% of the total cellular polyphosphate content. It is, therefore, possible that the phosphorus content of an algal culture could increase without observing an increase in the polyphosphate granule content of individual cells.

Previous work conducted in this PhD examined the conditions that influence the phosphorus content of a mixed WSP biomass (Chapter 3), and the conditions that influence polyphosphate granule accumulation in individual cells from an algal genus (Chapter 4). While the literature suggests both of these methods can be used to indicate if luxury uptake of phosphorus is

occurring, the only link between these metrics is that polyphosphate granules are observed when the phosphorus content of the biomass is above 1% (gP/gSS) (Harold 1966; Kuhl 1977; Elgavish *et al.* 1980; Bolier *et al.* 1992; Eixler *et al.* 2006). This link was briefly studied in Chapter 4, where it was observed that increasing the polyphosphate granule content of individual cells (μm^2 granules/μm^2 cell) did not necessarily increase the phosphorus content of the biomass (gP/gSS). This observation raises the question of what is the relationship between the 'phosphorus content of the biomass' and the 'polyphosphate granule content of individual cells', which is examined in this chapter.

5.2 Methodology

This section describes the methodology used to examine the relationship between the 'phosphorus content of the biomass' and the 'polyphosphate granule content of individual cells'. The *Scenedesmus* genus and *Chlamydomonas reinhardtii* species were used for this examination due to both algae being found in WSPs (Crimp *et al.* 2018), with *C. reinhardtii* being a common model organism (Harris 2001). In order to examine this relationship between the metrics, separate algal cultures from the *Scenedesmus* genus and *C. reinhardtii* species were exposed to different conditions, as outlined in the following sections.

5.2.1 *Scenedesmus* experimental reactors

Six one-litre batch reactors were started with 20% inoculum culture (inoculum described in section 2.2) with the remaining 80% synthetic wastewater according to Davis and Wilcomb (1967) (recipe given in Appendix 8.2.1), unless otherwise stated. Although the inoculum culture originated from a mixed genus WSP culture, it had become dominated by the *Scenedesmus* algal genus with no other algal genera observed under light microscopy. These reactors were given the same environmental conditions as the inoculum culture described in section 2.2, unless otherwise stated. The phosphorus concentration in the reactors was modified using KH_2PO_4, and the light intensity was manipulated using fluorescent lights (Philips daylight bulbs 36W) according to Table 5.1.

The phosphorus concentrations detailed in Table 5.1 are based on work conducted in Chapter 3 and Chapter 4 that showed increasing the phosphorus concentration should increase both the phosphorus content of the biomass (Chapter 3) and the polyphosphate granule content of individual *Scenedesmus* cells (Chapter 4). The high phosphorus concentrations of 34 and 48 mg $P\text{-}PO_4$/L are outside the range of normal WSP concentrations; however, they were used in this study to achieve high phosphorus accumulation.

Table 5.1: Phosphorus concentration and light intensity used in experimental reactors

Reactor	Phosphorus concentration (mg P-PO_4/L)	Light intensity at the surface of the reactor (µE/m^2.s)
1	0.0	150
2	0.6	150
3	2.5	150
4	7.5	150
5	34	60
6	48	60

The light intensity in this work was kept at 150 µE/m^2.s for reactors 1 to 4 and was decreased to 60 µE/m^2.s in reactors 5 and 6. While increasing the light is specified in Chapter 3 and Chapter 4 to increase the phosphorus accumulation, the aim of the work in this chapter was to obtain a range of different phosphorus contents of the biomass, which was still achieved under these conditions.

Samples of the six experimental reactors detailed in Table 5.1 were taken on day four of the batch experiment and analysed for suspended solids, phosphate concentration, total phosphorus concentration, and polyphosphate granule content. The experimental time of four days was based on findings in Chapter 3 that indicate that under the conditions in Table 5.1, four days should be sufficient time to reach the maximum phosphorus content of the biomass.

5.2.2 *Chlamydomonas reinhardtii* experimental reactors

125-mL axenic *C. reinhardtii* inoculum cultures were maintained in 250 mL Erlenmeyer-flasks with Minimal Media (Appendix 8.5.1) modified to a low phosphorus concentration of 1 mgP/L by minimising K_2HPO_4 and KH_2PO_4. The reactors were cultivated in a Minitron incubator (Infors HT, Switzerland), that was maintained at 25°C with an atmosphere of 2% CO_2 in air. The reactors were continuously agitated (180 RPM) and supplied continuous illumination from five fluorescent lights (18 W Polylux cool white tubes) producing a light intensity of 21 µE/m^2.s at the surface of the reactor. After seven days, 50 mL of the inoculum culture was transferred into a new 250 mL Erlenmeyer-flask containing 75 mL of autoclaved low phosphorus Minimal Media.

The experimental reactors were started with 5-day old *C. reinhardtii* inoculum culture. 500 mL of the inoculum culture was centrifuged (2900 g for 3.5 minutes) and re-suspended in 600 mL of Minimal Media without phosphorus in 1-litre Erlenmeyer flasks (high-P). A second experimental reactor was started the same way (low-P). One hour later (time = 0), K_2HPO_4/

KH_2PO_4 were added to the high-P reactor to achieve a phosphorus concentration of 10 mgP/L. The experimental reactors were maintained in the incubator under the same conditions as the inoculum culture unless being removed for sampling.

The experimental reactors were sampled for phosphate concentration, suspended solids, and polyphosphate granules at times of 0 minutes, 20 minutes, 24 hours, 48 hours, 72 hours, and 96 hours. Total phosphorus was sampled at the start and end of the experiment.

5.2.3 Analytical methods

The suspended solids and total phosphorus concentrations were analysed according to section 3.2.1.3. Phosphate concentration was analysed using ion-chromatography as described in section 2.2. Analysis of the polyphosphate granules was conducted according to section 4.2.1. The phosphorus content in the biomass was calculated using Equation 3.1 as shown in section 3.2.1.3. Light intensity was measured as described in section 2.2. The details of the *Scenedesmus* culture and analytical methods used for the scanning transmission electron microscopy coupled with energy dispersive X-ray spectroscopy (STEM-EDS) are given in section 4.2.1.1.

5.3 Results and Discussion

In order to identify the relationship between the 'phosphorus content of the biomass' and the 'polyphosphate granule content of individual cells', *Scenedesmus* cells were analysed for their polyphosphate granule content (μm^2 granule/μm^2 cell) from six reactors with different phosphorus contents of the biomass (gP/gSS). This resulted in multiple *Scenedesmus* cells being analysed for a single phosphorus content of the biomass. The resulting relationship between the 'phosphorus content of the biomass' and the 'polyphosphate granule content of individual *Scenedesmus* cells' is shown in Figure 5.1.

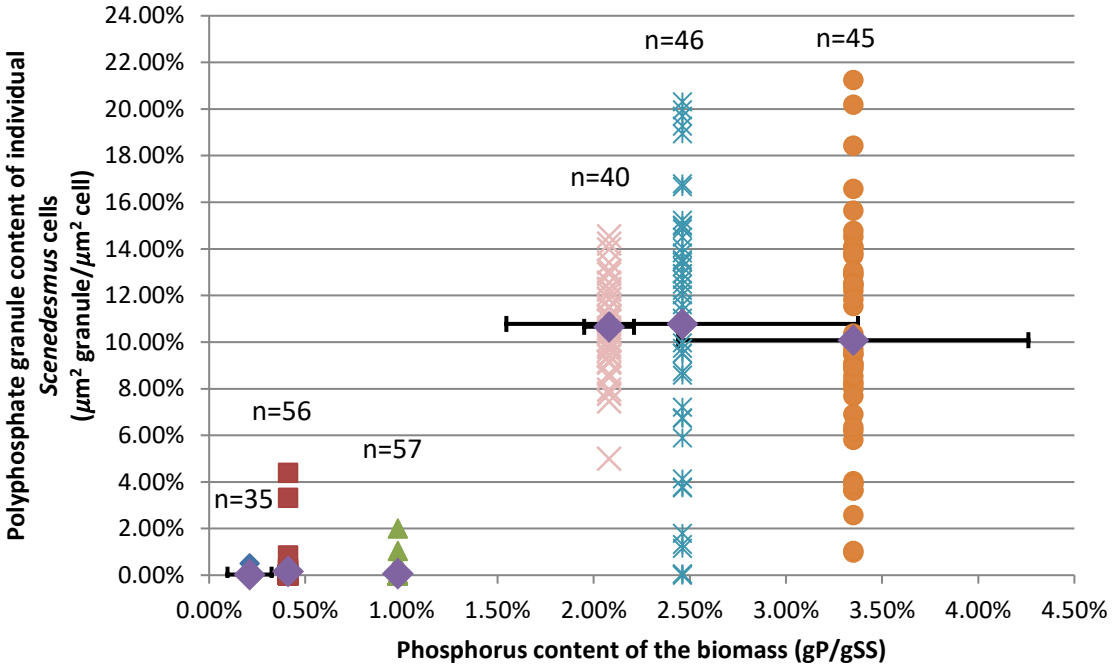

Figure 5.1: Relationship between the phosphorus content of the biomass (gP/gSS) and the polyphosphate granule content of individual cells (µm² granules/µm² cell) for the *Scenedesmus* genus. Purple diamonds represent the average polyphosphate granule content at the given phosphorus content of the biomass. Other markers represent the polyphosphate granule content from individual cells at the different phosphorus contents of the biomass. n refers to the number of individual *Scenedesmus* colonies.

Figure 5.1 shows that when the phosphorus content of the biomass is below 1% (gP/gSS), polyphosphate granules were detected in only a few (13%) of the individual cells. Conversely, when the phosphorus content of the biomass was increased above 1% (gP/gSS), polyphosphate granules were observed in nearly all (99%) of the individual cells. This finding agrees with the literature, where it is widely cited that algal cultures with phosphorus contents above 1% (gP/gSS) have polyphosphate granules (Harold 1966; Kuhl 1977; Elgavish *et al.* 1980; Bolier *et al.* 1992; Eixler *et al.* 2006).

An unexpected finding was made in Figure 5.1, where it was observed that wide variation in the polyphosphate granule content of individual cells occurred when the phosphorus content of the biomass is above 1% (gP/gSS). For example, at a phosphorus content in the biomass of 2.5% (gP/gSS), the polyphosphate granule content of individual *Scenedesmus* cells varied from 0% to over 20% (μm^2 granule/μm^2 cell). The variation appears larger for the low light intensity conditions, which may be a result of less photosynthetic energy available for growth and polyphosphate granule formation. This variation has never been reported in the literature and raises the question of what is causing this variation.

Additionally, Figure 5.1 shows that increasing the phosphorus content of the biomass above 2.1% (gP/gSS) had no effect on the average polyphosphate granule content. This observation is only significant when increasing the phosphorus content of the biomass from 2.1% to 3.4% (gP/gSS) due to the large error bars at the higher phosphorus contents of the biomass. This raises the question of what is causing the increase in the phosphorus content of the biomass if polyphosphate granules are not responsible. Although this work was beyond the original scope of the PhD, further investigation was conducted to examine possible reasons for these observations, as outlined below:

1. Does the staining and image analysis technique identify the polyphosphate granules correctly?
2. Do the species within a genus accumulate different amounts of polyphosphate granules?
3. What cellular processes are responsible for the variation in polyphosphate granule content?
4. Are there compounds other than polyphosphate granules responsible for phosphorus storage?

These potential reasons are explored further in the following sections.

5.3.1 Does the staining and image analysis technique identify the polyphosphate granules correctly?

The staining and image analysis technique was previously discussed in Chapter 4, with a brief summary given here of the main points.

The specificity of Ebel's cytochemical stain was analysed previously in section 4.2.1.2 by SEM-EDS of a stained algal cell with polyphosphate granules (Figure 4.4 and reproduced in Figure 5.2).

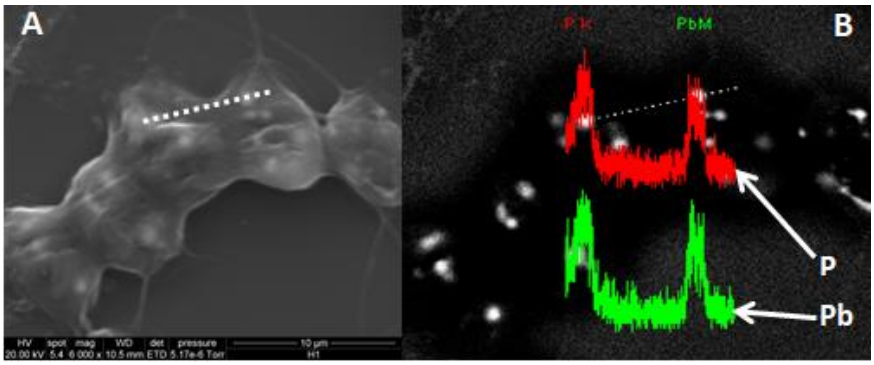

Figure 5.2: Electron microscope image of a Scenedesmus alga. (B): SEM backscatter detection image of Scenedesmus alga with overlaid phosphorus (P) in red/top and lead (Pb) in green/bottom EDS outputs. The white dotted line in all images shows the EDS laser path. Reproduced from Chapter 4)

Ebel's stain replaces the counter-ions contained in the polyphosphate granules with lead, therefore, a peak in phosphorus and lead are expected when the EDS laser passes over the granules. As shown in Figure 5.2, this is the case, with the llead peaks being simultaneously observed with a peak in phosphorus. This finding suggests that the stain is specific to polyphosphate granules, and therefore the black lead areas that are observed under light microscopy, and used in the image analysis program, should only be present when polyphosphate granules are present.

It is possible that using a 2-dimensional image to represent a 3-dimensional object could influence the quantification of polyphosphate granules in individual cells. This issue has two main points. The first being that the microscope needs to be focused to observe the 3-dimensional granules within the cell, and the second being that the image analysis program uses this 2-dimensional image to estimate the amount of polyphosphate granules in a 3-dimensional algal cell. This effect is discussed further in Appendix 8.4.2 where it was found that, while these issues may have a minor effect on the quantification of polyphosphate granules in a single cell, due to the large number of cells analysed, the results obtained using this image analysis method should not be affected.

5.3.2 Do the species within a genus accumulate different amounts of polyphosphate granules?

It has previously been shown in Chapter 4 that, depending on the conditions, certain algal genera can accumulate more polyphosphate granules than others. In addition to this, a species effect has previously been observed in the cyanobacteria *Microcystis* in natural systems, where the species *Microcystis flosaquae* could store more phosphorus than *Microcystis wesenbergii* (Yue *et al.* 2013). It is therefore plausible that different algal species within a genus could also

have different levels of polyphosphate granule accumulation, resulting in the variation observed in Figure 5.1. This hypothesis was tested by quantifying the polyphosphate granule content of individual cells in a pure strain of *Chlamydomonas reinhardtii*. While *C. reinhardtii* belongs to a different genus than the previously examined *Scenedesmus*, if similar variation is observed in *C. reinhardtii,* it can be assumed that the variation in Figure 5.1 is not due to the influence of different species within the genus. As was previously conducted for the *Scenedesmus* genus, this new comparison between the 'phosphorus content of the biomass' and the 'polyphosphate granule content of individual cells' in a pure culture of *C. reinhardtii* is shown in Figure 5.3.

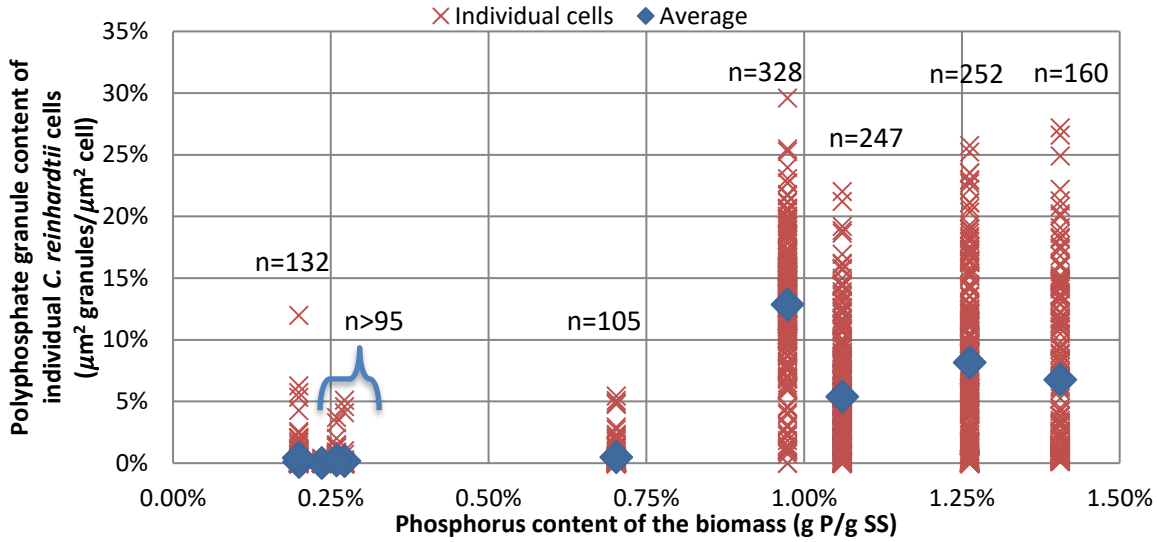

Figure 5.3: Relationship between the phosphorus content of the biomass (gP/gSS) and the polyphosphate granule content of individual *C. reinhardtii* cells (µm² granules/µm² cell). n refers to the number of individual cells. n>95 refers to the smallest number of individual cells analysed at that grouping of phosphorus contents of the biomass.

As can be seen in Figure 5.3, the *C. reinhardtii* species shows a similar trend to the *Scenedesmus* genus previously shown in Figure 5.1. Interestingly, more variation is observed in the *C. reinhardtii* species culture than in the *Scenedesmus* genus culture. For example, individual *C. reinhardtii* cells had polyphosphate granule contents varying from 0% to a maximum of 29% (μm^2 granule/μm^2 cell), while individual cells in the *Scenedesmus* genus varied from 0% to a maximum of 21% (μm^2 granule/μm^2 cell).

Since Figure 5.1 and Figure 5.3 show algae from two different genera, it is possible that the algal species will still cause some of the variation when studying at the algal genus level. However, since individual cells from the *C. reinhardtii* species had a similar variation to individual cells in the *Scenedesmus* genus, it seems unlikely that different species from the

same algal genus are the cause of the variation in polyphosphate granule content observed in Figure 5.1.

5.3.3 What cellular processes are responsible for the variation in polyphosphate granule content?

Phosphorus is widely used throughout the cell in a variety of compounds such as ATP, nucleotides, RNA, DNA, phospholipids, and polyphosphates (Kuhl 1977). While it is generally accepted that algal cells produce polyphosphate as a phosphorus storage reservoir (Kuhl 1977; Bolier *et al.* 1992; Eixler *et al.* 2006), alternative uses of polyphosphate within the algal cell have also been proposed. One of these alternatives involves the incorporation of cations within the polyphosphate granules. These cations are suggested to be included to counteract the negative charge of the polyphosphate (Lins & Farina 1999; Schonborn *et al.* 2001; Hupfer *et al.* 2008; Diaz *et al.* 2009), however, this cation incorporation may have further cellular functions such as regulating intracellular cation concentrations or detoxification (Chopin *et al.* 1997; Nishikawa *et al.* 2006; Adams *et al.* 2016). Another alternative function of polyphosphate was proposed by Werner *et al.* (2007) who suggested that polyphosphate would accumulate in the cell wall of *C. reinhardtii* as a defence mechanism against toxins or pathogens. If the polyphosphate granules are used for more than just phosphorus storage within the algal cell, then the granules may be produced or consumed as required by these other cellular functions, resulting in variation between individual cell requirements. However, this would only occur if the individual cells were responding differently to a stimulus, indicating the individual cells are at different stages of the cell cycle.

Indeed, changes in the polyphosphate content of algal cells have previously been linked to cell division (Miyachi & Miyachi 1961; Baker & Schmidt 1964; Herrmann & Schmidt 1965; Werner *et al.* 2007). For example, Baker and Schmidt (1963) found that in a synchronous *Chlorella* culture, acid-insoluble polyphosphate increased until cell division occurred, at which the lowest acid-insoluble polyphosphate concentration was detected. Similar findings were observed by Miyachi and Miyachi (1961) who identified that the polyphosphate fraction defined by Miyachi as “A” increased in concentration until cell division occurred, after which the concentration was drastically reduced. Furthermore, polyphosphate “A” has been linked to polyphosphate granules in both algae (Kulaev *et al.* 2004) and bacteria (Achbergerová & Nahálka 2011). This link between the cell cycle and polyphosphate granules is well established in bacterial systems (Henry & Crosson 2013; Racki *et al.* 2017). These findings give strong

evidence that the concentration of the polyphosphate granules will change with the cell life cycle.

For the effect of the cell life cycle to cause the variation in polyphosphate granule content observed in Figure 5.1 and Figure 5.3, the individual algal cells need to be at different stages of their life cycle. Algal cultures can have synchronous cell cycles if the experiment is set up to have specific illumination regimes and inhibitors (Zachleder *et al.* 2002). However, as this was not conducted in these experiments, the *Scenedesmus* and *C. reinhardtii* cultures are assumed to have asynchronous cell cycles. This is indeed what was observed in Figure 5.4. Individual *Scenedesmus* colonies were observed to have varying cell numbers from one to four cells, indicating different stages of the life cycle. While *Scenedesmus* are typically found in colonies of 2 cell multiples, single cell *Scenedesmus* colonies have previously been observed in the literature (Lurling & Van Donk 1997). This reasoning could explain the variation observed in Figure 5.1 and Figure 5.3.

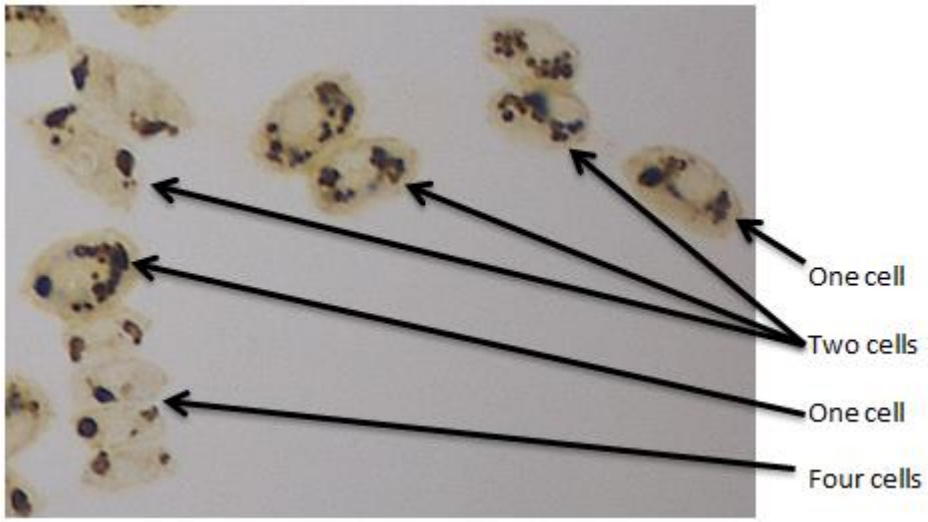

Figure 5.4: Example of the variation in the number of cells per colony seen in the *Scenedesmus* reactors.

5.3.4 Are there compounds other than polyphosphate granules responsible for phosphorus storage?

The results from Figure 5.1 previously revealed that increasing the phosphorus content of the biomass from 2.1% to 3.4% (gP/gSS) had no effect on the average polyphosphate granule content of the *Scenedesmus* cells. This observation was unexpected, as the literature states that polyphosphate is the main phosphorus storage compound in algae (Kuhl 1977; Bolier *et al.* 1992; Eixler *et al.* 2006), where it is typically incorporated into granules within the cell (Siderius *et al.* 1996; Diaz *et al.* 2009; Solovchenko *et al.* 2016). As the average polyphosphate granule content of the *Scenedesmus* did not increase when the phosphorus content of the biomass

was increased, it was hypothesised that a compound other than polyphosphate granules is responsible for the storage. This hypothesis was investigated through scanning transmission electron microscopy coupled with energy dispersive X-ray spectroscopy (STEM-EDS) of high phosphorus content *Scenedesmus* cells to identify any high phosphorus localisations within the cell. An example output from the STEM-EDS is shown in Figure 5.5.

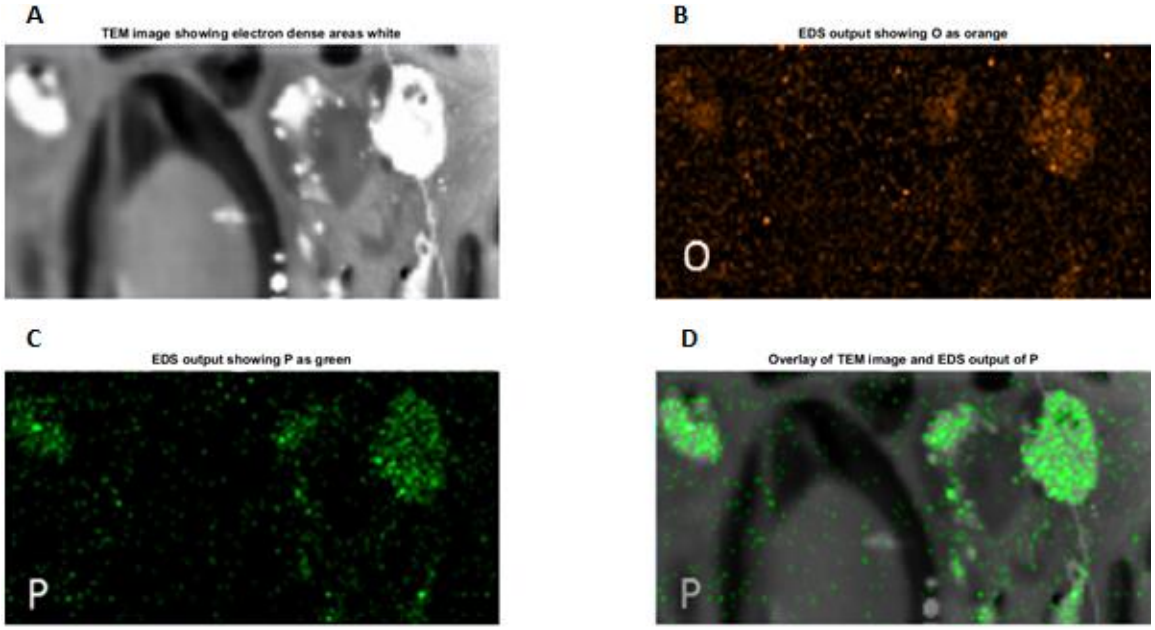

Figure 5.5: An example STEM-EDS output from a *Scenedesmus* algal cell with polyphosphate granules. A: STEM image of *Scenedesmus* cell (contrast inverted) showing electron-dense areas as white. B: Oxygen EDS output. C: Phosphorus EDS output. D: Phosphorus EDS output overlaid on top of the STEM image. Note: A brighter intensity shows an increased elemental abundance in the EDS outputs.

The STEM image in Figure 5.5A shows electron dense areas as white, while the EDS outputs in Figure 5.5B and C show an increase in the elemental abundance of oxygen and phosphorus respectively by a brighter intensity. The initial step to identifying high phosphorus areas that are not polyphosphate granules is first to identify the granules themselves. Polyphosphate granules are known to be electron dense (Hupfer *et al.* 2008) and contain an increased elemental abundance of phosphorus and oxygen. Therefore, to identify the polyphosphate granules, STEM is required first to visualise the electron dense areas within the cell, and then EDS is required to identify if these electron-dense areas have increased phosphorus and oxygen abundance. As shown in Figure 5.5A, electron-dense areas are present within the cell, which is the first evidence of polyphosphate granules. Polyphosphate granules are further demonstrated in Figure 5.5B and C where these electron-dense areas are also high in oxygen and phosphorus abundance. Combining these observations gives substantial evidence of polyphosphate granules, which matches the previous findings in this PhD (section 4.2.1.2).

Further analysis of Figure 5.5 was conducted outside of the electron-dense areas to identify any high phosphorus localisations that are not polyphosphate granules. As shown in Figure 5.5D, while there are some points of high phosphorus scattered across the cell, the phosphorus intensity is considerably lower (indicated by a lower brightness) than the electron-dense areas. Therefore, in terms of phosphorus density, polyphosphate granules indeed store more phosphorus than other cellular compounds. This finding agrees with the literature where polyphosphate granules have been shown to have twice the phosphorus density compared to the remainder of the cell (Diaz *et al.* 2009).

To understand the phosphorus storage contribution of polyphosphate granules to the cell, not only does the phosphorus density need to be accounted for, but also the amount of granules within the cell. As previously shown in Figure 5.1 and Figure 5.3, the amount of polyphosphate granules in individual cells varied from 0% to 29% (μm^2 granule/μm^2 cell) of the cell area. Using a mass balance, the granule areas of the individual cells were combined with the phosphorus densities from Diaz *et al.* (2009) of 7±2 $\mu gP/cm^2$ for the granules and 3±1 $\mu gP/cm^2$ for the remaining cell. The full mass balance is shown in Appendix 8.5.2, with the resulting contribution of polyphosphate granules to the overall phosphorus in the cell shown in Figure 5.6.

The phosphorus density used in this mass balance is based only on Diaz *et al.* (2009), and, therefore, it is possible that the phosphorus density could be different for the algal genera and conditions examined in this thesis. For this to influence the results, the phosphorus density would need to vary between the observed polyphosphate granules. While this may be possible, it would require a change in the structure of the granules by, for example, changing the counter-ion concentration within the granule themselves which would likely affect the stability of the polyphosphate granules (Harold 1966; Bental *et al.* 1990; Leitao *et al.* 1995). As shown previously in the STEM-EDS image in Figure 4.3 (Chapter 4), the phosphorus and calcium (common counter-ion) atomic percentages remain similar for both the granules examined. This suggests the phosphorus density did not vary, and therefore agrees with the findings of a consistent phosphorus density in polyphosphate granules proposed by Diaz *et al.* (2009).

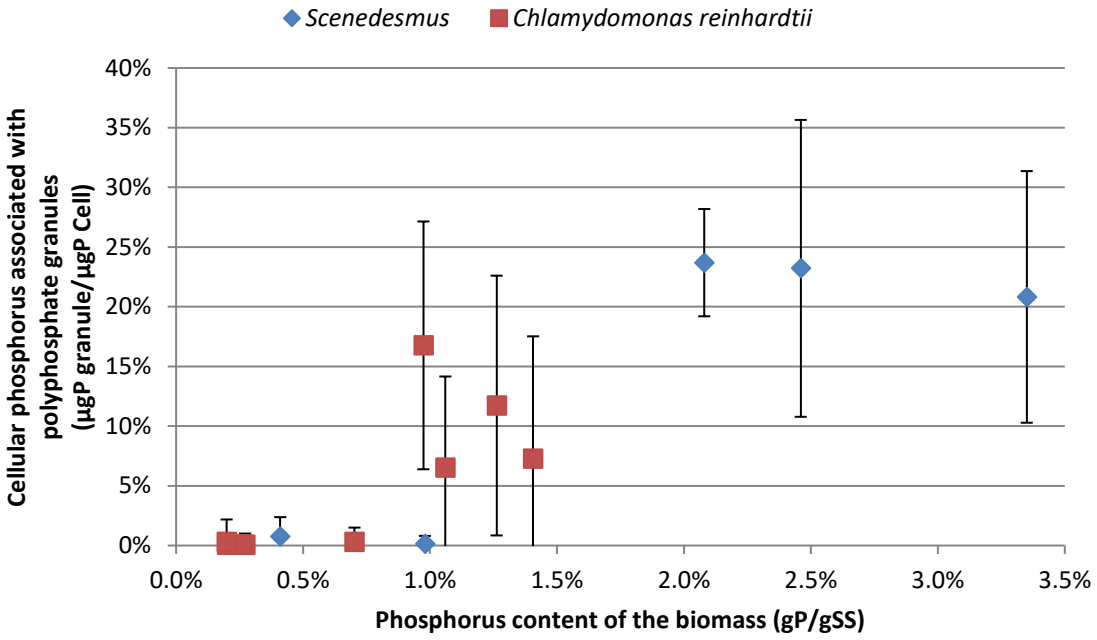

Figure 5.6: Phosphorus associated with the polyphosphate granules for *Scenedesmus* and *C. reinhardtii* cells shown in Figure 5.1 and Figure 5.3 respectively. Error bars are the standard deviation produced from the variation in polyphosphate granule area of individual cells.

Figure 5.6 shows the phosphorus contribution of polyphosphate granules to the overall phosphorus content of individual cells for *Scenedesmus* (blue diamond) and *C. reinhardtii* (red squares). As shown in Figure 5.6, polyphosphate granules contributed up to 35% and 27% of the total cellular phosphorus for *Scenedesmus* and *C. reinhardtii* respectively. This finding fits with Rhee (1973), who extracted total polyphosphate (which includes non-granular polyphosphate) from *Scenedesmus* cultures and found the total polyphosphate contributed between 10% to 40% of the total cellular phosphorus concentration.

Interestingly, when the phosphorus content of the biomass in the *Scenedesmus* culture was increased above 2% (gP/gSS), the amount of phosphorus associated with the granules did not increase. For example, increasing the phosphorus content of the biomass from 2.1% to 3.4% (gP/gSS) resulted in a phosphorus associated with the polyphosphate granules of 24% and 21% respectively, which, when accounting for the error bars, resulted in no significant difference being observed. This finding suggests that, while polyphosphate granules allow the algae to store phosphorus in high-density localisations as confirmed in Figure 5.5 by STEM-EDS, the polyphosphate granules were not responsible for increases in the phosphorus content of the *Scenedesmus* biomass above 2% (gP/gSS).

This increase instead may be due to a large number of the less intense phosphorus localisations mentioned previously. As seen in the STEM-EDS image in Figure 5.5, there are some small scatterings of high phosphorus spots spread across the cell (as indicated by the green intensity). Although these are less phosphorus dense then the granules (indicated by a lower brightness), it is possible that the large number of these spots could result in the increase in the phosphorus content of the biomass above 2% (gP/gSS). This would not be observed by Ebel's stain as this is specifically for the polyphosphate granules. These spots could be a variety of different phosphorus containing compounds, such as, non-granular polyphosphate, surface adsorbed phosphate, phospholipids, phosphoproteins, phosphorylated carbohydrates, ATP/ADP, and nucleotides to name a few. While the exact nature of these phosphorus compounds cannot be determined from this work, the results presented in Figure 5.6 suggest that for the phosphorus content of the culture to increase from 2% up to 3.4% (gP/gSS), at least one other phosphorus compound that is not polyphosphate granules must be responsible for this storage.

5.4 Conclusions

Individual cells from the same culture had varying polyphosphate granule contents from 0% to over 20% (μm^2 granule/μm^2 cell) when exposed to the same conditions. This variation was not only observed at the genus level in *Scenedesmus* but also at the species level in *Chlamydomonas reinhardtii*. Additionally, increasing the phosphorus content of the biomass from 2.1% to 3.4% (gP/gSS) had no significant effect on the average amount of phosphorus contributed by the polyphosphate granules. This indicates that the accepted understanding in the literature that polyphosphate granules are responsible for increases in the phosphorus content of the algae may be incorrect, as other forms of phosphorus storage must be responsible for attaining a highly elevated phosphorus content in the biomass.

Chapter 6
Conclusions and recommendations

6.1 Conclusions

Although the literature review indicated the variables cation concentration, prior phosphorus content in the algae, and biomass concentration were potentially significant, screening experiments identified these variables had no significant effect on algal phosphorus accumulation at the WSP levels examined. Conversely, in addition to the three variables phosphorus concentration, temperature, and light intensity identified from the literature, the screening experiments identified three further influential variables as the mixing intensity, organic load, and pH.

These six influential variables were further examined in 40 batch factorial experiments, in which nine significant main effects and interactions were identified that influence the phosphorus accumulation in a mixed genus WSP biomass (≥90% confidence). The significant effects and interactions were incorporated into a 'mixed genus' regression equation that successfully predicted seven out of the eight batch experiments from the literature. The 'mixed genus' regression equation predicted the combination of conditions to increase the phosphorus content of the biomass (gP/gSS) as:

- High phosphorus concentration (15 mgP/L), high mixing intensity (500 RPM), and high pH (11), while having a low organic load (0 mgCOD/L), and
- Temperature and light intensity need to be either both low (winter: 10°C and 60µE/m^2.s) or both high (summer: 25°C and 150µE/m^2.s).

A bench-scale 'luxury uptake' process, designed based on these conditions, was used to assess the prediction capability of the regression equation in a continuous flow system, in which three of the five conditions examined were successfully predicted. Of the two conditions predicted to increase the phosphorus content of the biomass, the summer condition successfully achieved a high phosphorus content in the biomass of 2.2%±0.4% (gP/gSS), which was within the 95% confidence bounds of the predicted value of 2.6%±0.3% (gP/gSS).

A new image analysis method was developed that could quantify stained polyphosphate granules in individual algal cells from a mixed genus WSP culture. Polyphosphate granules were confirmed to have a higher level of phosphorus compared to the remaining cell. All twelve algal genera identified in the WSP could accumulate polyphosphate granules. Of the

five most abundant algal genera, *Micractinium/Microcystis* had the highest average accumulation of polyphosphate granules (17% μm^2 granule/μm^2 cell), followed by *Scenedesmus* (12%), *Pediastrum* (11%), *Monoraphidium* (8%), and *Actinastrum* (4%). The variables and interactions that influence polyphosphate granule accumulation differed between these five algal genera:

- All genera studied preferred a high phosphorus concentration to increase polyphosphate granule accumulation.
- A high light intensity, high organic load, or high temperature was preferred by the algae if the variable was significant for that genus.

The conditions to increase polyphosphate granule accumulation in the *Scenedesmus* genus were incorporated into a regression equation that successfully predicted the polyphosphate granule content of *Scenedesmus* cells in all five 'luxury uptake' process conditions examined (95% confidence). This improved prediction capability indicates that an understanding of the algal genus present in a WSP system is required for accurate predictions of the phosphorus accumulation to be obtained, and the batch data can indeed be applied to a continuous process.

The literature indicated that the phosphorus content in the biomass (gP/gSS) increases as a result of the production of polyphosphate granules. Examining this relationship, it was observed that individual cells from the same species had varying polyphosphate granule contents from 0% to over 20% (μm^2 granule/μm^2 cell) when exposed to the same conditions. Additionally, contrary to what is believed in the literature, increasing the phosphorus content of the biomass from 2.1% to 3.4% (gP/gSS) had no significant effect on the average amount of phosphorus contributed by the polyphosphate granules. This finding indicates that phosphorus compounds other than polyphosphate granules must be responsible for attaining a highly elevated phosphorus content in the biomass.

These findings pave the way forward for the development of a new algal-based biotechnology capable of harvesting phosphorus from wastewater, which is further discussed in the following recommendations section.

6.2 Recommendations for future research

1. Investigation into the non-linear response observed in the predictive phosphorus content of the biomass equation (Equation 3.2) produced in Chapter 3.

While the non-linear response was only significant at 90% confidence, it is possible that the optimum conditions to elevate the phosphorus content of the biomass are between the high and low levels examined in this work. Future work should investigate this potential non-linear response to allow a better understanding of the optimum conditions and further refine the predictive model produced in this thesis.

2. Optimisation of the algal productivity and settleability in the growth stage of the 'luxury uptake' process.

A combination of a high phosphorus content in the biomass and a high biomass concentration which is easily settleable are required to achieve overall phosphorus removal from the 'luxury uptake' process. The work in Chapter 3 took the first step towards this and showed a high phosphorus content of the biomass can be achieved in the luxury uptake stage. This first step of achieving a high phosphorus content of the biomass was the focus of this thesis, however, to achieve phosphorus removal in the 'luxury uptake' process, the next step is to maintain this high phosphorus content of the biomass while also achieving a high biomass concentration. With the current 'luxury uptake' process design, a high biomass concentration could be achieved by optimising algal productivity and harvesting in the growth stage. This would then allow the biomass to be recycled back in to the luxury uptake stage.

3. Future research on luxury uptake should be conducted at the algal genus level.

As shown in Chapter 4, the combination of variables required to elevate polyphosphate granule accumulation are dependent on the algal genera studied. Furthermore, it was shown that understanding the algal genera present in the culture allowed for an improved predictive capability in the 'luxury uptake' process. In Chapter 5, however, it was shown that an increase in the polyphosphate granule content of individual algal cells does not necessarily result in an increase in the phosphorus content of the entire biomass. Therefore, future research should either be conducted using the traditional phosphorus content of the biomass (gP/gSS) method with single algal genera, or a method that can analyse the total phosphorus content of single algal cells from a mixed genus culture. A potential method to analyse the phosphorus content in single algal cells is scanning electron microscopy coupled with energy dispersive X-ray spectroscopy (SEM-EDS). SEM-EDS would allow the complete cell to be visualised, and

therefore identified, while also giving the elemental abundance of the algal cell, which would allow the phosphorus content to be calculated. The downside of this SEM-EDS method is the preparation time required to obtain useful elemental abundance results, and the SEM-EDS equipment required for the analysis.

4. Investigation into the variation in polyphosphate granules observed in individual cells.

While preliminary work was conducted and a hypothesis proposed to explain the cause of the variation in individual cells polyphosphate granule content, further research should be conducted to conclusively identify the cause. Investigating this phenomenon could lead to an improved understanding of phosphorus accumulation in algae, which could in turn influence the design and operation of the 'luxury uptake' process.

5. Further research into the compounds responsible for the increase in phosphorus content of the biomass above 2% (gP/gSS).

In Chapter 5 it was shown that polyphosphate granules may not be responsible for an increase in the phosphorus content of the biomass above 2% (gP/gSS). While the compound/s responsible were not identified in Chapter 5, understanding what is causing the increase above 2% (gP/gSS) may allow modifications to the 'luxury uptake' process to be conducted that would further improve phosphorus accumulation in algae.

6.3 Recommendations for the design and operation of a 'luxury uptake' process

The purpose of this section is to provide tentative design and operation guidelines for a 'luxury uptake' process based on achieving a high phosphorus content of the biomass (Chapter 3) and a high concentration of settleable biomass in the luxury uptake stage. It should be noted that these recommendations are based on small-scale laboratory experiments, and further research is needed before large scale application is considered.

The basic concept of the 'luxury uptake' process proposed here is essentially the same as used in Chapter 3, with a separate luxury uptake stage and growth stage which allows these two critical unit operations to remain uncoupled and optimised individually. It is important to stress that this thesis is the first stage in developing a 'luxury uptake' process and the design and operation guidelines proposed in this section cannot be considered final. These guidelines are simply the best guess at what the system could look like given the small-scale laboratory results produced in this thesis. Furthermore, this 'luxury uptake' process has only been designed for phosphorus removal, and therefore there is a potential that the other functions of the WSP system, such as pathogen removal, BOD removal and nitrogen removal, could be affected by these changes, and this requires further consideration.

6.3.1 Luxury uptake stage

The luxury uptake stage is designed to increase the phosphorus content of the biomass. The conditions to increase the phosphorus content of the biomass are taken from the operation of the bench-top luxury uptake process in Chapter 3, and are shown in Table 6.1. It is known that seasonal environmental changes affect algal pond performance (Craggs *et al.* 2014). While these seasonal environmental variables of light intensity and temperature are difficult to control in full-scale WSPs, a level of control can be possible through dynamic control of the pond depth (Bechet *et al.* 2016). However, as these environmental variables are predominantly set by the season, a 'summer' and 'winter' set of conditions for a temperate climate have been proposed in Table 6.1.

Table 6.1: Recommended conditions to operate the luxury uptake stage

	Light intensity ($\mu E/m^2.s$)	Temperature (°C)	Phosphorus (mgP/L)	Mixing intensity (RPM)	pH	Organic load (mgCOD/L)
Summer	150	25	15	500	Uncontrolled	105
Winter	60	10	5	100	Uncontrolled	105

According to Table 6.1, maintaining a higher in-pond phosphorus concentration is preferable in summer, while a lower in-pond phosphorus concentration is preferable in winter. This finding is based on the laboratory scale luxury uptake process, in which the inlet phosphorus concentration was varied. As the inlet concentration cannot be directly varied in a full-scale system, two alternative approaches have been proposed. The first approach, as shown in Figure 6.1, is to baffle the luxury uptake pond into smaller ponds and operate it in a plug-flow pattern in summer but a parallel 'CSTR' type flow pattern in winter.

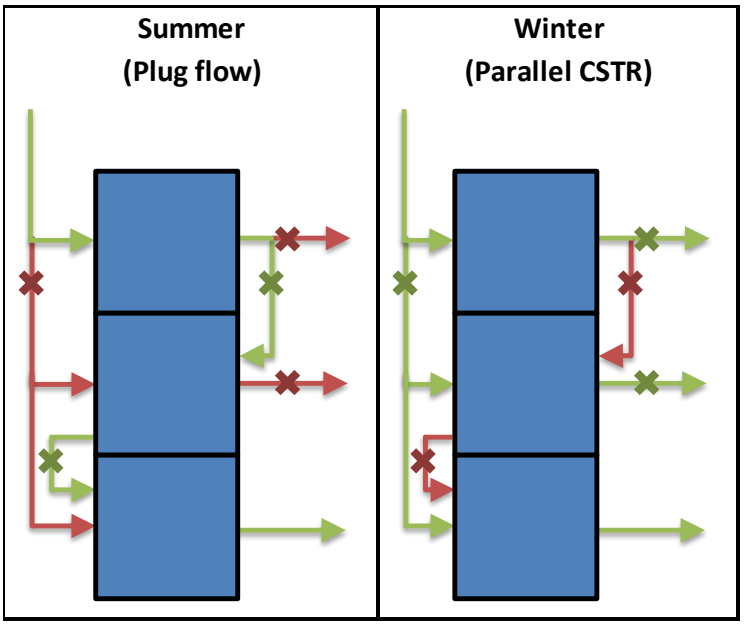

Figure 6.1: Possible changes in flow pattern for summer and winter flow. The 'X' represents valves, the green colour represents open valves and pipe flows, and the red colour represents closed valves and pipes with no flow.

Plug-flow should maintain a higher phosphorus concentration in the first reactor that receives the influent wastewater. This is essentially the same configuration that was used in the laboratory scale trials. In winter, with simply the change of five valves, the inlet can instead

divert into the three luxury uptake stage reactors in a parallel arrangement, as shown in Figure 6.1. This parallel arrangement should increase the dilution of the inlet resulting in a lower overall phosphorus concentration.

An alternative design could be dilution of the inlet wastewater with the already treated effluent wastewater. In summer the system can be designed similar to the summer design shown in Figure 6.1. However, when the lower phosphorus concentration is desired in winter, a recycle stream from the end of the 'luxury uptake' process (that will be low in phosphorus concentration) could be used to dilute the phosphorus concentration of the inlet wastewater. As both proposed methods for controlling the phosphorus concentration have not yet been examined, further research is required to ensure the desired effects are achieved.

The mixing intensity from the laboratory scale system was 500 RPM in summer and 100 RPM in winter. While the units of RPM are difficult to translate to full-scale, the mixing regime that describes these RPMs can be used to allow scale up from the small-scale testing. 500 RPM at small-scale resulted in a 'rapid mixing' regime, while 100 RPM resulted in a 'just suspended' mixing regime. For an algal based HRAP system, a mixing intensity of 1 W/m^3 should result in a 'just suspended' mixing regime (Chisti 2016). For activated sludge systems, a mixing intensity of 20 W/m^3 results in a 'rapid mixing' regime (Metcalf & Eddy 2003), and it is assumed that a similar mixing intensity would be suitable for achieving 'rapid mixing' in algal based systems. These different mixing intensities can be achieved in the luxury uptake stage by using mechanical mixers within the pond that can have a variable speed depending on the season.

In the laboratory results, an uncontrolled pH was found to increase phosphorus accumulation in the luxury uptake pond for both seasons. This uncontrolled pH is typical of WSP systems and therefore no implications on design or operation are required.

In both seasons, a low organic load should increase the phosphorus content of the biomass in the luxury uptake pond. To achieve a low organic load, either a primary anaerobic pond or primary facultative pond could potentially be used prior to the luxury uptake pond.

The effect of HRT and depth in the luxury uptake pond were not examined in this thesis. In Chapter 3, the HRT of the luxury uptake stage was set to 3 days for both seasons examined. This 3 day HRT is similar to what is used in HRAPs in the summer (Craggs *et al.* 2014), and is therefore likely suitable for the luxury uptake stage. As depth was also not examined in this thesis, a depth of 0.3 m in the luxury uptake stage is suggested based on the typical depth of

algal based HRAP systems (Craggs 2005). This typical HRAP depth should ensure the algae are intermittently exposed to the ambient light (Park *et al.* 2011a).

A settler is required at the end of the luxury uptake pond to ultimately remove the phosphorus rich biomass from the wastewater system. Settling of traditional facultative pond algae is often challenging, however algal settling ponds following HRAPs have been shown to successfully harvest the algae (García *et al.* 2000; Park *et al.* 2011b; Craggs *et al.* 2015). Removal of the harvested algal biomass before decay occurs is crucial to achieving overall phosphorus removal from the luxury uptake process (Powell *et al.* 2011b). The luxury uptake pond would need continuous biomass removal from the settler, or, at a minimum, daily removal to prevent decay of the biomass and release of the phosphorus from occurring (Craggs *et al.* 2014). In the work of Park *et al.* (2011b), recycling part of the harvested biomass has shown to improve settleability from 60% with no recycle to above 85% with recycling. It is therefore recommended to include a recycle of a small amount of the harvested biomass to improve settleability. In a pilot-scale HRAP in Cambridge, New Zealand, Craggs *et al.* (2015) used an algal harvesting pond with an HRT of 2 hours and a depth of 4m.

6.3.2 Growth stage

The growth stage is a separate pond designed to supply the biomass required in the luxury uptake pond. The biomass produced in the growth stage therefore needs to be settled from the effluent discharge and recycled into the luxury uptake stage. The growth stage was not optimised in this thesis; however, the desired algal characteristics from the growth stage are similar to what is commonly observed when using an HRAP. HRAPs are known to promote high algal concentrations that are more easily settleable compared to typical facultative WSPs (García *et al.* 2000; Park *et al.* 2011b; Craggs *et al.* 2015).

The HRT of an HRAP in a temperate climate is dependent on the season, with HRTs of 3 to 4 days in summer and 7 to 9 days in winter (Craggs *et al.* 2014). The depth of the HRAP also varies between 0.3 to 0.5 m (Craggs 2005). Taking a summer HRT and depth of 4 days and 0.3 m respectively, the depth would need to increase to 0.5 m to achieve the 7-day HRT in winter.

A paddlewheel mixer could be used to create circulation around the pond and introduce turbulence to improve algal cells exposure to sunlight (Craggs *et al.* 2014). A mixing intensity of 1 W/m^3 has been suggested by Chisti (2016) to achieve this mixing regime.

CO_2 addition could also be used to further improve the algal productivity in the growth stage. CO_2 addition has previously been used on pilot-scale HRAP systems, with increases in the biomass yield of up to 30% (Park & Craggs 2010; Zhou *et al.* 2012). The pH should be used to control the CO_2 addition, with a target pH of just below 8 being optimum (Craggs *et al.* 2014).

6.3.3 Final design

The final design, if this system was constructed from new, would look similar to that shown in Figure 6.2, with, in this example, a primary anaerobic pond being used at the start of the system.

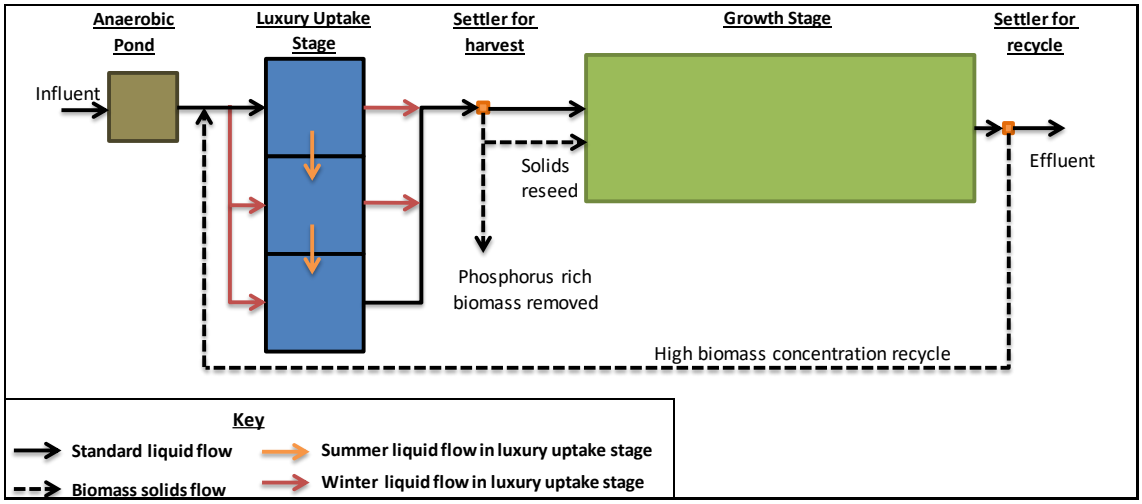

Figure 6.2: Scale diagram of the proposed 'luxury uptake' system. Note: Luxury uptake stage flow pattern has been described previously in Figure 6.1.

This system could also be retrofitted to existing WSP systems. To illustrate this, a design was also proposed for modifying the existing WSP system in Rongotea, New Zealand (600 people, flowrate is approximately 180 m^3/d). The existing WSP system at Rongotea consists of a primary facultative pond (4800 m^2), secondary facultative pond (1600 m^2), and an algal settler (330 m^2), as shown in the satellite image in Figure 6.3.

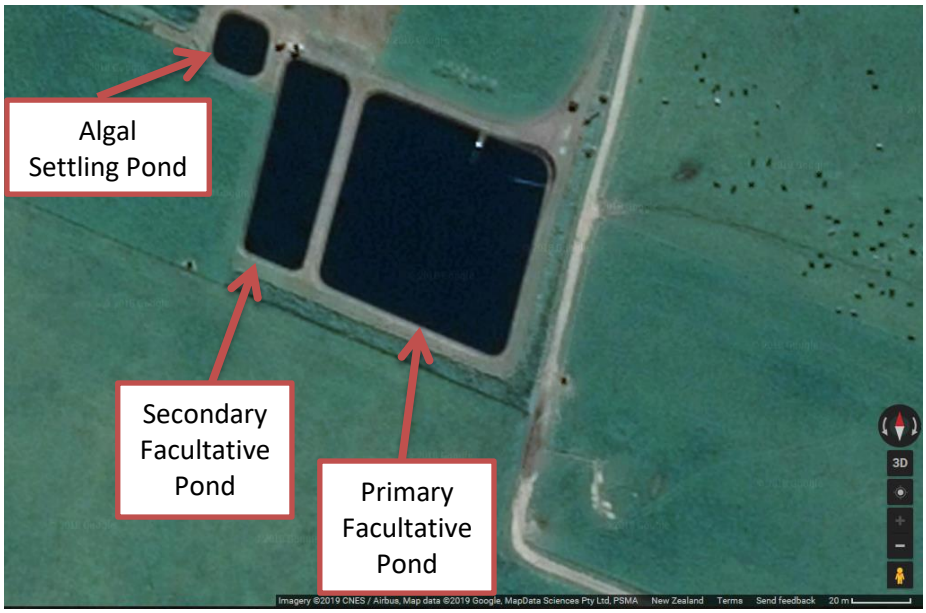

Figure 6.3: Satellite image of the current WSP system for Rongotea, New Zealand

Two alternative designs are given in Figure 6.4 for modifying the Rongotea WSP using either a primary facultative pond (middle) or a primary anaerobic pond (bottom). A rough guide to the size requirements of both of these primary ponds has been produced based on typical design guidelines from Mara (2005), assuming an influent BOD of 500 mgBOD/L (Rani & Dahiya 2008), an average temperature of 13°C, an average depth of 3m for the anaerobic pond, and 1.5m for the facultative pond (Mara 2005). This results in a primary anaerobic pond with an HRT of 3 days, or a primary facultative pond with an HRT of 55 days. As shown in Figure 6.4, if using a primary facultative pond, a new growth pond and one extra settler would be required. If instead a primary anaerobic pond is used, the flow direction could be reversed and then only two new algal settlers are required. Extra maturation ponds have been included in the anaerobic pond designed ‘luxury uptake’ system to utilise the space that is not required in the new retrofitted system.

As these recommendations are based on small-scale laboratory experiments that focused on increasing the phosphorus content of the biomass, further investigation into the other functions of a WSP system, such as pathogen removal, BOD removal, and nitrogen removal are required. As the total area of the WSP system does not change, one likely presumes that these functions are not negatively affected, however with the lower depths in the ‘luxury uptake’ system compared to a traditional facultative pond, there is potential for these other functions to be affected, and thus further research is needed before large scale application is considered.

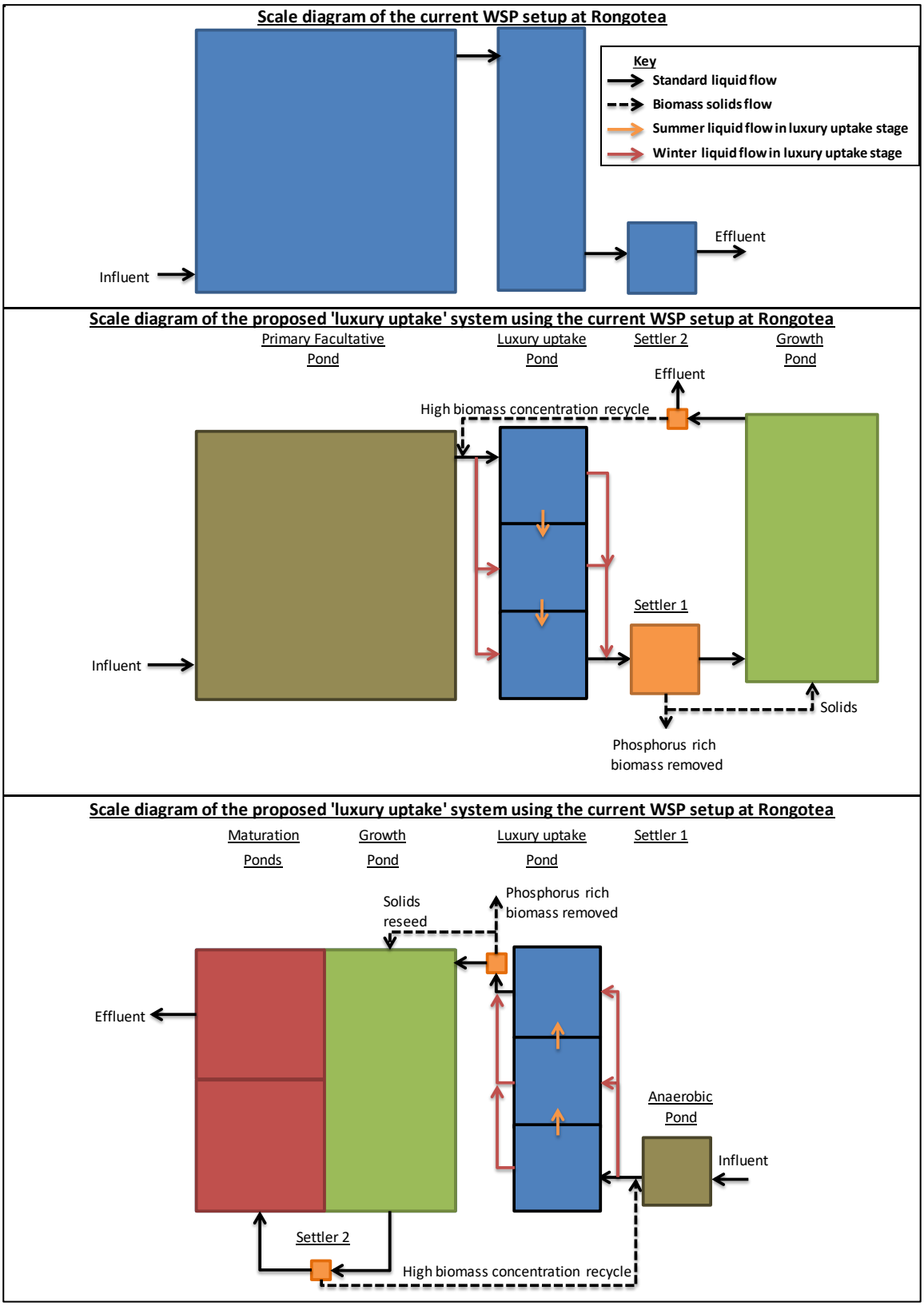

Figure 6.4: Proposed 'Luxury uptake' system based on the laboratory scale experiment using the current WSP setup at Rongotea. Top is the current setup, middle is the proposed setup using a primary facultative pond, and bottom is the proposed setup using a primary anaerobic pond. Note: maturation ponds are included in the bottom setup to utilise the remaining space leftover from the existing WSP at Rongotea. The flow patterns in the luxury uptake pond are shown earlier in Figure 6.1.

References

Achbergerová L. and Nahálka J. (2011). Polyphosphate - an ancient energy source and active metabolic regulator. *Microbial Cell Factories* **10**(1), 63.

Adams M. S., Dillon C. T., Vogt S., Lai B., Stauber J. and Jolley D. F. (2016). Copper Uptake, Intracellular Localization, and Speciation in Marine Microalgae Measured by Synchrotron Radiation X-ray Fluorescence and Absorption Microspectroscopy. *Environmental Science & Technology* **50**(16), 8827-39.

Aitchison P. A. and Butt V. S. (1973). The Relation between the Synthesis of Inorganic Polyphosphate and Phosphate Uptake by *Chlorella vulgaris*. *Journal of Experimental Botany* **24**(3), 497-510.

Ambarsari I., Brown B. E., Barlow R. G., Britton G. and Cummings D. (1997). Fluctuations in algal chlorophyll and carotenoid pigments during solar bleaching in the coral Goniastrea aspera at Phuket, Thailand. *Marine Ecology Progress Series* **159**, 303-7.

Arauzo M., Colmenarejo M. F., Martinez E. and Garcia M. G. (2000). The role of algae in a deep wastewater self-regeneration pond. *Water Research* **34**(14), 3666-74.

Arbib Z., Ruiz J., Alvarez-Diaz P., Garrido-Perez C., Barragan J. and Perales J. A. (2013). Effect of pH control by means of flue gas addition on three different photo-bioreactors treating urban wastewater in long-term operation. *Ecological Engineering* **57**, 226-35.

Ariesyady H. D., Fadilah R., Kurniasih K., Sulaeman A. and Kardena E. (2016). The Distribution of Microalgae in a Stabilization Pond System of a Domestic Wastewater Treatment Plant in a Tropical Environment (Case Study: Bojongsoang Wastewater Treatment Plant). *Journal of Engineering and Technological Sciences* **48**(1), 86-98.

Azad H. S. and Borchardt J. A. (1970). Variations in Phosphorus Uptake by Algae. *Environmental Science & Technology* **4**(9), 737-43.

Baker A. L. and Schmidt R. R. (1963). Intracellular distribution of phosphorus during synchronous growth of Chlorella pyrenoidosa. *Biochimica et Biophysica Acta* **74**, 75-83.

Baker A. L. and Schmidt R. R. (1964). Polyphosphate Metabolism during Nuclear Division in Synchronously Growing Chlorella. *Biochim Biophys Acta* **82**, 624-6.

Banat I., Puskas K., Esen I. and Al-Daher R. (1990). Wastewater treatment and algal productivity in an integrated ponding system. *Biological Wastes* **32**(4), 265-75.

Bechet Q., Shilton A. and Guieysse B. (2016). Maximizing Productivity and Reducing Environmental Impacts of Full-Scale Algal Production through Optimization of Open Pond Depth and Hydraulic Retention Time. *Environ Sci Technol* **50**(7), 4102-10.

Bental M., Pick U., Avron M. and Degani H. (1990). Metabolic studies with NMR spectroscopy of the alga Dunaliella salina trapped within agarose beads. *European Journal of Biochemistry* **188**(1), 111-6.

Bisgaard S. r. (1997). QUALITY QUANDARIES∗ Blocking Two-Level Factorials. *Quality Engineering* **9**(4), 753-9.

Blank L. M. (2012). The cell and P: from cellular function to biotechnological application. *Curr Opin Biotechnol* **23**(6), 846-51.

Bode G., Mauch F., Ditschuneit H. and Malfertheiner P. (1993). Identification of structures containing polyphosphate in Helicobacter pylori. *Journal of General Microbiology* **139**(12), 3029-33.

Bolier G., Dekoningh M. C. J., Schmale J. C. and Donze M. (1992). Differential Luxury Phosphate Response of Planktonic Algae to Phosphorus Removal. *Hydrobiologia* **243**, 113-8.

Bouarab L., Dauta A. and Loudiki M. (2004). Heterotrophic and mixotrophic growth of Micractinium pusillum Fresenius in the presence of acetate and glucose: effect of light and acetate gradient concentration. *Water Research* **38**(11), 2706-12.

Brahma S. K., Hargraves P. E., Howard W. F. and Nelson W. H. (1983). A Resonance Raman Method for the Rapid Detection and Identification of Algae in Water. *Applied Spectroscopy* **37**(1), 55-8.

Brown N. (unpublished). Quantification of polyphosphate in algae using Raman microscopy. In: *unpublished results*, Massey University.

Burczyk J. (1986). Cell wall carotenoids in green algae which form sporopollenins. *Phytochemistry* **26**(1), 121-8.

Carey C. C., Ibelings B. W., Hoffmann E. P., Hamilton D. P. and Brookes J. D. (2012). Eco-physiological adaptations that favour freshwater cyanobacteria in a changing climate. *Water Research* **46**(5), 1394-407.

Carrera J., Vicent T. and Lafuente J. (2004). Effect of influent COD/N ratio on biological nitrogen removal (BNR) from high-strength ammonium industrial wastewater. *Process Biochemistry* **39**(12), 2035-41.

Cembella A. D., Antia N. J. and Harrison P. J. (1982). The Utilization of Inorganic and Organic Phosphorus-Compounds as Nutrients by Eukaryotic Microalgae - a Multidisciplinary Perspective .1. *Crc Critical Reviews in Microbiology* **10**(4), 317-91.

Cembella A. D., Antia N. J. and Harrison P. J. (1984). The Utilization of Inorganic and Organic Phosphorus-Compounds as Nutrients by Eukaryotic Microalgae - a Multidisciplinary Perspective .2. *Crc Critical Reviews in Microbiology* **11**(1), 13-81.

Chisti Y. (2016). Large-Scale Production of Algal Biomass: Raceway Ponds. 21-40.

Chopin T., Lehmal H. and Halcrow K. (1997). Polyphosphates in the red macroalga *Chondrus crispus (Rhodophycea)*. *New Phytologist* **135**(4), 587-94.

Cohen J. (1992). A power primer. *Psychol Bull* **112**(1), 155-9.

Colthup N. B., Daly L. H. and Wiberley S. E. (1990). *Introduction to infrared and Raman spectroscopy*. Academic Press, Boston.

Cornet J. F., Dussap C. G. and Gros J. B. (1994). Conversion of radiant light energy in photobioreactors. *AIChE Journal* **40**(6), 1055-66.

Cornet J. F., Dussap C. G., Gros J. B., Binois C. and Lasseur C. (1995). A Simplified Monodimensional Approach for Modeling Coupling between Radiant Light Transfer and Growth-Kinetics in Photobioreactors. *Chemical Engineering Science* **50**(9), 1489-500.

Craggs R. (2005). Advanced integrated wastewater ponds. In: *Pond Treatment Technology* Shilton A (ed.), IWA Scientific and Technical Report Series, London, pp. 282-310.

Craggs R., Park J., Heubeck S. and Sutherland D. (2014). High rate algal pond systems for low-energy wastewater treatment, nutrient recovery and energy production. *New Zealand Journal of Botany* **52**(1), 60-73.

Craggs R., Park J., Sutherland D. and Heubeck S. (2015). Economic construction and operation of hectare-scale wastewater treatment enhanced pond systems. *Journal of Applied Phycology* **27**(5), 1913-22.

Crimp A. (2015). *Luxury uptake of phosphorus by microalgae in New Zealand waste stabilisation ponds*. Masters in Engineering, School of Engineering and Advanced Technology (SEAT), Massey University, Massey University.

Crimp A., Brown N. and Shilton A. (2018). Microalgal luxury uptake of phosphorus in waste stabilization ponds - frequency of occurrence and high performing genera. *Water Science and Technology* **78**(1-2), 165-73.

Cromar N. J., Fallowfield H. J. and Martin N. J. (1996). Influence of environmental parameters on biomass production and nutrient removal in a high rate algal pond operated by continuous culture. *Water Science and Technology* **34**(11), 133-40.

Curtis T. P., Mara D. D. and Silva S. A. (1992). Influence of pH, Oxygen, and Humic Substances on Ability of Sunlight To Damage Fecal Coliforms in Waste Stabilization Pond Water. *Applied and Environmental Microbiology* **58**(4), 1335-43.

Davies-Colley R. J., Donnison A. M., Speed D. J., Ross C. M. and Nagels J. W. (1999). Inactivation of faecal indicator micro-organisms in waste stabilisation ponds: interactions of environmental factors with sunlight. *Water Research* **33**(5), 1220-30.

Davis E. M. and Wilcomb M. J. (1967). Enzymatic Degradation and Assimilation of Condensed Phosphates by Green Algae. *Water Research* **1**(5), 335-8.

Dementjev A. and Kostkeviciene J. (2013). Applying the method of Coherent Anti-stokes Raman microscopy for imaging of carotenoids in microalgae and cyanobacteria. *Journal of Raman Spectroscopy* **44**(7), 973-9.

Diaz J., Ingall E., Vogt S., de Jonge M. D., Paterson D., Rau C. and Brandes J. A. (2009). Characterization of phosphorus, calcium, iron, and other elements in organisms at sub-micron resolution using X-ray fluorescence spectromicroscopy. *Limnology and Oceanography-Methods* **7**, 42-51.

Ebel J. P., Colas J. and Muller S. (1958). Presence de polyphosphates chez divers organismes inferieurs. *Experimental Cell Research* **15**(1), 36-42.

Eixler S., Karsten U. and Selig U. (2006). Phosphorus storage in Chlorella vulgaris (Trebouxiophyceae, Chlorophyta) cells and its dependence on phosphate supply. *Phycologia* **45**(1), 53-60.

Elgavish A., Elgavish G. A., Halmann M., Berman T. and Shomer I. (1980). Intracellular phosphorus pools in intact algal cells: 31P NMR and transmission electron microscopy studies. *FEBS Lett* **117**(1), 137-42.

Fagerbakke K. M., Heldal M. and Norland S. (1996). Content of carbon, nitrogen, oxygen, sulfur and phosphorus in native aquatic and cultured bacteria. *Aquatic Microbial Ecology* **10**(1), 15-27.

Furtado A. L. F. F., Calijuri M. D., Lorenzi A. S., Honda R. Y., Genuario D. B. and Fiore M. F. (2009). Morphological and molecular characterization of cyanobacteria from a Brazilian facultative wastewater stabilization pond and evaluation of microcystin production. *Hydrobiologia* **627**(1), 195-209.

Garcia J., Mujeriego R., Bourrouet A., Penuelas G. and Freixes A. (2000). Wastewater treatment by pond systems: experiences in Catalonia, Spain. *Water Science and Technology* **42**(10-11), 35-42.

García J., Mujeriego R. and Hernández-Mariné M. (2000). High rate algal pond operating strategies for urban wastewater nitrogen removal. *Journal of Applied Phycology* **12**(3-5), 331-9.

Ghazy M., El-Senousy W. M., Abdel-Aatty A. M. and Kamel M. (2008). Performance evaluation of a waste stabilisation pond in a rural area in Egypt. *American Journal of Environmental Science* **4**(4), 316-25.

Godos I. d., Blanco S., García-Encina P. A., Becares E. and Muñoz R. (2009). Long-term operation of high rate algal ponds for the bioremediation of piggery wastewaters at high loading rates. *Bioresource Technology* **100**(19), 4332-9.

Goldberg J., Gonzalez H., Jensen T. E. and Corpe W. A. (2001). Quantitative analysis of the elemental composition and the mass of bacterial polyphosphate bodies using STEM EDX. *Microbios* **106**(415), 177-88.

Goldman J. C. (1980). Physiological aspects in algal mass cultures. In: *Algae Biomass: Production and Use* G. Shelef CJS (ed.), Elsevier, Amsterdam.

Guiry M. D. and Guiry G. M. (2017). AlgaeBase. http://www.algaebase.org (accessed 02 February 2017).

Hadiyanto H., Elmore S., Van Gerven T. and Stankiewicz A. (2013). Hydrodynamic evaluations in high rate algae pond (HRAP) design. *Chemical Engineering Journal* **217**, 231-9.

Harold F. M. (1966). Inorganic polyphosphates in biology: structure, metabolism, and function. *Bacteriol Rev* **30**(4), 772-94.

Harris E. H. (2001). Chlamydomonas as a model organism. *Annual Review of Plant Physiology and Plant Molecular Biology* **52**(1), 363-406.

Healey F. P. (1979). Short-Term Responses of Nutrient-Deficient Algae to Nutrient Addition1. *Journal of Phycology* **15**(3), 289-99.

Henry J. T. and Crosson S. (2013). Chromosome replication and segregation govern the biogenesis and inheritance of inorganic polyphosphate granules. *Molecular Biology of the Cell* **24**(20), 3177-86.

Heo J., Cho D.-H., Ramanan R., Oh H.-M. and Kim H.-S. (2015). PhotoBiobox: A tablet sized, low-cost, high throughput photobioreactor for microalgal screening and culture optimization for growth, lipid content and CO2 sequestration. *Biochemical Engineering Journal* **103**, 193-7.

Heraud P., Wood B. R., Beardall J. and McNaughton D. (2006). Effects of pre-processing of Raman spectra on in vivo classification of nutrient status of microalgal cells. *Journal of Chemometrics* **20**(5), 193-7.

Herrmann E. C. and Schmidt R. R. (1965). Synthesis of Phosphorus-Containing Macromolecules during Synchronous Growth of Chlorella Pyrenoidosa. *Biochim Biophys Acta* **95**, 63-75.

Hupfer M., Gloss S., Schmieder P. and Grossart H. P. (2008). Methods for detection and quantification of polyphosphate and polyphosphate accumulating microorganisms in aquatic sediments. *International Review of Hydrobiology* **93**(1), 1-30.

Jacobson L., Halmann M. and Yariv J. (1982). The molecular composition of the volutin granule of yeast. *Biochemical Journal* **201**(3), 473-9.

Jones R. I. (1990). Phosphorus Transformations in the Epilimnion of Humic Lakes - Biological Uptake of Phosphate. *Freshwater Biology* **23**(2), 323-37.

Kaplan D., Richmond A. E., Dubinsky Z. and Aaronson A. (1986). Algal nutrition. In: *CRC Handbook of Microalgal Mass Culture* Richmond AE (ed.), CRC Press, Boca Raton.

Kayombo S., Mbwette T. S. A., Katima J. H., Ladegaard N. and Jorgensen S. E. (2004). *Waste Stabilization Ponds and Constructed Wetlands: Design Manual*. United Nations Environment Programme.

Kim J., Lee J. Y. and Lu T. (2014). Effects of dissolved inorganic carbon and mixing on autotrophic growth of Chlorella vulgaris. *Biochemical Engineering Journal* **82**, 34-40.

Kingsbury J. M. (1956). On Pigment Changes and Growth in the Blue-Green Alga, Plectonema Nostocorum Bornet Ex Gomont. *The Biological Bulletin* **110**(3), 310-9.

Kooijman S. A., Muller E. B. and Stouthamer A. H. (1991). Microbial growth dynamics on the basis of individual budgets. *Antonie Van Leeuwenhoek* **60**(3-4), 159-74.

Kornberg A., Rao N. N. and Ault-Riche D. (1999). Inorganic polyphosphate: a molecule of many functions. *Annual Review of Biochemistry* **68**, 89-125.

Krauss R. W. (1976). Inorganic Nutrition of Algae. In: *Algal Culture: From laboratory to pilot plant* Burlew JS (ed.), Carnegie Institution of Washington, Washington D.C., pp. 211-30.

Kuhl A. (1962). Inorganic phosphorus uptake and metabolism. In: *Physiology and biochemistry of algae*, Academic Press, New York, pp. 211-30.

Kuhl A. (1977). Phosphorus. In: *Algal physiology and biochemistry* Stewart WD (ed.), Blackwell Scientific Publications Ltd, Oxford, pp. 636-54.

Kulaev I. S., Vagabov V. M. and Kulakovskaya T. V. (2004). *The biochemistry of inorganic polyphosphates*. Wiley & Sons, Chichester, West Sussex.

Larsdotter K., La Cour Jansen J. and Dalhammar G. (2007). Biologically mediated phosphorus precipitation in wastewater treatment with microalgae. *Environmental Technology* **28**(9), 953-60.

Lau P. S., Tam N. F. Y. and Wong Y. S. (1995). Effect of algal density on nutrient removal from primary settled wastewater. *Environmental Pollution* **89**(1), 59-66.

Laws E. A. (1975). The Importance of Respiration Losses in Controlling the Size Distribution of Marine Phytoplankton. *Ecology* **56**(2), 419-26.

Lean D. R. (1984). Metabolic indicators for phosphorus limitation. *Journal of Verhandlungen des Internationalen Verein Limnologie* **22**, 211-8.

Lee Y.-K. and Shen H. (2007). Basic Culturing Techniques. In: *Handbook of Microalgal Culture*, Blackwell Publishing Ltd, pp. 40-56.

Leitao J., Lorenz B., Bachinski N., Wilhelm C., Müller W. and Schröder H. (1995). Osmotic-stress-induced synthesis and degradation of inorganic polyphosphates in the alga Phaeodactylumtricornutum. *Marine Ecology Progress Series* **121**, 279-88.

Leupold M., Hindersin S., Gust G., Kerner M. and Hanelt D. (2012). Influence of mixing and shear stress on Chlorella vulgaris, Scenedesmus obliquus, and Chlamydomonas reinhardtii. *Journal of Applied Phycology* **25**(2), 485-95.

Lins U. and Farina M. (1999). Phosphorus-rich granules in uncultured magnetotactic bacteria. *FEMS Microbiology Letters* **172**(1), 23-8.

Lurling M., Eshetu F., Faassen E. J., Kosten S. and Huszar V. L. M. (2013). Comparison of cyanobacterial and green algal growth rates at different temperatures. *Freshwater Biology* **58**(3), 552-9.

Lurling M. and Van Donk E. (1997). Morphological changes in Scenedesmus induced by infochemicals released in situ from zooplankton grazer. *Limnology and Oceanography* **42**(4), 783-8.

Majed N. and Gu A. Z. (2010). Application of Raman microscopy for simultaneous and quantitative evaluation of multiple intracellular polymers dynamics functionally relevant to enhanced biological phosphorus removal processes. *Environ Sci Technol* **44**(22), 8601-8.

Majed N., Li Y. and Gu A. Z. (2012). Advances in techniques for phosphorus analysis in biological sources. *Current Opinion in Biotechnology* **23**(6), 852-9.

Majed N., Matthaus C., Diem M. and Gu A. Z. (2009). Evaluation of Intracellular Polyphosphate Dynamics in Enhanced Biological Phosphorus Removal Process using Raman Microscopy. *Environmental Science & Technology* **43**(14), 5436-42.

Mara D. (2005). Pond process design - a practical guide. In: *Pond Treatment Technology* Shilton A (ed.), IWA Scientific and Technical Report Series, London, pp. 168-87.

Mara D. and Pearson H. (1998). *Design manual for waste stabilization ponds in Mediterranean countries*. Lagoon Technology International, Leeds, UK.

Markou G., Vandamme D. and Muylaert K. (2014). Microalgal and cyanobacterial cultivation: The supply of nutrients. *Water Research* **65**, 186-202.

Martinez M. E., Sanchez S., Jimenez J. M., El Yousfi F. and Munoz L. (2000). Nitrogen and phosphorus removal from urban wastewater by the microalga Scenedesmus obliquus. *Bioresource Technology* **73**(3), 263-72.

Maurer M., Abramovich D., Siegrist H. and Gujer W. (1999). Kinetics of biologically induced phosphorus precipitation in waste-water treatment. *Water Research* **33**(2), 484-93.

Mayo A. W. and Noike T. (1996). Effects of temperature and pH on the growth of heterotrophic bacteria in waste stabilization ponds. *Water Research* **30**(2), 447-55.

Mburu N., Tebitendwa S. M., van Bruggen J. J., Rousseau D. P. and Lens P. N. (2013). Performance comparison and economics analysis of waste stabilization ponds and horizontal subsurface flow constructed wetlands treating domestic wastewater: a case study of the Juja sewage treatment works. *Environmental Management* **128**, 220-5.

Mehrabadi A., Craggs R. and Farid M. M. (2016). Biodiesel production potential of wastewater treatment high rate algal pond biomass. *Bioresource Technology* **221**, 222-33.

Menya E., Wangi G. M., Amanyire F. and Ebangu B. (2013). Design of waste stabilization ponds for dairy processing plants in Uganda. *Agricultural Engineering International* **15**(3), 198-207.

Metcalf & Eddy I. (2003). *Wastewater Engineering - Treatment and Reuse*. Mc Graw Hill.

Minitab (2010). Minitab® 17 Statistical Software. In, Minitab Inc., State College, PA.

Miyachi S., Kanai R., Mihara S., Miyachi S. and Aoki S. (1964). Metabolic Roles of Inorganic Polyphosphates in Chlorella Cells. *Biochim Biophys Acta* **93**(3), 625-34.

Miyachi S. and Miyachi S. (1961). Modes of formation of phosphate compounds and their turnover in chlorella cells during the process of life cycle as studied by the technique of synchronous culture. *Plant and Cell Physiology* **2**(4), 415-24.

Miyachi S. and Tamiya H. (1961a). Distribution and turnover of phosphate compounds in growing chlorella cells. *Plant and Cell Physiology* **2**(4), 405-14.

Miyachi S. and Tamiya H. (1961b). Some observations on the phosphorus metabolism in growing Chlorella cells. *BBA - Biochimica et Biophysica Acta* **46**(1), 200-2.

Molina E., Fernández J., Acién F. G. and Chisti Y. (2001). Tubular photobioreactor design for algal cultures. *Journal of Biotechnology* **92**(2), 113-31.

Moss B. (1973). The Influence of Environmental Factors on the Distribution of Freshwater Algae: An Experimental Study: III. Effects of Temperature, Vitamin Requirements and Inorganic Nitrogen Compounds on Growth. *The Journal of Ecology* **61**(1), 179.

Moudříková Š., Sadowsky A., Metzger S., Nedbal L., Mettler-Altmann T. and Mojzeš P. (2017). Quantification of Polyphosphate in Microalgae by Raman Microscopy and by a Reference Enzymatic Assay. *Analytical Chemistry* **89**(22), 12006-13.

Nishikawa K., Machida H., Yamakoshi Y., Ohtomo R., Saito K., Saito M. and Tominaga N. (2006). Polyphosphate metabolism in an acidophilic alga *Chlamydomonas acidophila* KT-1 (*Chlorophyta*) under phosphate stress. *Plant Science* **170**(2), 307-13.

Nurdogan Y. and Oswald W. J. (1995). Enhanced Nutrient Removal in High-Rate Ponds. *Water Science and Technology* **31**(12), 33-43.

Nyholm N. (1978). Dynamics of phosphate limited algal growth: simulation of phosphate shocks. *Theoretical Biology* **70**(4), 415-25.

Oliveira S. C. and Von Sperling M. (2008). Reliability analysis of wastewater treatment plants. *Water Research* **42**(4-5), 1182-94.

Parab N. D. and Tomar V. (2012). Raman Spectroscopy of Algae: A Review. *Journal of Nanomedicine & Nanotechnology* **3**(2), 1-7.

Park J. B. and Craggs R. J. (2010). Wastewater treatment and algal production in high rate algal ponds with carbon dioxide addition. *Water Science and Technology* **61**(3), 633-9.

Park J. B., Craggs R. J. and Shilton A. N. (2011a). Wastewater treatment high rate algal ponds for biofuel production. *Bioresource Technology* **102**(1), 35-42.

Park J. B. K., Craggs R. J. and Shilton A. N. (2011b). Recycling algae to improve species control and harvest efficiency from a high rate algal pond. *Water Research* **45**(20), 6637-49.

Park J. B. K., Craggs R. J. and Tanner C. C. (2018). Eco-friendly and low-cost Enhanced Pond and Wetland (EPW) system for the treatment of secondary wastewater effluent. *Ecological Engineering* **120**, 170-9.

Pearson H. (2005). Microbiology of waste stabilisation ponds. In: *Pond Treatment Technology* Shilton A (ed.), IWA Publishing, London, pp. 14-48.

Pembrey R. S., Marshall K. C. and Schneider R. P. (1999). Cell surface analysis techniques: What do cell preparation protocols do to cell surface properties? *Appl Environ Microbiol* **65**(7), 2877-94.

Peng J. F., Wang B. Z., Song Y. H., Yuan P. and Liu Z. H. (2007). Adsorption and release of phosphorus in the surface sediment of a wastewater stabilization pond. *Ecological Engineering* **31**(2), 92-7.

Perez-Garcia O., Bashan Y. and Esther Puente M. (2011). Organic Carbon Supplementation of Sterilized Municipal Wastewater Is Essential for Heterotrophic Growth and Removing Ammonium by the Microalga Chlorella Vulgaris. *Journal of Phycology* **47**(1), 190-9.

Pham D. T., Everaert G., Janssens N., Alvarado A., Nopens I. and Goethals P. L. M. (2014). Algal community analysis in a waste stabilisation pond. *Ecological Engineering* **73**, 302-6.

Pollingher U. and Berman T. (1975). Autoradiographic screening for potential heterotrophs in natural algal populations of Lake Kinneret. *Microbial Ecology* **2**(4), 252-60.

Portielje R. and Lijklema L. (1994). Kinetics of luxury uptake of phosphate by algae-dominated benthic communities. *Hydrobiologia* **275-276**(1), 349-58.

Pottier L., Pruvost J., Deremetz J., Cornet J. F., Legrand J. and Dussap C. G. (2005). A fully predictive model for one-dimensional light attenuation by Chlamydomonas reinhardtii in a torus photobioreactor. *Biotechnol Bioeng* **91**(5), 569-82.

Powell N., Shilton A., Chisti Y. and Pratt S. (2009). Towards a luxury uptake process via microalgae - Defining the polyphosphate dynamics. *Water Research* **43**(17), 4207-13.

Powell N., Shilton A., Pratt S. and Chisti Y. (2006a). Luxury uptake of phosphorus by microalgae in waste stabilisation ponds. In: *Young Researchers 2006 (Water and Environment Management Series no. 12)*, IWA Publishing, pp. 249-56.

Powell N., Shilton A., Pratt S. and Chisti Y. (2011a). Luxury uptake of phosphorus by microalgae in full-scale waste stabilisation ponds. *Water Science and Technology* **63**(4), 704-9.

Powell N., Shilton A., Pratt S. and Chisti Y. (2011b). Phosphate release from waste stabilisation pond sludge: significance and fate of polyphosphate. *Water Science and Technology* **63**(8), 1689-94.

Powell N., Shilton A., Pratt S., Chisti Y. and Grigg N. (2006b). Factors effecting biological phosphorus removal in waste stabilisation ponds - A statistical analysis. In: *7th IWA specialist conference on waste stabilisation ponds*, Bangkok, Thailand.

Powell N., Shilton A. N., Pratt S. and Chisti Y. (2008). Factors influencing luxury uptake of phosphorus by microalgae in waste stabilization ponds. *Environmental Science & Technology* **42**(16), 5958-62.

Pruvost J., Van Vooren G., Cogne G. and Legrand J. (2009). Investigation of biomass and lipids production with Neochloris oleoabundans in photobioreactor. *Bioresource Technology* **100**(23), 5988-95.

Qu C.-B., Wu Z.-Y. and Shi X.-M. (2008). Phosphate assimilation by Chlorella and adjustment of phosphate concentration in basal medium for its cultivation. *Biotechnology Letters* **30**(10), 1735-40.

Racki L. R., Tocheva E. I., Dieterle M. G., Sullivan M. C., Jensen G. J. and Newman D. K. (2017). Polyphosphate granule biogenesis is temporally and functionally tied to cell cycle exit during starvation in Pseudomonas aeruginosa. *Proceedings of the National Academy of Sciences* **114**(12), E2440-E9.

Rani D. and Dahiya R. P. (2008). COD and BOD removal from domestic wastewater generated in decentralised sectors. *Bioresource Technology* **99**(2), 344-9.

Ren L., Rabalais N. N., Turner R. E., Morrison W. and Mendenhall W. (2009). Nutrient Limitation on Phytoplankton Growth in the Upper Barataria Basin, Louisiana: Microcosm Bioassays. *Estuaries and Coasts* **32**(5), 958-74.

Rhee G. Y. (1973). A continuous culture study of phosphate uptake. Growth rate and polyphosphate in *Scenedesmus* sp. *Journal of Phycology* **9**(4), 12.

Rice E. W., Baird R. B. and Eaton A. D. (2017). *Standard Methods for the Examination of Water and Wastewater*. 23rd edn. American Public Health Association, Washington, DC.

Rosemarin A. S. (1982). Phosphorus Nutrition of Two Potentially Competing Filamentous Algae, Cladophora Glomerata (L.) Kütz. and Stigeoclonium Tenue (Agardh) Kütz. from Lake Ontario. *Journal of Great Lakes Research* **8**(1), 66-72.

Ruiz-Marin A., Mendoza-Espinosa L. G. and Stephenson T. (2010). Growth and nutrient removal in free and immobilized green algae in batch and semi-continuous cultures treating real wastewater. *Bioresource Technology* **101**(1), 58-64.

Ruiz F. A., Marchesini N., Seufferheld M., Govindjee and Docampo R. (2001). The polyphosphate bodies of Chlamydomonas reinhardtii possess a proton-pumping pyrophosphatase and are similar to acidocalcisomes. *J Biol Chem* **276**(49), 46196-203.

Sánchez J. F., Fernández-Sevilla J. M., Acién F. G., Cerón M. C., Pérez-Parra J. and Molina-Grima E. (2008). Biomass and lutein productivity of Scenedesmus almeriensis: influence of irradiance, dilution rate and temperature. *Applied Microbiology and Biotechnology* **79**(5), 719-29.

Schelske C. L. and Sickogoad L. (1990). Effect of Chelated Trace-Metals on Phosphorus Uptake and Storage in Natural Assemblages of Lake-Michigan Phytoplankton. *Journal of Great Lakes Research* **16**(1), 82-9.

Schmidt J. J., Gagnon G. A. and Jamieson R. C. (2016). Microalgae growth and phosphorus uptake in wastewater under simulated cold region conditions. *Ecological Engineering* **95**, 588-93.

Schonborn C., Bauer H. D. and Roske I. (2001). Stability of enhanced biological phosphorus removal and composition of polyphosphate granules. *Water Research* **35**(13), 3190-6.

Schuster K. C., Urlaub E. and Gapes J. R. (2000). Single-cell analysis of bacteria by Raman microscopy: spectral information on the chemical composition of cells and on the heterogeneity in a culture. *J Microbiol Methods* **42**(1), 29-38.

Selig U., Michalik M. and Huebener T. (2006). Assessing P status and trophic level of two lakes by speciation of particulate phosphorus forms. *Journal of Limnology* **65**(1), 17-26.

Sells M. D., Brown N. and Shilton A. N. (2018). Determining variables that influence the phosphorus content of waste stabilization pond algae. *Water Research* **132**, 301-8.

Sforza E., Calvaruso C., La Rocca N. and Bertucco A. (2018). Luxury uptake of phosphorus in Nannochloropsis salina : Effect of P concentration and light on P uptake in batch and continuous cultures. *Biochemical Engineering Journal* **134**, 69-79.

Shanthala M., Hosmani S. P. and Hosetti B. B. (2009). Diversity of phytoplanktons in a waste stabilization pond at Shimoga Town, Karnataka State, India. *Environmental Monitoring and Assessment* **151**(1-4), 437-43.

Shelef G. (1982). High-Rate Algae Ponds for Wastewater-Treatment and Protein-Production. *Water Science and Technology* **14**(1-2), 439-52.

Shilton A. and Sweeney D. (2005). Hydraulic design. In: *Pond Treatment Technology* Shilton A (ed.), IWA Scientific and Technical Report Series, London, pp. 188-217.

Shilton A. and Walmsley N. (2005). Introduction to pond treatment technology. In: *Pond Treatment Technology* Shilton A (ed.), IWA Publishing, London, pp. 1-13.

Shilton A. N., Powell N. and Guieysse B. (2012). Plant based phosphorus recovery from wastewater via algae and macrophytes. *Current Opinion in Biotechnology* **23**(6), 884-9.

Siderius M., Musgrave A., Ende H., Koerten H., Cambier P. and Meer P. (1996). Chlamydomonas Eugametos (Chlorophyta) Stores Phosphate in Polyphosphate Bodies Together with Calcium. *Journal of Phycology* **32**(3), 402-9.

Silva-Benavides A. M. and Torzillo G. (2012). Nitrogen and phosphorus removal through laboratory batch cultures of microalga *Chlorella vulgaris* and cyanobacterium *Planktothrix isothrix* grown as monoalgal and as co-cultures. *Journal of Applied Phycology* **24**(2), 267-76.

Smith F. A. (1966). Active phosphate uptake by Nitella translucens. *Biochim Biophys Acta* **126**(1), 94-9.

Smith R. E. H. and Kalff J. (1982). Size-Dependent Phosphorus Uptake Kinetics and Cell Quota in Phytoplankton. *Journal of Phycology* **18**(2), 275-84.

Solovchenko A., Verschoor A. M., Jablonowski N. D. and Nedbal L. (2016). Phosphorus from wastewater to crops: An alternative path involving microalgae. *Biotechnology Advances* **34**(5), 550-64.

Sonmez C., Elcin E., Akın D., Oktem H. A. and Yucel M. (2016). Evaluation of novel thermo-resistant Micractinium and Scenedesmus sp. for efficient biomass and lipid production under different temperature and nutrient regimes. *Bioresource Technology* **211**, 422-8.

Spijkerman E. and Coesel P. F. M. (1998). Different Response Mechanisms of Two Planktonic Desmid Species (Chlorophyceae) to a Single Saturating Addition of Phosphate. *Journal of Phycology* **34**(3), 438-45.

Stevenson R. J. and Stoermer E. F. (1982). Luxury consumption of phosphorus by five Cladophora epiphytes in Lake Huron. *Transactions of the American Microscopical Society* **101**(2), 151-61.

Su Y., Mennerich A. and Urban B. (2012). Comparison of nutrient removal capacity and biomass settleability of four high-potential microalgal species. *Bioresource Technology* **124**, 157-62.

Sutherland D. L., Turnbull M. H., Broady P. A. and Craggs R. J. (2014). Wastewater microalgal production, nutrient removal and physiological adaptation in response to changes in mixing frequency. *Water Research* **61**, 130-40.

Suttle C. A., Stockner J. G. and Harrison P. J. (1987). Effects of Nutrient Pulses on Community Structure and Cell Size of a Freshwater Phytoplankton Assemblage in Culture. *Canadian Journal of Fisheries and Aquatic Sciences* **44**(10), 1768-74.

Torzillo G., Pushparaj B., Masojidek J. and Vonshak A. (2003). Biological constraints in algal biotechnology. *Biotechnology and Bioprocess Engineering* **8**(6), 338-48.

Turpin D. H. and Harrison P. J. (1979). Limiting Nutrient Patchiness and Its Role in Phytoplankton Ecology. *Journal of Experimental Marine Biology and Ecology* **39**(2), 151-66.

Voelz H., Voelz U. and Ortigoza R. O. (1966). The polyphosphate overplus phenomenon in *Myxococcus zanthus* and its influence on the architecture of the cell. *Archives of Microbiology* **53**(4), 371-88.

Walmsley N. and Shilton A. (2005). Solids and organics. In: *Pond Treatment Technology* Shilton A (ed.), IWA Publishing, London, pp. 66-76.

Wei X., Jie D. F., Cuello J. J., Johnson D. J., Qiu Z. J. and He Y. (2014). Microalgal detection by Raman microspectroscopy. *Trends in Analytical Chemistry* **53**, 33-40.

Weissman J. C., Goebel R. P. and Benemann J. R. (1988). Photobioreactor design: Mixing, carbon utilization, and oxygen accumulation. *Biotechnology and Bioengineering* **31**(4), 336-44.

Werner T. P., Amrhein N. and Freimoser F. M. (2007). Inorganic polyphosphate occurs in the cell wall of Chlamydomonas reinhardtii and accumulates during cytokinesis. *BMC Plant Biology* **7**(1), 51.

Whitton B. A., Grainger S. L., Hawley G. R. and Simon J. W. (1991). Cell-bound and extracellular phosphatase activities of cyanobacterial isolates. *Microbial Ecology* **21**(1), 85-98.

Woertz I., Feffer A., Lundquist T. and Nelson Y. (2009). Algae Grown on Dairy and Municipal Wastewater for Simultaneous Nutrient Removal and Lipid Production for Biofuel Feedstock. *Journal of Environmental Engineering* **135**(11), 1115-22.

Wood B. R., Heraud P., Stojkovic S., Morrison D., Beardall J. and McNaughton D. (2005). A portable Raman acoustic levitation spectroscopic system for the identification and environmental monitoring of algal cells. *Analytical Chemistry* **77**(15), 4955-61.

Wu L. F., Chen P. C. and Lee C. M. (2013). The effects of nitrogen sources and temperature on cell growth and lipid accumulation of microalgae. *International Biodeterioration & Biodegradation* **85**, 506-10.

Young P., Taylor M. and Fallowfield H. J. (2017). Mini-review: high rate algal ponds, flexible systems for sustainable wastewater treatment. *World Journal of Microbiology and Biotechnology* **33**(6).

Yue T., Zhang D. and Hu C. (2013). Comparative studies on phosphate utilization of two bloom-forming *Microcystis spp*. (cyanobacteria) isolated from Lake Taihu (China). *Journal of Applied Phycology* **26**(1), 333-9.

Zachleder V., Bisova K., Vitova M., Kubin S. and Hendrychova J. (2002). Variety of cell cycle patterns in the alga Scenedesmus quadricauda (Chlorophyta) as revealed by application of illumination regimes and inhibitors. *European Journal of Phycology* **37**(3), 361-71.

Zhang E., Wang B., Wang Q., Zhang S. and Zhao B. (2008). Ammonia–nitrogen and orthophosphate removal by immobilized Scenedesmus sp. isolated from municipal wastewater for potential use in tertiary treatment. *Bioresource Technology* **99**(9), 3787-93.

Zhao Y. T., Zhao P., Li T., Wang L. and Yu X. Y. (2013). The Influence of Glucose on Growth and Lipid Production under Heterotrophic and Mixotrophic Conditions for Monoraphidium sp. FXY-10. *Advanced Materials Research* **864-867**, 49-55.

Zhou W., Min M., Li Y., Hu B., Ma X., Cheng Y., Liu Y., Chen P. and Ruan R. (2012). A hetero-photoautotrophic two-stage cultivation process to improve wastewater nutrient removal and enhance algal lipid accumulation. *Bioresource Technology* **110**, 448-55.

Appendices

8.2 Appendix for Chapter 2: Screening of variables

8.2.1 Synthetic wastewater recipe

The standard synthetic wastewater recipe from Davis and Wilcomb (1967) is given in Table 8.1 and Table 8.2.

Table 8.1: Synthetic wastewater composition according to Davis and Wilcomb (1967)

Chemical	Concentration (mg/L)
$Ca(NO_3)_2$	60
KNO_3	70
NH_4Cl	57
KH_2PO_4	20
NaCl	70
$MgSO_4$	20
$NaHCO_3$	125
$Na_3C_6H_5O_7$	250
Na_2SiO_3	0.05 mL/L
Hutners trace elements	1 mL/L

Table 8.2: Hutners trace elements composition according to Davis and Wilcomb (1967)

Chemical	Concentration (mg/L)
EDTA	5.0
$ZnSO_4$	2.0
H_3BO_3	1.0
$CaCl_2$	0.662
$MnCl_2$	0.50
$FeSO_4$	0.50
$CoCl_2$	0.15
$CuSO_4$	0.15
$(NH_4)_6Mo_7O_{24}$	0.10

This synthetic wastewater was used as it represents a typical secondary wastewater (Davis & Wilcomb 1967). The synthetic wastewater contained chelating chemicals that prevent phosphorus precipitation at high pH to ensure phosphorus removal was due to biological uptake. Modifications to the phosphorus concentration were made by addition or removal of KH_2PO_4. The organic load was modified through the addition of glucose. Glucose was used to allow for rapid heterotrophic growth during the batch experiments.

8.2.2 Growth and phosphorus removal data used to calculate the phosphorus content of the biomass

8.2.2.1 Organic loading

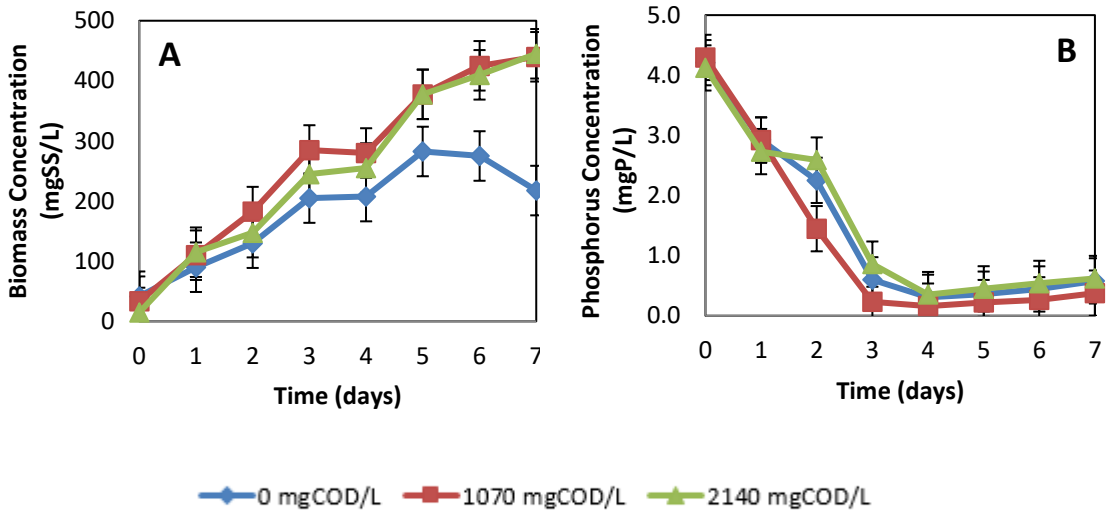

Figure 8.1: Effect of organic loading on biomass concentration (A) and phosphorus removal (B).

As seen in Figure 8.1, the addition of organic carbon resulted in an increased biomass concentration (A) while having no significant (90% confidence) effect on phosphorus removal (B). The increased biomass concentration is expected due to the heterotrophic growth of both algae and bacteria with the addition of organic carbon.

8.2.2.2 Cation concentration

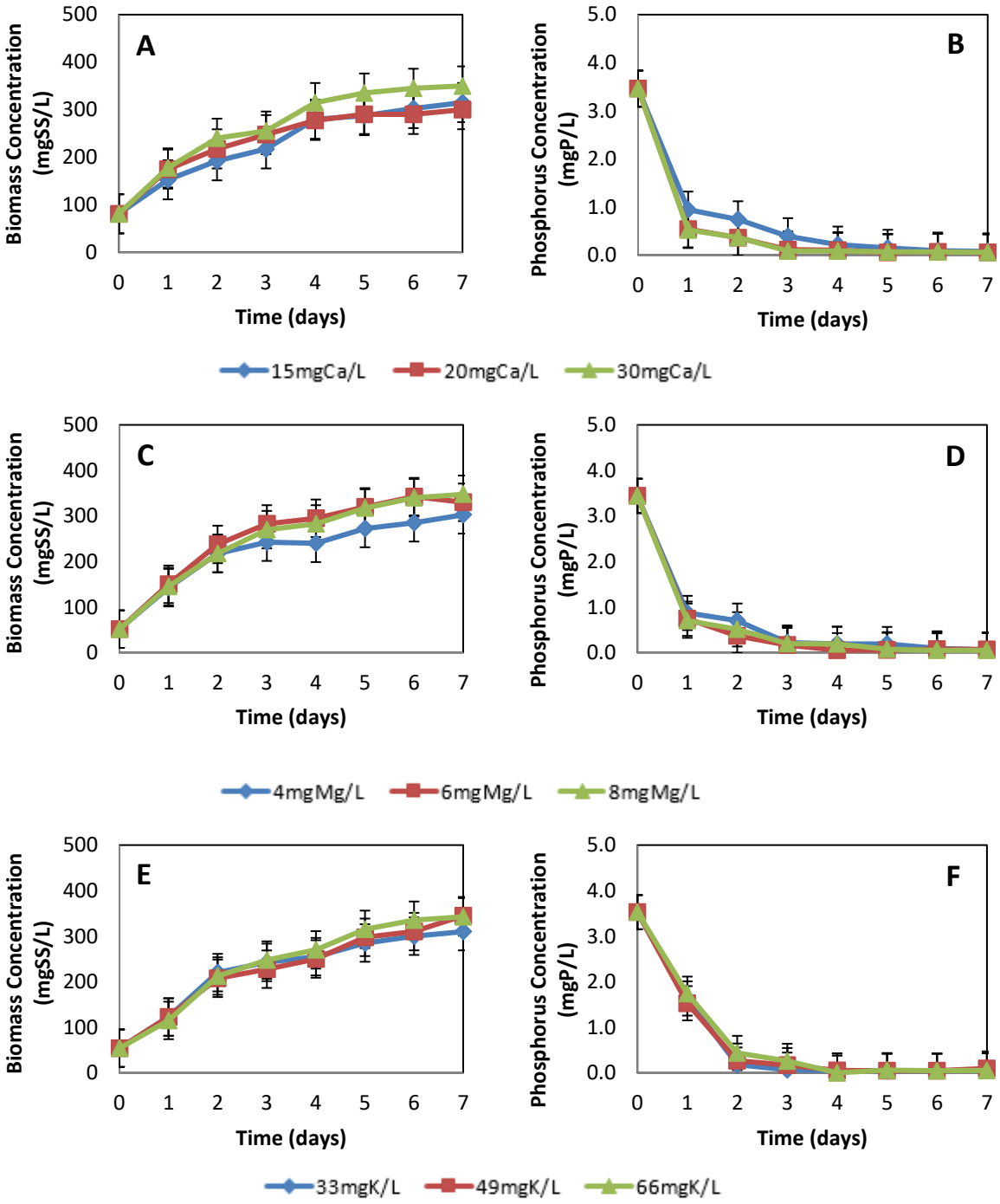

Figure 8.2: Effect of calcium, magnesium, and potassium concentration on the biomass concentration (A, C, E respectively) and phosphorus removal (B, D, F respectively).

As seen in Figure 8.2, the addition of calcium (A and B), magnesium (C and D), or potassium (E and F) had no significant effect (90% confidence) on the biomass concentration or phosphorus removal. This suggests the concentration of these cations in typical secondary wastewater (Davis & Wilcomb 1967) is not limiting for growth or phosphorus removal.

8.2.2.3 Prior phosphorus content of the biomass

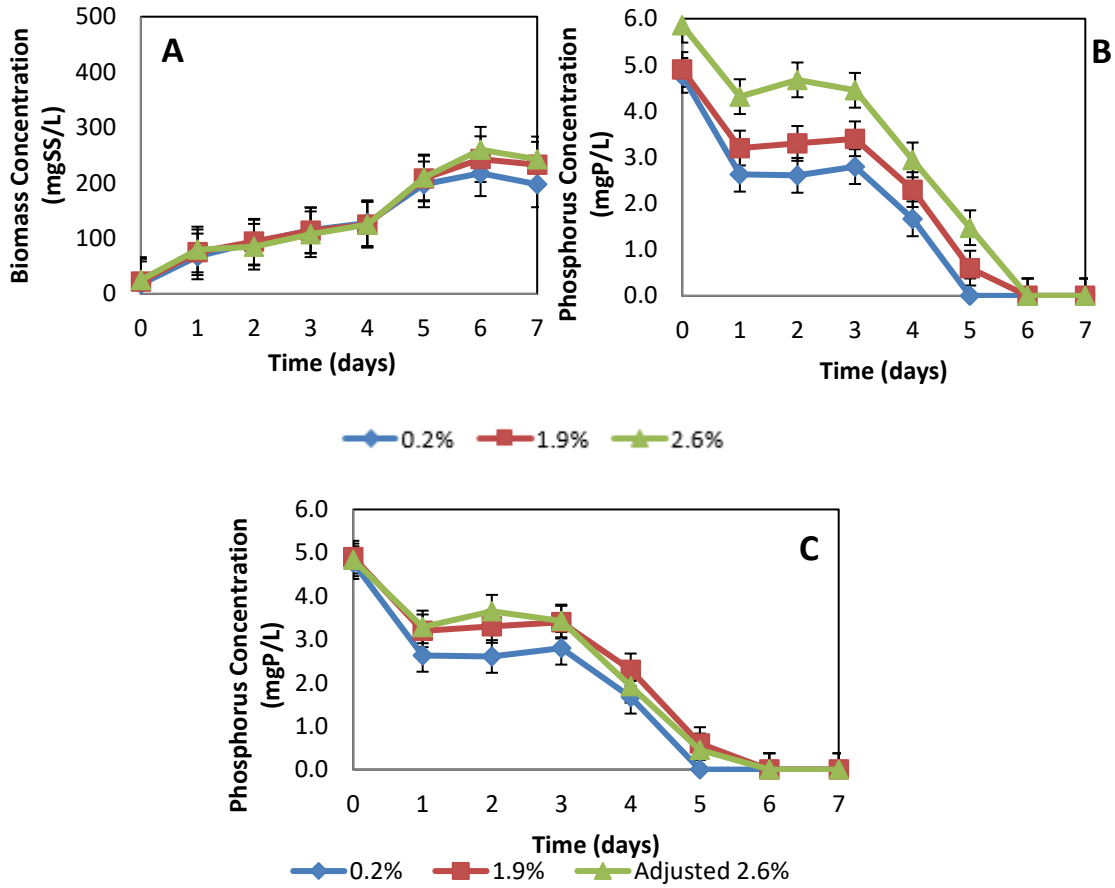

Figure 8.3: Effect of the prior phosphorus content of the biomass on the biomass concentration (A), phosphorus removal (B) and adjusted phosphorus removal (C). (Note: percentages in the legend are the phosphorus content (gP/gSS) of the initial inoculum cultures).

As seen in Figure 8.3, a higher prior phosphorus content of the biomass had no significant effect (90% confidence) on the biomass concentration (A) while significantly (90% confidence) affecting the phosphorus removal (B).

This significant effect on phosphorus removal is likely due to an artefact of the experimental design. To produce algal cultures of differing phosphorus contents, increasing amounts of phosphorus were added to the inoculum cultures (as described in the methods section 2.2). While the phosphorus concentration in the inoculum reactors of the 0.2% and 1.9% conditions was 0 mgP/L, the 2.6% inoculum reactor still had 7.9 mgP/L in the reactor solution when used as an inoculum. This residual phosphorus in the 2.6% inoculum reactor increased the starting phosphorus concentration as seen in Figure 8.3B. If this difference in starting phosphorus concentrations is adjusted for as shown in Figure 8.3C, the apparent 'significant' effect is no longer significant (90% confidence).

8.2.2.4 Biomass concentration

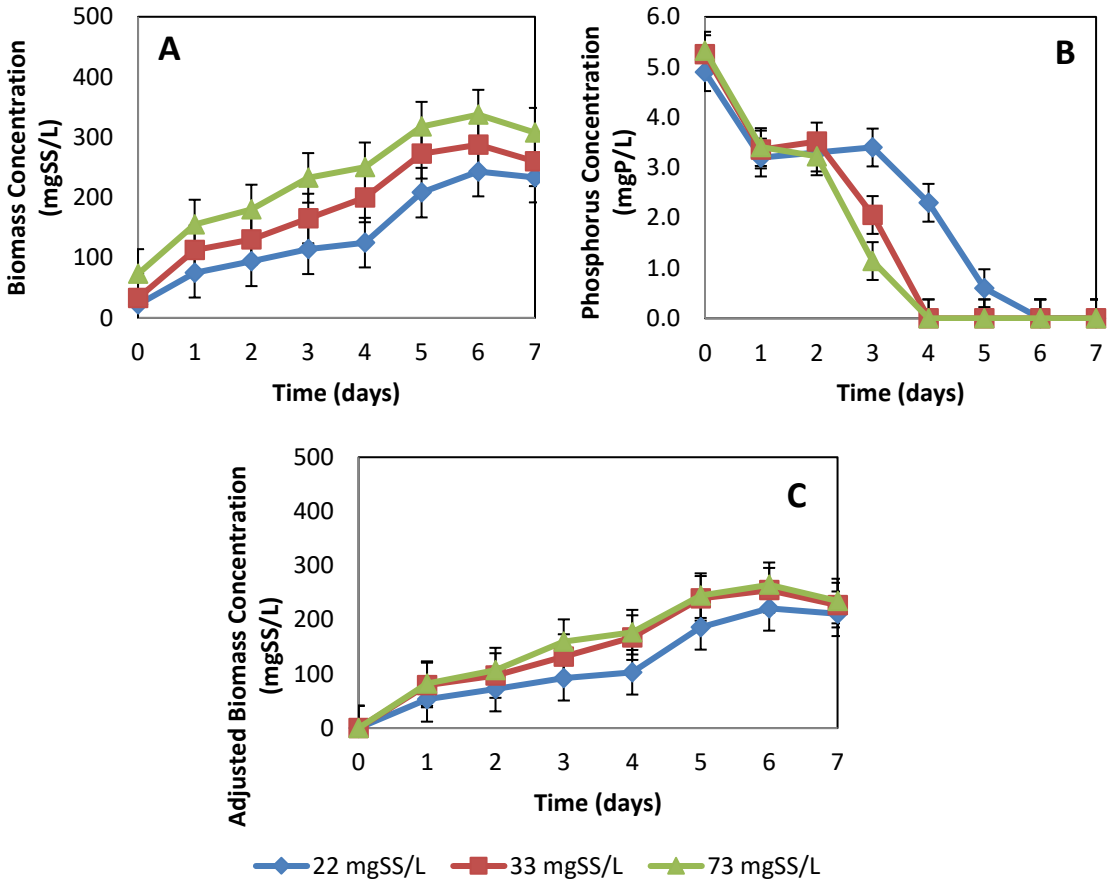

Figure 8.4: Effect of the initial biomass concentration on the biomass concentration (A), phosphorus removal (B), and adjusted biomass concentration (C) (Note: Legend shows starting biomass concentrations).

As might be expected, a higher initial biomass concentration allowed for increased biomass concentrations throughout the experiment (Figure 8.4A). While the difference between the 73 mgSS/L and 22 mgSS/L reactors is significant (90% confidence), if the different starting biomass concentrations are accounted for, as shown in Figure 8.4C, the effect is no longer significant

Figure 8.4B shows increasing the initial biomass concentration above 22 mgSS/L significantly (90% confidence) improved phosphorus removal. This improved phosphorus removal is likely due to the extra biomass and not phosphorus accumulation. This is shown in the main chapter (section 2.3.4), where no significant effect on the phosphorus content of the biomass was observed.

8.2.2.5 pH control

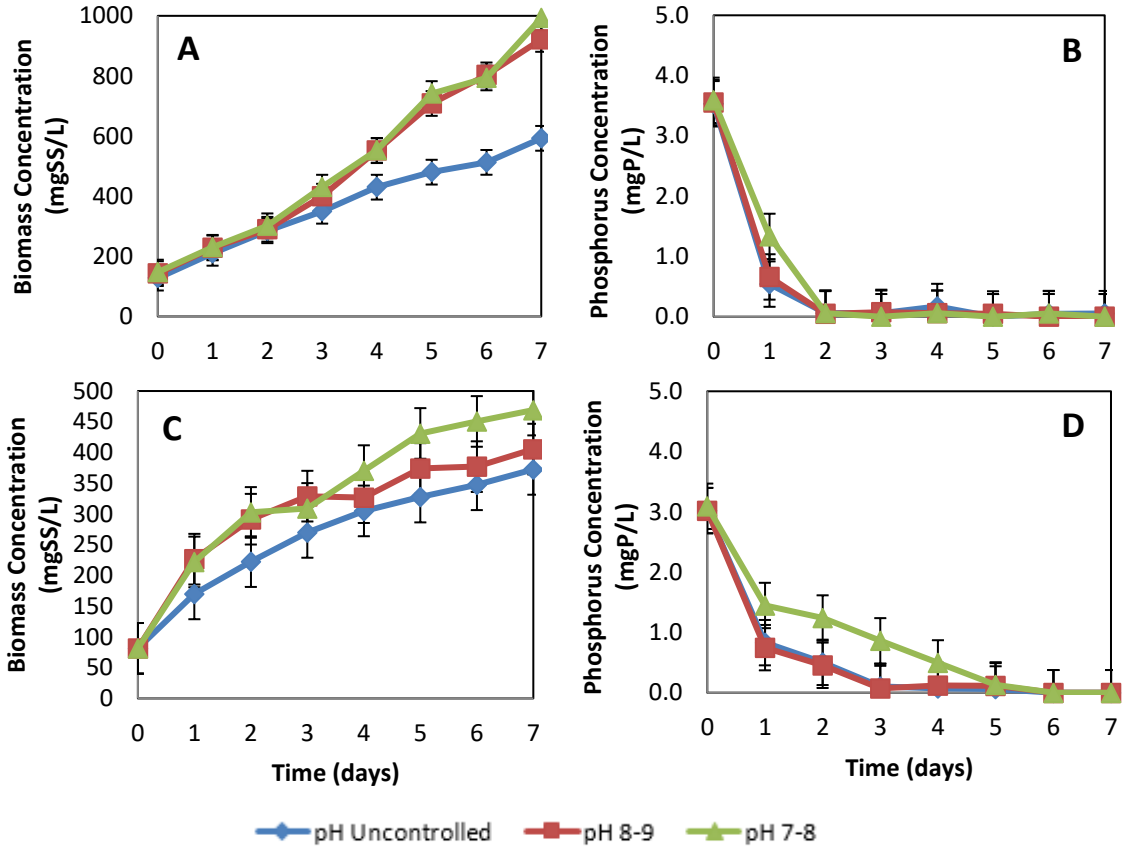

Figure 8.5: (Top) Effect of CO2 pH control on biomass concentration (A) and phosphorus removal (B). (Bottom) Effect of HCl pH control on biomass concentration (C) and phosphorus removal (D)

As expected, CO_2 pH control had a significant (90% confidence) positive effect on biomass concentration (Figure 8.5A) with CO_2 pH control allowing 400 mgSS/L more biomass by day 7. Although a large increase in biomass occurred, the phosphorus removal (Figure 8.5B) was not significantly affected (90% confidence).

A similar effect is observed when using HCl for pH control; however, the effect on biomass concentration is only significant (90% confidence) when comparing the pH 7-8 and pH uncontrolled reactors.

8.2.2.6 Mixing intensity

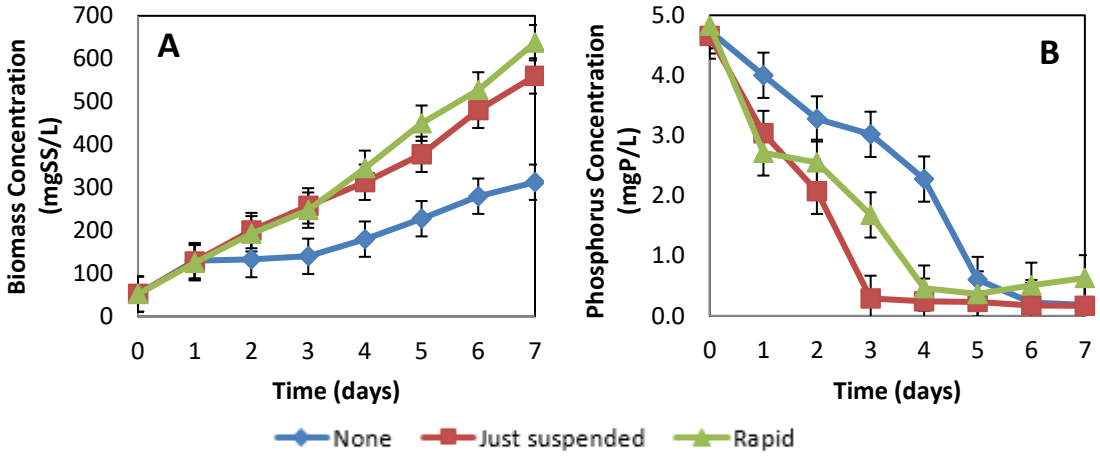

Figure 8.6: Effect of mixing intensity on biomass concentration (A) and phosphorus concentration (B).

As can be seen in Figure 8.6, increasing the mixing intensity from a non-mixed to a mixed state significantly (90% confidence) increases the biomass concentration (A) and phosphorus removal (B). Once mixing is occurring, further increasing of the mixing intensity has no effect on biomass concentration or phosphorus removal.

8.3 Appendix for Chapter 3: Variables affecting phosphorus accumulation in a mixed genus WSP

8.3.1 Analysis of local waste stabilisation ponds

Due to unforeseen circumstances with Rongotea WSP being desludged during the experimental work conducted in Chapter 3 and Chapter 4, analysis of suitable WSP sites in the wider Manawatu region was conducted to identify a replacement pond for the Rongotea WSP. The WSPs shown in Table 8.3 were selected to compare to Rongotea based on their geographical location. This comparison involved visual analysis of the algal diversity as shown in Table 8.4.

Table 8.3: Description of the sites sampled from the wider Manawatu region.

Pond	District	Type of system	Further notes
Rongotea	Manawatu	2 facultative ponds and 1 maturation pond	
Awahuri	Manawatu	Facultative pond	
Himatangi	Manawatu	Facultative pond and a floating wetland	
Fielding	Manawatu	3 facultative ponds	Treats supernatant from the digester.
PNCC	Manawatu	Pilot-scale WSP	Treats wastewater after primary sedimentation. Was seeded from Rongotea before desludging.
Woodville	Tararua	2 facultative ponds and 3 maturation ponds	Recently flooded and has minimal algal populations
Pahiatua	Tararua	3 facultative ponds	
Foxton Beach	Horowhenua	2 facultative ponds	
Shannon	Horowhenua	2 facultative ponds and a floating wetland	
Tokomaru	Horowhenua	Facultative pond and a wetland	

Table 8.4: Presence of algal genera in WSPs from the Manawatu region

Algal Genus	Rongotea	Awahuri	Himatangi	Fielding	PNCC	Woodville	Pahiatua	Foxton Beach	Shannon	Tokomaru
Scenedesmus	✓	✓	×	×	✓	×	✓	✓	✓	✓
Cyclotella	✓	×	×	×	×	×	×	✓	✓	✓
Closterium	✓	×	×	×	×	×	✓	✓	×	×
Pediastrum	✓	×	×	×	✓	×	×	×	×	×
Actinastrum	✓	×	×	×	✓	×	✓	✓	×	✓
Coelastrum	✓	✓	×	×	✓	×	✓	×	×	✓
Micractinium	✓	✓	✓	✓	✓	×	×	✓	✓	✓
Monoraphidium	✓	×	×	×	✓	×	✓	✓	✓	✓
Crucigeniella	✓	×	×	×	✓	×	×	×	✓	✓
Ankistrodesmus	✓	✓	×	×	×	×	×	×	×	×
Kirchneriella	✓	×	✓	×	×	×	✓	✓	✓	×
Number present	11	4	2	1	7	0	6	7	6	7

From Table 8.4, the PNCC, Foxton Beach, and Tokomaru WSPs have the highest number of similar algal genera present compared to Rongotea (7 out of the 11 algal genera commonly observed at Rongotea). Further consideration of these three ponds by analysis of the suspended solids concentration indicated that PNCC and Foxton Beach WSPs had viable amounts of solids for centrifugation (100 mg SS/L and 67 mg SS/L respectively).

Further experimentation was conducted on both PNCC and Foxton Beach WSPs by conducting a centre point run as described in the methods in section 3.2.1. This was then compared to the phosphorus content of the biomass (gP/gSS) from centre point runs previously conducted using Rongotea algae, which can be seen in Figure 8.7:

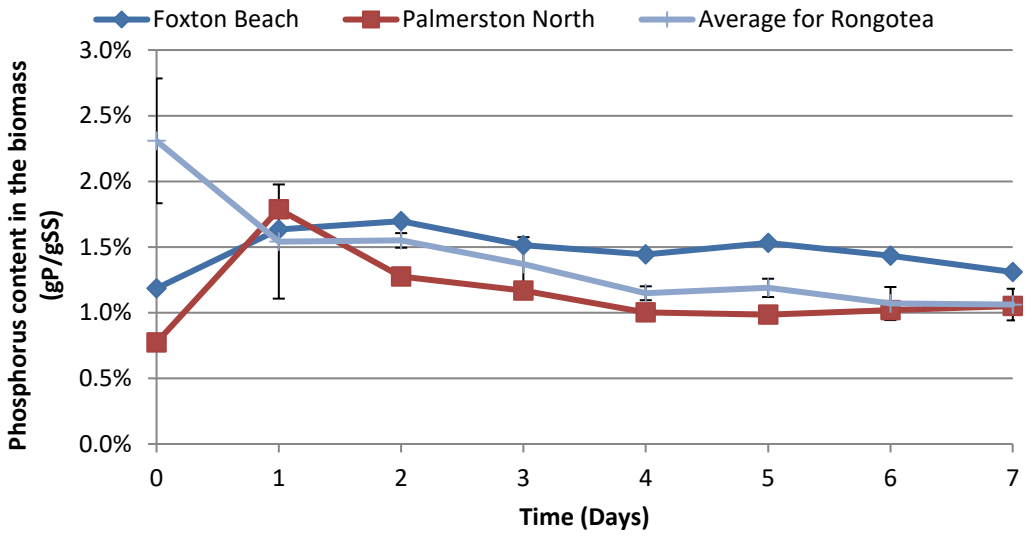

Figure 8.7: Comparison of centre point runs from Foxton Beach, PNCC, and Rongotea. Error bars are the 95% confidence intervals based on the average of 4 centre point runs using Rongotea algae.

As shown in Figure 8.7, both Foxton Beach and PNCC start at lower phosphorus contents in the biomass compared to Rongotea. However, from day 1 onwards, there is minimal difference between the ponds with the error bars from the Rongotea sampling overlapping mostly with the PNCC phosphorus content in the biomass. This was expected as the PNCC pond was initially seeded from Rongotea and therefore was expected to have a similar response. Based on this evidence, PNCC pond was chosen to continue the experimental work in Chapter 3 and Chapter 4 after Rongotea WSP was desludged.

8.3.2 Statistical analysis of inoculum sources

The centre point runs were conducted for two reasons. The first reason is they allow identification of any non-linear response occurring between the levels of the variables tested;

however, the variable responsible for this non-linear response cannot be identified. The second reason is they allow the reproducibility of the phosphorus content of the biomass to be estimated for all 40 experimental reactors. This is based on the assumption that the difference in phosphorus content of the biomass of the eight centre point reactors would be the same if any other condition was replicated. The centre point reactors were all given the same conditions and therefore expected to give similar values. The variation in phosphorus content of the biomass between these reactors can be seen in Figure 8.8.

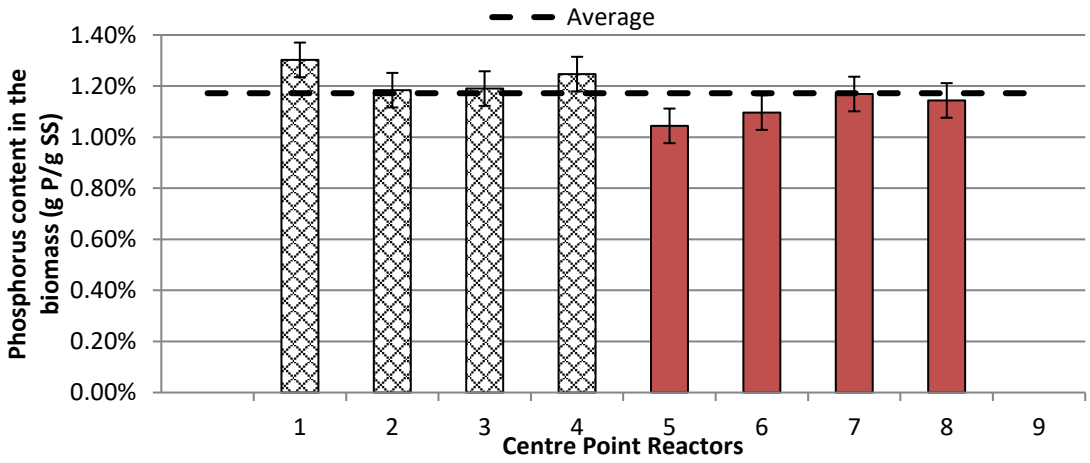

Figure 8.8: Phosphorus content in the biomass for the eight centre point control reactors. Reactors 1 to 4 (cross pattern) were inoculated from Rongotea WSP, and reactors 5 to 8 (solid red) were inoculated from Palmerston North WSP. The black dotted line is an average of all centre point reactors. Error bars are 95% confidence intervals.

As shown in Figure 8.8 there is good agreement between all eight centre point reactors with an average phosphorus content in the biomass of 1.17%±0.07% (95% confidence), showing a low error, and therefore suggesting that the results are reproducible. The error was calculated as a 95% confidence interval using the average phosphorus content of the biomass of the eight centre point reactors. Statistical analysis using a two-tailed T-test was conducted to identify any difference between the inoculum sources. This resulted in a p-value of 0.11 suggesting that the inoculum source did not significantly affect the phosphorus content of the biomass for the centre point reactors, and can, therefore, be assumed to have no significant effect on the factorial experimental results.

8.3.3 Confounding of interactions using the 2^{6-1} experimental design

Due to the fractional factorial design (2^{6-1}), confounding between variables and interactions can occur resulting in the effect of some variables being unable to be distinguished from the effect of others. The confounding in this experimental design means the effects of:

- Main effects are confounded with 5-way interactions (i.e. the effect of phosphorus concentration cannot be differentiated from the effect of the interaction between temperature x light intensity x mixing intensity x organic load x pH)
- 2-way interactions are confounded with 4-way interactions
- 3-way interactions are confounded with other 3-way interactions

Since four-way or higher interactions are unlikely to be significant, the effect of main effects and 2 way interactions are unlikely to be influenced by confounding. However, due to the inability to reliably differentiate between the effects of 3-way interactions (i.e. 3-way interactions are confounded with other 3-way interactions), the analysis was only conducted up to 2-way interactions.

8.3.4 Laboratory scale semi-continuous flow 'luxury uptake' process

The 'luxury uptake' process was designed based on the implications on WSP system design and operation in section 3.3.2. The initial methodology was described in section 3.2.2, with this section giving further details on the 'luxury uptake' process.

The major differences between the laboratory 'luxury uptake' process and the full-scale 'luxury uptake' process as proposed in section 3.3.2 are outlined below:

- The anaerobic pond can be removed in the laboratory scale 'luxury uptake' process as the organic load can instead be simply controlled through the synthetic wastewater feed.
- Part of the harvested biomass is reseeded into the 'growth pond' to encourage easily settleable algae to dominate the system. This was based on work from Park *et al.* (2011b) who previously found reseeding settled biomass improved harvest efficiency and increased the dominance of readily settleable algal species.

Pumps were required for feed, solids harvest, solids reseed, and solids recycle. These pumps were operated semi-continuously as outlined in Table 8.5. The biomass was harvested (clarifier 1) or recycled (clarifier 2) from the bottom of an Imhoff cone clarifier as shown in Figure 3.1 on page 76. As discussed in section 3.2.2, the HRT of the luxury uptake stage was increased to 5 days for only the third run of the 'luxury uptake' process (Experiment #3 in Table 3.5). This was done to coincide with the peak polyphosphate granule content for the operating conditions identified in Chapter 4. The increased HRT was achieved by reducing the feed pump flow rate, which is shown in Table 8.5. All other pump times remained the same.

Table 8.5: Pump times and flow rates

Pump	Times activated (Pump on per day)	Active time (min/time activated)	Total pump time (min active/d)	Flow rate (L/min active)	Flowrate (L/d)
Feed (Runs 1,2,4 and 5)	12	6	72	0.032	2.3
Feed (Run 3)	12	6	72	0.019	1.4
Solids harvest	4	1	4	0.1	0.4
Solids reseed	2	1	2	0.05	0.1
Solids recycle	12	2	24	0.07	1.7

The flow rate of the feed pump is based on the HRT in the 'luxury uptake' stage of either 3 days for runs 1, 2, 4, and 5, or 5 days for run 3. The solids harvest and recycle pump flow rates were set based on estimated volumes of solids collected in the clarifiers. The solids reseed flowrate was arbitrarily set. Optimisation of these flowrates was not conducted in this work.

The solids retention time (SRT) of the luxury uptake process was calculated using Equation 8.1:

Equation 8.1: SRT calculation for luxury uptake process. Where: SS = suspended solids (mgSS/L), LU = luxury uptake stage, V = volume (L), Growth = growth stage, and Q = flow rate (L/d).

$$SRT = \frac{(SS_{LU} \times V_{LU}) + (SS_{Clarifier\ 1} \times V_{Clarifier\ 1}) + (SS_{Growth} \times V_{Growth}) + (SS_{Clarifier\ 2} \times V_{Clarifier\ 2})}{(SS_{Harvest} \times Q_{Harvest}) + (SS_{Effluent} \times Q_{Effluent})}$$

The calculated SRT and hydraulic retention time (HRT) of the luxury uptake process operating under the different conditions are given in Table 8.6.

Table 8.6: HRT and average SRT of the entire luxury uptake process under the different operating conditions. Experiment number refers to the numbers given in Table 3.5.

Experiment number	Hydraulic retention time HRT (Days)	Average solids retention time SRT (Days)
#1 (Winter)	8	11.6
#2 (Summer)	8	11.0
#3	13.4	13.4
#4	8	9.1
#5	8	9.9

8.3.5 Identifying the HRT required for the luxury uptake stage of the 'luxury uptake' process

In order to identify the hydraulic retention time (HRT) for the luxury uptake stage in section 3.3.3, analysis of the day that the maximum phosphorus content of the biomass (gP/gSS) was achieved in each of the 40 batch experiments was conducted and is shown in Figure 8.9.

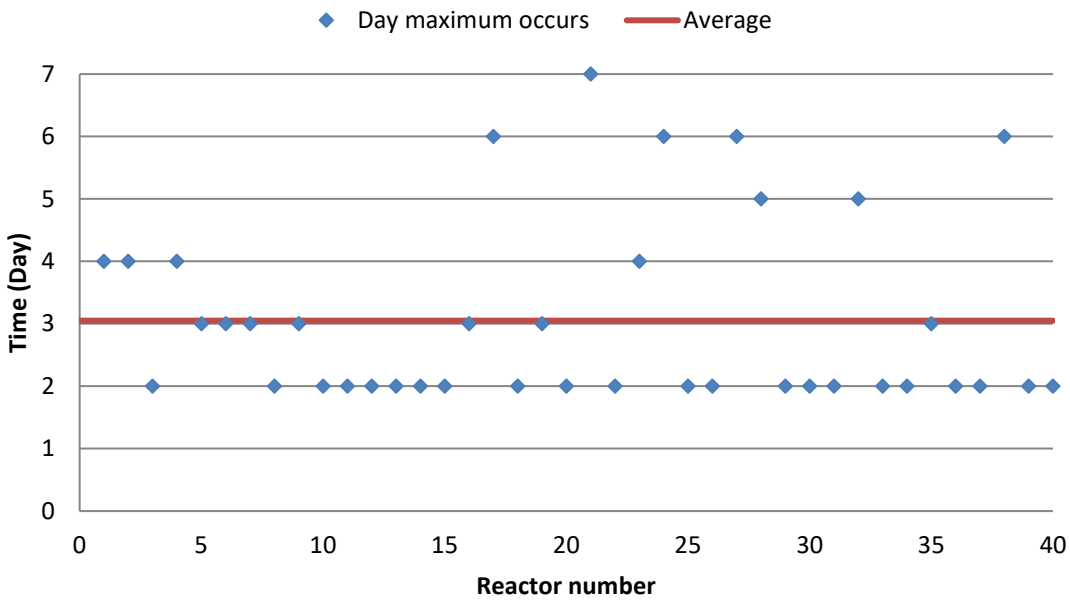

Figure 8.9: Day that the maximum phosphorus content of the biomass (gP/gSS) was achieved. Reactor number refers to the run order given in Table 3.2.

While the maximum day varies across the 40 reactors, Figure 8.9 shows the average day the maximum phosphorus content of the biomass occurred was 3 days. Therefore, the HRT for the luxury uptake stage in section 3.3.3 was set to 3 days. Note: since run 3 of the 'luxury uptake' process is based on the findings of Chapter 4, a different HRT than the one proposed here was used for that specific experiment.

8.3.6 Residual analysis of the linear regression fitted to produce Equation 3.2 that is used to predict the phosphorus content in the biomass

The regression equation was produced in Minitab using stepwise regression with an alpha to enter and remove of 0.1. Up to 2-way interactions were included and non-significant main effects that had a significant interaction were included in the regression equations to maintain statistical hierarchy. When conducting linear regression, the residual plots should be analysed to ensure the assumption of normal distribution of the residuals is correct. This residual analysis was produced using Minitab with the residual plots shown in Figure 8.10.

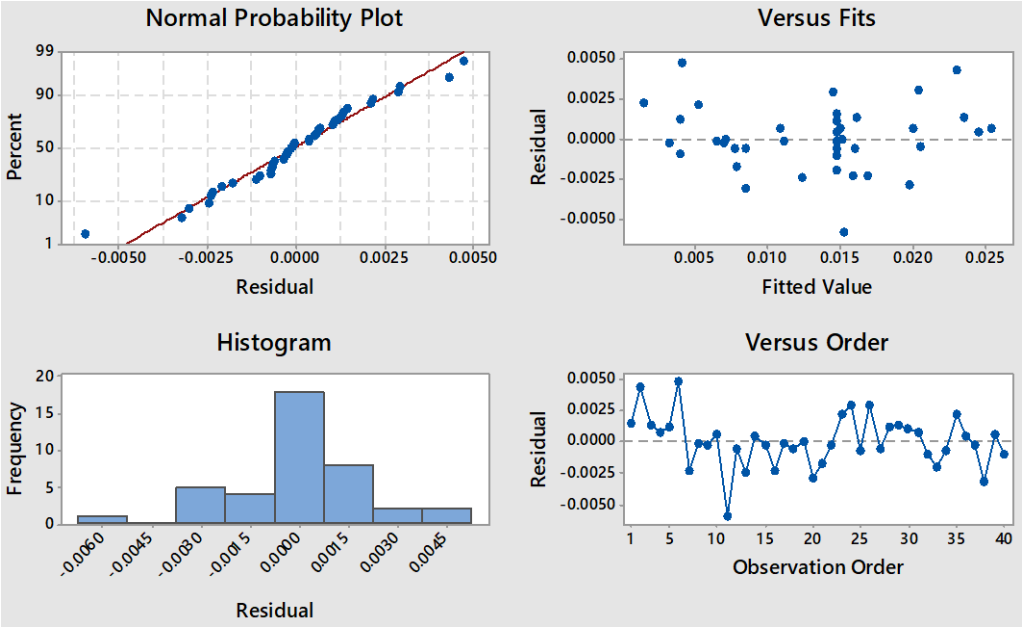

Figure 8.10: Residual plots for Equation 3.2 that is used to predict the phosphorus content of the biomass

Analysing the 'normal probability plot' in Figure 8.10, the residuals appear to be normally distributed as they follow the line of best fit. This can also be seen in the 'histogram' that shows a general normal distribution shape. No trend can be seen in the 'versus order' plot. A slight parabolic trend can be seen in the 'versus fit' plot that agrees with the significant curvature (90% confidence) identified in the Minitab analysis. As further shown in the experimental vs predicted plot in Figure 8.11, apart from the slight curvature previously mentioned, the linear regression appears to fit the data well. This agrees with the adjusted R^2 and predicted R^2 values of 86% and 76% respectively, suggesting the linear regression is a good fit to the data.

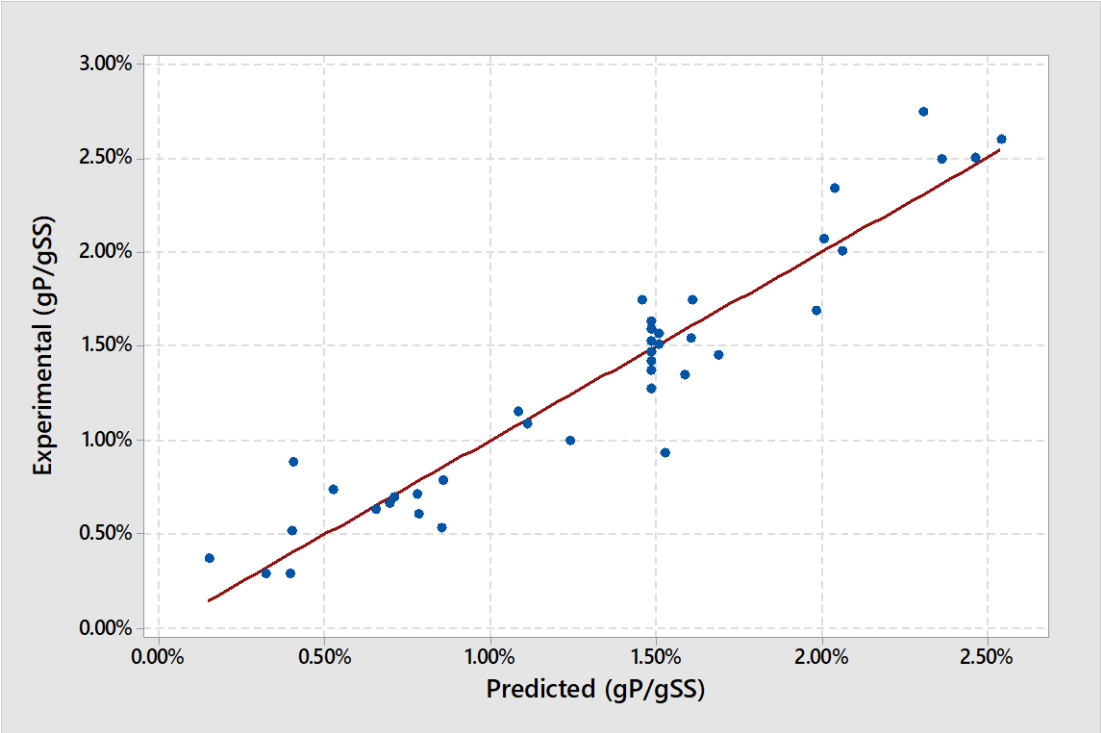

Figure 8.11: Actual experimental value vs predicted value using Equation 3.2.

8.3.7 Regression equation for biomass growth under batch conditions

This section discusses the effect of the variables and interactions on the biomass growth over seven days under batch conditions. The regression equation was produced in Minitab using stepwise regression with an alpha to enter and remove of 0.05. Up to 2-way interactions were included and non-significant main effects that had a significant interaction were included in the regression equations to maintain statistical hierarchy. The standardised effects of the variables are shown in Table 8.7. Variables with a p-value of less than 0.05 are statistically significant at the 95% confidence.

Table 8.7: The standardised effects of significant variables and interactions on the biomass growth. *Denotes an interaction between variables, [a] not applicable due to the variable not having a significant effect.

Variable	Effect	P value	Significance
Temperature	11.47	0.003	95% Confidence
Phosphorus concentration	N/A[a]	0.885	Not Significant
Light	28.85	0.000	95% Confidence
Mixing	N/A[a]	0.710	Not Significant
Organic load	19.12	0.000	95% Confidence
pH	-14.23	0.000	95% Confidence
Temperature*Light	12.74	0.001	95% Confidence
Light*pH	-15.10	0.000	95% Confidence
Mixing*Organic load	-9.29	0.013	95% Confidence

From Table 8.7, of the 21 variables and interactions examined, only seven were found to be significant at the 95% confidence level. These significant variables and interactions were used to produce a regression equation that is shown in Equation 8.2.

Equation 8.2: Regression equation to predict the biomass growth over seven days under batch conditions

$$Growth\left(\frac{gSS}{d}\right) = -33.3 - 1.22(T) + 0.75(L) + 0.027(M) + 0.047(C) + 5.25(pH) + 0.019(T \times L) - 0.084(L \times pH) - 0.000066(M \times C)$$

Where: T = temperature (°C), L = light intensity (µE/m^2.s), M = mixing intensity (RPM), C = organic load (mgCOD/L), and pH = pH. '×' refers to an interaction effect between the variables.

The adjusted R^2 and prediction R^2 of Equation 8.2 were calculated in Minitab to be 80% and 70% respectively, suggesting the linear regression is a good fit to the data. A high prediction R^2,

such as the one observed here, suggests Equation 8.2 should have a reasonable prediction capability for new observations outside of the 40 experimental reactors described in section 3.2.1.

Analysis of the residual plots shown in Figure 8.12 suggests the residuals are normally distributed, and no clear trend in the 'versus fit' or 'versus order' plots can be observed. This suggests the linear regression is a good fit to the data.

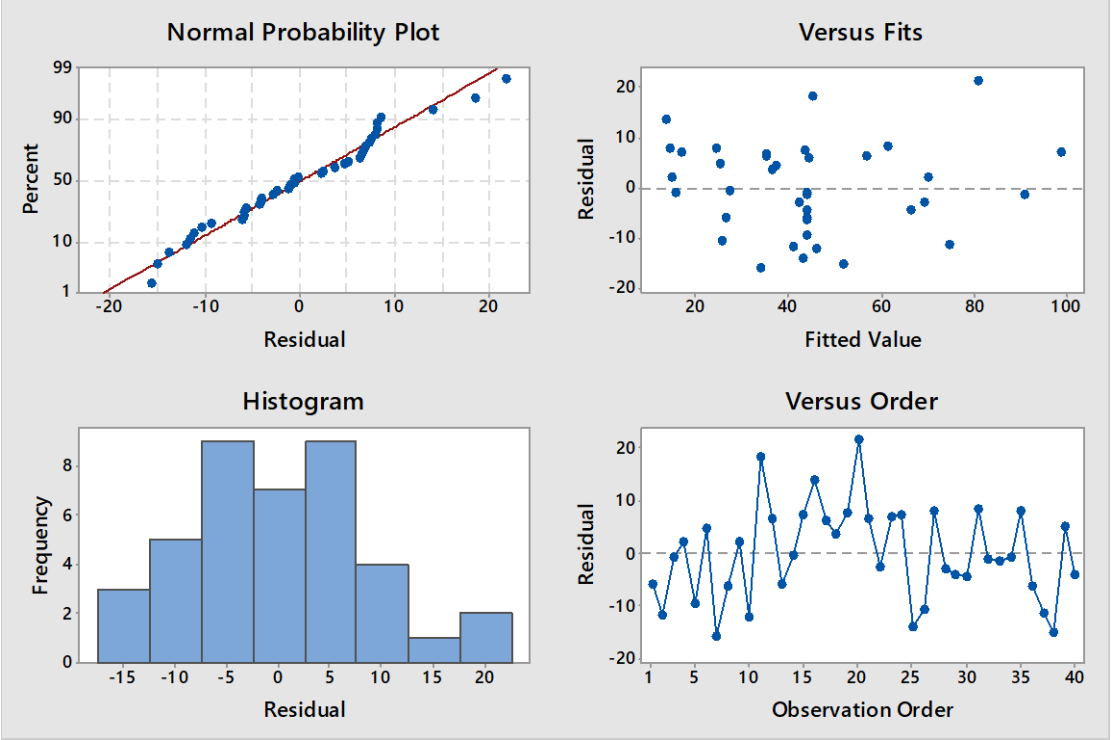

Figure 8.12: Residual plots produced in Minitab when producing the growth regression equation

8.3.8 Additional experimental data from luxury uptake process

This section summarises additional experimental data taken from the luxury uptake process under the different operational conditions. The operating conditions are shown in Table 8.8 and the additional experimental data in Table 8.9. It should be noted that as the growth stage was not optimised, the phosphorus removal in the system was also not optimised as both a high phosphorus content in the biomass and high biomass concentrations are required to remove phosphorus.

Table 8.8: Operating conditions for the luxury uptake process

Experiment Number	Phosphorus Concentration (mgP/L)	Mixing Intensity (RPM)	pH	Organic load (mgCOD/L)	Temperature (°C)	Light Intensity (μE/m^2.s)
#1 (Winter)	15	500	No control	105	10	60
#2 (Summer)	15	500		105	25	150
#3	15	500		805	25	150
#4	5	100		105	25	150
#5	5	100		105	10	60

Table 8.9: Additional experimental data obtained when operating the luxury uptake process under the different experimental conditions shown in Table 8.8.

Experiment number	pH (pH)		Dissolved oxygen (mgDO/L)		Solids concentration at end of stage (mgSS/L)			Phosphorus concentration at end of stage (mgP-PO_4/L)	
	LU stage	Growth stage	LU stage	Growth stage	LU stage	Harvest	Growth stage	LU stage	Growth stage
#1 (Winter)	8.8	8.8	11.0	11.6	170	510	290	11.7	11.7
#2 (Summer)	9.9	10.6	12.3	12.9	640	2350	100	7.1	5.5
#3	8.2	8.8	3.7	6.7	1182	3902	1880	2.6	3.0
#4	10.5	10.8	14.1	13.7	390	1910	360	0.0	0.0
#5	8.7	8.9	10.8	11.2	90	450	240	2.1	2.3

8.4 Appendix for Chapter 4: The effect of individual algal genera on phosphorus accumulation

8.4.1 Matlab code used for image analysis quantification of polyphosphate granules

In order to quantify the polyphosphate granules observed under light microscopy, an image analysis method was required. This image analysis method was developed in the computer software Matlab. In general, this method measures the area of the polyphosphate granules and the area of the algal cell to give a percentage of the cell that is polyphosphate granules. This method is described in section 4.2.1.2. The Matlab code used is given in sections 8.4.1.1, 8.4.1.2, and 8.4.1.3.

8.4.1.1 "Algal selection" Matlab code

```
function varargout = Algae_Selection(varargin)
% ALGAE_SELECTION MATLAB code for Algae_Selection.fig
% Begin initialization code - DO NOT EDIT
gui_Singleton = 1;
gui_State = struct('gui_Name',       mfilename, ...
                   'gui_Singleton',  gui_Singleton, ...
                   'gui_OpeningFcn', @Algae_Selection_OpeningFcn, ...
                   'gui_OutputFcn',  @Algae_Selection_OutputFcn, ...
                   'gui_LayoutFcn',  [] , ...
                   'gui_Callback',   []);
if nargin && ischar(varargin{1})
    gui_State.gui_Callback = str2func(varargin{1});
end

if nargout
    [varargout{1:nargout}] = gui_mainfcn(gui_State, varargin{:});
else
    gui_mainfcn(gui_State, varargin{:});
end
% End initialization code - DO NOT EDIT

% --- Executes just before Algae_Selection is made visible.
function   Algae_Selection_OpeningFcn(hObject,   eventdata,   handles,
varargin)
global k m z a1 a2 a3 a4 a5
z = input('Initial image number           ');
if z == 0;
        k2 = 'image.tif';
        y = 0;
elseif z < 10;
        k2 = sprintf('image000%d.tif', z);
        y = 0;
elseif z < 100;
        k2 = sprintf('image00%d.tif', z);
        y = 0;
elseif z < 1000;
        k2 = sprintf('image0%d.tif', z);
        y = 0;
else
```

```
        k2 = sprintf('image_%d.tif', z);
        y = 0;
end
k = imread(k2);
m = 1; a1 = 1; a2 = 1; a3 = 1; a4 = 1; a5 = 1;
axes(handles.axes1);
imshow(k);

% Choose default command line output for Algae_Selection
handles.output = hObject;

% Update handles structure
guidata(hObject, handles);


% --- Outputs from this function are returned to the command line.
function  varargout  =  Algae_Selection_OutputFcn(hObject,  eventdata,
handles)

varargout{1} = handles.output;
% --- Executes on button press in select.
function select_Callback(hObject, eventdata, handles)
global k BW
axes(handles.axes1);
imshow(k);
BW = imcrop;
imshow(BW);

% --- Executes on button press in original.
function original_Callback(hObject, eventdata, handles)
global k
axes(handles.axes1);
imshow(k);

% --- Executes on button press in quit.
function quit_Callback(hObject, eventdata, handles)
close

% --- Executes on button press in next.
function next_Callback(hObject, eventdata, handles)
global z k
z = z+1;
if z < 10;
k = sprintf('image000%d.tif', z);
y = 0;
elseif z < 100;
k = sprintf('image00%d.tif', z);
y = 0;
elseif z < 1000;
k = sprintf('image0%d.tif', z);
y = 0;
else
k = sprintf('image_%d.tif', z);
y = 0;
end
imshow(k);
```

```
% --- Executes on button press in Previous_Image.
function Previous_Image_Callback(hObject, eventdata, handles)
global z k
z = z-1;
if z<0;
    z=0;
end
if z == 0;
k = 'image.tif';
y = 0;
elseif z < 10;
k = sprintf('image000%d.tif', z);
y = 0;
elseif z < 100;
k = sprintf('image00%d.tif', z);
y = 0;
elseif z < 1000;
k = sprintf('image0%d.tif', z);
y = 0;
else
k = sprintf('image_%d.tif', z);
y = 0;
end
imshow(k);

% --- Executes on button press in Micractinium.
function Micractinium_Callback(hObject, eventdata, handles)
global a1 BW k
filename = sprintf('Micractinium%d.tif', a1);
imwrite(BW, filename, 'tif');
imshow(k);
a1=a1+1;

% --- Executes on button press in Scenedesmus.
function Scenedesmus_Callback(hObject, eventdata, handles)
global a2 BW k
filename = sprintf('Scenedesmus%d.tif', a2);
imwrite(BW, filename, 'tif');
imshow(k);
a2=a2+1;

% --- Executes on button press in Actinastrum.
function Actinastrum_Callback(hObject, eventdata, handles)
global a3 BW k
filename = sprintf('Actinastrum%d.tif', a3);
imwrite(BW, filename, 'tif');
imshow(k);
a3=a3+1;

% --- Executes on button press in Monoraphidium.
function Monoraphidium_Callback(hObject, eventdata, handles)
global a4 BW k
filename = sprintf('Monoraphidium%d.tif', a4);
imwrite(BW, filename, 'tif');
imshow(k);
a4 = a4+1;

% --- Executes on button press in Pediastrum.
```

```
function Pediastrum_Callback(hObject, eventdata, handles)
global a5 BW k
filename = sprintf('Pediastrum%d.tif', a5);
imwrite(BW, filename, 'tif');
imshow(k);
a5=a5+1;
```

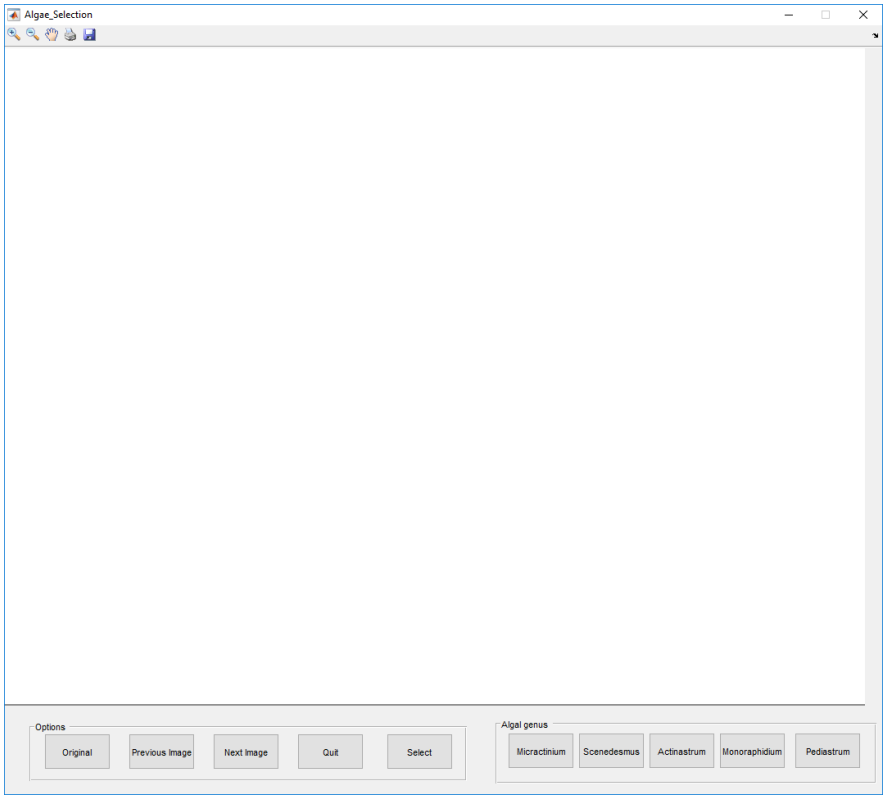

Figure 8.13: Algal section user interface

8.4.1.2 "Polyphosphate granule quantification" Matlab code

```
clc
clear all
close all
global a n q t Algae b_meanb no_bg
display('Notes:');
display('1) This will overwrite any images called Algae_#');
display('2) Ensure that background removal and pixel counts are
checked');
display('3) Images must be .tif and numbered sequentially from 1');
display(' ')

%% Overwrite Results Excel Sheet
Erase     =     questdlg('Results     Excel     File     Exist?','Excel
file?','Yes','No','Cancel','No');
switch Erase;
    case 'Yes';
        Erase_A = xlsread('Results.xlsx','Area');
        Erase_V = xlsread('Results.xlsx','Volume');
        Erase_N = xlsread('Results.xlsx','GNumber');
        if ~isempty(Erase_A)
            xlswrite('Results.xlsx',zeros(size(Erase_A))*nan, 'Area');
```

```
        end
        if ~isempty(Erase_V)
            xlswrite('Results.xlsx',zeros(size(Erase_V))*nan,
'Volume');
        end
        if ~isempty(Erase_N)
            xlswrite('Results.xlsx',zeros(size(Erase_N))*nan,
'GNumber');
        end
    case 'No';
    case 'Cancel';
        return%               Stop code
end
%% Selecting values
number=input('Number of images to analyse         ');
n=1;
z=zeros(4,1,number);
x_v=zeros(5,1,number);
x_g=zeros(3,1,number);

display('Micractinium       = 1')
display('Scenedesmus        = 2')
display('Actinastrum        = 3')
display('Monoraphidium      = 4')
display('Pediastrum         = 5')
display('Other              = 6')
display('Background removed = 9')
display(' ')
Algae = input('Algae Type          ');
display(' ')

if     Algae == 1; % Micractinium
       b_t = 3.5;                                %Background removal
       d_r = 6;                                   %Dilation factor (whole
numbers only)
       gradient = 0.003820;
       intercept = -0.095;
elseif Algae == 2; % Scenedesmus
       b_t = 3.5;                                % Background removal
       d_r = 2;                                         % Dilation factor
(whole numbers only)
       gradient = 0.003791;
       intercept = -0.1269;
elseif Algae == 3; % Actinastrum
       b_t = 3;                                  % Background removal
       d_r = 4;                                         % Dilation factor
(whole numbers only)
       gradient = 0.003820;
       intercept = -0.095;
elseif Algae == 4; %Monoraphidium
       b_t = 2.9;                                % Background removal
       d_r = 6;                                         % Dilation factor
(whole numbers only)
       gradient = 0.003820;
       intercept = -0.095;
elseif Algae == 5; % Pediastrum
       b_t = 3;                                  % Background removal
       d_r = 6;                                         % Dilation factor
(whole numbers only)
```

```
        gradient = 0.003791;
        intercept = -0.1;
elseif Algae == 6; % Other algae. May need to change values depending
on algae
        b_t = 3.5;                                  % Background removal
        d_r = 6;                                          % Dilation factor
(whole numbers only)
        gradient = 0.003703;
        intercept = -0.1157;
elseif Algae == 9; % If background has already been removed
        b_t = 1;                                     %
        d_r = 1;                                     %
        gradient = 0.003820; %May need to change depending on algae
        intercept = -0.095;  %May need to change depending on algae
end

while n<number+1;
no_bg = 0;
if Algae == 1
f=sprintf('Micractinium%d.tif', n);
elseif Algae == 2
f=sprintf('Scenedesmus%d.tif', n);
elseif Algae == 3
f=sprintf('Actinastrum%d.tif', n);
elseif Algae == 4
f=sprintf('Monoraphidium%d.tif', n);
elseif Algae == 5
f=sprintf('Pediastrum%d.tif', n);
elseif Algae == 6
f=sprintf('Other%d.tif', n);
else
f=sprintf('Algae_%d.tif', n);
end
a=imread(f);
%%                  If background already removed
if Algae == 9;
a_f = a;
original = a;
else
%%                   Start of algae background removal/isolation
original = a;
%%                   Background Removal (b)
b = a(:,:,3);                          % Select blue channel
b_mean = mean(b(:));                   % Mean pixel value
b_meanb = mean(b(b>b_mean));           % Mean of background
b_std = std(double(b(b>b_mean)));      % Std deviation of background
b_threshold = b_meanb - b_std*b_t;   % Empirically calculated threshold
level to separate(This use to be: thr = mn2 - st2*4)
b_mask = b < b_threshold;              % Create a mask image of algae
b_fill = imfill(b_mask,'holes');       % Fill in interior holes

%%                  Making full RGB image with background removal
a_br = a(:,:,1);                       % Red channel
a_br(~b_fill)=255;                      % Remove everything from a_br that
is not in image b_fill
a_bg = a(:,:,2);                       % Green channel
a_bg(~b_fill)=255;                      % Remove everything from a_bg that
is not in image b_fill
a_bb = a(:,:,3);                       % Blue channel
```

```
a_bb(~b_fill)=255;                    % Remove everything from a_bb that
is not in image b_fill
a_bf = a;                            % Simple copy
a_bf(:,:,1) = a_br;                  % Combine red channel
a_bf(:,:,2) = a_bg;                  % Combine green channel
a_bf(:,:,3) = a_bb;                  % Combine blue channel

%%                  Small object removal (c)
c = bwlabel(b_fill,4);                                  % Label regions
to allow measurements
c_prop = regionprops(c, 'all');                                 % Obtain
properties of objects
c_A = [c_prop.Area];                                     % Areas from
stats obtained previously
c_minA = max([c_prop.Area]) - 4*std([c_prop.Area]);     % Selects the
minimum object size
if  c_minA > 200;                                      % Incase minArea
becomes negative
    c_Aallowed = c_A > c_minA;                          % Remove small
objects if standard deviation is small (i.e. lots of small objects
present).
else
    c_Aallowed = c_A > max([c_prop.Area])/4;            % Remove small
objects if standard deviation is large
end
c_keepIndex = find(c_Aallowed);                        % Makes an array
of allowable objects
c_f = ismember(c, c_keepIndex);                         % Re-label with
only the cell areas kept.

%%                  Making full RGB image with small object removal
a_cr = a(:,:,1);                    % Red channel
a_cr(~c_f)=255;                      % Remove everything from a_cr that
is not in image c_f
a_cg = a(:,:,2);                    % Green channel
a_cg(~c_f)=255;                      % Remove everything from a_cg that
is not in image c_f
a_cb = a(:,:,3);                    % Blue channel
a_cb(~c_f)=255;                      % Remove everything from a_cb that
is not in image c_f
a_cf = a;                           % Simple copy
a_cf(:,:,1) = a_cr;                 % Combine red channel
a_cf(:,:,2) = a_cg;                 % Combine green channel
a_cf(:,:,3) = a_cb;                 % Combine blue channel

%%                  Edge correction (d)
d_edge1 = edge(c_f,'Canny');                            % Display only
the edges of the cell
d_dil1 = imdilate(d_edge1,strel('disk',d_r));           % Dilate the
edges so that it is larger than original
d_dil1(c_f) = 1;                                       % Everything in
c_f is also in d_dil1 (Ensuring that imfill works on boundary images)
d_fill1 = imfill(d_dil1,'holes');                       % Fill in the
edges

d_edge2 = edge(d_fill1,'Canny');                        % Get edge of
new larger shape
```

```
d_dil2 = imdilate(d_edge2,strel('disk',d_r));            % Dilate the
edges of larger shape (Want the inner boundary)
d_fill2 = imfill(d_dil2,'holes');                        % Fill in the
edges
d_fill2(d_dil1) = 1;                                     % Everything in
d_dil1 is also in d_fill2 (Ensuring that imfill works on boundary
images)

d_edge3 = edge(d_fill2,'Canny');                         % Get edge of
new larger shape
d_pad = padarray(d_edge3, [1 1], 1, 'both');             % Add white
border to allow dilation to occur correctly
d_dil3 = imdilate(d_pad,strel('disk',1));                % Dilate edges
of larger shape by 1(Gives original size of image)
d_dimen = d_dil3(2:end-1,2:end-1);                       % Reset image
dimensions
d_dil4 = imdilate(d_dimen,strel('disk',(d_r*2)-1));      % Finish
dilation of edges (Gives original size of image)

d2 = d_fill1;                                            % Simple copy
d2(d_dil4) = 0;                                          % Remove
everything from image d2 that is in image d_dil3

%%                  Making full RGB image with background removed
a = original;
a_er = a;
a_er = a(:,:,1);   % Red channel
a_er(~d2)=255;     % Remove everything from a_er that is not in image
d2
a_eg = a;
a_eg = a(:,:,2);   % Green channel
a_eg(~d2)=255;     % Remove everything from a_eg that is not in image
d2
a_eb = a;
a_eb = a(:,:,3);   % Blue channel
a_eb(~d2)=255;     % Remove everything from a_eb that is not in image
d2
a_f = a;
a_f(:,:,1) = a_er; % Combine red channel
a_f(:,:,2) = a_eg; % Combine green channel
a_f(:,:,3) = a_eb; % Combine blue channel

%% Watershed transform to remove any abnormalities
e2 = d2;
e = -bwdist(~e2);
e_water = watershed(e);
e2(e_water == 0) = 0;

e2_Seg = bwlabel(e2);                                    % Label regions to
allow measurements
e2_Seg_prop = regionprops(e2_Seg, 'all');                % Obtain properties
of objects
e2_Seg_allowed = [e2_Seg_prop.Area] > max([e2_Seg_prop.Area])/15;  %
Remove small objects if standard deviation is large
e2_Seg = ismember(e2_Seg, find(e2_Seg_allowed));  % Re-label with only
large segment areas kept.
```

```
e2_edge = edge(e2_Seg,'Canny');                          % Get edges of all
segments
e2_dilate = imdilate(e2_edge, strel('disk',10));  % Dilate edge
e2_dilate(e2_Seg) = 1;                                   %
e2_fill = imfill(e2_dilate,'holes');                     % Fill in edges
(Segments are now larger)
e2_edge2 = edge(e2_fill,'Canny');                        % Take edge of
larger granules
e2_dilate2 = imdilate(e2_edge2,strel('disk',10)); % Dilate by same
factor as previously used
e2_fill(e2_dilate2) = 0;                                 % Anything in large
dilated image thats also in g1_2 is removed

e2_Seg = bwlabel(e2_fill);                               % Label regions to
allow measurements
e2_Seg_prop = regionprops(e2_Seg, 'all');                % Obtain properties
of objects
e2_Seg_allowed = max([e2_Seg_prop.Area]);                % Remove small
objects if standard deviation is large
e2_Seg = ismember(e2_Seg, find(e2_Seg_allowed));  % Re-label with only
large segment areas kept.

e3_erode = imerode(e2_Seg, strel('disk',10));
e3_Seg = bwlabel(e3_erode);                              % Label regions to
allow measurements
e3_Seg_prop = regionprops(e3_Seg, 'all');                % Obtain properties
of objects
e3_Seg_allowed = [e3_Seg_prop.Area] < max([e3_Seg_prop.Area]);  %
Remove small objects if standard deviation is large
e3_Seg = ismember(e3_Seg, find(e3_Seg_allowed));  % Re-label with only
large segment areas kept.
e3_Seg = imdilate(e3_Seg,strel('disk',10));
e2_Seg(e3_Seg)=0;


e3_Seg = bwlabel(e2_Seg);                                % Label regions to
allow measurements
e3_Seg_prop = regionprops(e3_Seg, 'all');                % Obtain properties
of objects
e3_Seg_allowed = [e3_Seg_prop.Area] < max([e3_Seg_prop.Area]);  %
Remove small objects if standard deviation is large
e3_Seg = ismember(e3_Seg, find(e3_Seg_allowed));  % Re-label with only
large segment areas kept.
e2_Seg(e3_Seg)=0;

%%                    Making full RGB image with watershed transform
a = original;
e_er = a;
e_er = a(:,:,1);    % Red channel
e_er(~e2_Seg)=255;  % Remove everything from a_er that is not in image
d2
e_eg = a;
e_eg = a(:,:,2);    % Green channel
e_eg(~e2_Seg)=255;  % Remove everything from a_eg that is not in image
d2
e_eb = a;
e_eb = a(:,:,3);    % Blue channel
```

```
e_eb(~e2_Seg)=255;  % Remove everything from a_eb that is not in image
d2
e_f = a;
e_f(:,:,1) = e_er;  % Combine red channel
e_f(:,:,2) = e_eg;  % Combine green channel
e_f(:,:,3) = e_eb;  % Combine blue channel

%%          Manual UI required?
figure('units','normalized','outerposition',[0 0 1 1]);
set(gcf,'name','1','numbertitle','off')
subplot(2,2,1); imshow(a); title('Original (a)');
subplot(2,2,2);  imshow(a_cf);  title('Background  and  SO  removed  (a
cf)');
subplot(2,2,3); imshow(a_f); title('Edge correction (a f)');
subplot(2,2,4); imshow(e_f); title('Watershed correction(e_f)');
w  =  questdlg('Corrections  required?',  'Extra  removal',  'Watershed',
'User interface', 'None', 'None');
switch w
    case 'Watershed';
        a_f = e_f;
    case 'User interface';
        q = 0;              % Makes program wait for UI to finish
        t = 1;              % Used in UI
        GUI_Removal;        % Start UI
        while q == 0;       % When UI finished q changes to 1
        uiwait(GUI_Removal);% Wait for UI to finish
        end
        a_f = a;            % Simple copy to use later
    case 'None';
end
close all
%%                  Saves image without background
filename = sprintf('Algae_%d.tif', n);
imwrite(a_f, filename, 'tif');
end

%%                  Pixel Counter
m  =  mean(a_f(a_f<250));                  %  Mean  of  image  with  white
background excluded
e_threshold = gradient*m+intercept;% Based on threshold testing data

image_seg1=im2bw(a_f,e_threshold    -    0.1);    %Applying    different
thresholds to isolate granules
image_seg2=im2bw(a_f,e_threshold     -     0.05);%Applying     different
thresholds to isolate granules
image_seg3=im2bw(a_f,e_threshold);                 %Applying  different
thresholds to isolate granules
image_seg12=im2bw(a_f,0.99);               %Turning algae to black and
white
filename_1 = sprintf('Threshold %d', e_threshold - 0.05);
filename_2 = sprintf('Threshold %d', e_threshold);
filename_3 = sprintf('Threshold %d', e_threshold + 0.05);
filename_12 = ('Threshold 0.99');

%                  Finds and counts the black pixels
size1=(find(image_seg1==0));
size2=(find(image_seg2==0));
size3=(find(image_seg3==0));
```

```
size4=(find(image_seg12==0));
size_1=size(size1,1);
size_2=size(size2,1);
size_3=size(size3,1);
size_4=size(size4,1);

%                  Constructs the array for saving
black=[size_1 size_2 size_3 size_4]';
z(:,1,n)=black(:,1,1);

%% Calculating volume of granules compared to volume of cell (Assuming
sphericity)
% Identifying cell and calculating radii (Assuming sphericity)
clear al_stat g1_stat g2_stat g3_stat
al=original(:,:,2);  % Copy with red selected
al(al>0)=0;
al(~image_seg12)=255;% Mask cell only (use to be image seg12
al = al > 254;       % Remove everything that is not cell

if Algae == 9;       % Remove artifacts if bg already removed
als = bwlabel(al,4);
als_prop = regionprops(als, 'all');
als_A = [als_prop.Area];
als_MinA = max([als_prop.Area])/4;
als_Alow = als_A > als_MinA;
als_keepIndex = find(als_Alow);
alf = ismember(als, als_keepIndex);
al(~alf)=0;
end

al_stat                                                                =
regionprops('table',al,'Centroid','MajorAxisLength','MinorAxisLength')
;   % Obtain statistics on cell
al_radii                 =                mean([al_stat.MajorAxisLength
al_stat.MinorAxisLength],2)/2;              % Calculate radius of algae
(Assuming sphericity)
al_volume       =       4/3       *       pi       *       (al_radii.^3);
% Calculate volume of algae (Assuming sphericity)
al_volume_oval    =    4/3    *    pi    *    al_stat.MajorAxisLength    .*
(al_stat.MinorAxisLength.^2);%  Calculate  volume  of  algae  (Assuming
oval)
al_volume_total                      =                    sum(al_volume);
% Sum volume of sphere algae (incase previous volume was split)
al_volume_total_oval                 =               sum(al_volume_oval);
% Sum volume of oval algae (incase previous volume was split)

% Identifying granules and calculating radii (Assuming sphericity)
% Threshold 1
g1=original(:,:,2);     % Copy with red selected
g1(g1>0)=0;
g1(~image_seg1)=255;    % Mask granules only
g1 = g1 > 254;          % Remove everything that is not granules

g1_edge1 = edge(g1,'Canny');                          % Get edges of all
granules
g1_dil1 = imdilate(g1_edge1,strel('disk',8)); % Dilate edge
g1_dil1(g1) = 1;
```

```
g1_fill1 = imfill(g1_dil1,'holes');                    % Fill in edges
(Granules are now larger)
g1_edge2 = edge(g1_fill1,'Canny');                % Take edge of larger
granules
g1_dil2 = imdilate(g1_edge2,strel('disk',8)); % Dilate by same factor
as previously used
g1_2 = g1_fill1;                                  % Simple copy
g1_2(g1_dil2) = 0;                                     % Anything in large
dilated image thats also in g1_2 is removed

g1_stat                                                                 =
regionprops('table',g1_2,'Centroid','MajorAxisLength','MinorAxisLength
');  % Obtain statistics on granules
g1_radii                  =                 mean([g1_stat.MajorAxisLength
g1_stat.MinorAxisLength],2)/2;  % Calculate radius of all granules
(Assuming sphericity)
g1_volume       =       4/3       *       pi       *       (g1_radii.^3);
% Caculate volume of all granules (assuming sphericity)
g1_volume_total                     =                   sum(g1_volume);
% Sum volume of all granules
g1_granule_number                   =                 size(g1_radii,1);
% Number of individual granules identified
% Threshold 2 - Repeat with different threshold
g2=original(:,:,2);
g2(g2>0)=0;
g2(~image_seg2)=255;
g2 = g2 > 254;
g2_edge1 = edge(g2,'Canny');
g2_dil1 = imdilate(g2_edge1,strel('disk',8));
g2_dil1(g2) = 1;
g2_fill1 = imfill(g2_dil1,'holes');
g2_edge2 = edge(g2_fill1,'Canny');
g2_dil2 = imdilate(g2_edge2,strel('disk',8));
g2_2 = g2_fill1;
g2_2(g2_dil2) = 0;
g2_stat                                                                 =
regionprops('table',g2_2,'Centroid','MajorAxisLength','MinorAxisLength
');
g2_radii                  =                 mean([g2_stat.MajorAxisLength
g2_stat.MinorAxisLength],2)/2;
g2_volume = 4/3 * pi * (g2_radii.^3);
g2_volume_total = sum(g2_volume);
g2_granule_number = size(g2_radii,1);
% Threshhold 3 - Repeat with different threshold
g3=original(:,:,2);
g3(g3>0)=0;
g3(~image_seg3)=255;
g3 = g3 > 254;
g3_edge1 = edge(g3,'Canny');
g3_dil1 = imdilate(g3_edge1,strel('disk',8));
g3_dil1(g3) = 1;
g3_fill1 = imfill(g3_dil1,'holes');
g3_edge2 = edge(g3_fill1,'Canny');
g3_dil2 = imdilate(g3_edge2,strel('disk',8));
g3_2 = g3_fill1;
g3_2(g3_dil2) = 0;
g3_stat                                                                 =
regionprops('table',g3_2,'Centroid','MajorAxisLength','MinorAxisLength
');
```

```
g3_radii                =                mean([g3_stat.MajorAxisLength
g3_stat.MinorAxisLength],2)/2;
g3_volume = 4/3 * pi * (g3_radii.^3);
g3_volume_total = sum(g3_volume);
g3_granule_number = size(g3_radii,1);

%       Constructs the array for saving
granule_stats       =       [g1_granule_number       g2_granule_number
g3_granule_number]';
volume     =     [g1_volume_total     g2_volume_total     g3_volume_total
al_volume_total al_volume_total_oval]';
x_v(:,1,n) = volume(:,1,1);
x_g(:,1,n) = granule_stats(:,1,1);
n=n+1;

%%                  Display Summary

gr1 = imfuse(a_f,g1_2, 'blend');
gr2 = imfuse(a_f,g2_2,'blend');
gr3 = imfuse(a_f,g3_2, 'blend');
filename_num = sprintf('Figure %d',(n-1)/number);
figure('Name',  filename_num,'units','normalized','outerposition',[1  0
0.8 0.8]) %Left number: if 1 is right screen, if 0 is left screen
subplot(2,3,1); imshow(original); title('Original image');
subplot(2,3,2); imshow(a_f); title('Final Image (a f)');
subplot(2,3,3);             imshow(a_f);             hold             on;
viscircles(al_stat.Centroid,al_radii,'LineWidth',0.5);     hold     off;
title('Spherical cell assumption');
subplot(2,3,4);             imshow(gr1);             hold             on;
viscircles(g1_stat.Centroid,g1_radii,'LineWidth',0.5);     hold     off;
title('Low Threshold');
subplot(2,3,5);             imshow(gr2);             hold             on;
viscircles(g2_stat.Centroid,g2_radii,'LineWidth',0.5);     hold     off;
title('Typical Threshold');
subplot(2,3,6);             imshow(gr3);             hold             on;
viscircles(g3_stat.Centroid,g3_radii,'LineWidth',0.5);     hold     off;
title('High Threshold');
end

%% Saving results
%                   Puts results into saveable format
i=1;
while i<number+1;
results_area(:,i)=z(:,1,i);
results_volume(:,i)=x_v(:,1,i);
results_number(:,i)=x_g(:,1,i);
i=i+1;
end
%                    Calculating area (r) and volume (g) percentage
r_end = results_area(end,:);
r_other = results_area(1:end-1,:);
x_v_end = results_volume(end-1,:);
x_v_other = results_volume(1:end-2,:);
r=1;
while r<number+1;
results_area_percent(:,r) = r_other(:,r)/r_end(:,r);
results_volume_percent(:,r) = x_v_other(:,r)/x_v_end(:,r);
r=r+1;
```

```
end
%                   Saving
save('Area.csv', 'results_area', '-ascii', '-tabs')
save('Volume.csv', 'results_volume', '-ascii', '-tabs')
save('Number.csv', 'results_number', '-ascii', '-tabs')
xlswrite('Results.xlsx', results_area, 'Area')
xlswrite('Results.xlsx', results_volume, 'Volume')
xlswrite('Results.xlsx', results_number, 'GNumber')
display('Sphere is 2nd to bottom. Oval is bottom')
```

8.4.1.3 User interface for "Polyphosphate granule quantification" Matlab code

```
function varargout = GUI_Removal(varargin)
% GUI_REMOVAL MATLAB code for GUI_Removal.fig

% Begin initialization code - DO NOT EDIT
gui_Singleton = 1;
gui_State = struct('gui_Name',       mfilename, ...
                   'gui_Singleton',  gui_Singleton, ...
                   'gui_OpeningFcn', @GUI_Removal_OpeningFcn, ...
                   'gui_OutputFcn',  @GUI_Removal_OutputFcn, ...
                   'gui_LayoutFcn',  [] , ...
                   'gui_Callback',   []);
if nargin && ischar(varargin{1})
    gui_State.gui_Callback = str2func(varargin{1});
end

if nargout
    [varargout{1:nargout}] = gui_mainfcn(gui_State, varargin{:});
else
    gui_mainfcn(gui_State, varargin{:});
end
% End initialization code - DO NOT EDIT

% --- Executes just before GUI_Removal is made visible.
function GUI_Removal_OpeningFcn(hObject, eventdata, handles, varargin)
global a k
k=a;
axes(handles.axes1);
imshow(k);
% Choose default command line output for GUI_Removal
handles.output = hObject;
% Update handles structure
guidata(hObject, handles);
% --- Outputs from this function are returned to the command line.
function   varargout   =   GUI_Removal_OutputFcn(hObject,   eventdata,
handles)
varargout{1} = handles.output;
% --- Executes on button press in select.
function select_Callback(hObject, eventdata, handles)
global k BW
axes(handles.axes1);
imshow(k);
BW = roipoly;
% --- Executes on button press in next.
function next_Callback(hObject, eventdata, handles)
global a q k
a = k;
q = 1;
```

```
close
% --- Executes on button press in save.
function save_Callback(hObject, eventdata, handles)
global n k
filename = sprintf('GUI%d.tif', n);
imwrite(k, filename, 'tif');

% --- Executes on button press in original.
function original_Callback(hObject, eventdata, handles)
global k a
k=a;
clear BW;
axes(handles.axes1);
imshow(k);

% --- Executes on button press in Keep.
function Keep_Callback(hObject, eventdata, handles)
global k BW no_bg a
k(~BW) = 0;
k = k(:,:,1);
k(not(BW))=255;
clear ui_edge ui_fill;                    % Clear value of variables
ui_edge = edge(k,'Canny');                % Takes edge of UI image
ui_fill = imfill(ui_edge,'holes');          % Fills in edge to make a
mask with the UI image selected as '1s' and the background as '0s'
ui_cr = a(:,:,1);                         % Red channel
ui_cr(~ui_fill)=255;                          % Remove everything from
a_er that is not in image d2
ui_cg = a(:,:,2);                         % Green channel
ui_cg(~ui_fill)=255;                          % Remove everything from
a_eg that is not in image d2
ui_cb = a(:,:,3);                         % Blue channel
ui_cb(~ui_fill)=255;                          % Remove everything from
a_eb that is not in image d2
k = a;                                    % Simple copy
k(:,:,1) = ui_cr;                         % Combine red channel
k(:,:,2) = ui_cg;                         % Combine green channel
k(:,:,3) = ui_cb;                         % Combine blue channel
imshow(k);
no_bg = 1;
```

Figure 8.14: The graphical user interface for background removal

8.4.2 Is the Matlab methodology robust?

To ensure that the Matlab methodology is robust, testing of the method was conducted to identify the effect, if any, of the following issues:

1. Specificity of Ebel's cytochemical stain to polyphosphate granules
2. The ability of the image analysis program to detect the stained polyphosphate granules
3. Using a 2-dimensional image to represent a 3-dimensional object

8.4.2.1 Specificity of Ebel's cytochemical stain

The specificity of Ebel's cytochemical stain was analysed in section 4.2.1.2. From work in section 4.2.1.2, it was identified that the algae store phosphorus in localised granules indicative of polyphosphate. As further shown in section 4.2.1.2, SEM-EDS analysis of algal cells stained with Ebel's cytochemical stain showed that phosphorus and lead peaks occurred simultaneously within electron dense areas. This suggests that (1) the stain is specific to polyphosphate granules as there was no stain accumulation in other areas of the cell, and (2) it is unlikely that granules were not stained as the phosphorus peaks had an associated lead peak.

8.4.2.2 The ability of the image analysis program to detect polyphosphate granules

The ability for the image analysis program to detect polyphosphate granules is dependent on a threshold value used in the Matlab code that distinguishes between the cell and the polyphosphate granules. A static threshold is not suitable due to variations in cell colour which can be caused by changes in environmental conditions, production of carotenoids, variations in chlorophyll concentrations (Kingsbury 1956; Burczyk 1986; Ambarsari *et al.* 1997), and differences in microscope settings. It was therefore required to produce a relationship between the observed cell colour and granule detection threshold to allow a reliable distinction between cell and granules. An example of this relationship is shown in Figure 8.15 for *Scenedesmus*.

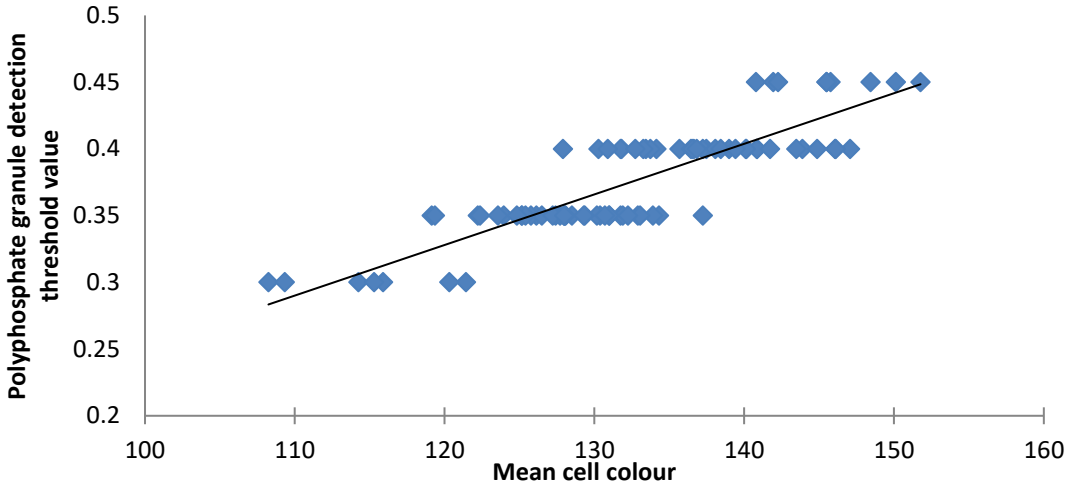

Figure 8.15: The empirical relationship between mean cell colour and polyphosphate granule detection threshold (Note: a higher cell colour result in a lighter cell. 0 is black, and 255 is white)

The empirical relationship shown in Figure 8.15 was produced by manual selection of a suitable threshold to distinguish cell and polyphosphate granules for a range of different cells. A linear trend line was fitted to produce an empirical relationship shown in Equation 8.3.

Equation 8.3: The empirical relationship between the detection threshold and cell colour

$$Detection\ threshold = 0.0038(Mean\ cell\ colour) - 0.1269$$

This empirical relationship has an R^2 of 0.75 suggesting a good fit. This empirical relationship was implemented into the Matlab code to increase the accuracy for detection of the polyphosphate granules.

Further to this, manual inspection of every processed cell was conducted to ensure that (1) the cell was isolated from the background without any debris or unwanted background, and (2) granule detection identified and counted all polyphosphate granules within the algal cell. An example of the detection using the empirical relationship shown in Equation 8.3 can be seen in Figure 8.16.

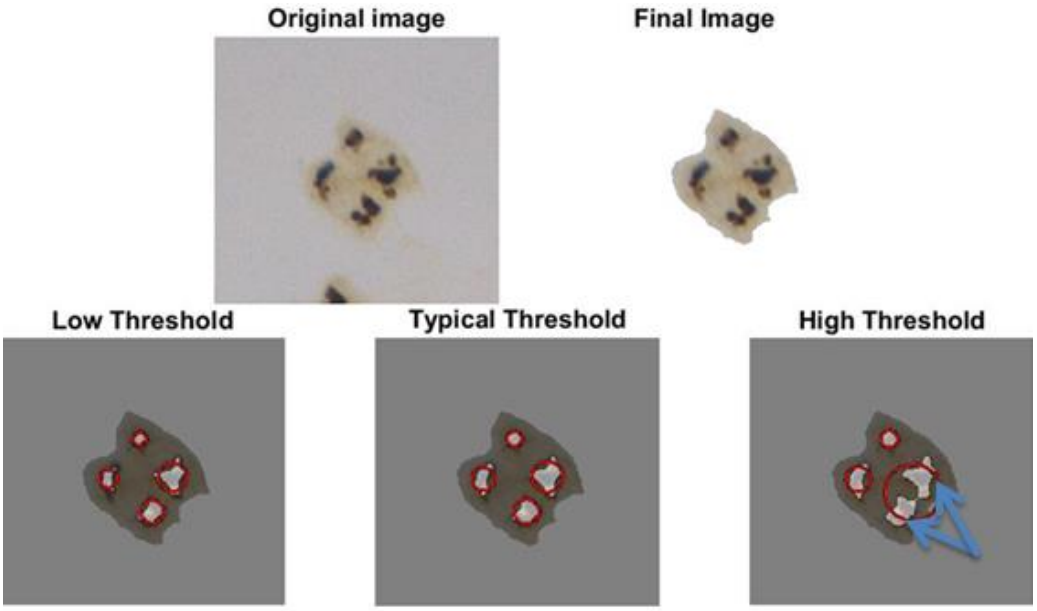

Figure 8.16: Example of the empirical detection threshold to identify polyphosphate granules. Top images show the separation of the cell from the background, while the bottom images show the granule detection at different thresholds. The typical threshold value is 0.41 as calculated using Equation 8.3 with a mean cell colour of 141, the low threshold value is 0.36 (typical value – 0.05), and the high threshold value is 0.46 (typical value + 0.05). Red circles show a spherical assumption based on the granule length and width. Blue arrows show the two separate granules that are combined into one granule when using the high detection threshold.

As shown in Figure 8.16, the low threshold was unable to detect all of the granules, resulting in a lower granule area of 9% (µm² granule/µm² cell). The high threshold overestimated the amount of granules, resulting in the bottom right two granules (indicated by the blue arrows in Figure 8.16) being detected as one large granule, and a consequent higher granule area of 15% (µm² granule/µm² cell). The typical threshold accounts for the majority of the granules while still ensuring the granules are separated. This typical threshold value resulted in a granule area of 12% (µm² granule/µm² cell). Therefore, while slight changes in the detection threshold could influence the granule detection; this effect should be minimised by manual inspection of the processed cells.

8.4.2.3 Using a 2-dimensional image to represent a 3-dimensional object

It is possible that using a 2-dimensional image to represent a 3-dimensional object could influence the quantification of polyphosphate granules in individual cells. This issue has two main points. The first being that the microscope needs to be focused to observe the 3-dimensional granules within the cell, and the second being the image analysis program uses this 2-dimensional image to estimate the amount of polyphosphate granules in a 3-dimensional algal cell.

This first issue is dependent on the focus of the granules. To address this potential issue, the microscope was always focused on the granules within the cells. If taking pictures of multiple algae in a single field of view, the focus point to ensure the granules are observed in all algae may differ, requiring multiple photos at different focus points for the same field of view. While it was attempted to ensure all the granules were in focus, it is still possible that some granules, especially when multiple granules are present in one cell, would be out of focus. To reduce the impact of this, the Matlab program applies an edge smoothing function to remove "fuzzy" edges due to focus, allowing a close estimation of the true granule area. Combined with a large number of cells analysed per sample, it is unlikely that the microscope focus has a large impact on the detection process.

A spherical assumption was made in the image analysis program that estimates the cell and granule volumes to understand the relationship between the 2-dimensional images and 3-dimensional objects. This assumption takes the average of the longest and shortest distances of the cell in the 2-dimensional image to estimate the diameter that can be used in a spherical assumption. Similarly, the same process is conducted for each individual granule within the cell. This relationship was studied using the round alga *Chlamydomonas reinhardtii* (culture described in section 5.2.2). An example of the spherical cell assumption is shown in Figure 8.17.

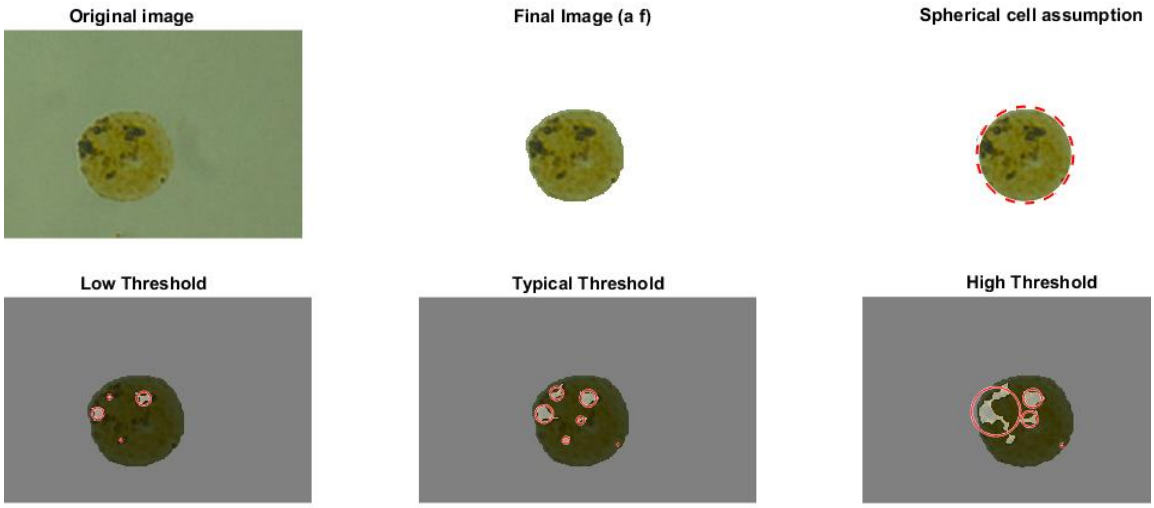

Figure 8.17: Example of a typical *C. reinhardtii* cell used for the volume calculations. From top left to right: original image, background removed image, and background removed image with the red dotted outline showing the circumference used for the spherical estimation. From bottom left to right: low granule threshold, typical granule threshold as predicted by the empirical threshold relationship for *C. reinhardtii*, and high granule threshold. Red circles show the detected granules and the circumference used in the spherical estimation.

As shown in Figure 8.17, the *C. reinhardtii* cell has a good fit to the spherical assumption. Further to this, the typical granule detection threshold discussed in section 8.4.2.2 (and labelled 'typical threshold' in Figure 8.17) shows the majority of the polyphosphate granules are detected with minimal detection of the non-granular cell. While there is some variation in the granule sphericity, without any 3-dimensional imaging, the spherical assumption is a good estimate of the granule volume.

A comparison between the polyphosphate granule volume and the polyphosphate granule area for individual *C. reinhardtii* cells was conducted using the spherical assumption as shown in Figure 8.18.

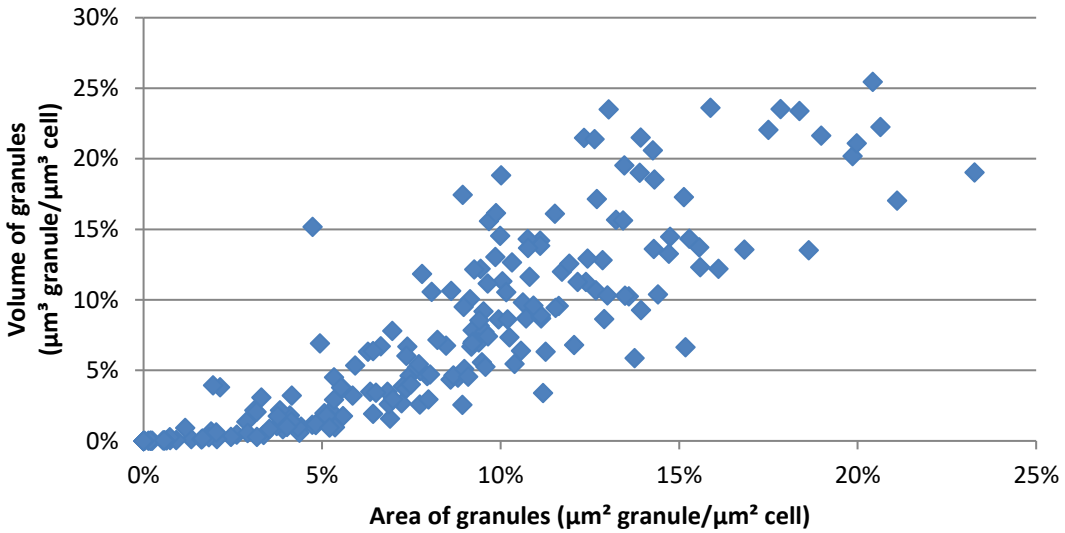

Figure 8.18: Comparison between area and volume calculations of polyphosphate granules in *C. reinhardtii* cells.

As shown in Figure 8.18, a general trend of increasing granule area and an increase in the granule volume can be observed. Since the spherical assumption does not hold for all algal genera in the WSP (i.e. *Scenedesmus*), using a spherical assumption would consequently bring in more variation if applied to those algae. Therefore, the granule area was used in the image analysis method to quantify the polyphosphate granules.

8.4.3 Regression equation used to incorporate the effects of variables on polyphosphate granule formation in the genera studied

The following sections show the regression equations for each genus that were produced in Minitab by using stepwise regression with an alpha to enter and remove of 0.1. Up to 2-way interactions were included and non-significant main effects that had a significant interaction were included in the regression equations to maintain statistical hierarchy. The values used in the Minitab analysis to produce these regression equations are from the fractional factorial experiment described in section 4.2.2.1.

For all the regression equations: T = temperature (°C), P = phosphorus concentration (mgP/L), L = light intensity ($\mu E/m^2.s$), M = mixing intensity (RPM), C = organic load (mgCOD/L), and pH = pH. '×' refers to an interaction effect between the variables.

8.4.3.1 Scenedesmus

$$\text{Polyphosphate granule area } \left(\frac{\mu m^2 \text{ granule}}{\mu m^2 \ cell}\right)$$
$$= 0.0584 - 0.00103(\text{T}) - 0.00456(\text{P}) - 0.000684(\text{L}) + 0.000025(\text{M})$$
$$- 0.000030(\text{C}) - 0.00015(\text{pH}) + 0.000019(\text{T} \times \text{L}) + 0.000052(\text{P} \times \text{L})$$
$$+ 0.000004(\text{P} \times \text{C}) + 0.01492(\text{Ct Pt})$$

$$R^2_{Adjusted} = 48\%$$

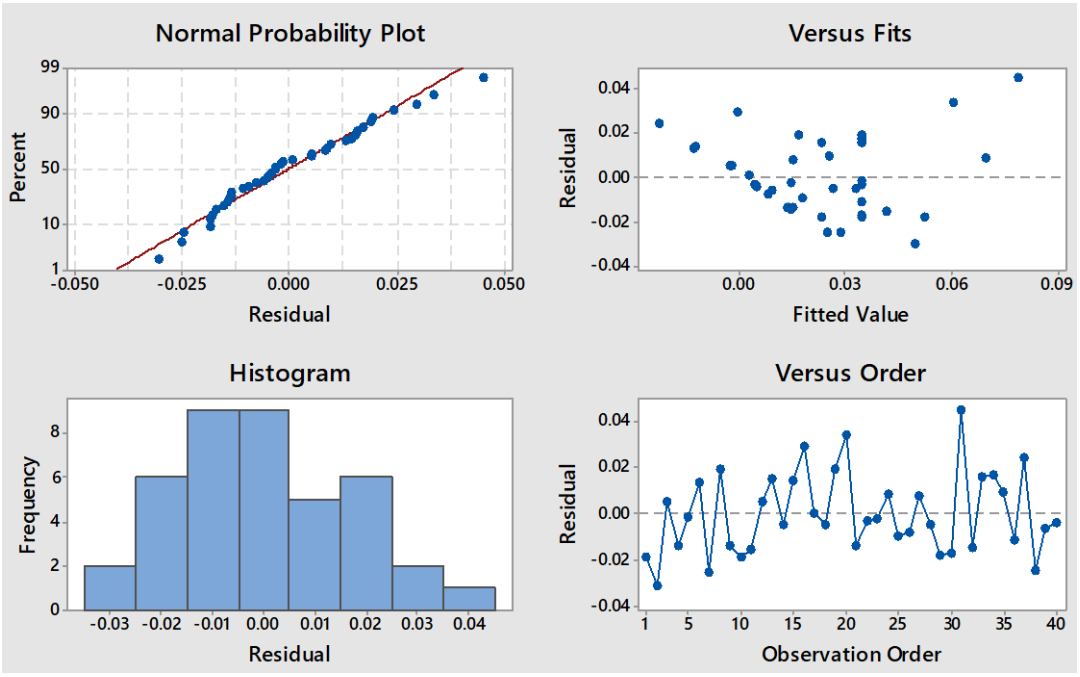

Figure 8.19: Residual plots for the *Scenedesmus* regression equation

Analysing the 'normal probability plot' in Figure 8.19, the residuals appear to be normally distributed as they follow the line of best fit. This can also be seen in the 'histogram' that shows a general normal distribution shape. This suggests the assumption of normal distribution to make the linear regression was correct. No trend can be seen in the 'versus order' plot.

A trend can be observed in the 'versus fit' plot in Figure 8.19. This trend suggests a non-linear response, which was also indicated in the Minitab analysis by the inclusion of the centre point term in the regression equation for *Scenedesmus*. Due to the experimental design, the variable or variables responsible for this non-linear response cannot be identified.

8.4.3.2 Micractinium/Microcystis

$$\text{Polyphosphate granule area } \left(\frac{\mu m^2 \text{ granule}}{\mu m^2 \ cell}\right)$$
$$= -0.0524 + 0.00328(T) + 0.00331(P) - 0.000704(L) + 0.000030(M)$$
$$+ 0.000007(C) + 0.01236(pH) + 0.000025(T \times L) - 0.000540(T \times pH)$$
$$+ 0.000039(P \times L) + 0.000004(P \times C) - 0.000730(P \times pH)$$
$$- 0.0000004(M \times C)$$

$$R^2_{Adjusted} = 42\%$$

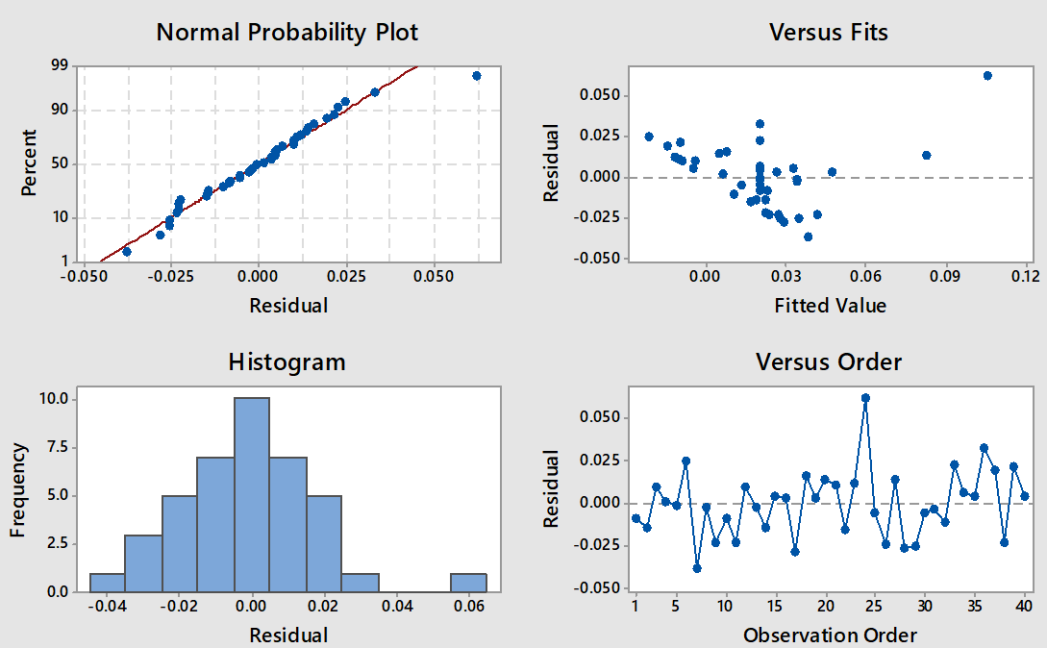

Figure 8.20: Residual plots for the *Micractinium/Microcystis* regression equation

Analysing the 'normal probability plot' in Figure 8.20, the residuals appear to be normally distributed as they follow the line of best fit. A large residual can be observed at the top right of the 'normal probability plot' which appears to be an outlier. A similar trend is also shown in the 'histogram'. This suggests the assumption of normal distribution to make the linear regression was correct. No trend can be seen in the 'versus order' plot.

A slight trend can be observed in the 'versus fit' plot in Figure 8.20. While this may suggest a non-linear response, Minitab did not find curvature, which is used to indicaite non-linearity, to be significant (p-value of 0.402).

8.4.3.3 Pediastrum

Polyphosphate granule area $\left(\frac{\mu m^2 \text{ granule}}{\mu m^2 \ cell}\right)$

$$= -0.0112 + 0.00600(T) - 0.00783(P) - 0.000337(L) - 0.000047(C)$$
$$+ 0.00986(pH) + 0.000203(T \times P) - 0.000731(T \times pH)$$
$$+ 0.000035(P \times L) + 0.000004(P \times C)$$

$$R^2_{Adjusted} = 38\%,$$

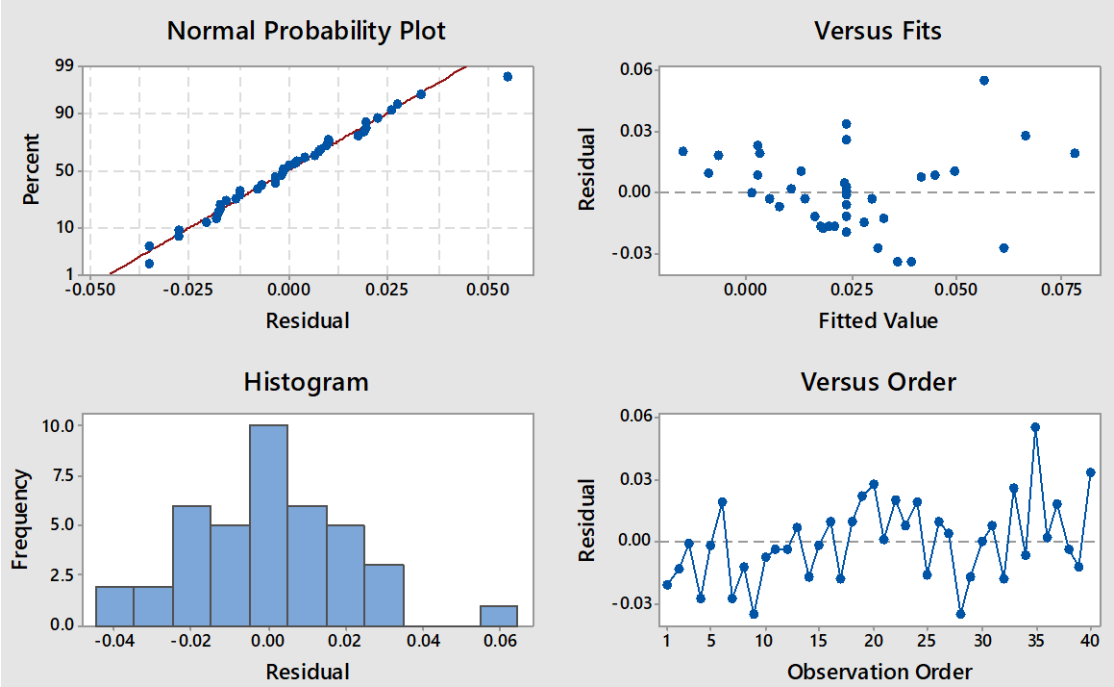

Figure 8.21: Residual plots for the *Pediastrum* regression equation

Analysing the normal probability plot in Figure 8.21, the residuals appear to be normally distributed as they follow the line of best fit. A large residual can be observed at the top right of the 'normal probability plot' which appears to be an outlier. A similar trend is also shown in the 'histogram'. This suggests the assumption of normal distribution to make the linear regression was correct. No trends can be seen in the 'versus fit' and 'versus order' plots.

8.4.3.4 Monoraphidium

$$\text{Polyphosphate granule area } \left(\frac{\mu m^2 \text{ granule}}{\mu m^2 \ cell}\right)$$
$$= 0.0598 - 0.00116(P) - 0.000124(L) - 0.000094(M) - 0.000051(C)$$
$$- 0.00579(pH) + 0.000022(P \times L) + 0.000011(M \times pH)$$
$$+ 0.000006(C \times pH)$$

$$R^2_{Adjusted} = 27\%$$

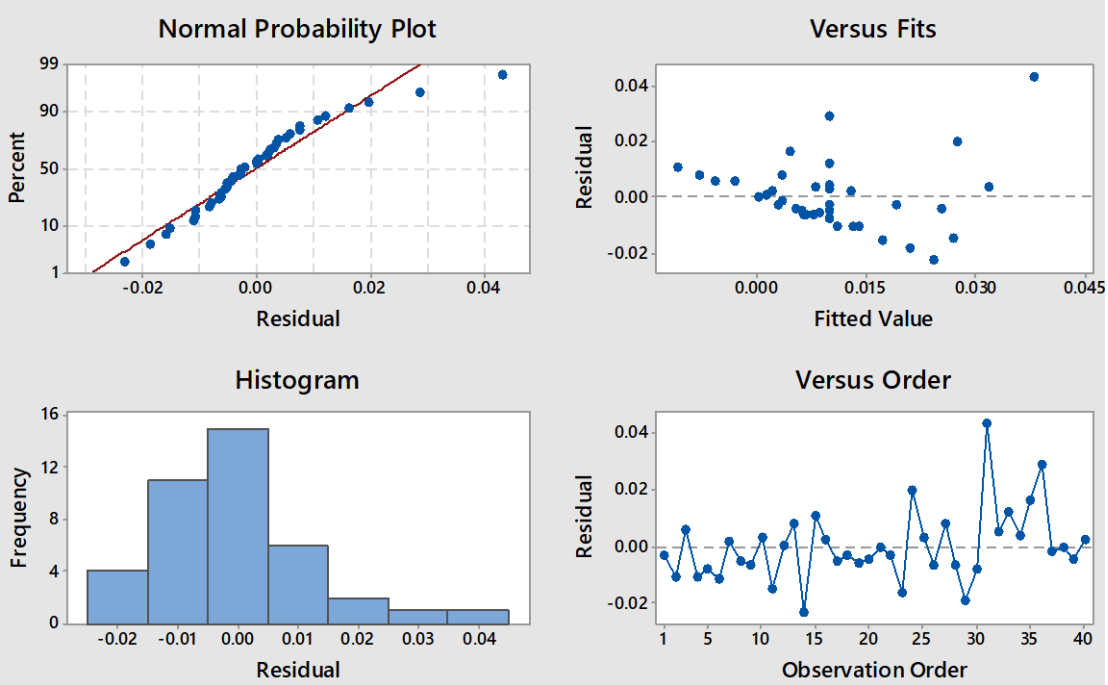

Figure 8.22: Residual plots for the *Monoraphidium* regression equation

As shown in the 'normal probability plot' in Figure 8.22, most of the residuals are normally distributed, however, there are two large residuals in the top right of the plot which may be outliers. This suggests the assumption of normal distribution to make the linear regression is correct for most of the residuals. No trend can be seen in the 'versus order' plot.

A slight parabolic trend can be observed in the 'versus fit' plot in Figure 8.22. While this may suggest a non-linear response, Minitab did not find curvature, which is used to indicaite non-linearity, to be significant (p-value of 0.515).

8.4.3.5 Actinastrum

Polyphosphate granule area $\left(\frac{\mu m^2 \text{ granule}}{\mu m^2 \ cell}\right)$

$$= -0.0687 + 0.003149(T) + 0.00335(P) + 0.000028(M) + 0.00675(pH) - 0.000306(T \times pH) - 0.000003(P \times M) - 0.000277(P \times pH)$$

$$R^2_{Adjusted} = 27\%$$

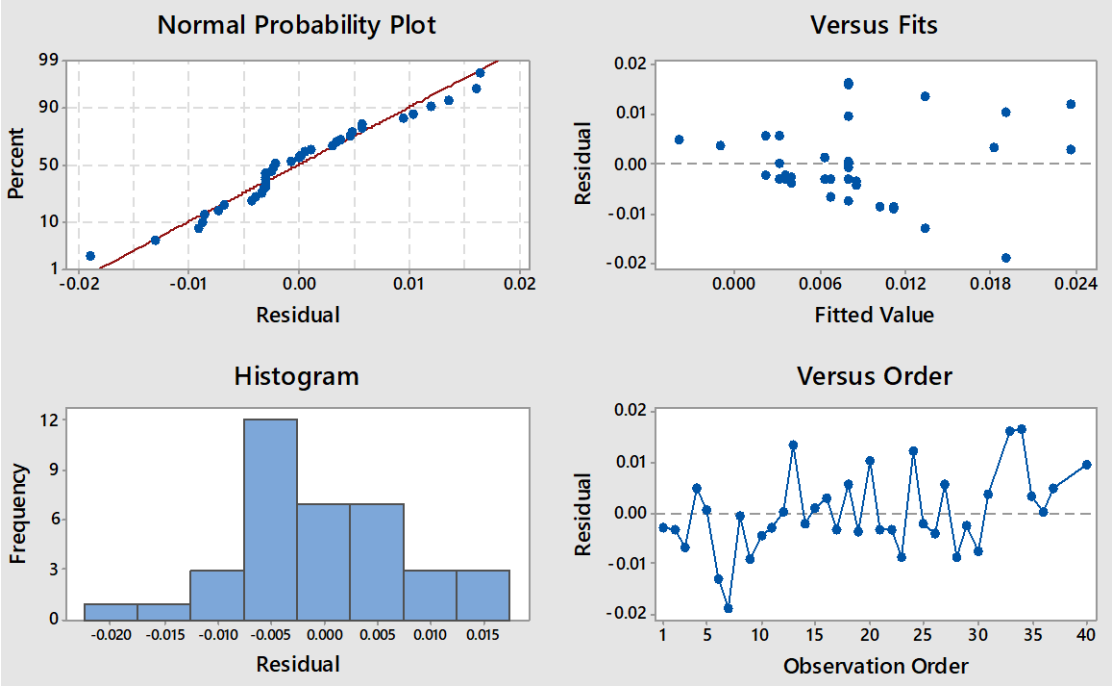

Figure 8.23: Residual plots for the *Actinastrum* regression equation

Analysing the 'normal probability plot' in Figure 8.23, the residuals appear to be normally distributed as they follow the line of best fit. This suggests the assumption of normal distribution to make the linear regression was correct. No trends can be seen in the 'versus fit' and 'versus order' plots.

8.5 Appendix for Chapter 5: Relating polyphosphate granules in algal cells to the phosphorus content of the biomass

8.5.1 Minimal medium

The minimal medium was used for experiments with the *Chlamydomonas reinhardtii* species. The synthetic wastewater recipe for this media is given in Table 8.10.

Table 8.10: Minimal medium used for the *Chlamydomonas reinhardtii* species work

Chemical	Concentration g/L
K_2HPO_4	0.034
KH_2PO_4	0.018
$NaNO_3$	0.63
NH_4Cl	0.4
$MgSO_4.7H_2O$	1.0
$CaCl_2.2H_2O$	0.5
Hutner Trace element	**Concentration mg/L**
$Na_2EDTA.2H_2O$	50.0
H_3BO_3	11.4
$MnCl_2{\cdot}4H_2O$	5.10
$ZnSO_4.7H_2O$	22.0
$CuSO_4.5H_2O$	1.57
$Na_2MoO_4{\cdot}2H_2O$	1.01
$CoCl_2{\cdot}6H_2O$	1.61
$FeSO_4.7H_2O$	4.99

8.5.2 Mass balance on phosphorus in polyphosphate granules

This section describes the mass balance that was conducted to estimate the contribution of phosphorus from polyphosphate granules to the overall cells phosphorus content. In Chapter 5, polyphosphate granules within algal cells have been shown to:

1. Vary from 0% up to 29% (μm^2 granule/μm^2 cell) of the total cell area as polyphosphate granules (Figure 5.1 and Figure 5.3), and
2. Polyphosphate granules have an increased phosphorus concentration of 7±2 $\mu gP/cm^2$, which is double the concentration of 3±1 $\mu gP/cm^2$ found in the remainder of the cell (Diaz *et al.* 2009).

Both of these points were used to conduct a mass balance to compare the amount of phosphorus associated with the granules and the amount of phosphorus associated with the remaining cell.

Step 1: Convert the area of granules and cells from pixels^2 to micron^2

In order to conduct the mass balance, the area of the granules and cell needed to be converted from pixels^2 to micron^2. This conversion was achieved by using a calibration constant in the image analysis method to convert between the two areas. The constant was calculated by using image analysis on the scale bar in the images (which is a known length) and comparing it to the number of pixels counted by the image analysis program, resulting in a calibration value of $213\,\frac{pixel^2}{micron^2}$. This calibration constant was then used to convert the areas of the granules and cell from pixels^2 to micron^2 on all cells in Figure 5.1 and Figure 5.3.

For example, if a cell had 608 pixel^2 of granules and 23516 pixel^2 of cell:

$$Granule\ area = \frac{608\ pixel^2}{213\ \frac{pixel^2}{micron^2}} = 2.9\ micron^2$$

$$Cell\ area = \frac{23516\ pixel^2}{213\ \frac{pixel^2}{micron^2}} = 110.4\ micron^2$$

Step 2: Account for the different phosphorus densities of the cell and polyphosphate granules given by Diaz *et al.* (2009)

The average phosphorus densities of the polyphosphate granules and the cell were used in this calculation, which corresponds to 7 $\mu gP/cm^2$ and 3 $\mu gP/cm^2$ respectively. These phosphorus

densities were then multiplied by the areas of the polyphosphate granules and cell calculated in step 1 for all cells in Figure 5.1 and Figure 5.3.

For example, if a cell had 2.9 micron^2 of granules and 110.4 micron^2 of cell:

$$Phosphorus\ in\ granule = \frac{2.9\ micron^2}{1 \times 10^8 \frac{cm^2}{micron^2}} \times 7 \frac{\mu gP}{cm^2} = 2 \times 10^{-7}\ \mu gP$$

$$Phosphorus\ in\ cell = \frac{110.4\ micron^2}{1 \times 10^8 \frac{cm^2}{micron^2}} \times 3 \frac{\mu gP}{cm^2} = 3.3 \times 10^{-6}\ \mu gP$$

Step 3: Calculate the percentage of the cellular phosphorus that is polyphosphate granules

The phosphorus in the granules is divided by the non-granular phosphorus in the cell for all algae shown in Figure 5.1 and Figure 5.3:

$$Percentage\ of\ cellular\ phosphorus\ that\ is\ granules = \frac{Phosphorus\ in\ granule}{Phosphorus\ in\ cell}$$

For example, if a cell had $2 \times 10^{-7}\ \mu gP$ of granules and $3.3 \times 10^{-6}\ \mu gP$ of cell:

$$Percentage\ of\ cellular\ phosphorus\ that\ is\ granules = \frac{2 \times 10^{-7}\ \mu gP}{3.3 \times 10^{-6}\ \mu gP} = 6\%$$

Step 4: Plot the 'average cellular phosphorus associated with polyphosphate granules (µgP granule/µgP Cell)' against the 'phosphorus content of the biomass (gP/gSS)'

The 'cellular phosphorus associated with polyphosphate granules (µgP granule/µgP Cell)' of all the cells at a given 'phosphorus content of the biomass (gP/gSS)' were averaged to obtain one point. This then allowed the comparison between the phosphorus associated with the granules and the phosphorus associated with the biomass to be conducted as shown in section 5.3.4 and reproduced here in Figure 8.24.

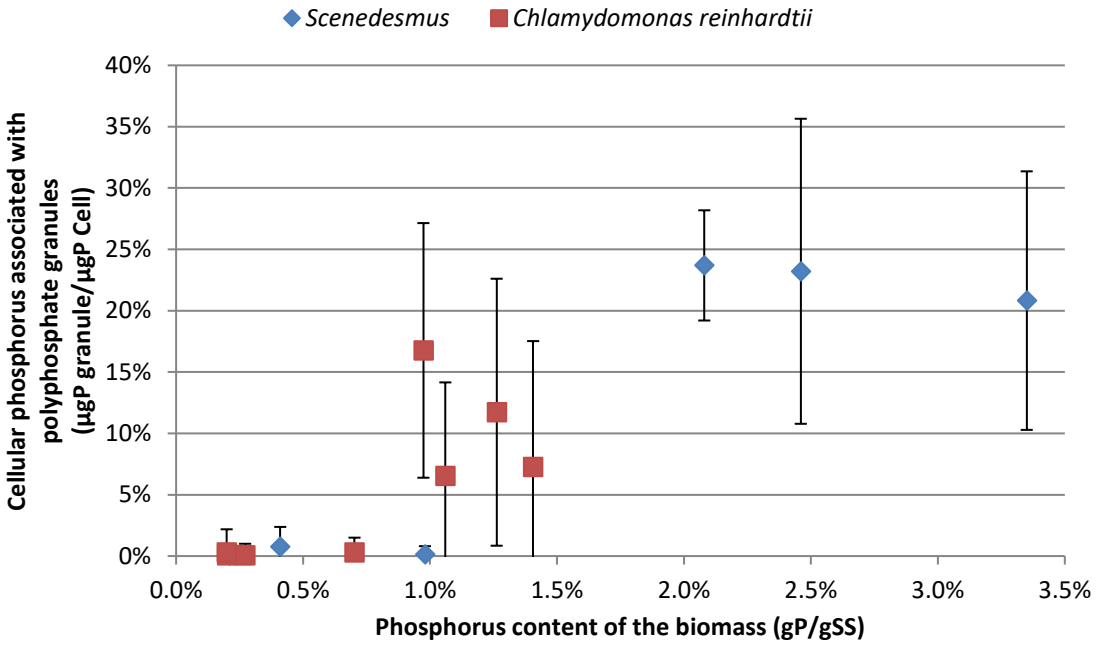

Figure 8.24: Phosphorus associated with the polyphosphate granules for *Scenedesmus* and *C. reinhardtii* cells shown in Figure 5.1 and Figure 5.3 respectively. Error bars are the standard deviation produced from the variation in polyphosphate granule area of individual cells.

Statement of contribution to doctoral thesis containing publications – Chapter 2

DRC 16

MASSEY UNIVERSITY
GRADUATE RESEARCH SCHOOL

STATEMENT OF CONTRIBUTION
TO DOCTORAL THESIS CONTAINING PUBLICATIONS

(To appear at the end of each thesis chapter/section/appendix submitted as an article/paper or collected as an appendix at the end of the thesis)

We, the candidate and the candidate's Principal Supervisor, certify that all co-authors have consented to their work being included in the thesis and they have accepted the candidate's contribution as indicated below in the *Statement of Originality*.

Name of Candidate: Matthew Sells

Name/Title of Principal Supervisor: Prof. Andrew Shilton

Name of Published Research Output and full reference:

Determining variables that influence the phosphorus content of waste stabilization pond algae

Sells, M. D., Brown, N., & Shilton, A. N. (2018). Determining variables that influence the phosphorus content of waste stabilization pond algae. Water Research, 132, 301-308. doi:10.1016/j.watres.2018.01.013

In which Chapter is the Published Work: Chapter 2

Please indicate either:

- The percentage of the Published Work that was contributed by the candidate:

  and / or

- Describe the contribution that the candidate has made to the Published Work:

  M. Sells was the main contributor of the manuscript. He conducted the experimental work, analysed the data and wrote most of the manuscript.

Candidate's Signature

31/07/18
Date

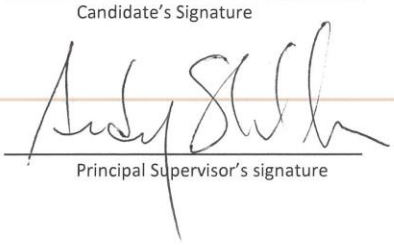

Principal Supervisor's signature

31/07/18
Date

GRS Version 3– 16 September 2011